ISSN 0003-2654
VOL. 119 NO. 3 MARCH 1994

THE ROYAL SOCIETY OF CHEMISTRY
Founded 1841

The Analyst

An international analytical science journal

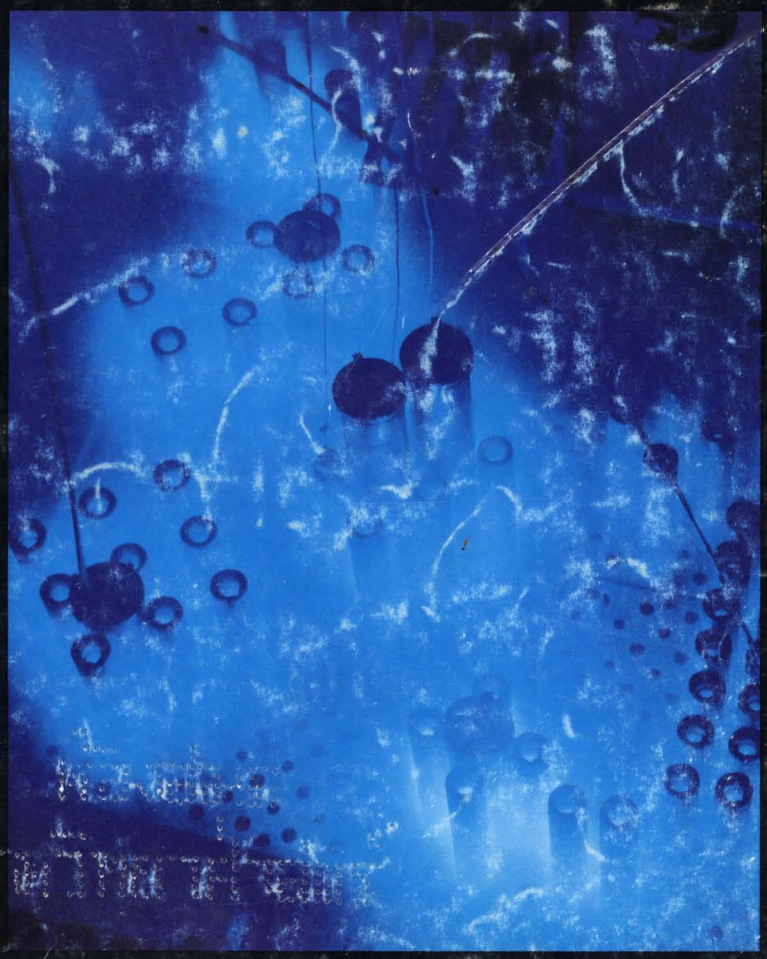

The Analyst

The Analytical Journal of The Royal Society of Chemistry

Editorial Manager, Analytical Journals: Janice M. Gordon

Editor, *The Analyst*
Harpal S. Minhas
The Royal Society of Chemistry,
Thomas Graham House, Science Park,
Milton Road, Cambridge, UK CB4 4WF
Telephone +44(0)223 420066.
Fax +44(0)223 420247. Telex No. 818293 ROYAL.

US Associate Editor, *The Analyst*
Dr Julian F. Tyson
Department of Chemistry,
University of Massachusetts,
Amherst MA 01003, USA
Telephone +1 413 545 0195
Fax +1 413 545 4490

Assistant Editors
Sarah Williams Yasmin Khan

Editorial Secretary: Claire Harris

Advertisements: Advertisement Department, The Royal Society of Chemistry, Burlington House, Piccadilly, London, UK W1V 0BN. Telephone +44(0)71-287 3091. Telex No. 268001. Fax +44(0)71-494 1134.

Information for Authors

Full details of how to submit material for publication in *The Analyst* are given in the Instructions to Authors in the January issue. Separate copies are available on request.

The Analyst publishes papers on all aspects of the theory and practice of analytical chemistry, fundamental and applied, inorganic and organic, including chemical, physical, biochemical, clinical, pharmaceutical, biological, environmental, automatic and computer-based methods. Papers on new approaches to existing methods, new techniques and instrumentation, detectors and sensors, and new areas of application with due attention to overcoming limitations and to underlying principles are all equally welcome. There is no page charge.

The following types of papers will be considered:

Full research papers.

Communications, which must be on an urgent matter and be of obvious scientific importance. Rapidity of publication is enhanced if diagrams are omitted, but tables and formulae can be included. Communications receive priority and are usually published within 5–8 weeks of receipt. They are intended for brief descriptions of work that has progressed to a stage at which it is likely to be valuable to workers faced with similar problems. A fuller paper may be offered subsequently, if justified by later work. Although publication is at the discretion of the Editor, communications will be examined by at least one referee.

Full critical reviews, which must be a critical evaluation of the existing state of knowledge on a particular facet of analytical chemistry.

Every paper (except Communications) will be submitted to at least two referees, by whose advice the Editorial Board of *The Analyst* will be guided as to its acceptance or rejection. Papers that are accepted must not be published elsewhere except by permission. Submission of a manuscript will be regarded as an undertaking that the same material is not being considered for publication by another journal.

Regional Advisory Editors. For the benefit of potential contributors outside the UK and N. America, a Group of Regional Advisory Editors exists. Requests for help or advice on matters related to the preparation of papers and their submission for publication in *The Analyst* can be sent to the nearest member of the Group. Currently serving Regional Advisory Editors are listed in each issue of *The Analyst.*

Manuscripts (four copies typed in double spacing) should be addressed to:

H. S. Minhas, Editor, *or*
J. F. Tyson, US Associate Editor

Particular attention should be paid to the use of standard methods of literature citation, including the journal abbreviations defined in Chemical Abstracts Service Source Index. Wherever possible, the nomenclature employed should follow IUPAC recommendations, and units and symbols should be those associated with SI.

All queries relating to the presentation and submission of papers, and any correspondence regarding accepted papers and proofs, should be directed either to the Editor, or Associate Editor, *The Analyst.* Members of the Analytical Editorial Board (who may be contacted directly or *via* the Editorial Office) would welcome comments, suggestions and advice on general policy matters concerning *The Analyst.*

Fifty reprints are supplied free of charge.

The Analyst (ISSN 0003–2654) is published monthly by The Royal Society of Chemistry, Thomas Graham House, Science Park, Milton Road, Cambridge, UK CB4 4WF. All orders, accompanied with payment by cheque in sterling, payable on a UK clearing bank or in US dollars payable on a US clearing bank, should be sent directly to The Royal Society of Chemistry, Turpin Distribution Services Ltd., Blackhorse Road, Letchworth, Herts, UK SG6 1HN. Turpin Distribution Services Ltd., is wholly owned by the Royal Society of Chemistry. 1994 Annual subscription rate EC £340.00, USA $641.00, Canada £384.00 (excl. GST), Rest of World £366.00. Purchased with *Analytical Abstracts* EC £718.00, USA $1351.00, Canada £811.00 (excl. GST), Rest of World £772.00. Purchased with *Analytical Abstracts* plus *Analytical Proceedings* EC £851.00, USA $1601.00, Canada £961.00 (excl. GST), Rest of World £915.00. Purchased with *Analytical Proceedings* EC £432.00, USA $812.00, Canada £487.00 (excl. GST), Rest of World £432.00. Air freight and mailing in the USA by Publications Expediting Inc., 200 Meacham Avenue, Elmont, NY 11003.

USA Postmaster: Send address changes to: *The Analyst,* Publications Expediting Inc., 200 Meacham Avenue, Elmont, NY 11003. Second class postage paid at Jamaica, NY 11431. All other despatches outside the UK by Bulk Airmail within Europe, Accelerated Surface Post outside Europe. PRINTED IN THE UK.

Editorial

The continuing evolution of *The Analyst*

The Analyst is the oldest continuously-published, English language analytical science journal: volume 1 appeared in 1877. However, *The Analyst* has moved with the times keeping abreast of all that is new in analytical chemistry, maintaining its excellent reputation acquired over a century and a half.

The rapid pace of development in analytical science has led to an even greater expansion of the content of the journal, thus in order to meet the changing needs of both our readers and authors, the evolution of the journal (that began in January 1993 with the introduction of Tutorial Reviews, a conference diary, conference reports and faster publication times) has continued. You may have noticed that the cover has been modernised, with the inclusion of colour photographs relevant to the content. Colour will continue to be included within the scientific content of the journal too, where it is justifiable as an aid to understanding the text. The Editor, Harp Minhas, would be pleased to consider photographs from authors and special issue conference organizers for inclusion on the cover.

Some would have liked to have seen a change in the name of the journal, but changes in name are not popular with librarians, and, in these times of difficult financing, there is always the possibility of being viewed as a completely new (and, therefore, unaffordable) journal. *The Analyst* grew up in the times of classical analysis, and it has always been concerned to publish methods that work well in real situations, *e.g.*, in industrial laboratories; even a few years ago it was not unknown for steel analysts in Sheffield, for example, acting as referees, to have a proposed method tested in their laboratory as part of the refereeing process. The Analytical Editorial Board (AEB) and permanent journals staff have aimed, with some success, to broaden the scope of the analytical chemistry topics appearing in *The Analyst* and in order to meet the needs and interests of its readers and authors worldwide. Clearly, our current readers and authors are better termed analytical scientists than analytical chemists or just analysts, so we have now included the term analytical science on the cover. The name of the journal remains as it was in 1876: it is an honourable name.

The other changes that have been introduced over the past two years or so have catalysed changes to our sister journal *Analytical Proceedings* (see *Anal. Proc.*, 1994, **30**, 1 for more details). This now has the subtitle, 'Including Analytical Communications', and has been re-launched as a refereed, rapid publication, analytical communications journal. This change will increase the international status of *Analytical Proceedings Including Analytical Communications*, and make the two journals more complementary. For this reason it is intended that *The Analyst* will no longer publish communications, these being redirected, with the author's permission, to *Analytical Proceedings Including Analytical Communications*. For some time now papers based on plenary lectures at conferences have been included in *The Analyst*, rather than in *Analytical Proceedings*.

As a result of our success in broadening the scope of *The Analyst* and ensuring its wider acceptance amongst the international scientific community and analytical scientists in Europe and worldwide, we welcome Yngvar Thomassen from Norway as our first member on AEB from outside the British Isles.

Many authors appreciate the quality of editing and presentation in the journals of The Royal Society of Chemistry, and the personal attention they receive at all stages in the publication process. If you would like further information about publishing in *The Analyst* please write, fax or telephone the editor.

Arnold G. Fogg
Chairman, Analytical Editorial Board

New Editorial Board Members

Dr Yngvar Thomassen

Yngvar Thomassen was born in Porsgrunn, Norway, on March 25, 1947. Dr. Thomassen's academic training was obtained in the Department of Analytical Chemistry at the University of Oslo from where he graduated in 1973. He spent one year at the Norwegian Defence Research Institute before taking a postdoctoral research associate position at the Department of Analytical Chemistry at the University of Oslo, where he conducted research for 2½ years. In 1978 he visited The University of Toronto, Department of Environmental Studies and Geology, for one year with a Royal Norwegian Grant (visiting scientist).

He is currently employed as a senior research scientist at the National Institute of Occupational Health in Oslo where he has spent 16 years of his professional life. Dr. Thomassen is the author or co-author of over 125 scientific publications on atomic spectroscopy and other spectroscopic methods for the determination of essential and toxic elements in the environment with special emphasis on electrothermal atomic absorption spectrometry (ETAAS). He is best known for his research on the use of ETAAS in the determination of selenium and other toxic elements in human health and disease.

He is on the Editorial Advisory Board of *Journal of Trace Elements, and Electrolytes in Health and Disease* and *Scandinavian Journal of Work, Environment and Health*, and he has given over 130 presentations on various aspects of his research, of which 45 were invited lectures at major conferences and symposia. In the period 1983–91 he has been a member of the Commission on Toxicology, International Union of Pure and Applied Chemistry, titular member from 1986, where he has initiated the development of human body fluids as quality assurance materials for the measurement of minor, trace and ultra-trace elements and organic metabolites.

Dr. Thomassen has organized a number of Nordic, national and international conferences on topics dealing with analytical chemistry, atomic spectroscopy and environmental and biological issues.

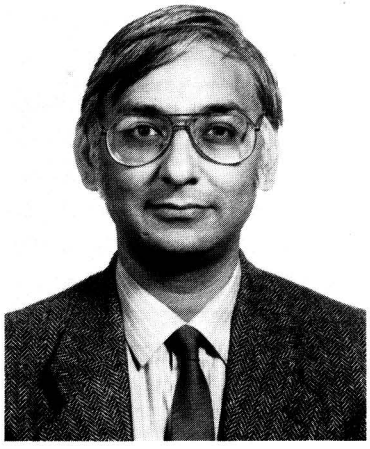

Professor Pankaj Vadgama

Pankaj Vadgama is Professor of Clinical Biochemistry in the Department of Medicine at the University of Manchester, Honorary Consultant Chemical Pathologist at Hope Hospital, and Head of the Department of Medicine. He was born in Nairobi, Kenya, February 16, 1948, and after schooling at Kings School in Harrow, he qualified in Medicine at the University of Newcastle-upon-Tyne in 1971. However, his professor (A. L. Lather) wished Pankaj to obtain a more thorough grounding in Chemistry as preparation for a career in clinical biochemistry. This he did (still at Newcastle) and gained first class honours in chemistry in 1976 and subsequently, a PhD in 1984 under the supervision of K. G. M. M. Alberti. His main interest is in the use of biosensors for clinical monitoring. He commenced work on enzyme-based biosensors as an MRC Training Fellow and, following a 2 year period as a Clinical Biochemist in the NHS, returned to work on biosensors at Newcastle, holding the title of Director of the Biosensor Group. Professor Vadgama has so far authored over 100 published articles in the field of biosensors.

Introduction to Control Charts in the Analytical Laboratory

Tutorial Review

Eamonn Mullins

Industrial Statistics Unit, Department of Statistics, Trinity College, Dublin, Ireland

The use of control charts in the analytical laboratory is introduced. Examples are provided to illustrate the use of control charts in assessing the performance of a measurement system; these are followed by a discussion of the assumptions and theory underlying the charts and of rules that are used to signal measurement problems. Next, some practical issues involved in setting up control charts are outlined. In particular, the problems arising in calculating an appropriate standard deviation, for establishing control limits for a chart, are considered: among these are the need to avoid partial replication and to include between-analyst, between-instrument and short-term temporal variation, where appropriate, in the estimate of random error. Aspects of the routine use of charts are then considered, including the recording of extra information about the assay on the control chart, so that it can be used for retrospective analyses of system performance and as a basis for assay improvement studies. Reference is made to the use of control charts as a kind of laboratory database, where the information required for planning future experimental studies is stored. Finally, brief reference is made to other types of control chart not discussed in the paper.

Keywords: *Shewhart control charts; normal distribution; measurement stability; full and partial replicates*

Introduction

Statistical quality control (QC) charts are a simple but powerful tool for monitoring the stability of an analytical procedure. Conceptually they are very simple: a standard material is measured regularly and the analytical responses are plotted in time order on a chart; if the chart displays other than random variation around the expected result it suggests that something has gone wrong with the measurement process. To help decide if this has happened control limits are plotted on the chart: the responses are expected to remain inside these limits. Rules are decided upon which will define non-random behaviour.

Control charts were developed to control engineering production processes rather than measurement systems. However, any apparent differences between the two situations disappear when we think of a measurement system as a production process the output of which is measurements. The most commonly used charts were developed by Shewhart[1] in Bell Laboratories in the 1920s. He described random measurement errors as being due to 'chance causes' and distinguished the latter from 'assignable causes', which would be anything that could change the level of a measurement (*i.e.*, cause bias) or change the precision. If a measurement system is stable such that it exhibits random variation around a given reference value and the size of that variation (as measured by the standard deviation) remains constant, he would say it is 'in statistical control' or simply 'in control'. The objective in using control charts is to achieve and maintain this state of statistical control.

The following sections of this paper begin with two examples to illustrate the use of control charts in assessing the performance of a measurement system; these are followed by a discussion of the assumptions and theory underlying the charts and of rules that are used to signal measurement problems. Next, some practical issues involved in setting up control charts are outlined. In particular, the problems arising in calculating an appropriate standard deviation for establishing control limits for a chart are considered: among these are the need to avoid partial replication and to include between-analyst, between-instrument and short-term temporal variation, where appropriate, in the estimate of random error. Aspects of the routine use of charts are then considered, including the recording of extra information about the assay on the control chart, so that it can be used for retrospective analyses of system performance and as a basis for assay improvement studies. Reference is made to the use of control charts as a kind of laboratory database, where the information required for planning future experimental studies is stored. Finally, brief reference is made to other types of control chart not discussed in the paper.

Examples

Example 1

Fig. 1 shows a control chart for a high-performance liquid chromatography (HPLC) potency assay of a pharmaceutical product.

The data displayed in the chart were collected over several months. At each time point, two replicate measurements were

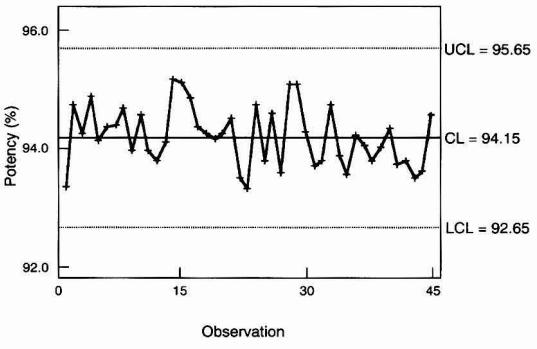

Fig. 1 Control chart for an HPLC potency assay

carried out on a control material. These results were averaged and it is the average that is plotted in the chart. For now, the centre line (CL) and control limits (upper and lower control limits, UCL and LCL) will be taken as given; later, the rationale for the limits and how they are set up in practice will be discussed.

There is no universal agreement on how control charts are to be used. Different companies use different rules. For example, the Ford Motor Co.[2] suggests that action is required if any of the following occur:

- 'any point outside of the control limits';
- 'a run of seven points all above or all below the central line';
- 'a run of seven intervals up or down' (*i.e.*, eight consecutive points running upwards or downwards);
- 'any other obviously non-random pattern'.

The same basic principle underlies all the rules: a system that is in statistical control should exhibit purely random behaviour—these rules correspond to improbable events on such an assumption. Accordingly, violation of one of the rules suggests that a problem has developed in the measurement system and that action is required. The rationale for the rules is discussed in the theory section below.

The measurement system to which Fig. 1 refers appears, by these rules, to be in statistical control. No points are outside the control limits and there are no long runs of points upwards of downwards or at either side of the CL.

Example 2

Fig. 2 represents 49 measurements on a water QC sample made up to contain 50 ppb of Fe. The sample was analysed by an inductively coupled plasma (ICP) spectrometer over a period of months.

The diagram in Fig. 2 shows a measurement system that is clearly out of control; in fact, two gross outliers were removed before this chart was drawn. The data were collected retrospectively from the laboratory records as a first step towards implementing a measurement-control system. They are presented here because they exhibit the classic features of an out-of-control system: several points outside the control limits, a run of points above the CL and a run of points downwards. There is an obvious need to stabilize this measurement system.

There are two ways in which control charts are used, *viz.*, for assessing the performance of a measurement system (as has been done by using Figs 1 and 2) and for maintaining the stability of a measurement system, which is their routine use once stability has been established. Where a chart is being used to control an assay we would not expect to see a pattern such as is exhibited between observations 17 and 32 of Fig. 2, where 16 points are all either on or above the CL. Use of a control chart should lead to the positive bias suggested here being corrected before such a long sequence of out-of-control points could develop.

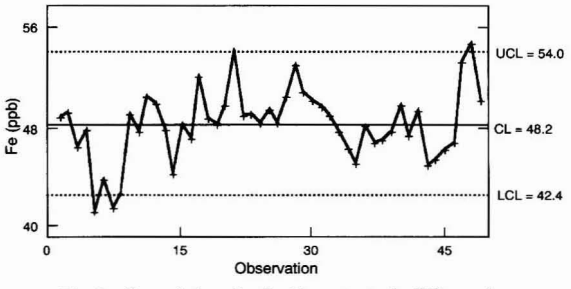

Fig. 2 Control chart for the Fe content of a QC sample

Theory Underlying the Control Limits

The CL for the control chart is taken to be the average value around which the measurements are varying. For control purposes we would like this to be the 'true value' of the control sample being measured, but in practice, we would usually take it as the average of the most recent observations considered to be 'in control' this average should preferably be based on 30 or more observations.

The control limits are usually placed three standard deviations above and below the CL (three standard errors if we are dealing with averages; see below). This choice is based on the assumption that the frequency distribution of measurement errors will follow a normal or Gaussian curve. A distribution curve can be thought of as an idealized histogram: the area under the curve between any two values on the horizontal axis yields the relative frequency with which observations occur between these two values. Hence, as shown in Fig. 3, 99.74% of the area under any normal curve lies within three standard deviations (3σ) of the long-run average (μ). The assumption of a normal distribution for measurement errors has both an empirical and theoretical basis. Experience suggests that if the same quantity is measured a large number of times and a histogram is drawn of the resulting values, a normal curve will afford a very good approximation to the histogram. It can also be shown mathematically that the cumulative effect on a system of very many small chance perturbations will be to produce a normal distribution for the measured response.

For individual measurements the control limits are:

$$\begin{aligned} \text{UCL} &= \text{CL} + 3\sigma \\ \text{LCL} &= \text{CL} - 3\sigma \end{aligned} \qquad (1)$$

where σ is the standard deviation of individual measurements.

If the point to be plotted is the average of a number of measurements, say J, then an adjustment has to be made to take account of the fact that averages, rather than individual measurements, are being plotted. Anyone who performs measurements knows (instinctively, almost) that averages are less variable than individual measurements. If individual measurements yield a frequency distribution, as shown in Fig. 3, with mean μ ('true value') and standard deviation σ, then a very large number of averages, each based on J measurements from the same measurement system, would produce a similar frequency distribution centred on μ, but the width would be defined by $\sigma/\sqrt{J}$ (now called the standard error rather than the standard deviation), *i.e.*, the distribution would be tighter and more of the values would be close to μ. This simply quantifies the extent to which averages are less variable than individual measurements.

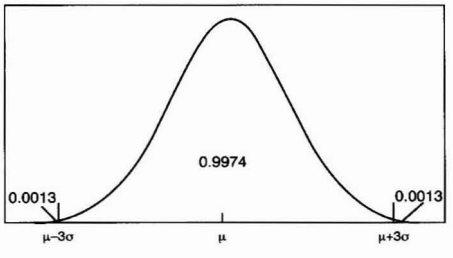

Fig. 3 Areas under the normal curve

To obtain the correct control limits when plotting averages, we simply replace σ by $\sigma/\sqrt{J}$ in the definitions given above and obtain:

$$\begin{aligned} \text{UCL} &= \text{CL} + 3\sigma/\sqrt{J} \\ \text{LCL} &= \text{CL} - 3\sigma/\sqrt{J} \end{aligned} \quad (2)$$

where σ is (as before) the standard deviation of individual measurements.

The limits described above are known as 'three sigma limits (3σ)' for obvious reasons. They were first proposed by Shewhart in the 1920s and have become the conventionally accepted rule. Their principal justification is that if the measurement system is in control, then the probability of a point going outside the control limits is very small: about 3 in 1000. Accordingly, they give very few false alarm signals. If a point does go outside the control limits it seems much more likely that a problem has arisen with the measurement system (*e.g.*, it has become biased upwards or downwards) than that the system is stable and, just by chance, the measurement errors have combined to yield a highly improbable result. This is the rationale for the first Ford rule, quoted above.

The basis for the second Ford rule (a run of seven points all above or all below the CL) is that, if the system is in control, the probability that any one measurement is above or below the CL is 1/2. Accordingly, the probability that seven in a row will be at one side of the CL is $(1/2)^7 = 1/128$; so it is 1/64 that there will be a run either above or below it. Again, such an occurrence would suggest that the measurement system has become biased upwards or downwards. The third rule (eight consecutive points running upwards or downwards) has a similar rationale: if successive measurements are varying at random about the CL, we would not expect long runs in any one direction.

The last catch-all rule (any other obviously non-random pattern) is one to be careful of: the human eye is adept at finding patterns, even in random data. The advantage of having clear-cut rules that do not allow for subjective judgement is that the same decisions will be made irrespective of who is using the chart. Having said this, if there really is 'obviously non-random' behaviour in the chart (*e.g.*, cycling of results between day and night shift, perhaps indicating a need for better temperature control of a chromatographic column) it would be foolish to ignore it.

Some writers[3,4] suggest a second set of control limits called 'warning limits' at a distance of 2σ from the CL. Two consecutive points outside the warning limits are taken as an out-of-control signal. The eight rules set out in the Appendix (based on the Western Electric[5] approach to control charts) are a more elaborate version of this proposal.

The assumption that the data follow a normal frequency distribution is more critical for charts based on individual measurements than for those based on averages. Averages tend to follow the normal distribution unless the distribution of the measurements on which they are based is quite skewed. In principle, this tendency holds when the averages are based on very large numbers of observations, but in practice samples of even four or five will often be well behaved in this regard. If there is any doubt concerning the distribution of the measurements, a normal probability plot can be used to check the assumption.[6]

Setting up Control Charts

It is clear from the foregoing that two system parameters are required for setting up a control chart: a CL that is defined by the average level of the measurements and a standard deviation that measures the variability of the measurements, and hence defines the control limits. Since the routine use of a control chart is to maintain the measurement system in statistical control, these two parameters should be determined from data that reflect the system in control.

How Many Control Samples?

The principal considerations governing the number and frequency of control samples are cost (either financial cost of analyses or, more frequently, the analyst's time) and the stability of the measurement system. If a system is very stable and not prone to going out of control, a low level of monitoring is adequate. If, one the other hand, the system is not very stable and is known to go out of control a high level of monitoring is required, if accuracy is to be assured. A general guideline on frequency would be to include at least one set of control samples with every batch of analyses and more than one set if the batch is large or the stability of the system is in any way suspect.

The larger the number of samples in the control set the more likely it is that a measurement bias, if present, will be detected. The minimum level is obviously one. Many laboratories, however, use two, which, while improving the chances of detecting bias, also provide a check on precision and on gross errors: if the two measured values are unacceptably far apart it indicates a problem with the measurement system. This can be incorporated into a control chart to monitor precision (usually a range chart; see below) or simply provide a rule that the measurements are unacceptable if more than a certain distance apart. This distance might, for example, be set at the repeatability of the measurement, *i.e.*, $2\sqrt{2\sigma^2}$, where σ is the standard deviation.

In instances where the measurement precision is poor, the final result for a product sample could be the average of a number of replicates (say J). In such circumstances it would be natural for the control set also to contain J replicates. The traditional approach in statistical process control for components is to take regular samples of J components (where J is typically 4 or 5) and plot both the average and range, thereby providing a check on the target value (average) for the quality characteristic and its variability (range). Range charts involve plotting the difference between the smallest and largest measured values in the control set; the technical basis for calculating control limits for these charts is different, but conceptually range charts are the same as, and are used in exactly the same ways as, the charts already discussed. The Analytical Methods Committee[4] (see below) provide an example where five replicates were analysed for arsenic, and both average and range charts were plotted to ensure lack of bias and good precision. Wetherill and Brown[3] provide a more technical discussion of the issues involved in deciding on number of replicate.

Calculating the Limits

The CL is the value about which the individual measurements should be varying at random. Accordingly, if we have a stable measurement system we can obtain a reasonable estimate of this by taking a series of measurements (say n, preferably 30 or more) and calculating the average:

$$\text{CL} = \bar{X} = \frac{\Sigma X_i}{n} \quad (3)$$

The method of calculating the standard deviation will depend on the way the data have been collected.

Single measurements

Where single measurements are performed the method of calculating the standard deviation is still a research question.[7,8] Two methods will be considered here. The simplest of

these involves using the usual formula for calculating a standard deviation from a sample of independent observations:

$$S = \sqrt{\frac{\Sigma(X_i - \bar{X})^2}{n-1}} \quad (4)$$

where n is the number of observations. If the number of measurements is very large we could regard our calculated value as the long-run standard deviation (σ) of the measurement system; in practice, this is rarely the case and so we replace the symbol σ by S in eqns. (1) and (2). In Example 1 the two replicates were averaged and then this method of calculating S was used, essentially treating the averages as if they were individual measurements.

An alternative approach is through using the differences between successive observations as a measure of random variation: the magnitudes of the differences between successive measurements, *i.e.*, $|X_2 - X_1|$, $|X_3 - X_2|$, *etc*, are averaged (the result is the mean of the moving ranges, $\bar{R}$), then

$$S = \frac{\bar{R}}{1.128} \quad (5)$$

is an estimate of the standard deviation (more elaborate moving-range methods and a discussion of the issues dictating a choice between them can be found in Wetherill and Brown[3]). This method was applied to the ICP data of Example 2 to produce the control chart of Fig. 2. If this method is applied to the HPLC data of Example 1, virtually the same standard deviation is obtained: $S = 0.46$ as opposed to $S = 0.50$ from eqn. (4). This is because the data are in control. The ICP data of Example 2 are not in control and would yield $S = 2.84$, by using eqn. (4), whereas $S = 1.94$ is obtained from eqn. (5). The control limits based on the larger standard deviation estimate are so wide that the large of observations (21 and 48) are within the UCL. The instability of the ICP measurement system has affected the moving-range calculation much less than the over-all estimate of standard deviation.

In each instance the control limits are

$$\bar{X} \pm 3S \quad (6)$$

Several measurements

Sometimes the points to be plotted will be averages based on several replicates. For example, the Analytical Methods Committee[4] report data referring to five replicate analyses for arsenic in a bulk reference material, in 43 successive batches each of 50 samples. In general, it would not be advisable to treat the averages of five replicates as single observations and follow the methods discussed above: this would ignore a great deal of the information in the data regarding random measurement error (there are, however, occasions when averaging is desirable; these are discussed later). Within each sub-group of size J (here, $J = 5$) an estimate of the squared standard deviation (also called the variance) can be calculated:

$$S_i^2 = \frac{\sum_{j=1}^{J} (X_{ij} - \bar{X}_i)^2}{J-1} \quad (7)$$

where X_{ij} is the j^{th} observation in sub-group i; $j = 1,2...J$, $i = 1,2...K$, *i.e.*, there are K sub-groups in all; $\bar{X}_i$ is the average result for sub-group i. These can then be averaged, and the square root yields an estimate of the standard deviation:

$$S = \sqrt{\frac{\sum_{i=1}^{K} S_i^2}{K}} \quad (8)$$

In this instance the CL is given by

$$CL = \bar{\bar{X}} = \frac{\sum_{i=1}^{K} \bar{x}_i}{K} \quad (9)$$

and the control limits by

$$UCL = CL + 3S/\sqrt{J}$$
$$LCL = CL - 3S/\sqrt{J} \quad (10)$$

as discussed in the theory section.

Data Scrutiny

The requirement that the observations used reflect a measurement system that is in control is an important one: it would be unreasonable to expect a control chart based on unstable data to maintain stability in future data! To check that the system is in control what is usually done is to calculate control limits, as described above, using all the available data, draw the control chart and apply a set of rules (such as that discussed earlier) to identify out-of-control points. When these are identified, reasons for their being out of control should be sought. If explanations are forthcoming the points should be dropped and the CL and control limits re-calculated on the basis of the remaining points. This process may have to be repeated as it can happen that points which previously appeared in control will fall outside the revised control limits when outliers are discarded. This happens because very large or very small values can inflate the standard deviation estimate and thus give wider control limits than are justified by the in-control data, and also because the CL may be biased upwards or downwards by outliers. Assuming that a computer package is available for the exploratory data analysis described above (MINITAB[9] was used here) it could well be worthwhile to use both eqns. (4) and (5) to calculate the standard deviation when analysing single observations.

Nature of Replicates

If the latter method (*i.e.*, pooling within-subgroup estimates) of calculating the standard deviation is to be applied, it is important that the replicates are full replicates, *i.e.*, each is subject in their preparation to all the possible sources of random error. This means that all the steps in the preparation of a sample for analysis must be carried out separately for each replicate. If some are carried out jointly we end up with partial replicates, and differences between their measured values will not fully represent the possible random differences that can arise between replicate analyses of the routinely analysed material that is of primary concern. An extreme example will, perhaps, make this point clearer.

Suppose the preparation and analysis of a control sample involves drying, weighing, dilution and subsequent injection on to an HPLC column and that what are considered to be two replicates simply involve two injections of a single sample prepared in this way on to the column. Clearly, the only factors that can produce differences between the measured results are those that operate from the injection stage onwards, *viz.*, injection, separation and detection. Two genuine replicates, on the other hand, not only involve differences due to all these factors, but also differences due to drying error, to weighing error and to dilution error. Accordingly, the partial replicates could seriously under-

estimate the size of the random error present in the measurement. They would, therefore, lead to control limits that are too narrow for the system being studied and result in the appearance of false alarm signals. In consequence, much analytical effort could be expended trying to bring into control a system that is already in control. This will inevitably lead to disillusionment on the part of the analysts and very likely the abandonment of the control chart; a potentially useful tool will, accordingly, be dismissed not only as useless, but as positively disruptive. Partial replicates should, therefore, not be collected for the purposes of plotting control charts. If, for other reasons, partial rather than full replicates are collected, they should be averaged and treated as individual observations for the purpose of setting up and plotting control charts.

Even where true replicates are available, care must be taken to ensure that the appropriate standard deviation is determined; what this is will depend on how the measurement will be carried out on a routine basis.

What Error is Random?

The standard deviation we calculate is intended to measure the extent of purely random error; it should not include non-random sources of variation. The distinction between these is not, however, always immediately obvious. For example, a routine purity assay in a pharmaceutical-manufacturing plant might involve two replicate control material measurements for each batch of product samples (Example 1 is a case in point). For any one batch of product, the samples will invariably be analysed by the same analyst with the same equipment. For different batches, the assay could be carried out by a single analyst with a single set of equipment, or, perhaps, several analysts and several sets of equipment could be involved.

Where only one analyst is involved we could calculate the standard deviation from the variation within the pairs of replicates [following the method described by eqns. (7) and (8)]. Ideally, we would do this in the latter case, also. However, as this calculation takes no account of the fact that several sets of equipment have been used by several analysts, any variation between instruments or between analysts will not be included in the estimate of random error (which, consequently, will be smaller than if these sources of variation had been included). Accordingly, variation between analysts or between instruments are potential assignable causes, which could lead to out-of-control signals. If the assay is under very tight control, such an approach could well be justified. In many instances, however, we will be forced, pragmatically, to accept that small differences occur both between analysts and between instruments and to regard this as part of the random variation in the measurement system. In such a case the pairs should be averaged and the standard deviation calculated by using either eqns. (4) or (5); in either instance (assuming stability is established) the calculation includes between-assay variation as part of the random error. If there is any doubt about the assay stability, eqn. (5) will be preferable, as it explicitly includes only localized between-assay variation (*i.e.*, immediate neighbours) as measuring random error.

Even where the assay is routinely performed by a single analyst using a single set of equipment there could be reasons why the within-assay variation will not form the basis for calculating the standard deviation. Suppose a batch of samples is analysed every day and the assay exhibits a certain amount of day-to-day variation (perhaps related to environmental conditions), then, again, we may decide (pragmatically) to accept this as part of the random measurement error of the system. If so, the replicates should be averaged and the standard deviations, based on the resulting values, regarded as individual observations.

Where more than two replicates are analysed and it is desired that between sub-group variation should be included in the estimate of random error, then simply averaging the results for each sub-group and treating the averages as individual observations could be a very inefficient use of the available information. A more sophisticated approach, based on a combination of variation within the sub-groups and variation between the averages, will be appropriate.[3]

Control Material

The standard material being analysed may be a certified standard reference material, a control sample made up to have certain characteristics, or a single batch of product whose 'true value' is considered known from extensive testing (the Analytical Methods Committee[4] discuss and provide examples of the important characteristics of control materials). Irrespective of the nature of the standard material it is important that it be stable, and appropriate measures should be taken to ensure that it is; any instability in the control material could otherwise be falsely attributed to the measuring system. Because of the possibility of matrix interference effects, the matrix of the standard material used for the control chart should be as close as possible to that of the material normally analysed by the measurement system. It is important, also, that the standard material be treated in exactly the same manner as routine samples. If special care is taken in the analysis of standards they will no longer be representative of routine analyses and their value will be diminished, if not entirely lost.

Testing for Bias

It is pointless asking if the measuring system is unbiased until measurement stability is established. Unless the system is in statistical control we cannot assume our next reading is going to be a good one (*i.e.*, in control) or a bad one (*i.e.*, out of control). If the system is not in control, the fact that the average of recent measurements (perhaps, the last 30) coincides with the true value is irrelevant. Accordingly, the strategy should be to achieve measurement stability first and correct bias afterwards, if necessary.

A statistical test (a Student's t-test, see, *e.g.*, Miller and Miller[10]) can be carried out to establish whether any difference between the CL and the 'true value' of the control material is consistent with random variation or whether a systematic difference is likely to be present. If a systematic difference is present, two possibilities are suggested: the control material has changed over time (or was made up incorrectly) or the measurement system is biased. If the control material is known (or at least assumed with good reasons) to be stable, an investigation of possible sources of bias is required. These will depend on the nature of the analysis, but would typically include: poorly defined standard operating procedures, differences between analysts or instruments, problems with reagents, instability of standards, and calibration problems.

Using Control Charts

Using control charts, once they are properly set up, is simply a matter of plotting the points and applying whatever set of rules has been decided on. There are, however, a few practical points worth considering.

1. Apart from acting as a working tool to monitor measurement stability, a control chart is a very useful historical record of the measurement process. As such, the more information it contains the better. A control chart should not be pretty! A pristine control chart, such as one

produced by computer, which has nothing but plotted points and control lines, is infinitely less useful than a grubby piece of paper with marks indicating, *e.g.*, changes of chromatographic column, mobile phase, new standards, problems with the automatic integrator requiring manual integration of peaks, *etc.* A very busy analyst will rarely have time to reflect on problems encountered in a particular assay; however, if the problems are noted on the chart, recurring problems will eventually be identified and action to rectify them should follow.

2. Where the control chart contains extra information, such as a code for the instrument used and for the analyst who performed the assay, it is worthwhile examining these records periodically: even if instruments or analysts give acceptably close results when the charts are first set up, it does not mean that they will continue to do so forever afterwards. If the control chart data are maintained as a computer record, as well as on the paper chart in the laboratory, it makes such retrospective investigations much easier.

3. In planning experimental studies of any kind, the standard deviation is a key parameter in determining the appropriate sample size.[11] Control charts contain all the information required for determining the standard deviation and are, therefore, a kind of laboratory database. It is important, however, to use the right control chart in any given situation.

Control charts based on a series of measurements on standard reference materials or a single batch of control material contain information on measurement error only. As such they contain the key information for planning method comparison studies or for studies on the performance of trainee analysts. They are not, however, the place to look for information on the likely variability that will be experienced in a study on the effects of a process change. A control chart based on production samples will provide us this information: it will contain batch-to-batch variability as well as measurement error.

4. If a measurement system has poor precision a control chart does not, in itself, improve this state of affairs. The poor precision will be reflected in a large standard deviation that will result in wide control limits. Provided that the system is in statistical control the routine measurements will stay within these limits and no action will be signalled. Control charts are, however, a useful starting point for any quality improvement programme that attempts to improve the precision of an assay, *i.e.*, reduce measurement error. For example, it was noted earlier that we would expect better precision, in many instances, from a single analyst using a single instrument than from multiple analysts using multiple instruments. If the last is our current regime we might wish to see what improvement could be obtained by moving to the former regime.

If we have two (or more) replicate measurements on our control samples, then from each pair we can obtain an estimate of the standard deviation being achieved by a single analyst on a single instrument at any one time and can combine all these estimates into a single pooled estimate [with use of eqns. (7) and (8)]. This estimate is what we would use in determining the repeatability of the method. As such it estimates the very best precision that is achievable under current conditions. Accordingly, it provides a benchmark against which to judge current performance. If current performance (including between-analyst and between-instrument variation) is very much worse than this, it may be possible to improve precision substantially by assigning a single analyst and/or a single instrument to this assay. Alternatively, it may be possible by careful study of the measurement process to reduce the variation between analysts and between instruments. If, on the other hand, the current standard deviation is close to that based on within-run variation, it is unlikely that the assay can be substantially improved by such studies: if better precision is required, a very detailed study of the sources of error present even for a single analyst using one set of equipment must be carried out and ways of eliminating or reducing such errors identified. Alternatively, it might be more fruitful to examine different analytical methods for the assay.

Concluding Remarks

This paper has attempted to introduce the theory and practice of control charts by focusing on just one chart; this, however, is the chart most commonly used in analytical laboratories. There are many different control charts for different purposes.[3] For example, brief reference was made to Shewhart's range chart, which can be used to monitor the precision of the measurement system if the standard control material is analysed a number of times. CUSUM (cumulative sum) charts plot the accumulated difference between a target value and the measured value; they are claimed to pick up small biases faster than the Shewhart chart described above (the Analytical Methods Committee[4] provides an example that illustrates the use of both range and CUSUM charts). Some QC activities involve monitoring many responses simultaneously: monitoring whiskey production, for example, involves the determination of more than 20 flavour compounds, ranging in magnitude from single figure to hundreds of parts per million levels. Multivariate control charts[3,6] were developed for such situations; they are, however, not widely used and are still very much a research topic. The examples provided earlier assumed a normal distribution for the measurement errors; where the procedure involves counting (*e.g.*, the membrane-filter method for measuring airborne asbestos concentrations), assuming that the data have a Poisson frequency distribution would be more appropriate in many instances, and charts based on this assumption can be constructed. The concepts underlying the use of all such charts are, however, fundamentally the same, and a thorough grasp of the foregoing material should enable the reader to evaluate their potential for use in his or her own laboratory.

APPENDIX

There are many variants on the rules used for defining out-of-control signals. An extensive set (based on that developed by Western Electric[5]) is implemented in the MINITAB statistical package.[9,12] These rules involve dividing the control chart into zones as shown below, and counting appropriate events defined in terms of these zones. The control limits, upper and lower, are labelled as the 'three sigma limits', while the zones are defined by 1 and 2 sigma lines (*i.e.*, CL ± 1 σ and CL ± 2 σ).

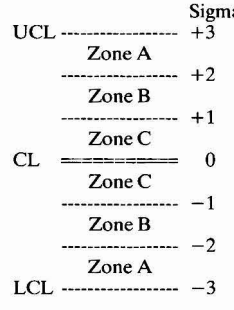

Rule 1. One point beyond zone A.

Rule 2. Nine points in a row in zone C or beyond (on one side of the CL).

Rule 3. Six points in a row, all increasing or all decreasing.

Rule 4. Fourteen points in a row, alternating up and down.

Rule 5. Two out of three points in a row in zone A or beyond.

Rule 6. Four out of five points in a row in zone B or beyond (on one side of the CL).

Rule 7. Fifteen points in a row in zone C (above and below the CL).

Rule 8. Eight points in a row beyond zone C (above and below the CL).

I am grateful to Jill Ahern, Imelda Averill, Norman Allott, John Buckley, Hazel Graham, Des McAteer, Kevin McNamara, Liam Murphy and Michael Stuart, all of whom have influenced this paper either through discussions on the use of control charts in analytical laboratories or by their suggestions and comments on an earlier draft of the paper. Any errors or obscurities are my own.

References

1 Shewhart, W. A., *Economic Control of the Quality of Manufactured Products*, Macmillan, London, 1931.
2 Ford Motor Co., *Continuing Process Control and Process Capability Improvement*, Ford Motor Co., Dearborn, MI, 1983.
3 Wetherill, G. B., and Brown, D. W., *Statistical Process Control: Theory and Practice*, Chapman and Hall, London, 1991.
4 Analytical Methods Committee, *Analyst*, 1989, **114**, 1497.
5 Western Electric Corp., *Statistical Quality Control Handbook*, AT&T Technologies, Indianapolis, IN, 1956.
6 Ryan, T. P., *Statistical Methods for Quality Improvement*, Wiley, New York, 1989.
7 Cryer, J. D., and Ryan, T. P., *J. Qual. Technol.*, 1990, **22**, 187.
8 Roes, K. C. B., Does, R. J. M., and Schurink, Y., *J. Qual. Technol.*, 1993, **25**, 188.
9 Minitab Inc., *MINITAB Statistical Software, Release 8*, Minitab, State College, PA, 1991.
10 Miller, J. C., and Miller, J. N., *Statistics for Analytical Chemistry*, Ellis Horwood, Chichester, 2nd edn., 1988.
11 Davies, O. L., ed., *The Design and Analysis of Industrial Experiments*, Longman, London, 1978.
12 Nelson, L., *J. Qual. Technol.*, 1984, **16**, 237.

Paper 3/05111k
Received August 24, 1993
Accepted October 13, 1993

Fast Atom Bombardment Mass Spectrometry of Sodium and Potassium Oxalates—Mass Spectrometric Evidence for the Existence of (Sodium–oxalate)$^-$ and (Potassium–oxalate)$^-$ Ion Pairs in Aqueous Solutions

Raj P. Singh, Ian D. Brindle,* Timothy R. B. Jones and Jack M. Miller*

Chemistry Department, Brock University, St. Catharines, Ontario, Canada L2S 3A1

Mikio Chiba

Agriculture Canada, Vineland Station, Ontario, Canada L0R 2E0

Mass spectrometric evidence for the formation of (sodium–oxalate)$^-$ ($NaC_2O_4^-$) and (potassium–oxalate)$^-$ ($KC_2O_4^-$) ion pairs in aqueous solutions of potassium oxalate and sodium oxalate was obtained by analysing different concentrations of sodium and potassium oxalates in water containing 10% glycerol. The results suggest that fast atom bombardment mass spectrometry can be used to reveal the behaviour of ionic species in aqueous solutions. The $KC_2O_4^-$ and $NaC_2O_4^-$ ion pairs form clusters with neutral molecules of potassium oxalate and sodium oxalate and glycerol. No ion pair or cluster formation was observed when dry salts (without glycerol) were analysed. This behaviour differs from what has been observed for alkali halides under similar experimental conditions.

Keywords: Mass spectrometry; fast atom bombardment; (sodium–oxalate)$^-$ ion pair; (potassium–oxalate)$^-$ ion pair

Introduction

Ion-association models are used extensively to explain the characteristics of aqueous environmental and biological solutions.[1,2] The ion-association models used for the speciation and calculation of the supersaturation index of urine for calcium oxalate phases (the principal components of kidney stones) consider ion pairing of urinary cations with oxalate. These ion pairs include (calcium–oxalate)^0 ($CaC_2O_4^0$), (magnesium–oxalate)^0 ($MgC_2O_4^0$), (proton–oxalate)$^-$ ($HC_2O_4^-$), (sodium–oxalate)$^-$ ($NaC_2O_4^-$) and (potassium–oxalate)$^-$ ($KC_2O_4^-$).[3] However, on the basis of conductivity measurements of sodium oxalate solutions, Berland *et al.*[4] assumed sodium oxalate to be a completely dissociated electrolyte.

In urine, where the sodium concentration is very high, omission of the $NaC_2O_4^-$ ion pair (if it really does exist) in the equilibrium calculations of calcium oxalate phases will result in significantly higher supersaturation values of urine with respect to calcium oxalate monohydrate and dihydrate phases than is actually the case. Correction for the existence of $KC_2O_4^-$ and $NaC_2O_4^-$ ion pairs in equilibrium calculations is therefore necessary to calculate the correct supersaturation value of urine for calcium oxalate phases that form kidney stones. Corrections for ion pairing of oxalate with sodium and potassium also need to be applied in speciation calculations for environmental waste solutions; oxalate, being an industrial pollutant and naturally occurring ligand, is ubiquitous in environmental solutions[5] along with sodium and potassium cations.

The presence of $KC_2O_4^-$ and $NaC_2O_4^-$ ion pairs in aqueous solutions containing potassium, sodium, and oxalate ions has been demonstrated by solubility,[6,7] potentiometry[8] and Raman spectroscopy.[9] Although a stability constant ($k = [NaC_2O_4^-]/[Na^+]\,[C_2O_4^-]$) of 13.2 $dm^3\ mol^{-1}$ has been reported for the $NaC_2O_4^-$ ion pair,[6] a value of 10 $dm^3\ mol^{-1}$ is typical of most (sodium/potassium–anion)$^-$ ion pairs such as $KC_2O_4^-$, KSO_4^-, $NaC_2O_4^-$ and $NaSO_4^-$. Caprioli,[10] and Johnstone and Rose[11] demonstrated that fast atom bombardment mass spectrometry (FABMS) can provide accurate knowledge of ionic equilibria existing in solutions. Caprioli[10] determined the dissociation constants of weak acids in aqueous solutions using FABMS; the results compared well with the literature values. Further, Johnstone and Rose[11] reported that FABMS can be used routinely to examine complex formation between metal cations and macrocyclic ligands in solution. In view of the controversy raised by Berland *et al.*[4] we decided to use FABMS to investigate the existence of $KC_2O_4^-$ and $NaC_2O_4^-$ ion pairs in solutions containing sodium or potassium and oxalate ions.

Experimental

Chemicals

Spectrophotometric grade glycerol was obtained from Aldrich, Milwaukee, WI, USA. Analytical-reagent grade sodium oxalate and potassium oxalate salts were obtained from BDH, Toronto, Canada.

Instrumentation and Procedures

A Concept IS double-focusing mass spectrometer with *E/B* (Electric field/magnetic field) configuration (Kratos Analytical, Urmston, Greater Manchester, UK) and fast atom bombardment source was used for mass spectrometric analyses. The instrument was controlled by a Kratos DS 90 Data General Eclipse computer system. A Kratos Mach 3 data system running on a SUN SPARC station was used for further data work-up. For all low resolution studies, a nominal resolving power of 1000 was used. High resolution analysis of potassium oxalate solution was carried out at a resolution of 7500. Iodide ion (m/z 126.9045) was used as standard. The spectrometer was fitted with an Ion Tech saddle field atom gun and xenon was used as the fast atom beam. The fast atom beam energy was 7.5 keV, and the density corresponding to an

* Authors to whom correspondence should be addressed.

emission current was about 1 mA. The source was operated at room temperature and an accelerating potential of 8 kV. The scan rate was 10 s decade^{-1}. Solutions (1 μl) of different concentrations of sodium oxalate and potassium oxalate, prepared in 10% glycerol were placed on the probe tip for determination by FABMS.

Results and Discussion

Representative fast atom bombardment mass spectra of solutions of sodium oxalate and potassium oxalate are shown in Figs. 1 and 2, respectively. The peaks due to the $NaC_2O_4^-$ (*m/z* 111) and $KC_2O_4^-$ (*m/z* 127) ion pairs are clearly seen. The base peak in all the spectra obtained for dilute solutions of potassium oxalate or sodium oxalate was due to (glycerol–H)$^-$ [(Gly–H)$^-$, *m/z* 91]. All the spectra for different concentrations of sodium oxalate or potassium oxalate in 10% glycerol and 10% pure glycerol showed a number of ions at low *m/z* (*e.g.*, *m/z* 71, 59, 45, 17). These ions are due to the gas-phase dissociation of (Gly–H)$^-$ $(Gly)_n$, n = 0–5, were also present. Both oxalate ion pairs, *i.e.*, $NaC_2O_4^-$ and $KC_2O_4^-$, formed a series of clusters with glycerol, the most intense ones being those at *m/z* 203 [$NaC_2O_4^-$(Gly)] and 219 [$KC_2O_4^-$(Gly)]. In fact, the ions at *m/z* 203 and 219 formed as a result of the association of the ion pairs $NaC_2O_4^-$ and $KC_2O_4^-$ with Gly were the most intense peaks after the base peak (*m/z* 91) in all the spectra of dilute solutions of sodium oxalate and potassium oxalate. The $NaC_2O_4^-$ and $KC_2O_4^-$ ion pairs also form series

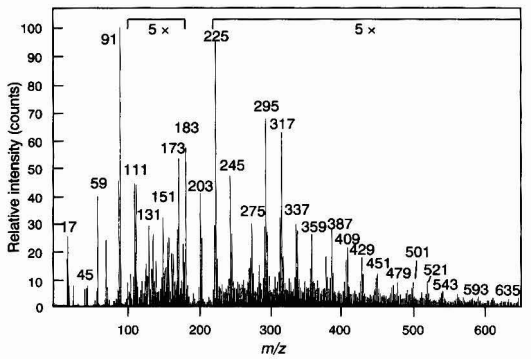

Fig. 1 Fast atom bombardment mass spectrum of 80 mmol dm^{-3} sodium oxalate in 10% glycerol. Scale magnification is indicated

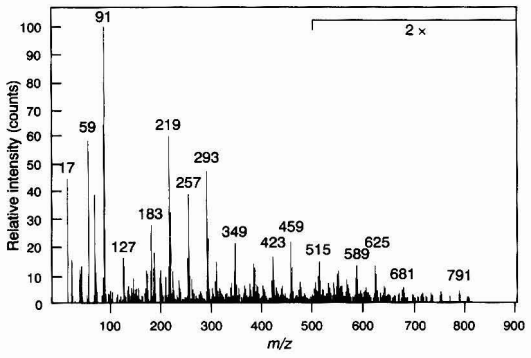

Fig. 2 Fast atom bombardment mass spectrum of 50.0 mmol dm^{-3} potassium oxalate in 10% glycerol. Scale magnification is indicated

of clusters with neutral molecules of $Na_2C_2O_4$ [$NaC_2O_4^-$ $(Na_2C_2O_4)_n$, n = 0–3; *m/z* 111, 245, 379, 513] and $K_2C_2O_4$ [$KC_2O_4^-$ $(K_2C_2O_4)_n$, n = 0–3; *m/z* 127, 293, 459, 625].

In addition to $NaC_2O_4^-$ and $KC_2O_4^-$, ion pairs such as $HC_2O_4^-$, M(Gly–2H)$^-$, M_2(Gly–3H)$^-$ (M = Na or K), and Gly(Gly–H)$^-$$(Gly)_n$, n = 0–4 are also observed in oxalate solutions. The formation of these ion pairs can be suggested on the basis of the following equilibria:

$$\text{Gly} \rightleftharpoons (\text{Gly–H})^- + \text{H}^+ \quad (1)$$

$$(\text{Gly–H})^- + \text{Na}^+ \rightleftharpoons \text{Na(Gly)–2H})^- + \text{H}^+ \quad (2)$$

$$\text{Na(Gly–2H)}^- + \text{Na}^+ \rightleftharpoons \text{Na}_2\text{(Gly–3H)}^- + \text{H}^+ \quad (3)$$

$$\text{H}^+ + \text{C}_2\text{O}_4^{2-} \rightleftharpoons \text{HC}_2\text{O}_4^- \quad (4)$$

$$\text{Gly} + (\text{Gly–H})^- \rightleftharpoons \text{Gly(Gly–H)}^- \quad (5)$$

It seems that the formation of the $HC_2O_4^-$ ion pair through pairing of H^+ with $C_2O_4^{2-}$ drives the dissociation reaction of glycerol [eqn. (1)] to the right, as the abundances of (Gly–H)$^-$ and (Gly–H)$^-$(Gly) were higher in 10% glycerol solution containing potassium oxalate and sodium oxalate than in pure 10% glycerol. All the anions and anion pairs discussed earlier formed clusters with neutral molecules of $Na_2C_2O_4$ (and $K_2C_2O_4$) and glycerol as follows: (Gly–H)$^-$$(Na_2C_2O_4)_n$, n = 0–4, *m/z* 91, 225, 359, 493, 627; Gly(Gly–H)$^-$$(Na_2C_2O_4)_n$, n = 0–3, *m/z* 183, 317, 451, 585; Na(Gly–2H)$^-$$(Na_2C_2O_4)_n$, n = 0–3, *m/z* 113, 247, 381, 515; Na_2(Gly–3H)$^-$$(Na_2C_2O_4)_n$, n = 0–2, *m/z* 135, 269, 403; $HC_2O_4^-$$(Na_2C_2O_4)_n$, n = 0–4, *m/z* 89, 223, 357, 491, 625; (Gly–H)$^-$$(Gly)_n$, n = 0–3, *m/z* 91, 183, 275, 363; Na(Gly–2H)$^-$$(Gly)_n$, n = 0–4, *m/z* 113, 205, 297, 389, 481; Na_2(Gly–3H)$^-$$(Gly)_n$, n = 0–3, *m/z* 137, 229, 321, 413; and $HC_2O_4^-$ $(Gly)_n$, n = 0–5, *m/z* 89, 181, 273, 365, 457, 549.

$NaC_2O_4^-$ also showed cluster formation with glycerol and glycerol–sodium oxalate clusters: $NaC_2O_4^-$$(Gly)_n$, n = 0–5, *m/z* 111, 203, 295, 387, 479, 571; and $NaC_2O_4^-$–Gly$(Na_2C_2O_4)_n$, n = 0–4, *m/z* 203, 337, 471, 605, 739. The following clusters were formed: $NaC_2O_4^-$–Na(Gly– 2H)$^-$$(Gly)_n$, or $Na_2C_2O_4$–(Gly–H)$^-$$(Gly)_n$, n = 0–4, *m/z* 225, 317, 409, 501, 593; and $HC_2O_4^-$$(GlyNa_2C_2O_4)_n$, n = 0–4, *m/z* 89, 181, 315, 449, 583. Analogous cluster formation was observed for potassium oxalate solutions (Fig. 2).

There are two possible mechanisms by which ion pair and ion cluster formation can occur in solution during FABMS. By mechanism **1**, the ions and ion clusters form by recombination of ions and neutral molecules in the gas phase. In mechanism **2** it is assumed that the ions and ion clusters determined by FABMS are already present in solution. In the latter instance, the results should indicate similarities with the ionic equilibria occurring in liquid solutions. These mechanisms for the formation of ions and ion clusters by FABMS have been debated by many researchers.[12] In order to investigate whether the results obtained by FABMS, which relate to the distribution of ions in the gas phase, closely resemble those of ionic equilibria in the liquid phase (*i.e.*, sodium and potassium oxalate solutions in 10% glycerol), we analysed sodium oxalate and potassium oxalate solutions at different concentrations using FABMS.

The results for the analyses of $Na_2C_2O_4$ and $K_2C_2O_4$ solutions seem to indicate that the abundances of ion clusters and ion pairs determined by FABMS are closely related to possible solution equilibria. At low concentrations of potassium oxalate (*e.g.* 1.0 mmol dm^{-3}) there was no evidence of significant amounts of the $KC_2O_4^-$ ion pair or its clusters. This can be explained on the basis of equilibrium calculations for 1.0 mmol dm^{-3} potassium oxalate solution. Assuming a stability constant of 10.0 dm^3 mol^{-1} for $KC_2O_4^-$, we estimated that in 1.0 mmol dm^{-3} potassium oxalate solution, the concentration of the $KC_2O_4^-$ ion pair would be too small, *i.e.*, <0.01 mmol dm^{-3}, to be determined by FABMS. We can argue here that if ion pair formation was taking place in the gas

phase, we would have detected the $KC_2O_4^-$ ion pair in 1.0 mmol dm^{-3} potassium oxalate solution because the concentration of desorbed K^+ and $C_2O_4^{2-}$ ions should have been sufficiently high in the gas phase to form a $KC_2O_4^-$ ion pair.

For 10.0, 20.0, 40.0, 50.0, and 80.0 mmol dm^{-3} concentrations of potassium oxalate and/or sodium oxalate, the concentrations of the $KC_2O_4^-$ or $NaC_2O_4^-$ ion pairs were estimated to be 0.5, 1.5, 4.5, 6.4, and 13.3 mmol dm^{-3}, respectively. Therefore, in $Na_2C_2O_4$ and $K_2C_2O_4$ solutions $\geq$10.0 mmol dm^{-3} (containing approximately 0.5 mmol dm^{-3} of ion pairs), $KC_2O_4^-$ or $NaC_2O_4^-$ ion pairs and their clusters should be detected in the corresponding mass spectra. Indeed, as the spectra of all potassium oxalate and sodium oxalate solutions of concentrations $\geq$10.0 mmol dm^{-3} showed significant abundances of $KC_2O_4^-$ or $NaC_2O_4^-$ ion pairs and their clusters.

Fig. 3 shows the mass spectrum of 10.0 mmol dm^{-3} potassium oxalate with a small peak due to the $KC_2O_4^-$ ion pair at *m/z* 127 and to that of its cluster with $K_2C_2O_4$ at *m/z* 293. Of the peaks that were derived from the $KC_2O_4^-$ ion pair in potassium oxalate solution, the most intense was that of the $KC_2O_4^-$(Gly) cluster at *m/z* 219. This peak was not present in the mass spectrum of 1.0 mmol dm^{-3} potassium oxalate solution in 10% glycerol. In fact, the peaks of ion clusters $NaC_2O_4^-$(Gly) and $KC_2O_4^-$(Gly) at *m/z* 203 and 219, respectively, for solutions of $Na_2C_2O_4$ and $K_2C_2O_4$ in glycerol can be regarded as confirmatory peaks for the formation of $NaC_2O_4^-$ and $KC_2O_4^-$ ion pairs as their intensities are much higher than those of the peaks of other clusters containing sodium oxalate and potassium oxalate ion pairs. The abundances of the $NaC_2O_4^-$ $(Na_2C_2O_4)_n$ and $KC_2O_4^-$ $(K_2C_2O_4)_n$, clusters were very much dependent on the concentration of ion pairs in solution. For example, at 10.0 and 20.0 mmol dm^{-3}, the concentration of $KC_2O_4^-$ or $NaC_2O_4^-$ ion pairs was not sufficient for the formation of clusters with neutral molecules of sodium oxalate and potassium oxalate. However, as the concentrations of the $NaC_2O_4^-$ and $KC_2O_4^-$ ion pairs increased in solution, the abundances of $NaC_2O_4^-$ $(Na_2C_2O_4)_n$ and $KC_2O_4^-$ $(K_2C_2O_4)_n$ ion clusters increased (Figs. 4 and 5). These results suggest that the abundances of $NaC_2O_4^-$ and $KC_2O_4^-$ ion pairs and their clusters are closely related to their concentrations in solution.

Fig. 6 shows the relative abundances of Na(Gly–2H)$^-$, Na_2(Gly–3H)$^-$ $HC_2O_4^-$, and $NaC_2O_4^-$ ion pairs as functions of sodium oxalate concentration. The increase in the relative abundances of these ion pairs with increasing sodium oxalate concentration in sodium oxalate–10% glycerol solutions is expected on the basis of solution equilibria eqns. (1)–(4). This again suggests that results obtained by FABMS are representative of solution equilibria occurring in sodium oxalate–10% glycerol solutions. In Fig. 6 the relative abundances of the $HC_2O_4^-$ ion pair are much higher than the relative abundances of the Na(Gly–2H)$^-$, Na_2(Gly–3H)$^-$, and $NaC_2O_4^-$ ion pairs. This can be explained on the basis of the larger stability constant of the $HC_2O_4^-$ ion pair, estimated to be 15 000 dm^3 mol^{-1}, compared with that of the $NaC_2O_4^-$ ion pair (approximately 10 dm^3 mol^{-1}). The stability constants of

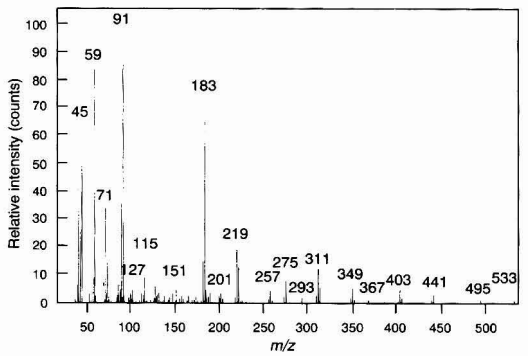

Fig. 3 Fast atom bombardment mass spectrum of 10.0 mmol dm^{-3} potassium oxalate in 10% glycerol

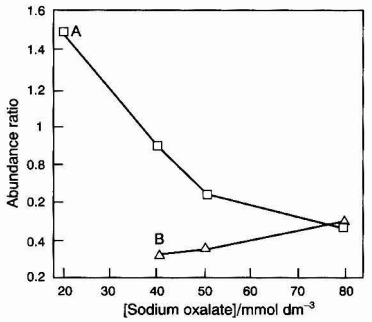

Fig. 4 Plot of the ratios of relative abundances for A, $NaC_2O_4^-$ (*m/z* 111) and $NaC_2O_4^-(Na_2C_2O_4)$ (*m/z* = 245), and B, $NaC_2O_4^-(Na_2C_2O_4)_2$ (*m/z* 379) and $NaC_2O_4^-$ $(Na_2C_2O_4)$ against the sodium oxalate concentration in 10% glycerol

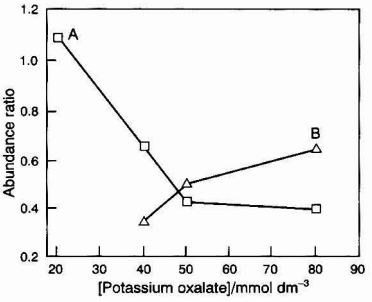

Fig. 5 Plot of the ratios of relative abundances for A, $KC_2O_4^-$ (*m/z* 127) and $KC_2O_4^-(K_2C_2O_4)$ (*m/z* = 293), and B, $KC_2O_4^-$ $(K_2C_2O_4)_2$ (*m/z* 459) and $KC_2O_4^-(K_2C_2O_4)$ against the potassium oxalate concentration in 10% glycerol

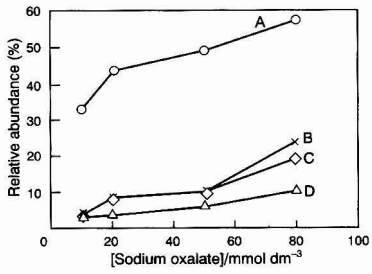

Fig. 6 Relative abundances of A, $HC_2O_4^-$ (*m/z* 89), B, Na(Gly–2H)$^-$ (*m/z* 113), C, $NaC_2O_4^-$ (*m/z* 111), and D, Na_2(Gly–3H)$^-$ (*m/z* 135) ion pairs as functions of sodium oxalate concentration in 10% glycerol

the NaGly–2H)$^-$ and Na_2(Gly–3H)$^-$ ion pairs are not known. As expected, the relative abundances of the clusters of all these ion pairs with glycerol and sodium oxalate increased with increasing sodium oxalate concentration.

The relative abundances of glycerol clusters with the sodium oxalate ion pair (*i.e.*, $NaC_2O_4^-(Gly)_n$ also increased with increasing sodium oxalate concentration, especially in dilute solutions as shown in Fig. 7. Fig. 8 shows the relative abundances of (Gly–H)$^-$ ions and its ion clusters with glycerol and $Na_2C_2O_4$. The (Gly H)$^-$ peak (A) was the base peak in all the spectra of sodium and potassium oxalate solutions up to 80 mmol dm^{-3}, despite strong binding with $Na_2C_2O_4$ (or $K_2C_2O_4$) molecules to form the (Gly–H)$^-Na_2C_2O_4$ cluster (D) at *m/z* 225, the relative abundance of which increased with increasing $Na_2C_2O_4$ concentration. The high abundance of (Gly–H)$^-$ obtained by FABMS can be explained on the basis of equilibria equations (1) and (4). The relative abundance of the (Gly–H)$^-$Gly cluster (B) at *m/z* 183, however, decreased sharply as the concentration of sodium oxalate increased from 10 to 80 mmol dm^{-3}. Perhaps the formation of the (Gly–H)$^-$Gly–$Na_2C_2O_4$ cluster (E) at *m/z* 317, the relative abundance of which increased with increasing sodium oxalate concentration, caused the decrease in the abundance of (Gly–H)$^-$Gly. The relative abundances of $Na_2C_2O_4$–(Gly–H)$^-(Gly)_n$ (n = 0–4; *m/z* 225, 317, 409, 501) also increased with increasing sodium oxalate concentration (Fig. 8).

In the mass spectrum of a solution containing a very high concentration of potassium oxalate (10% glycerol saturated with potassium oxalate), (Gly–H)$^-$ was no longer the base peak. The relative abundance of all glycerol-containing ion pairs and clusters was substantially lower in this spectrum, as shown in Fig. 9. The gas-phase ions of glycerol and clusters of $NaC_2O_4^-(Na_2C_2O_4)_n$ were relatively more abundant.

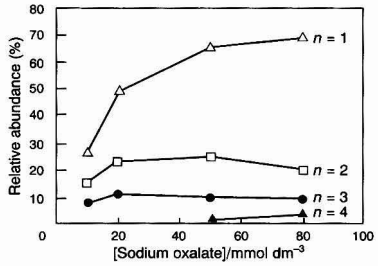

Fig. 7 Relative abundances of glycerol clusters with the sodium oxalate ion pair [*i.e.*, $NaC_2O_4^-(Gly)_n$ (n = 1–4; *m/z* 203, 295, 387, and 479)] as functions of sodium oxalate concentration in 10% glycerol

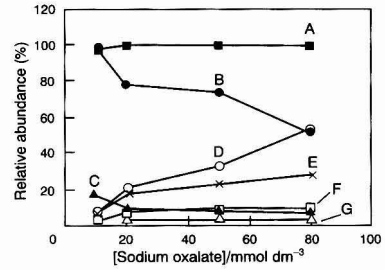

Fig. 8 Relative abundances of (Gly–H)$^-$ ions and its ion clusters with glycerol and $Na_2C_2O_4$ [*i.e.*, (Gly–H)$^-(Gly)_n$ (n = 0–2; *m/z* A, 91, B, 183, and C 275), and $Na_2C_2O_4^-$(Gly–H)$^-(Gly)_n$ (n = 0–4; *m/z* D, 225, E, 317, F, 409, and G, 501] as functions of sodium oxalate concentration in 10% glycerol

The mass spectrum of a solution containing 40.0 mmol dm^{-3} each of sodium sulfate and potassium oxalate (Fig. 10) indicates the presence of $NaSO_4^-$ (*m/z* 119) and KSO_4^- (*m/z* 135) ion pairs in addition to $NaC_2O_4^-$ (*m/z* 111) and $KC_2O_4^-$ (*m/z* 127) ion pairs. The relative abundances of the $NaSO_4^-$ and KSO_4^- ion pairs are similar to those of the $NaC_2O_4^-$ and $KC_2O_4^-$ ion pairs, this result was expected on the basis of the similar stability constants of these ion pairs. The peak due to the $KC_2O_4^-$ ion pair was mixed with a glycerol (matrix) peak of similar mass and hence appears to be larger than the KSO_4^- ion pair peak. Investigation of mixed solutions of potassium sulfate and potassium oxalate by high resolution FABMS confirmed that the relative abundance of the $KC_2O_4^-$ ion pair is similar to that of the KSO_4^- ion pair. These results suggest that the abundances of various ion pairs and ion pair clusters determined by FABMS in mixed solutions of sodium sulfate and potassium oxalate are closely related to the corresponding concentrations in solution.

Analysis by FABMS of solid potassium oxalate (without glycerol) did not indicate ion pair or ion pair cluster formation. This suggested that the $KC_2O_4^-$ ion pair and its clusters, determined in solutions, were not desorbed from the sputtered solid. It seems that mass spectrometric results for potassium oxalate and sodium oxalate show different behaviour than those obtained in analyses of alkali halides by FABMS.[12,13] In the study of alkali halides by FABMS, very

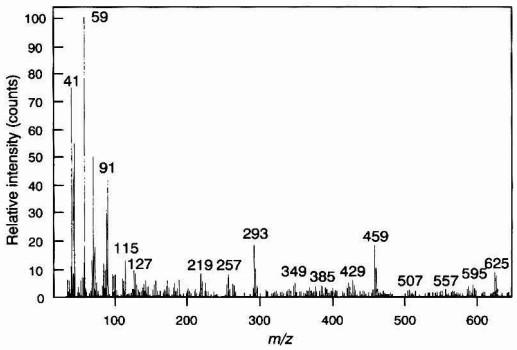

Fig. 9 Fast atom bombardment mass spectra of 10% glycerol saturated with potassium oxalate

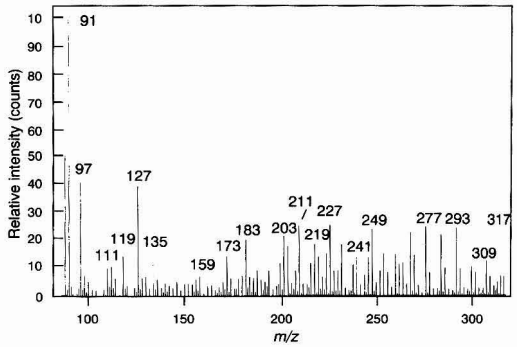

Fig. 10 Fast atom bombardment mass spectra of a mixture of 40.0 mmol dm^{-3} each of potassium oxalate and sodium sulfate in 10% glycerol

similar cluster formation was observed both from the sputtered solid and from solutions.

Although the results of the low-resolution analyses by FABMS of potassium oxalate or sodium oxalate solutions and mixed solutions of sodium sulfate and potassium oxalate, reported here are consistent with the formation of $NaC_2O_4^-$ and $KC_2O_4^-$ ion pairs, the presence of some of these ion pairs was confirmed by high-resolution analysis. Analysis of an 80.0 mmol dm^{-3} solution of potassium by high-resolution FABMS using I^- (*m/z* 126.9045) as standard, confirmed the presence of $KC_2O_4^-$ ions at *m/z* 126.9383 (calculated mass = 126.9434). The presence of $NaC_2O_4^-$, $HC_2O_4^-$, $NaSO_4^-$, and KSO_4^- ion pairs was also confirmed by high-resolution FABMS.

In conclusion, the results reported here have provided fast atom bombardment mass spectrometric evidence for the existence of $NaC_2O_4^-$ and $KC_2O_4^-$ ion pairs in solutions containing sodium, potassium, and oxalate ions. This contrasts with the assumption of Berland *et al.*[4] that sodium oxalate is a completely dissociated electrolyte. The results are consistent with those of the analysis by FABMS carried out by Caprioli,[10] and Johnstone and Rose,[11] who demonstrated that FABMS can reveal the existence of ionic equilibria in solutions.

We thank the NSERC for financial support in providing equipment grants for the purchase of the Kratos Concept IS double-focusing mass spectrometer. The authors also thank the Ontario Ministry of Environment and Energy for funding this project (Grant No. 1384).

References

1 Sposito, G., *Soil Sci. Soc. Am. J.*, 1984, **48**, 531.
2 Werness, P. G., Brown, C. M., Smith, L. H., and Finlayson, B., *J. Urol.*, 1985, **134**, 1242.
3 Singh, R. P., Gaur, S. S., Sheehan, M. E., and Nanacollas, G. H., *J. Crystal Growth*, 1988, **87**, 318.
4 Berland, Y., Olmer, M., Gandvuillemin, M., Lundager-Madsen, H. E., and Boistelle, R., *J. Crystal Growth*, 1988, **87**, 494.
5 Mesuere, K., and Fish, W., *Environ. Sci. Technol.*, 1992, **26**, 2357.
6 Singh, R. P., *Bull. Chem. Soc. Jpn.*, 1989, **52**, 2205.
7 Finlayson, B., and Roth, R. A., *Urology*, 1973, **1**, 142.
8 Daniele, P. G., Rigano, C., and Sammartano, S., *Thermochim. Acta*, 1981, **46**, 103.
9 Kanamori, K., Mihara M., and Kawai, K., *Bull. Chem. Soc. Jpn.*, 1979, **52**, 2205.
10 Caprioli, R. M., *Anal. Chem.*, 1983, **55**, 2387.
11 Johnstone, R. A. W., and Rose, M. E., *J. Chem. Soc., Chem. Commun.*, 1983, 1268.
12 Sunner, J., *J. Am. Soc. Mass Spectrom.*, 1993, **4**, 410.
13 Miller, J. M., and Theberge, R., *Org. Mass Spectrom.*, 1985, **20**, 600.

Paper 3/05151J
Received August 26, 1993
Accepted September 24, 1993

Interlaboratory Comparison of Instruments Used for the Determination of Elements in Acid Digestates of Solids

David Eugene Kimbrough and Janice Wakakuwa

California Environmental Protection Agency, Department of Toxic Substances Control, Southern California Laboratory, 1449 W. Temple Street, Los Angeles, CA 90026-5698, USA

This paper presents data from an interlaboratory study involving 160 accredited hazardous materials laboratories; the accuracy and precision of four different analytical techniques, inductively coupled plasma atomic emission spectrometry (ICP-AES) and inductively coupled plasma mass spectrometry, flame atomic absorption spectrometry, electrothermal atomic absorption spectrometry, and hydride generation atomic absorption spectrometry (HGAAS) are compared. Each laboratory performed a mineral acid digestion on five soils spiked with different concentrations of arsenic, cadmium, molybdenum, selenium and thallium. The resulting digestates were analysed on one of the instruments under investigation. The results show that at most concentrations ICP-AES has significantly higher precision and accuracy than the other techniques, but also the highest rates of false positives and negatives. Consistently, HGAAS provided the lowest precision and accuracy.

Keywords: *Inductively coupled plasma atomic emission spectrometry; electrothermal atomic absorption spectrometry; flame atomic absorption spectrometry; hydride generation atomic absorption spectrometry; acid digestate*

Introduction

One of the most commonly requested analyses in environmental chemistry is the analysis of solids for 'metals'. The term 'metal' usually refers to any regulated element such as chromium, lead, or arsenic, whether or not it is technically classified as a metal. In this paper, the term element is used in place of 'metal'.

There are a large number of possible objectives for this type of analysis, including verification that a material is legally defined as 'hazardous waste.' The term 'solids' covers an extremely wide range of matrices, soils, sludges, sediments, mine tailings, mill tailings, industrial wastes, press cakes, slags, tank bottoms, clarifier bottoms, *etc.* Likewise, the range of concentrations extends from tens of per cent to parts per billion.[1] The most commonly used procedure for this analysis is to solubilize the elements in question using an acid digestion procedure, and analyse the resulting liquid digestate in either an atomic absorption or atomic emission instrument.

The range of techniques used includes inductively coupled plasma atomic emission spectrometry (ICP-AES), flame atomic absorption spectrometry (FAAS), and electrothermal atomic absorption spectrometry (ETAAS). In the USA, these are the only analytical methods approved by the Federal Environmental Protection Agency (USEPA) for solids analysis in Manual SW846.[2] Inductively coupled plasma mass spectrometry (ICP-MS) is approved in draft form. Informally, hydride generation atomic absorption spectrometry (HGAAS) techniques are also used. The corresponding instruments are generally treated as being equivalent for the purposes of determining elements in solids. However, data from these instruments have only been compared at trace-level concentrations in aqueous matrices. Data at concentrations of regulatory interest in solids have not been reviewed for instrumental bias.

This paper examines the applicability of these analytical instruments to the analysis of acid digestates of solid materials based on how they perform in real-sample analysis. It draws on the data accumulated from 160 environmental laboratories accredited by the State of California to analyse solids for 'toxic metals' (certificates refer to these laboratories as 'hazardous materials laboratories').

In this work, these same USEPA-approved analytical techniques were used to analyse five soils spiked with five regulated toxic elements, arsenic, cadmium, molybdenum, selenium and thallium. The range of concentrations covered four orders of magnitude.

Regulatory Background

Under Federal[3] and Californian law[4] a material is considered hazardous if it exhibits the 'characteristic of toxicity'. Under Federal law this characteristic is determined by an acetic acid leaching procedure [known as the Toxicity Characterization Leaching Procedure (TCLP), Method 1311 in SW 846[2]]. The resulting leachate is then analysed by the methods described earlier. If any of the seven listed toxic elements leach out of a solid at concentrations greater than regulatory limits, then the material is legally classified as 'hazardous'. As this procedure is extremely complicated and expensive to run, it is common practice to analyse for the total concentration of these elements first. Method 3050,[2] a mineral acid digestion procedure, is usually the method of choice.

Under Californian law there are seven tests for the characteristic of toxicity, one of which is the total concentration of 17 toxic elements, as determined by Method 3050.[2] Another of the methods is the TCLP. The third is a citric acid leaching test known as the Waste Extraction Test (WET). In each instance, the digestates or leachates are analysed using the analytical techniques described earlier.

Therefore there are regulatory and scientific implications to the choice of instrumentation for the analysis of solids. The State of California has an interest in ensuring that laboratories analysing solids for regulated elements perform an adequate job. Perhaps the most crucial reason is for comparability of data. It is essential for legal and scientific reasons to have methods that produce comparable results so that any number of laboratories can analyse the same material and agree on its composition.

Experimental

Experimental Design

A set of five soil samples were prepared. The samples were spiked with five water-soluble salts of arsenic, cadmium, molybdenum, selenium and thallium. The goal was for each sample to have four different concentrations of spiked analytes and less than 1 mg kg^{-1} of the fifth analyte. This was not true for arsenic, which had a natural background value of 5 mg kg^{-1}, a typical value for Californian soils.[5] Hence each element would be determined over a range of four orders of magnitude along with a 'blank' sample (see Table 1).

The soil was then validated both in-house and by 23 reference laboratories that used a wider variety of analytical techniques than EPA SW 846 allows. (A more complete discussion of these steps is provided in refs. 6 and 7.) The samples were then distributed among the accredited hazardous materials laboratories where they were digested and analysed; the results were returned.

Analytical Methods

The accredited laboratories used two acid digestions, SW 846 Method 3050 and draft Method 3055, which for the elements studied yield equivalent results.[8,9] Method 3050 involves the repeated digestion of sample (2.0 g), first with nitric acid and then with hydrogen peroxide to destroy the matrix. Hydrochloric acid is added after the digestion and the digestate is refluxed to solubilize certain elements if ICP-AES or FAAS is being used. If ETAAS is to be used, then no HCl is added. Either way, the sample is made up to a 100 ml final volume. If HGAAS is to be used, 50 ml of the digestate must be redigested. Concentrated nitric acid (10 ml) and sulfuric acid (12 ml, 9 mol l^{-1}) are added. The digestate is then evaporated until white fumes are observed (SO_3, about 20 ml). Analytical-reagent grade water (20 ml) is added and the evaporation is repeated to drive off oxides of nitrogen. The mixture is allowed to cool and 40 ml of concentrated HCl are added to a final volume of 100 ml. Method 3055 is an *aqua regia* method suitable only for ICP-AES and FAAS; only a few laboratories used this method.

Instrumentation methods include EPA SW 846 Methods 6010 (for ICP-AES), 6020 (for ICP-MS), 7060 (arsenic by ETAAS), 7061 (arsenic by HGAAS, zinc slurry), 7130 (cadmium by FAAS), 7131 (cadmium by ETAAS), 7480 (molybdenum by FAAS), 7481 (molybdenum by ETAAS), 7740 (selenium by ETAAS), 7741 (selenium by HGAAS, zinc slurry), 7840 (thallium by FAAS), and 7841 (thallium by ETAAS). A few laboratories used FAAS for arsenic and selenium. The reference laboratories used either these methods or very similar ones. For comparison, energy dispersive X-ray fluorescence spectroscopy (EDXRF) was also used. The samples were ground to pass through a US Standard Sieve No. 200 for this analysis.

False Positives and Negatives

A false positive is a result that reports the presence of an analyte in a sample above the reporting limit when, in fact, the concentration of the analyte is below the reporting limit. For example, if for a sample containing less than 1.0 mg kg^{-1} of thallium the laboratory reports 10 mg kg^{-1}, this is a false positive. If the laboratory reported 0.01 mg kg^{-1} of thallium, it would not be a false positive as 0.01 is less than 1. In this work there is no way of verifying if the reported value of 0.01 mg kg^{-1} is either qualitatively true or quantitatively accurate, but the validated value of less than 1.0 mg kg^{-1} is not contradicted. In Tables 3–6, results from the unspiked samples are included to measure the false positive rates. These soils may have small amounts of these elements, but the concentrations are well below 1.0 mg kg^{-1}.

False negatives are the results where an analyte is present in a sample and reported at a value 'less than' the spiked value. For example, if a sample containing 5 mg kg^{-1} of cadmium was reported as containing 'less that 1 mg kg^{-1}', by a laboratory, it would be considered a false negative. A laboratory report for this sample of 'less than 10 mg kg^{-1}' (10 mg kg^{-1}>) would not be a false negative, as there is, in fact, less than 10 mg kg^{-1} of cadmium. For a more thorough discussion of these definitions of false positives and negatives see ref. 10.

Results

Table 1 shows the final concentrations of the samples and the over-all results for each sample: results that were more than ten times the spiked value or less than one tenth the spiked value were excluded from the calculations. Not all of the laboratories determined all the five elements. Tables 2–6 list the mean values, standard deviations (s), relative standard deviations (s_r), number of results (n), number of results 'less than' the reporting limits (RL>), and number of false negatives (FNs), and false positives (FPs) for each instrument type for each sample and analyte.

Only four data points were excluded from the calculations for Tables 2–6. Two results for arsenic by ETAAS were so wildly high that their inclusion in calculating the result would have presented an unrealistic picture of ETAAS performance (see Table 2). The two ICP data points removed for molybdenum (see Table 4) were obtained in the same laboratory. Sequential, simultaneous and mass spectrometer ICPs are combined in the ICP category; ICP-MS data are also reported separately (Table 4). Only two laboratories reported ICP-MS data, so in the three instances where there were significant differences between the two sets of results, the more accurate result is reported in parentheses (Tables 2 and 4). The results for EDXRF are also shown for comparison. Table 7 shows the results from the laboratories that used

Table 1 Over-all results for each element using all the studied methods

Analyte	Sample	Spiked value/ mg kg^{-1}	Mean value/ mg kg^{-1}	Standard deviation/ mg kg^{-1}	Number of results
As*	A	4000	4080	1000	118
	B	500	484	388	121
	C	55	58.4	52.3	117
	D	10	12.2	14.2	107
	E	5	4.30	4.3	87
Cd	E	5000	4930	833	127
	A	500	509	157	126
	B	50	50.7	12.1	126
	C	5.0	6.15	2.35	126
Mo	D	5000	4490	1120	118
	E	500	460	174	121
	A	30	40.3	20.0	119
	B	5	7.89	7.19	96
Se	C	5000	4710	1320	115
	D	500	446	199	118
	E	50	52.7	55.8	116
	A	5	5.28	7.18	89
Tl	B	4400	4140	953	121
	C	500	456	113	121
	D	50	58.7	59.2	121
	E	5	8.86	8.06	85

* For arsenic, the 'spiked value' represents the amount spiked plus the amount of arsenic in the native soil (5 mg kg^{-1}). None of the other elements are present in native soil at concentrations above 1 mg kg^{-1}.

HGAAS for all of the arsenic samples (some laboratories used HGAAS for only the lower concentration samples).

Discussion

The results that are presented here represent how the various types of instrument perform under the normal situations of actual environmental laboratory conditions. What is not shown is that there were laboratories using each of these instrument types that produced accurate results. Any of these instrument types can be used to generate accurate and reproducible elemental analyses of acid digestates of solids given the proper conditions. What the results of this study show is how difficult it is to achieve those conditions under routine situations for each instrument type. Put another way, the results here can measure the robustness of the instrument.

One measure of the robustness of an instrument is the standard deviation. The higher the standard deviation is, the greater are the differences between laboratories analysing the same homogeneous material. The bias in the mean result gives an indication of what types of error are being made. Two types of error were made in this study, qualitative and quantitative. Qualitative errors are false positives and negatives, *i.e.*, a misidentification of the presence or absence of an element. These values are given in Tables 2–6 and do not show up in the mean values. Quantitative errors are those where the element is correctly identified as being present, but the concentration is incorrectly quantified. These are represented by the bias in the mean.

The most obvious trend in the data is that instrument performance is concentration dependent; some instrument types perform better at different concentrations. There are several reasons why this should be expected. One is that there is an extremely wide range of linear dynamic ranges. The atomic absorbance technologies tend to have linear dynamic ranges of 1–2 orders of magnitude, whereas the emission technologies have linear dynamic ranges of 4–6 orders of magnitude. Not only are some linear dynamic ranges wider than others, but they also cover very different concentration ranges.

The instruments used in ETAAS and HGAAS are very sensitive, with low and narrow linear dynamic ranges [low ng ml^{-1} (ppb) range]. Flame atomic absorption spectrometry has a linear dynamic range of comparable width to those of HGAAS and ETAAS, but at considerably higher concentrations [low mg ml^{-1} (ppm) range]. Three laboratories performed no dilutions on any of the digestates for analysis by ETAAS and reported the results directly from the instrument. When this occurred, all the spiked samples were reported with the same results. These analysts had no working concept of linear dynamic range.

Samples with high concentrations of analyte require large dilutions to bring them within the linear dynamic range, and these are always sources of error. For example, in order to analyse sample A for arsenic by ETAAS using Method 3050, one would digest 2 g of sample and make the digestate up to 100 ml. This would produce an arsenic concentration of 80 mg l^{-1}. A typical linear dynamic range for ETAAS is from 1 to 40 ng ml^{-1} so that at least a 1 + 1999 and up to as much as a 1 + 9999 dilution is needed.

Generally, ETAAS and HGAAS provided more accurate and reproducible results at lower concentrations than at higher concentrations. The ICPs consistently provided the most precise results for the highest concentration samples. They were also generally more accurate at the higher

Table 2 Arsenic results by technique

Sample	Parameter*	ICP	ICP-MS	FAAS	ETAAS	HGAAS	EDXRF
A	Mean	4250	63690 (4380)†	4240	4430	3650	4920
	s	757	2340	363	5430	2150	—
	s_r	18	44	8.5	122	59	—
	n	46	2	7	54	15	1
	RL>	0	0	0	0	0	0
	FN	0	0	0	0	0	0
B	Mean	472	425	462	483	438	565
	s	87	21.2	76.5	580	178	—
	s_r	18	5.0	17	120	41	—
	n	46	2	6	54	16	1
	RL>	0	0	0	0	0	0
	FN	0	0	0	0	0	0
C	Mean	60.8	42.5	49.9	55.2	45.1	50>
	s	51.2	34.7	10.6	61.5	34.3	—
	s_r	84	82	21	111	76	—
	n	43	2	5	55	16	0
	RL>	1	0	0	0	0	1
	FN	1	0	0	0	0	1
D	Mean	28.8	9.44	14.4	9.30	5.50	50>
	s	49.0	—	14.1	8.45	3.83	—
	s_r	170	—	98	93.9	69.6	—
	n	29	1	4	61	16	0
	RL>	6	1	0	2	5	1
	FN	5	1	0	2	3	0
E	Mean	39.4	4.57	8.26	3.56‡	7.62	50>
	s	68.1	2.22	9.13	3.05	19.7	—
	s_r	174	49	111	86	258	—
	n	18	2	3	56	15	0
	RL>	13	0	1	9	3	1
	FN	9	0	0	7	3	0

* Mean is in units of mg kg^{-1}; *s* = standard deviation (mg kg^{-1}); s_r = per cent relative standard deviation (mg kg^{-1}); *n* = number of results; RL> = number of results less than the reporting limit; and FN = false negative.

† One of the two ICP-MS results was very inaccurate, the result in parentheses is the more accurate one.

‡ Two results were removed, 814 and 160 mg kg^{-1} from two different laboratories.

concentrations, but less dramatically so. This is partly because no dilutions were needed to analyse even the samples with the highest concentrations.

Another factor that influenced the concentration-dependent performance of the instruments was the presence of interferents. Generally, emission technologies are more subject to inter-element interferences, both positive and negative. Interferents have the largest impact at lower concentrations where the signal from the analyte is comparable to the signal from the interferent. This is especially true

Table 3 Cadmium results by technique

Sample	Parameter*	ICP	ICP-MS	FAAS	ETAAS	EDXRF
E	Mean	4840	5170	4780	3890	5300
	s	787	226	1680	1940	—
	s_r	16.3	4.4	35.2	49.9	—
	n	83	2	36	5	1
	RL>	0	0	0	0	0
	FN	0	0	0	0	0
A	Mean	490	522	553	496	538
	s	61.1	12.0	272	136	—
	s_r	12.5	2.31	49.1	27.5	—
	n	82	2	37	5	1
	RL>	0	0	0	0	0
	FN	0	0	0	0	0
B	Mean	50.7	51.0	49.7	40.9	58
	s	14.2	3.89	10.9	19.0	—
	s_r	28.0	7.6	22.0	46.3	—
	n	83	2	36	5	1
	RL>	0	0	0	0	0
	FN	0	0	0	0	0
C	Mean	6.00	5.75	6.46	6.50	6
	s	2.26	0.35	1.54	5.27	—
	s_r	37.7	6.0	23.7	81.1	—
	n	80	2	35	8	1
	RL>	1	0	0	0	0
	FN	1	0	0	0	0
D	RL>	46	1	20	10	1
	FP	34	1	12	2	0

* Mean is in units of mg kg^{-1}; *s* = standard deviation (mg kg^{-1}); s_r = per cent relative standard deviation (mg kg^{-1}); *n* = number of results; RL> = number of results less than the reporting limit; FN = false negative; and FP = false positive.

Table 4 Molybdenum results by technique

Sample	Parameter*	ICP	ICP-MS	FAAS	ETAAS	EDXRF
D	Mean	4510	5340	4180	3360	4790
	s	920	658	2070	1920	—
	s_r	20.4	12.3	49.6	57.0	—
	n	87	2	29	5	1
	RL>	1	0	0	0	0
	FN	1	0	0	0	0
E	Mean	422†	497	588	384	505
	s	48.9	30.4	312	136	—
	s_r	11.6	6.1	53.1	35.3	—
	n	86	2	29	6	1
	RL>	0	0	0	0	0
	FN	0	0	0	0	0
A	Mean	34.4‡	40.4	56.1	50.9	52
	s	7.75	2.19	27.9	39.7	—
	s_r	22.6	5.4	49.8	79.4	—
	n	83	2	27	8	1
	RL>	1	0	2	0	0
	FN	1	0	1	0	0
B	Mean	6.53	6.56	14.7	10.9	12
	s	4.31	0.71	12.9	21.1	—
	s_r	66.1	10.8	88.1	195	—
	n	66	2	17	12	1
	RL>	16	0	11	0	0
	FN	11	0	1	0	0
C	RL>	50	0	20	11	1
	FP	30	2	8	3	0

* Mean is in units of mg kg^{-1}; *s* = standard deviation (mg kg^{-1}); s_r = per cent relative standard deviation (mg kg^{-1}); *n* = number of results; RL> = number of results less than the reporting limit; FN = false negative; and FP = false positive.

Table 5 Selenium results by technique

Sample	Parameter*	ICP	ICP-MS	FAAS	ETAAS	HGAAS	EDXRF
C	Mean	4680	4740	5410	4250	4490	5030
	s	500	—	1380	1440	3380	—
	s_r	10.7	—	25.5	34.0	75.2	—
	n	43	1	8	52	15	1
	RL>	0	0	0	1	0	0
	FN	0	0	0	1	0	0
D	Mean	441	540	568	403	459	465
	s	92.3	—	151	142	495	—
	s_r	20.9	—	26.6	35.3	108	—
	n	43	1	8	53	15	1
	RL>	0	0	0	0	0	0
	FN	0	0	0	0	0	0
E	Mean	67.8	58	85.0	41.4	31.3	53
	s	87.8	—	78.1	14.1	14.9	—
	s_r	130	—	91.9	34.0	47.8	—
	n	37	1	8	56	16	0
	RL>	2	0	0	0	0	0
	FN	1	0	0	0	0	0
A	Mean	55.3	3	52.4	4.41	1.80	12
	s	110	—	101	5.86	1.52	—
	s_r	199	—	193	133	84.1	—
	n	23	1	4	56	17	0
	RL>	11	0	1	4	3	0
	FN	6	0	0	2	0	0
B	RL>	21	1	3	54	17	1
	FP	12	0	2	7	3	0

* Mean is in units of mg kg^{-1}; *s* = standard deviation (mg kg^{-1}); s_r = per cent relative standard deviation (mg kg^{-1}); *n* = number of results; RL> = number of results less than the reporting limit; FN = false negative; and FP = false positive.

for analytes with principal wavelengths below 200 nm, for the metalloids, such as arsenic (with wavelengths of 189, 193 and 197 nm), selenium (196 nm) and thallium (190 nm), the accuracy and precision of the ICPs was poor at lower concentrations. This was most probably due to spectral problems such as baseline and overlap, which are especially intense below 200 nm. The determinations of the two transition metal elements cadmium (214, 226 and 228 nm) and molybdenum (202 and 203 nm) by ICP techniques had either superior or comparable accuracy and precision to the other techniques used, even at the lowest spiked concentrations. For the same reasons, the ICPs consistently had the highest rates of false negatives and positives.

The FAAS results for molybdenum, selenium and thallium all showed some reproducible positive interferences. Molybdenum is a refractory element that requires the use of ion suppressants, such as aluminium. Laboratories not using this will have a positive bias in their data. Electrothermal atomic absorption spectrometry is subject to many interferences, especially if the proper matrix modifiers are not used. Hydride generation atomic absorption spectrometry is subject to interferences from copper, lead and nickel at concentrations at or greater than 1 mg l^{-1}, which would commonly occur in acid digestates. The presence of reduced nitrogen oxides resulting from nitric acid digestion procedures can also reduce the instrumental response for some elements.[8]

Hydride generation gave the poorest performance at all concentrations in terms of precision and accuracy. In addition to the problems listed above, hydride methods are based on the chemical reduction of weakly oxidizing elements by powerful reducing agents, commonly sodium tetrahydroborate(III). In drinking and surface waters, elements such as arsenic and selenium, are readily reduced to form gaseous hydrides. In a strong acid solution, however, the tetrahydroborate(II) will react more freely with the stronger oxidizing agents present, such as nitric acid, hydrochloric acid, and especially chlorine, than with the target elements. This means that it is very difficult to achieve reproducible generation of gaseous hydrides.[11] This can be seen in Table 7. Only three of the laboratories (2, 11 and 15) produced accurate results for all five arsenic samples. Five laboratories (3, 5, 7, 8 and 16) got almost all of them wrong. The remaining eight laboratories all had more accurate results at higher concentrations than at lower concentrations. The only logical explanation is that the very large dilutions required to bring the analyte within the linear dynamic range also diluted the acids to the point where they were no longer a problem. The ETAAS technology generally suffered from poor precision at all concentrations, but had better accuracy at lower concentrations. The ETAAS method is not robust, it is very analyst-sensitive. To obtain accurate results, the exact temperature programme, chemical modifiers, and other variables have to be set for each sample, a skill that is not widespread. With sufficient laboratories employing inexperienced analysts,[11] interlaboratory variance and accuracy is bound to suffer.

The greatest problem with FAAS is sensitivity. Most laboratories followed SW 846 Methods that require the digestion of 2.0 g of soil, and the digestate to be made up to a final volume of 100 ml. This means that for the lowest concentration samples, the concentration in the extract would be 0.1 mg l^{-1}. For most analytes, this is below the ability of the equipment used for FAAS to read accurately (cadmium being an exception, as the data show). Under the best circumstances, a concentration of 0.1 mg l^{-1} would produce a signal of only a few absorbance units. If the instrument drifted only five absorbance units, a very small amount, the calculated concentration could be out by 100 or 200%. Selenium and arsenic are difficult elements to determine by FAAS owing to their electron stability (and hence resistance to absorbing ultraviolet light). Selenium suffers interference from acetylene. This is why few laboratories use FAAS for these elements.

The ICP-MS data showed very good precision and accuracy. One exception to this was the arsenic result for sample A

Table 6 Thallium results by technique

Sample	Parameter*	ICP	ICP-MS	FAAS	ETAAS	HGAAS	EDXRF
B	Mean	4010	4260	4500	3750	4135	5556
	s	728	235	9800	1480	—	—
	s_r	18.2	5.5	217	39.4	—	—
	n	56	2	31	35	1	1
	RL>	0	0	0	0	0	0
	FN	0	0	0	0	0	0
C	Mean	443	515	488	421	454	552
	s	128	9.90	86.0	143	—	—
	s_r	28.8	1.92	17.7	34.0	—	—
	n	53	2	31	35	1	1
	RL>	0	0	0	0	0	0
	FN	0	0	0	0	0	0
D	Mean	70.1	129 (53.4)†	53.4	44.4	44.5	44
	s	93.3	106	15.5	14.1	—	—
	s_r	132	82.7	29.1	31.8	—	—
	n	44	2	32	39	1	1
	RL>	7	0	1	0	0	0
	FN	7	0	1	0	0	0
E	Mean	40.9	66.3 (5.6)†	9.96	5.15	—	8
	s	71.9	85.8	4.17	3.04	—	—
	s_r	176	129	41.8	59.0	—	—
	n	29	2	19	46	0	1
	RL>	18	0	8	3	1	0
	FN	10	0	4	2	0	0
A	RL>	32	1	18	42	1	1
	FP	14	1	10	3	0	1

* Mean is in units of mg kg^{-1}; s = standard deviation (mg kg^{-1}); s_r = per cent relative standard deviation (mg kg^{-1}); n = number of results; RL> = number of results less than the reporting limit; FN = false negative; FP = false positive.

† One of the two ICP-MS results suffered severe positive interference. The results in parentheses represent the other ICP-MS result.

where one of the laboratories reported a result of 8000 mg kg^{-1} that appeared to be a calculation error. The other exception was some positive interferences for thallium at lower concentrations for one of the laboratories. With only one or two data points in this study, it is not possible to draw broad conclusions; however, this does indicate that ICP-MS may be a useful tool for the elemental analysis of solids. The main area of concern is the very low concentration of dissolved solids required for ICP-MS to prevent clogging of the sampling cone. This means that large dilutions must be made, possibly resulting in the dilution and calculation errors seen in the arsenic results. The two laboratories in this study seem to be doing an adequate job of controlling this problem, but more widespread use of this technology may introduce the type of problems seen for GFAAS and HGAAS.

The EDXRF data were interesting, as the results were fairly accurate over a wide concentration range. There was negative interference for arsenic owing to the presence of large amounts of selenium. There was a small positive interference for thallium. The standard used was carefully matrix-matched to the samples. Like ICP-MS, this may become a useful analytical technique for the environmental laboratory.

Conclusions

Among the four techniques examined, ICP technology was generally the most accurate and precise technique for the determination of elements in solids in the ppm range. This was due to the wide linear dynamic range of the ICP instruments, which necessitated fewer dilutions. Over the range of concentrations studied, the ICP is as sensitive as the other techniques for some elements. Most significantly it is a robust technique that a large number of laboratories can apply independently to the same material and obtain very similar results. Its major drawback is the frequency of false positives and negatives at low concentrations.

Hydride generation should not be used for the analysis of acid digestates of solids. As the data show, HGAAS is neither accurate nor reproducible for this type of analysis. Electrothermal atomic absorption spectrometry is accurate and precise at low concentrations, but not at higher concentrations. This is not to say that ETAAS can never be used for the analysis of high concentration samples, some laboratories did use it. Rather, it takes significant expertise to do so. Most laboratories are not able to make the technology work in a reproducible and accurate fashion for solids analysis.

Flame atomic absorption spectrometry fell between ICP and ETAAS. It had comparable or better accuracy and precision to ETAAS for most elements at many concentrations. It had poorer precision and accuracy at the lowest concentrations for the reasons discussed earlier.

Both ICP-MS and EDXRF show potential for future use in this application. For the average laboratory situation where acid digestion is used to determine elemental concentrations in the ppm (mg kg^{-1}) range in a solid material, the technique of choice is ICP. Flame atomic absorption spectrometry and ETAAS should be used for lower concentrations and as confirmation for ICP data where interferences are a problem. This is especially important for analyses for regulatory purposes where more than one laboratory will analyse the same material. It is important that accurate and reproducible results are obtained.

Table 7 HGAAS results for arsenic

	Concentration/mg kg^{-1}				
Laboratory	Sample A	Sample B	Sample C	Sample D	Sample E
1	4600	520	66	0.5	2.9
2	4145	467	28	12	2
3	149	259	2.31	0.375	0.66
4	4580	490	54	3.8	2.1
5	2200	330	8.7	3.3	0.8
6	3800	410	120	7.5	3.1
7	707	383	54.5	3.5	78.5
8	510	78.7	7.0	1.6	0.6
9	3300	370	45	6	2
10	3661	355	16.8	<0.02	0.56
11	5680	356	36.8	9	3.75
12	3900	460	48.8	2.84	2.7
13	4632	602	75.2	<0.125	<0.125
14	4600	513	3.7	1.75	1.8
15	4460	501	56.2	9.2	4.7
16	8512	920	99.2	6	7

References

1 Kimbrough, D. E., and Wakakuwa, J. R., in *Proceedings of the Sixth Annual USEPA Symposium on Solid Waste Testing and Quality Assurance*, US Government Printing Office, Washington, DC, July 1990, pp. ii–214; *Environ. Sci. Technol.*, 1992, **26**, 173.

2 *Test Methods for Evaluating Solid Wastes (EPA SW 846 Volume 1A)*, Office of Solid Waste and Emergency Response, US Environmental Protection Agency, US Government Printing Office, Washington, DC, 3rd edn., November 1986.

3 *Code of Federal Regulations*, Title 40, Chapter 1, Subchapter 1, Part 261, Subpart C, 261.24. United States Printing Office, Washington, DC, 1993.

4 *Code of California Regulations*, Title 22, Division 4.5, Chapter 11, Article 3, Section 66261.24 subsection (a)(2)(a). ed. Ayres, K., Barkelys Law Publishers, San Francisco, 1993.

5 *Arsenic*, ed. Committee on Medical and Biological Effects of Environmental Pollutants, National Academy of Science, Washington, DC, 1979.

6 Kimbrough, D. E., and Wakakuwa, J. R., in *Proceedings of the Seventh Annual USEPA Symposium on Solid Waste Testing and Quality Assurance*, US Government Printing Office, Washington, DC, July 1991, p. 165–179.

7 Kimbrough, D. E., and Wakakuwa, J. R., *Enrivon. Sci. Technol.*, 1992, **26**, 2095–2100.

8 Kimbrough, D. E., and Wakakuwa, J. R., in *Proceedings of the Fifth Annual USEPA Symposium on Solid Waste Testing and Quality Assurance*, US Government Printing Office, Washington, DC, July 1989, pp. 1–166; in *Waste Testing and Quality Assurance*, ed. Tatsch, C. E., American Society for Testing and Materials, Philadelphia, PA, 1991, p. 231–244.

9 Kimbrough, D. E., and Wakakuwa, J. R., *Environ. Sci. Technol.*, 1989, **23**, 898.

10 Kimbrough, D. E., and Wakakuwa, J. R., *Environ. Sci. Technol.*, 1993, **27**, 2692.

11 *Standard Methods for the Examination of Water and Wastewater*, APHA/AWWA/WEF, American Publich Health Association, Washington, DC, 18th edn, 1992, method 3114 C, pp. 3–32.

Paper 3/01954C
Received April 6, 1993
Accepted September 20, 1993

Determination of Low Levels of Nitrogen Oxides in Gas Streams by High-performance Liquid Chromatographic Determination of the Saltzman Complex

Julie D. Willis, Chris J. Dowle, Andrew P. Malyan, Robert D. Liversidge and Peter Cullen

ICI Wilton Research Centre, P.O. Box 90, Wilton, Middlesbrough, Cleveland, UK TS90 8JE

The use of high-performance liquid chromatography is described as an alternative analytical finish to the Saltzman method for the determination of nitrogen oxides (NO_x) by the formation of a diazonium salt. This method can be applied to the determination of NO_x in the range 1–50 ppb v/v in hydrocarbon gas stream matrices.

Keywords: High-performance liquid chromatography; nitrogen oxides (NO_x) determination; NO_x Saltzman complex; NO_x in process streams

Introduction

This paper presents an alternative strategy for the determination of various nitrogen oxides (NO_x) as found in effluent and process streams. This example focuses on tail gas consisting of saturated hydrocarbons. Nitrogen monoxide (NO) can combine with traces of oxygen at cold train temperatures to form nitrogen oxides (N_2O_3 and N_2O_4),[1] which accumulate in the coldest parts of the plant over years of operation. If these deposits come into contact with dienes during the warm-up processes (in plant shutdowns or upsets), unstable nitroso gums may be formed, which can decompose explosively.[2] Even small concentrations may accumulate over years of operation and create a hazard. One method in use to determine these levels in the defined matrix is that devised by Saltzman.[3] In this method, the gas stream is bubbled through acidified potassium permanganate, which oxidizes any NO to nitrogen dioxide (NO_2), which is then reacted with sulfanilic acid in acidic solution. The resulting diazonium salt is coupled with *N*-1-naphthylethylenediamine dihydrochloride to form a purple–pink azo dye (Saltzman complex), which is determined spectrophotometrically at 550 nm. In the matrix under consideration there is the possibility of other species interfering with this measurement, and therefore a more specific analytical finish was required and developed. High-performance liquid chromatography (HPLC) was found to be specific for the azo dye complex derived from NO_x and of sufficient sensitivity for the example illustrated.

In the Saltzman method, calibration solutions for the NO_x are based on sodium nitrite. Saltzman determined empirically that 1 mol of NO_x (as the Saltzman complex) has an absorbance 0.72 times that of the sodium nitrite-derived NO_x (as the Saltzman complex), but did not provide conclusive evidence to explain why this should be so. This was seen as a major weakness in the method; for example, does this factor of 0.72 indicate that the efficiency of conversion of NO through to the Saltzman complex is 72% and hence Saltzman's experimental conditions need to be exactly reproduced? Therefore, the sample pre-treatment stages, *i.e.*, conversion of NO into NO_2 and then into the Saltzman complex prior to analysis, were investigated with the aim of experimentally determining the efficiency of conversion.

Experimental

Reagents

The HPLC solvents were obtained from Fisons. All the other reagents and solvents were of analytical-reagent grade (if available) from BDH and Fluka. The water used must have a resistivity greater than 18 MΩ cm^{-1}. NO and NO_2 gas standards were supplied by Warren Spring Laboratory and a 400 ppm v/v NO gas standard was obtained from Electrochem Gases.

Apparatus

For the generation of known concentrations of NO_x, the apparatus consisted of a Labotron LDP 11A syringe pump with the gas supply controlled by a Fischer Porter 103237N rotameter-type flow meter and measured by a rotary gas meter, a Drechsel bottle, a Model 42 chemiluminescence NO–NO_2–NO_x analyser, (Thermo Environmental Instruments) (Fig. 1) and a 1 ml gas-tight syringe.

For formation of the azo dye complex, the absorbing apparatus consisted of a sintered-glass absorber, a rotary gas meter and a Drechsel bottle (Fig. 2) The HPLC system consisted of a Hewlett-Packard HP 1090M liquid chromatograph with an ultraviolet (UV)–visible diode-array detector. The column used was RP Basic (250 × 4.6 mm i.d.), supplied by Hichrom.

Procedure

Preparation of reagent, calibration and validation solutions

N-1-*Naphthylethylenediamine dihydrochloride solution*, 0.1% *m/v*. Dissolve 0.1 g of the reagent in 100 ml of water. This is the stock solution, X.

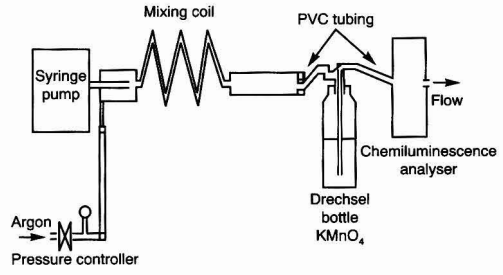

Fig. 1 Apparatus for generation of known NO_x concentrations to be measured by chemiluminescence

Saltzman absorbing reagent. Dissolve 5 g of sulfanilic acid in approximately 800 ml of water in a 1 l calibrated flask. Add 50 ml of glacial acetic acid and 50 ml of X and dilute to 1 l. This solution must be stored in a refrigerator.

Acidified potassium permanganate solution, 2.5% m/v in 2.5% v/v sulfuric acid. To prepare 2.5% v/v sulfuric acid, slowly and with constant stirring and cooling add 25 ml of concentrated sulfuric acid to approximately 800 ml of water. When cool, dilute to 1 l with water. Purge the permanganate solution with nitrogen at approximately 20 l h^{-1} for 15 min immediately before use to remove chlorine, which is evolved from chlorides present as impurities in the reagent.

Sodium nitrite standard solutions. Dissolve 0.41 g of sodium nitrite in 1 l of water. This is the stock solution, Y. Pipette 1 ml of Y into a 100 ml calibrated flask and dilute to volume with water. This is the stock solution, Z. Rinse a series of 100 ml Lifetime Red calibrated flasks three times with water and then once with Saltzman absorbing reagent. Pipette 0.5, 1.5, 3, 4 and 5 ml of solution Z into the flasks and dilute to volume with Saltzman absorbing reagent. These standards are equivalent to 1, 3, 6, 8 and 10 μl of NO_x, respectively (use of Saltzman factor to relate sodium nitrite-derived NO_x to NO_x in the sample). All standards and samples must be stored at 0 °C in the dark. This reagent is then stable for 2 weeks.

Gas stream sampling

Pipette 10 ml of Saltzman absorbing reagent into the sintered-glass absorber. Measure approximately 400 ml of permanganate solution into a Drechsel bottle and by means of a needle valve adjust the sample flow rate to 20 l h^{-1}. Using a short length of poly(vinyl chloride) (PVC) tubing, connect the absorber outlet to the gas meter and the sample point to the Drechsel bottle inlet. Allow gas to pass through the permanganate solution for 1 min. Note the initial reading of the gas meter, then connect the Drechsel bottle outlet to the absorber inlet. Allow 10 l of sample gas stream to pass through the absorber, then replace the permanganate solution and repeat.

Generation of standard atmospheres

For example, for the generation of a 10 ppb v/v standard of NO_x in argon, measure approximately 400 ml of permanganate solution into a Drechsel bottle. Set the argon gas flow rate to 1 l min^{-1}. Fill a 1 ml gas-tight syringe with 400 ppm v/v of NO and set the syringe pump flow rate to 25 μl min^{-1}. Allow the system to equilibrate for 15 min before measuring the actual level of NO_x using the chemiluminescence detector.

Measurement of NO_x concentrations

Measure the level of NO_x in the sample by HPLC. The HPLC conditions are as follows: mobile phase, 1% trifluoroacetic acid in water–1% trifluoroacetic acid in methanol (75 + 25 v/v); column temperature, 40 °C; flow rate, 1.5 ml min^{-1}; injection volume, 50 μl; and UV detection wavelength, 550 nm. Calculate the concentration as follows:

$$NO_x\,(\text{ppb v/v}) = \frac{1000NA}{G}$$

where N = NO_x (μl ml^{-1} from calibration), A = volume (ml) of Saltzman reagent in the absorber and G = volume (l) of gas passed through the absorber.

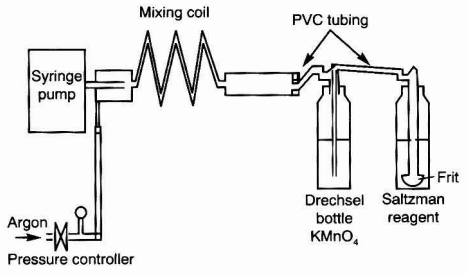

Fig. 2 Apparatus for generation of NO_x azo dye complex

Results and Discussion

HPLC Optimization

Initially ion-pair conditions were explored, which under alkaline conditions gave a UV chromophore for the ionized azo dye at 420–430 nm with a major impurity (thought to be some form of chlorine derivative[3,4]) at 480 nm. This is shown in Figs. 3 and 4. The conditions finally chosen give the UV chromophore for the azo dye at 550 nm, which has a molar absorptivity over 100 times greater than that at 420–430 nm and has improved selectivity, being much higher on the wavelength scale and eluting after the major impurity. This is shown in Figs. 5 and 6.

Stability of the Azo Dye

Effect of temperature

The levels of azo dye in two standards prepared by treating the Saltzman reagent with sodium nitrite equivalent to 6 μl of NO concentration (see Experimental), one stored in the dark at 0 °C and the other at room temperature (25 ± 3 °C), were compared over a 192 h period. The standard at room

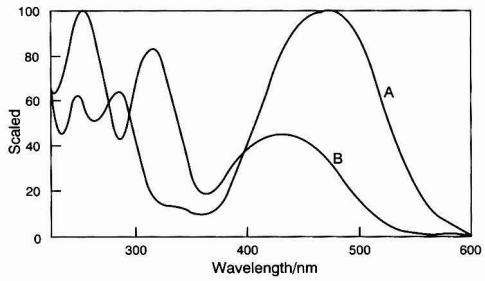

Fig. 3 UV spectra of Saltzman derivative (A) and its degradation product (B) (original HPLC method)

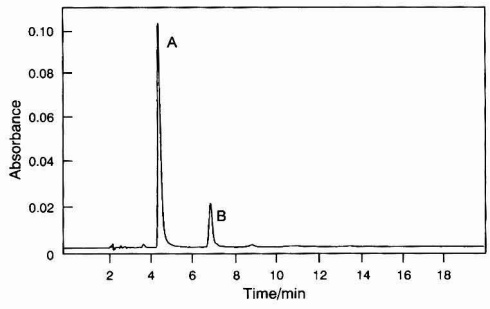

Fig. 4 Chromatogram of Saltzman derivative (A) and its degradation product (B) (original HPLC method)

temperature was found to have degraded considerably. The results are given in Table 1.

Effect of light

The levels of azo dye in two standards equivalent to 6 μl of NO concentration prepared by treating the Saltzman reagent with sodium nitrite, one stored in a dark cupboard and the other in direct sunlight for 72 h, were compared. The solution in the sunlight had changed colour to yellow and on examination by HPLC an unknown peak was detected at 3.3 min. A UV spectrum was taken at the apex of the peak which was found to have a maximum absorbance at 480 nm.

Validation Studies

The aim of these validation studies was to generate a known concentration of NO (using the apparatus in Fig. 1) to be measured by chemiluminescence analysis and then compare this value with that of the NO_x azo dye complex measured by HPLC. This HPLC-derived value incorporates the Saltzman factor (0.72) into its calibration and therefore, if the efficiency of conversion of NO into NO_2 and then into azo dye is measured as 100%, this is not equivalent to 100% conversion of NO but 72% calibration. Then any correction factor could be incorporated into the calculations of NO_x in the gas streams and the 'true' conversion efficiency of NO into the Saltzman complex would be known. This would thereby avoid relying on Saltzman's factor by exactly reproducing Saltzman's sampling conditions.

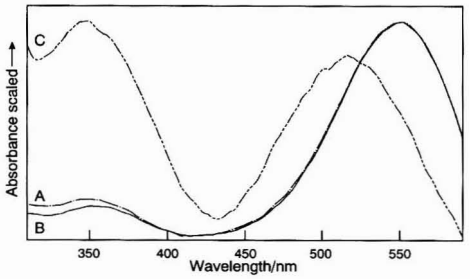

Fig. 5 UV spectra of Saltzman derivative (A and B) and its degradation product (C) (final HPLC method)

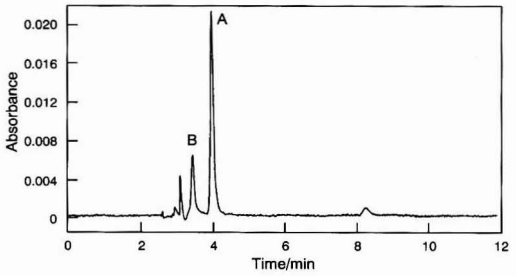

Fig. 6 Chromatogram of Saltzman derivative (A) and its degradation product (B) (final HPLC method)

Table 1 Effect of temperature on azo dye stability

	Decrease in peak area (μV s) of standards (%)	
Time/h	0 °C	25 ± 3 °C
0	0	0
24	0.4	6.0
48	1.3	11.0
120	3.8	22.0
192	3.8	31.0

Results

NO standards of 5, 10, 15 and 20 ppb v/v in argon were bubbled through potassium permanganate solution (flow rate 1 and 2 l min^{-1}) and passed through the chemiluminescence analyser. The recovery of NO was 62.0 ± 7.0% (mean ± standard deviation, n = 11) and was independent of the two flow rates. At this stage the first areas of uncertainty are introduced as the chemiluminescence analyser is inefficient at flow rates lower than 1 l min^{-1} whereas the experimental method requires 20 l h^{-1}. Also, there is no way of determining the efficiency of the NO_x Saltzman reaction that takes place in-line after the permanganate bubblers. Therefore, two assumptions were made: (*i*) the efficiency of NO conversion to NO_x by the permanganate is linear down to 20 h^{-1} and is taken to be 55%; this is an assumption of the worst possible case to err on the side of safety, but it is postulated that the conversion efficiency would be improved using the decreased flow rates through the bubblers; and (*ii*) there is full conversion of this NO_x to the Saltzman complex.

The argon flow rate was decreased to 0.5 l min^{-1}, the Saltzman absorbing reagent placed in-line and the above NO standards were bubbled through the system (as depicted in Fig. 2). The Saltzman complex was then determined by HPLC, incorporating the Saltzman factor into the calibration with sodium nitrite solution. The recovery of NO was 104.1 ± 14.7% (mean ± standard deviation, n = 8) over the concentration range covered, suggesting that the conversion of NO into NO_x and then into the Saltzman complex is indeed more efficient at the lower argon flow rates.

Replacing the argon with the hydrocarbon gas stream matrix under consideration initially created problems with the potassium permanganate oxidation of NO to NO_2 stage. Oxidations of various hydrocarbons in the gas stream matrix meant that large amounts of manganese dioxide were precipitated, causing restrictions in bubbling the NO through the potassium permanganate. Therefore, the potassium permanganate had to be renewed and the bubblers checked for blockages after every run. Initial NO recoveries were encouraging at 80.6 ± 8.3% (mean ± standard deviation, n = 5) compared with 104.1 ± 14.7% (slightly greater than the Saltzman conversion) in the inert matrix. It is hoped that further development work will help to increase this value.

Linearity and Precision Data

A linear relationship was observed between the peak areas for the azo dye complex and levels of NO generated from sodium nitrite over the range 0.001–0.1 μl ml^{-1} NO in Saltzman reagent; the correlation coefficient of the calibration graph was 0.99994. This is shown in Fig. 7.

The precision of the method was established by repeated analyses of two different standards: for the 0.06 μl ml^{-1} NO standard the relative standard deviation was 0.3% (n = 9) and for the 0.001 μl ml^{-1} NO standard it was 7.8% (n = 8).

Conclusions

This work has shown that the specific determination of NO_x at levels of 1–50 ppb v/v is possible in gas streams using HPLC

determination of the Saltzman-derived NO_x complex. This complex is stable for up to 2 weeks when stored at 0 °C in the dark. Preliminary studies on the sample pre-treatment prior to analysis indicate an efficiency of conversion of NO into NO_x and then into the Saltzman complex that is slightly less than the Saltzman factor, but further studies are required.

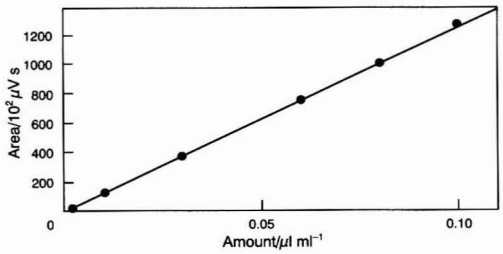

Fig. 7 Linearity data for NO_x Saltzman derivative. Constant = -1.027×10^3; 1st degree = 1.267×10^6; curve fit = linear; correlation coefficient = 0.99994; standard error = 6.13×10^2

Future Work

Further studies need to be carried out with the hydrocarbon gas stream matrix to clarify the value for the conversion efficiency. If it is found that the final value is indeed less than the Saltzman factor, then the conversion apparatus will be modified in an attempt to improve on this value.

References

1 Henstock, W. H., *Plant Oper. Prog.*, 1986, **5**, 4.
2 Hasebe, S., *Chem. Eng. Prog.*, 1966, **62**, 4.
3 Saltzman, B. E., *Anal. Chem.*, 1954, **26**, 12.
4 *ICI Internal Standard Analytical Method*, PCD/AR/23/14, ICI Wilton, 1976.

Paper 3/04685K
Received August 4, 1993
Accepted September 23, 1993

Determination of Octadecadienoic Acids in Human Serum: a Critical Appraisal

Gordon Read and Nigel R. Richardson

Department of Chemistry, University of Exeter, Stocker Road, Exeter, UK EX4 4QD

David G. Wickens

Department of Chemical Pathology, Whittington Hospital, London, UK N19 5NF

The method based on high-performance liquid chromatography currently used to determine the lipid levels of octadeca-9(*Z*),11(*E*)-dienoic acid in human serum fails to distinguish between this acid and octadeca-10(*E*),12(*Z*)-dienoic acid. Adducts with the fluorescent dienophile 4-[3-(1-propenyl)propyl]-1,2,4-triazoline-3,5-dione permit the separation of these two isomeric acids as does gas–liquid chromatography of their methyl esters, but these alternatives produce equivocal results when applied to biological samples.

Keywords: Octadeca-9(Z),11(E)-dienoic acid; fluorescent adduct; high-performance liquid chromatography; gas–liquid chromatography

Introduction

Concentrations of conjugated diene components in biological materials are commonly determined by measuring the ultraviolet (UV) absorption at 235 nm.[1,2] When coupled with high-performance liquid chromatography (HPLC), this technique supports a convenient and relatively sensitive mode of analysis. Such an analysis has been used extensively to determine levels of octadeca-9(*Z*),11(*E*)-dienoic acid (**I**) in clinical samples,[3] where particular focus has centred on the molar ratio of **I** to octadeca-9(*Z*),12(*Z*)-dienoic acid, linoleic acid (**II**).[4–17] We report in this paper a study of the chromatographic characteristics of **I** and derivatives of **I** with those of two isomeric acids, octadeca-9(*E*),11(*E*)-dienoic acid (**III**) and octadeca-10(*E*),12(*Z*)-dienoic acid (**IV**), and their corresponding derivatives that underlines the limited confidence that must accompany measurements on biological material based on a single analytical technique.

I $CH_3(CH_2)_5CH \overset{E}{=} CH\text{-}CH \overset{Z}{=} CH(CH_2)_7CO_2H$

II $CH_3(CH_2)_4CH \overset{Z}{=} CH\text{-}CH_2\text{-}CH \overset{Z}{=} CH(CH_2)_7CO_2H$

III $CH_3(CH_2)_5CH \overset{E}{=} CH\text{-}CH \overset{E}{=} CH(CH_2)_7CO_2H$

IV $CH_3(CH_2)_4CH \overset{Z}{=} CH\text{-}CH \overset{E}{=} CH(CH_2)_8CO_2H$

V $CH_3(CH_2)_4CH(OH)CH \overset{E}{=} CH\text{-}CH \overset{Z}{=} CH(CH_2)_7CO_2H$

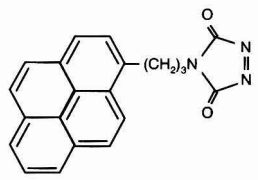

VI TAD

Experimental

Apparatus

The apparatus employed for the gas–liquid chromatographic (GLC) detection of the methyl esters was a modified Pye Unicam PV 400 instrument fitted with an inlet splitter and a flame ionization detector. The column was a 30 m × 0.32 mm i.d. capillary coated with Superox polyethylene glycol. The column temperature was 185 °C, the inlet and detector temperatures were both 225 °C and the linear velocity of the carrier gas (H_2) was 60 cm s^{-1}.

The HPLC assembly was a Waters-Millipore Model 6000A delivery system, a Pye Unicam PV 4020 UV–Visible detector and a Model SE 120 BBC Goerz Metrawatt chart recorder. Injections were made through a 20 μl loop on to a Waters-Millipore Nova-Pack C_{18} stainless-steel column (300 × 3.9 mm i.d.) protected by a similarly packed Anachem Type C-130-B precolumn (20 × 2 mm i.d.). Detection wavelengths of 234 and 340 nm were used for the free acids and the triazolinedione adducts, respectively. The mobile phase was prepared from HPLC-grade solvents (FSA Laboratories), which were filtered and purged with helium before use.

Materials

An authentic sample of octadeca-9(*Z*),11(*E*)-dienoic acid(*I*), synthesized from ricinolenic acid, was supplied by Professor Gunstone, University of St. Andrews. Authentic octadeca-9(*E*),11(*E*)-dienoic acid (**III**) was supplied by the Paint Research Association.

Octadeca-9(Z),11(E)-*dienoic acid* (**I**) and *octadeca*-10(E),12(Z)-*dienoic acid* (**IV**) 1 + 1 *mixture*. The mixture of **I** and **IV** was synthesized from linoleic acid (**II**) following the method of Nichols *et al.*[18] Co-crystallization from acetonitrile, at −15 °C gave colourless crystals, m.p. 4–6 °C.

Methyl esters. Standard acid (about 1 × 10^{-9} mol l^{-1}) in ethanol (0.2 ml) (capped Eppendorf tube) was reacted with excess of ethereal diazomethane[19] in the dark for 45 mins. Excess of reagent and solvents were removed under a stream of nitrogen. The residue was dissolved in ethyl acetate (10 μl) prior to injection (1 μl) into the GLC apparatus.

1,3,4-*Triazoline*-2,5-*dione* (*TAD*) adducts. The adducts were prepared in dry ethyl acetate from the acid standards (normally about 3 × 10^{-9} mol l^{-1}) by treatment with freshly

prepared TAD (**VI**) (2×10^{-7} mol l^{-1}) in ethyl acetate. The procedures detailed in ref. 20 for the preparation of the reagent, generation of the adduct and analysis of the adduct were followed.

Results and Discussion

The standards used in this study were **I**, **III** and a 1 + 1 mixture of **I** and **IV**. The mixture is readily obtained by isomerizing **II** under strong alkaline conditions.[18] It should be noted that Nichols *et al.*[18] based their assignment of the geometric arrangements in the two isomeric dienic acids produced by this reaction on UV spectral comparisons with authentic analogues. The assumption that the *Z*-bond which does not migrate will remain *Z* under the reaction conditions and theoretical considerations concerning the planarity of the anionic intermediate and steric influences were also used to support their argument for the structures of the products obtained. We have confirmed the positions of the double bonds in the two compounds by classical degradation.[21] The proximity of the chemical shifts in pairs of methine carbon signals observed in the ^{13}C NMR spectrum of the mixture leaves little doubt that both dienic acids have the same geometry about their double bonds. Further, the similarity between these shifts and those of 13-hydroxyoctadeca-9(*Z*),11(*E*)-dienoic acid (**V**) (sample provided by N. M. Maguire, University of Exeter) strongly support the (*Z*)(*E*) assignments made by Nichols *et al.* (see Table 1). The lack of symmetry in the shifts of the alkenic carbon signals rules out (*E*)(*E*) geometry.[22] As this paper will show, one product of the base-catalysed isomerization is indistinguishable from the synthetic 9,11-dienoic acid standard **I**. Only one isomer of the 10,12-dienoic acid is produced in the reaction and we believe therefore that this has the 10(*E*),12(*Z*) stereochemistry, in agreement with the proposal of Nichols *et al.*, rather than 10(*Z*),12(*E*) which is not rigorously excluded on the evidence.

A portion of each sample of dienoic acid was converted into the methyl ester.[19] A second portion of each sample was converted into the adduct of 4-[3-(1-pyrenyl) propyl]-1,2,4-triazoline-3,5-dione (TAD)(**VI**), a highly fluorescent dienophile developed for the determination of low levels of a dienic compound.[20] The free acids were examined by HPLC under conditions that had previously been optimized for **I**, **II** and **III**.[4] HPLC of the TAD adducts utilized the same reversed-phase column. The methyl esters were examined by GLC. After optimization of the operating conditions (see Experimental) for the adducts and methyl esters, the retention times for the above standards were as given in Table 2.

It is apparent from the data in Table 2 that the isomeric 9(*Z*),11(*E*)- and 10(*E*),12(*Z*)-dienoic acids, **I** and **IV**, cannot be distinguished by the method employed in the biomedical studies.[4–17] However, the TAD derivatives of these two acids are well separated under appropriate chromatographic conditions. Perversely, the TAD adducts of the 9(*E*)11(*E*)- and 10(*E*)12(*Z*)dienoic acids, **III** and **IV**, respectively, cannot be resolved by this method. No more than signal broadening was observed with mixed samples (see Fig. 1). Attempts to fine tune the chromatographic conditions to resolve the overlapping peaks were unsuccessful. Capillary GLC of the methyl esters completely resolves the three isomers but, of course,

Table 1 ^{13}C NMR ($CDCl_3$) chemical shifts for methine carbons in a mixture of (*E*)(*Z*)-conjugated dienic acids **I** and **IV** and in **V**

δ (ppm)		
I + **IV**		**V**
125.61	125.72	125.62
128.63	128.76	127.88
129.79	130.06	132.59
134.47	134.70	136.03

Table 2 Retention times for octadecadienoic acids **I**, **III** and **IV**, their methyl esters and their TAD adducts

	t_R/min		
Compound	**I** [9(*Z*),11(*E*)]	**III** [9(*E*),11(*E*)]	**IV** [10(*E*),12(*Z*)]
Free acid*	11.2	12.8	11.2
Free acid†	8.5	—	8.5
TAD adduct‡	20.6	19.1	18.8
Methyl ester	10.74	13.54	11.15

* Acetonitrile–0.1 mol l^{-1} acetic acid (80 + 20), flow rate 2.0 ml min^{-1}.

† Acetonitrile–0.1 mol l^{-1} acetic acid (90 + 10), flow rate 1.2 ml min^{-1}.

‡ Acetonitrile–0.1 mol l^{-1} acetic acid (80 + 20), flow rate 1.5 ml min^{-1}.

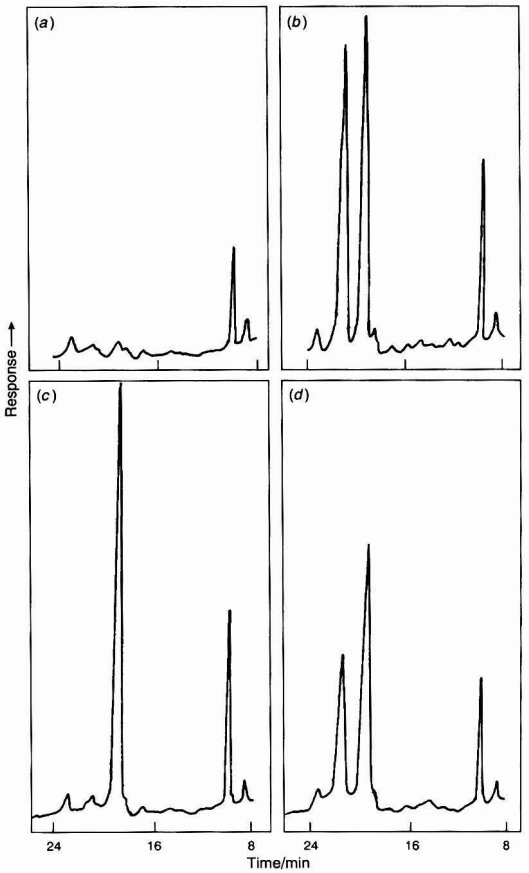

Fig. 1 HPLC chromatograms of TAD adducts from standard dienoic acids: (*a*) blank; (*b*) 1 : 1 mixture of octadeca-9(*Z*),11(*E*)-dienoic acid and octadeca-10(*E*),12(*Z*)-dienoic acid adducts; (*c*) octadeca-9(*Z*),12(*Z*)-dienoic acid adduct; (*d*) a mixture of (*b*) and (*c*). (See Experimental section for conditions)

fails to screen selectively for conjugated dienoic acids. Analysis by GLC is further limited by interference from a trace of by-product from diazomethane decompositions sufficient to affect quantitative measurements of **IV** at very low levels.

Our results clearly show that **I** and **IV** can be distinguished on the basis of HPLC analysis of their TAD adducts or by GLC analysis of their methyl esters. For mixtures of **I**, **III** and **IV** either a combination of HPLC of the free acids and HPLC of the TAD adducts or, more simply, GLC of their methyl esters may be employed.

Analysis by the above methods of the conjugated dienic acid components from phospholipase treatment of human serum proved to be more difficult. Results from many earlier studies on free acids, using the HPLC conditions described above, have firmly established that a relatively abundant unsaturated component appears in the HPLC trace at 11.2 min followed by a second component at 12.8 min. The abundance of the latter rarely exceeds 2% of the former. Other more polar components absorbing at 235 nm elute much earlier (4–8 min). The results of spiking studies associated the 9(*Z*),11(*E*)-dienoic acid **I** and the 9(*E*),11(*E*)-dienoic acid **III** with the bands appearing at 11.2 and 12.8 min, respectively.

With this background in view, the total acid fractions were isolated, as previously reported,[3] from five serum samples. TAD adducts obtained from these samples were analysed under the conditions described above. The HPLC traces showed a group of four polar components eluting between 12 and 15 min, labelled A in Fig. 2, which may be hydroperoxydienic acids. Consistent with analyses of the free acids, these traces also showed components, B and C in Fig. 2, with retention times of 19.0 and 20.6 min, associated with the adducts of **III** and/or **IV** and of **I**, respectively. Only a very small peak was expected at 19.0 min relative to the size of the latter peak; it was of some surprise, therefore, that the size of this signal, rather than being the expected 1–2% of the latter, varied from 28 to 106% (average 50%) of that found at 20.6 min.

These findings raised the possibility that in the earlier investigations up to 50% of the signal attributed to **I** on the sole basis of HPLC of the dienic acids might be due to **IV**. Further evidence from the GLC analysis of the methyl esters of the acid extract was sought. However, the complexity and the much greater abundance of many of the components prevented any realistic estimates of the minor esters key to this study. The putative **I** band from a further serum sample was therefore isolated by fractionation of the HPLC eluate.

HPLC analyses of the free acid obatined in this manner indicated that the level of **III** in the sample did not exceed 0.5% that of **I** and/or **IV**. HPLC analysis of the TAD adduct, backed by a spiking study, suggested that the level of **III** and/or **IV** was 12% of that of **I**. Collectively, these findings indicated that 11.5% of the 11.2 min signal in the free acid analysis of this sample could be due to **IV**. The GLC trace of the methyl esters of this acid fraction was much simpler than those from the total acid fractions but still included signals from numerous acids not active at 235 nm. A signal consistent with the presence of the methyl ester of **I** was observed in the critical 10–14 min time interval together with a peak with retention time very close to that shown by the methyl derivative of **IV**. The latter carried a shoulder from a marginally faster eluting component [Fig. 3(*a*)]. Careful measurement and a spiking study with the methyl esters of a 1 + 1 mixture of authentic **I** and **IV** [Fig. 3(*b*)] supported the case for the presence of the methyl ester of **I** but showed that neither the peak close to 11.15 min nor the accompanying shoulder coincided exactly with the signal from the methyl ester of **IV**. However, the spiking study could not eliminate the presence of the methyl ester of **IV** in the unspiked sample at a level corresponding to 10% of the corresponding ester from **I**, as its GLC signal may completely underlie the larger signal observed which was 57% that of the signal from the latter ester. The signal at 13.42 min, attributed to the methyl ester of octadeca-9(*E*),11(*E*)-dienoic acid (**III**), was equivalent to only three times the noise level.

Three observations in this study merit emphasis. First, the protocol adopted in earlier studies for the determination of octadeca-9(*Z*),11(*E*)-dienoic acid **I** does not permit a distinction between **I** and at least one closely related dienoic acid. It

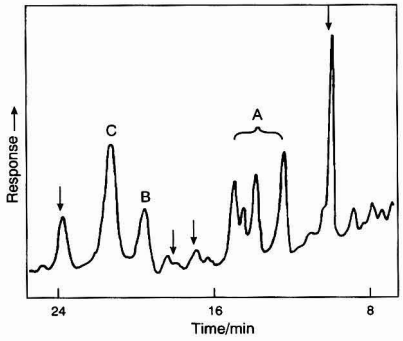

Fig. 2 HPLC chromatograms of TAD adduct from the total acid fraction of phospholipase treated human serum (background peaks arrowed). (See Experimental section for conditions)

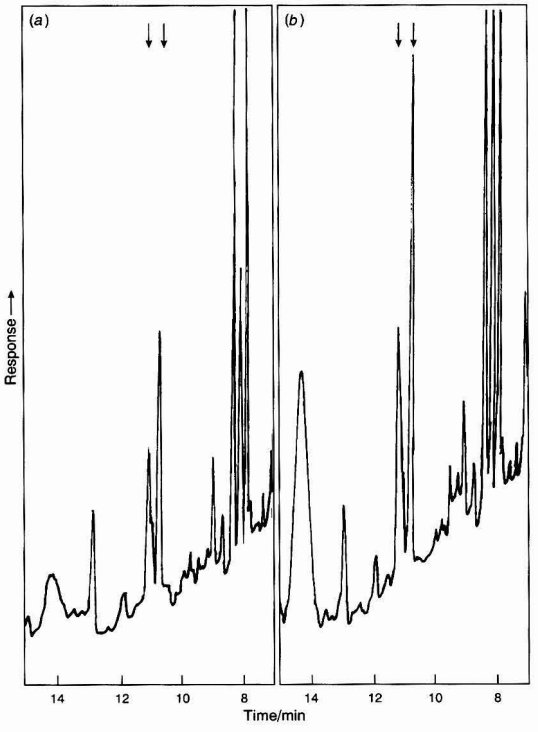

Fig. 3 GLC chromatograms of methyl esters from partially purified total acid fraction of phospholipase treated human serum: (*a*) before 'spiking' with 1:1 mixture of methyl octadeca-9(*Z*),11(*E*)-dienoate and methyl octadeca-10(*E*),12(*Z*)-dienoate; (*b*) after 'spiking'

may be noted that there are eight geometric isomers in the octadeca-9,11- and -10,12-dienoic acid series. Second, there appears to be a substantial conjugated dienoic acid fraction in phospholipase-treated human serum which gives a TAD derivative with characteristics indistinguishable by HPLC from those of the TAD derivative of octadeca-10(*E*),12(*Z*)-dienoic acid (**IV**). Third, and of much greater importance, is the observation that the confidence level that can be accorded to a single HPLC protocol as a means of identifying a compound is low. This is not a novel finding but one which is repeatedly overlooked. The chemical and biochemical literature[23,24] contains numerous examples of identifications made on the basis of a chromatographic technique which have been subsequently invalidated by employing more refined instrumentation, alternative analytical methods or (more valuably) combinations of analytical methods. Clearly, with further work, resolutions high enough to separate co-eluting components in the studies reported here might be achieved. However, one further aspect of such analyses is routinely overlooked. In analytical studies (and sadly in the teaching of chemistry), one important underlying tenet of the scientific method is ignored, namely in principle, differences between two different entities can be unequivocally demonstrated but the identity of two identical entities cannot, as a level must be set on the confidence of any measurement. In identification, a subjective step in the deductive exercise is always required. The need for a clear statement of the level of confidence in the identification of an analyte within complex mixtures encountered in medicinal chemistry is probably greater than in any other branch of science.

The authors gratefully acknowledge a postgraduate studentship (N. R. R.) from the SERC.

References

1 Gibian, M. J., and Vandenberg, P., *Anal. Biochem.*, 1987, **163**, 343.
2 Dormandy, T. L., and Wickens, D. G., *Chem. Phys. Lipids*, 1987, **45**, 353.
3 Iversen, S. A., Cawood, P., Madigan, A. J., Lawson, A. M., and Dormandy, T. L., *Febs. Lett.*, 1984, **171**, 320.
4 Griffin, J. F. A., Wickens, D. G., Tay, S. K., Singer, A., and Dormandy, T. L., *Clin. Chim. Acta*, 1987, **163**, 143.
5 Cawood, P., Wickens, D. G., Iversen, S. A., Braganza, J. M., and Dormandy, T. L., *FEBS Lett.*, 1983, **162**, 239.
6 Erskine, K. J., Iversen, S. A., and Davies, R., *Lancet*, 1985, **i**, 554.
7 Iversen, S. A., Cawood, P., and Dormandy, T. L., *Ann. Clin. Biochem.*, 1985, **22**, 137.
8 Tay, S. K., Singer, A., Griffin, J. F. A., Wickens, D. G., and Dormandy, T. L., *Clin. Chim. Acta*, 1987, **163**, 149.
9 Singer, A., Tay, S. K., Griffin, J. F. A., Wickens, D. G., and Dormandy, T. L., *Lancet*, 1987, **i**, 537.
10 Lawson, N., McGuigan, J., Watson, D. C. T., Collins, F. J., and Pandor, H. I., *Ann. Clin. Biochem.*, 1988, **25**, Suppl., 145s.
11 Green, A. J. E., Starkey, B. J., Halloran, S. P., McKee, G., Sutton, C. J. G., Manners, B. T. B., and Walker, A. W., *Lancet*, 1988, **ii**, 309.
12 Fairbank, J., Ridgway, L., Griffin, J., Wickens, D. G., Singer, A., and Dormandy, T. L., *Lancet*, 1988, **ii**, 329.
13 Coleman, D. V., Taylor, A., and Thomas, B. S., *Lancet*, 1988, **ii**, 329.
14 Green, A. J. E., Starkey, B. J., McKee, G., Hallovan, S. P., Sutton, C., Manners, B., and Walker, A. W., *Ann. Clin. Biochem.*, 1988, **25**, Suppl., 67s.
15 Fairbank, J., Hollingworth, A., Griffin, J., Ridgway, E., Wickens, D., Singer, A., and Dormandy, T., *Clin. Chim. Acta*, 1989, **186**, 53.
16 Wickens, D. G., Davies, M. J., Fairband, J., Tay, D. K., Slater, T. F., and Dormandy, T. L., *Am. J. Obstet. Gynecol.*, 1990, **162**, 854.
17 Ashworth, J., Wickens, D. G., Maurice, P. D. L., Lewis, G., Dormandy, T. L., and Breathnach, S. M., *Br. J. Dermat.*, 1990, **122**, 59.
18 Nichols, P. L., Herb, S. F., and Reimenschneider, R. W., *J. Am. Chem. Soc.*, 1951, **73**, 247.
19 Lawson, N., McGuigan, J., and Watson, D. C., *Ann. Clin. Biochem.*, 1988, **25**, 154.
20 Jordan, P. H., Read, G., and Hargreaves, T., *Analyst*, 1991, **116**, 1347.
21 Richardson, N. R., *PhD Thesis*, University of Exeter, 1990
22 Batchelor, J. G., Cushley, R. C., and Prestegard, J. H., *J. Org. Chem.*, 1974, **39**, 1698.
23 Bolton, A. A., *Nature (London)*, 1971, **231**, 22.
24 Johnson, T., and Sheppard, R. C., in *Molecular Recognition, Chemical and Biochemical Problems*, ed. Roberts, S. M., Royal Society of Chemistry, Cambridge, 1989, pp. 128–130.

Paper 3/05288E
Received September 3, 1993
Accepted September 22, 1993

Determination of Free myo-Inositol in Milk and Infant Formula by High-performance Liquid Chromatography

Harvey E. Indyk
Anchor Products, P.O. Box 7, Waitoa, New Zealand
David C. Woollard
Lynfield Food Services Centre, Ministry of Agriculture and Fisheries, P.O. Box 41, Auckland, New Zealand

A high-performance liquid chromatographic method is described for the determination of supplemental myo-inositol in infant formulas based on cows' milk. The technique incorporates pre-column derivatization with phenylisocyanate followed by reversed-phase gradient chromatography and ultraviolet detection. The protocol was also applied to a survey of free inositol at endogenous levels in the milk of cows, goats and humans. Nutritional preparations containing inositol at pharmacological levels are also amenable to a simplified isocratic analysis.

Keywords: High-performance liquid chromatography; myo-inositol; milk; infant formula; premix

Introduction

The first cyclohexitol to be isolated, myo-inositol, remains the only known biologically active isomer of the C_6 sugar alcohols. It is widely distributed in plant and animal tissues, both free and bound within several important phospholipids and inositol phosphates. It has been demonstrated that it contributes to important functional and structural roles[1] including cellular signalling,[2] lipotrophic action,[3] calcium mobilization[4] and surfaction in the lung,[5] and several neuropathies have been implicated in nerve inositol depletion.[6]

Its necessity in the diet has not been demonstrated for adult humans in view of the efficient renal and extrarenal biosynthesis of myo-inositol.[1,6,7] However, its occurrence at high levels in humans' milk implies a possible conditional or mandatory requirement during early infant development, and it is therefore increasingly added to infant formulas to ensure against deficiency.

The growing interest in this nutrient and the inherent problems with its detection are reflected in the diverse analytical approaches that have been reported. Hence, myo-inositol levels in tissues and body fluids have been estimated by microbial,[8,9] enzymic,[10–12] gas chromatographic[5,13–17] and high-performance liquid chromatographic methods,[18–27] although comparatively little progress has been made in the area of food analysis.

The principal aim of this study was to develop a technique facilitating the routine determination of supplemental inositol in infant formulations. In addition, it was considered of importance to characterize the levels of endogenous free inositol in various milk powders, and to compare its concentration in the milk of different species.

Experimental

Equipment

The high-performance liquid chromatography (HPLC) system consisted of a Model 510 and Model 501 pump with a Model 680 gradient controller, an 8 × 10 radial-compression module and a Resolve octadecylsilica (5 μm) column (Waters, Milford, MA, USA), a Rheodyne 7125 injector with 5 μl loop, a Model L-4200 spectrophotometric detector (240 nm), and a Model D-2500 integrator (Hitachi, Tokyo, Japan). During validation studies, an HP1040A diode-array detector (Hewlett Packard, Palo Alto, CA, USA) and a VG 70S magnetic sector mass spectrometer (VG Instruments, Manchester, UK) were used, the last of these under the following conditions: dithiothreitol + dithioerythritol (4 + 1 v/v) FAB matrix (1 μl on the probe); normal scanning mode, 20 keV Cs^+ beam (current 2 μA); source potential, 6000 V; resolution power, 1500; and scan time, 5 s.

A VP100 two-stage vacuum pump (Savant, Farmingdale, NY, USA) connected to an all-glass manifold with cold-trap was employed during sample preparation. Other apparatus included a forced-air oven maintained at 55 °C, a pH meter and screw-capped borosilicate glass vials (1.8 ml), compatible with possible autosampler use. For safety reasons a fume hood was essential during derivatization.

Reagents

myo-Inositol was obtained from Sigma (St. Louis, MO, USA), pyridine (analytical-reagent grade), methanol and acetonitrile (HPLC grade) from BDH (Merck, Poole, Dorset, UK), and phenylisocyanate from Serva (Heidelberg, Germany). Other saccharides included galactitol, D-sorbitol, D-mannitol, α- and β-D-glucose, α-lactose, D-galactose, and sucrose (Sigma). High quality water to at least 18 MΩ resistance was obtained from a Milli-Q system (Millipore, Milford, MA, USA) and was used throughout.

Preparation of Standards

Approximately 100 mg of myo-inositol were accurately weighed directly into a calibrated flask (100 ml) and dissolved to volume with water. A working standard was prepared by diluting the stock standard 100-fold in water to approximately 10 μg ml^{-1}. Other concentrations were used during validation studies. Standards of other saccharides considered likely to be present in milk were also prepared to equivalent concentrations, and others were evaluated as possible internal standards. All standards were stable at 4 °C for at least 2 months.

Sample Preparation

Approximately 2.0 g of milk powder or 15.0 g of liquid milk were accurately weighed into a beaker. A control reference sample and reagent blank were included with each analytical run to monitor method performance. The samples were made to about 25 ml with water by dissolving or dilution, as

appropriate. Protein was precipitated by titrating to pH 4.5 with hydrochloric acid (1.0 mol l^{-1}), after which the slurry was made to volume (100 ml) with water and filtered. Aliquots (100 μl) of clear sample filtrate and working standard were transferred to glass vials and lyophilized under vacuum (approximately 0.70 Pa).

Vitamin premixes containing inositol at pharmacological doses were also assayed after appropriate dilution in water. Aliquots (100 μl) were then lyophilized and treated as for milks.

In an attempt to extend the method to determine total inositol, some samples (2.0 g) were also subjected to acid hydrolysis under autoclave (121 °C, 3 h). Following pH adjustment, sample preparation was then completed as already described.

Derivatization

To each of the lyophilized samples and standards were added dry pyridine (70 μl) and phenylisocyanate (20 μl). The vials were capped and incubated at 55 °C for 70 min after which they were cooled on ice. Methanol (20 μl) was carefully added and the incubation was allowed to continue for a further 10 min at 55 °C to destroy excess phenylisocyanate. The reaction mixture was diluted with pyridine (90 μl) to a total volume of 200 μl ready for injection into the HPLC system. Extracts could then be conveniently stored overnight at 4 °C prior to analysis, although the high stability of the derivative would facilitate longer term storage, if required.

Chromatography

Derivatized extracts and standards (5 μl) were injected under the gradient elution conditions summarized in Table 1. Detection was at 240 nm with attenuation held at 0.16 a.u.f.s. between 25 and 40 min and at 0.64 a.u.f.s. between 0 and 25 and 40 and 47 min. Integration parameters were expediently set to analyse the chromatographic region of interest, subsequent to elution of reagent peaks. The system pressure under initial conditions was approximately 60 kg cm^{-2}.

Quantification was based upon comparison of the peak area or height of the myo-inositol sample with that of the external standard.

Results

Chromatography

Fig. 1 shows the chromatograms obtained under the described gradient conditions for a reagent blank, myo-inositol standard (10 μg ml^{-1}), and a typical unsupplemented cows' milk.

Optimum resolution of sample extracts was found to require a column providing ≥8500 plates per column (acenaphthene; acetonitrile + water, 70 + 30 v/v).

Tentative identification of other carbohydrates present in bovine milk was made by comparison of retention times with authentic standards. Sugars predictably eluted in order of the number of free hydroxyl groups available for derivatization in the parent compound. Non-reducing sugars and sugar alcohols produced single peaks while reducing saccharides (glucose, galactose and lactose) appeared as enantiomeric pairs as indicated in Fig. 1.

Milk from humans yielded a chromatographic profile broadly equivalent to that of cows' milk, but with unique and significant additional contributions in the later-eluting oligosaccharide region.

Although three minor peaks of the blank potentially interfere with glucose and galactose, there are no chromatographic artefacts compromising the estimation of either myo-inositol or later-eluting carbohydrates.

While galactitol was shown to be a potentially useful internal standard, eluting between inositol and sorbitol, the external calibration method was found to be more reliable for this study.

Table 1 Gradient conditions for the HPLC analysis

Time/min	Flow rate/ ml min^{-1}	Water (%)	Acetonitrile (%)	Curve*
Initial	2.0	45	55	—
30	2.0	35	65	8
38	2.0	35	65	6
40	2.5	10	90	6
46	2.5	10	90	6
48	2.0	45	55	6

* Curve number designated by the Waters Model 680 pump controller: curve 8 is a concave, and curve 6 a linear gradient.

Peak Identification

Confirmation of putative myo-inositol in sample extracts was achieved through several strategies. Thus, co-elution with authentic standard was observed under varying gradient conditions and with equivalent quantitative results. On-line photodiode-array detection was also employed, as illustrated in Fig. 2, where conventional spectra and three-dimensional ultraviolet isograms of milk and infant formula myo-inositol are compared with standard material.

Spectral equivalence was observed throughout elution of the alleged peak with a match factor against standard (calculated by the peak purity analysis program) of 997.92 for milk, and 999.33 for an inositol supplemented infant formula. A perfect match is defined instrumentally as 1000. This experiment showed a wavelength maxima of 233 nm for the derivatives, although routine analysis was performed at 240 nm.

Mass spectrometry under fast-atom bombardment conditions [*i.e.* fast atom bombardment mass spectrometry (FAB-MS)] was also performed, subsequent to semi-preparative chromatographic collection of authentic and alleged myo-inositol derivative peaks. Unlike the high concentration standard, the greater complexity of sample extracts required multiple collection and refractionation to achieve the necessary purity and amount for off-line FAB-MS. Approximately 2 μg of suspected and 100 μg of authentic compound were prepared for the MS analysis. Both extracts showed the equivalent and strong ions expected of fully derivatized inositol at *m/z* 895 and 917, corresponding to the typical MH^+ and $(M + Na)^+$ ions found under positive-ion FAB conditions. Fragment ions at *m/z* 419, 538, 639 and 758 were also found, probably associated with sequential loss of phenylisocyanate adducts.

Method Validation

Calibration curves for myo-inositol standards were linear (0.1–4.0 μg; $r = 0.9998$, where r is the correlation coefficient) over the range required for the analysis of all the samples studied. The high molar absorptivity of the chromophore easily allowed detection to at least one order of magnitude lower than that required for this application.

The recovery of myo-inositol during the over-all procedure was assessed after its addition to an unfortified milk powder; it was 102.9% at the 1.0 mg and 98.6% at the 2.0 mg spike level.

Instrument precision was estimated after replicate analysis of a derivatized standard yielding a relative standard deviation of 1.8% (5 μl fixed-volume injection).

Analytical repeatability was evaluated subsequent to replicate between-run analysis of a myo-inositol supplemented

infant formula; the relative standard deviation was 4.8% ($\bar{x}$ = 65.2 mg per 100 g, $\sigma_{n-1} = 3.1$, $n = 6$, where $\bar{x}$ is the mean result, σ, the standard deviation, and n, the number of determinations).

Method accuracy was assessed by comparing the free inositol levels of a range of bovine-milk powders obtained using the proposed HPLC method with the results of a microbial assay based on the growth of *Saccharomyces uvarum* (ATCC 9080). The latter technique was also used to obtain values of total inositol after acid hydrolysis. These data are given in Table 2, which also indicates the suitability of the technique for the routine analysis of nutritional milk powder and supplemented products.

The data obtained for free inositol using HPLC and microbial assay, were subjected to the paired Students *t*-test and showed no significant difference at the 95% confidence level. The correlation coefficient was 0.9946 with the regression equation $y = 0.894x + 4.365$.

The variation in myo-inositol levels between the milks of different species was investigated and these values are listed in Table 3. It is evident that humans' milk contains a comparatively higher inositol content than either bovine or caprine milk.

Discussion

Many liquid chromatographic systems have been described for the analysis of major sugars and polyhydric alcohols in foods. These systems have usually incorporated refractive index detection coupled with ion-exchange or amino-phase separation.[28–30] The relatively poor sensitivity associated with this viewing mode has precluded its application to the determination of low concentration, biologically active carbohydrates. The absence of chromophoric and fluorophoric functional groups within inositol and other saccharides, has stimulated the search for alternative sensitive and selective detection modes, including those based on pre-column[18–24,30] and post-column derivatization,[25,30] as well as pulsed amperometric oxidation following post-column manipulation of eluent pH.[25,27,30] A recent report compares detection limits achievable by these means, although it is restricted to reducing sugars only.[31]

Pre-column formation of the ultraviolet absorbing *p*-nitrobenzoate esters of low level sugars and polyols in lyophilized tissue extracts has been described, employing normal-phase HPLC separation on silica.[20,21] Despite excellent sensitivity, this derivatization protocol incorporates several time-consuming washes and has been recently described as failing in the estimation of myo-inositol and sorbitol in biological samples, unless extracts are initially fractionated on a cation-exchange HPLC system.[24]

An alternative pre-column derivatization approach, based on reaction with phenylisocyanate yielding the ultraviolet-active phenylurethanes, and using the more robust reversed-phase chromatographic mode has also been reported.[18,19,23] The isocyanates have high reactivity with almost any compound possessing active hydrogen and have been demonstrated by infrared and ^{13}C nuclear magnetic resonance spectroscopy to result in highly stable derivatives with carbohydrates and sugar alcohols, permitting detection to nanogram levels.[18]

In the analysis of unbound milk carbohydrates, proteins and fat can be conveniently coprecipitated and removed by treatment with dilute acid. Following lyophilization, sample derivatization is similar to previously described methods for biological tissues.[23] Chromatography with isocratic elution, as

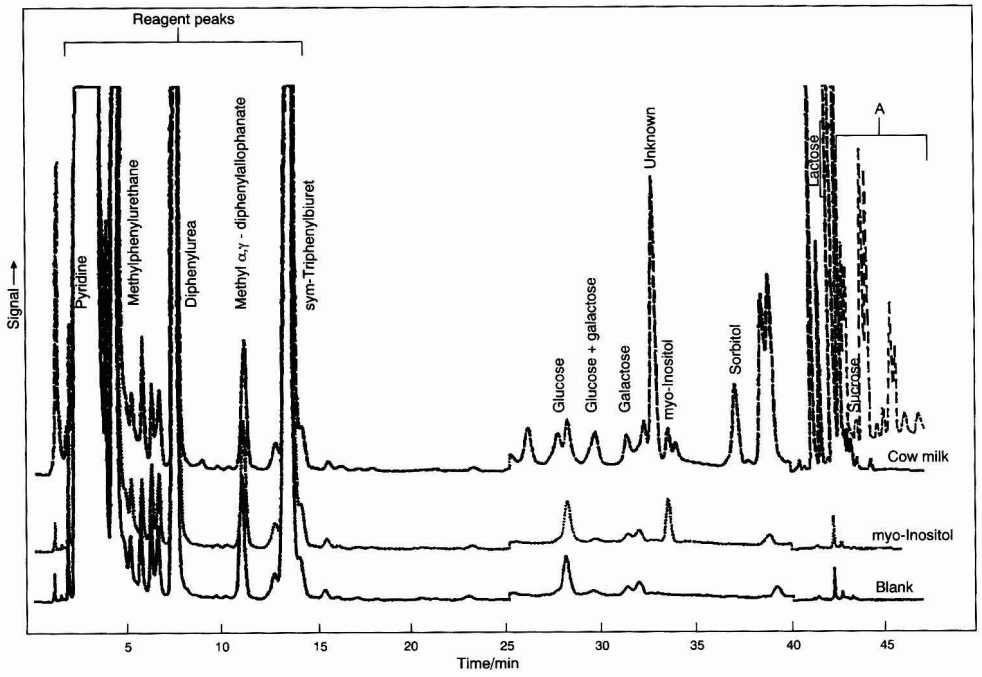

Fig. 1 Overlay chromatograms of phenylurethane derivative extracts of lyophilizates. Column: 5 μm Resolve C_{18}; gradient elution as described in Table 1. Detection: 240 nm; 0.16 a.u.f.s. (25–40 min). Injection volume, 5 μl. A, components unique to human milk

recommended in earlier reports,[19,23] provided insufficient resolution of the low level myo-inositol in milk and concave gradient conditions were found to be essential.

The high reactivity of the isocyanates leads to extraneous side reactions with solvents, producing low relative molecular mass reagent peaks eluting early in the chromatogram. These 'blank' components were the subject of a recent study, and several of the major byproducts were identified by both liquid chromatography-thermospray MS and photodiode-array detection.[32] The present work has facilitated a tentative identification of reagent peaks (Fig. 1), in view of the comparable chromatography in this elution region.

A recent study used a simplex procedure to investigate the optimum phenylisocyanate derivatization conditions required for monosaccharide standards.[33] The conditions recommended in this paper are essentially equivalent to the optimum, with a large excess of reagent over that established for maximum conversion.

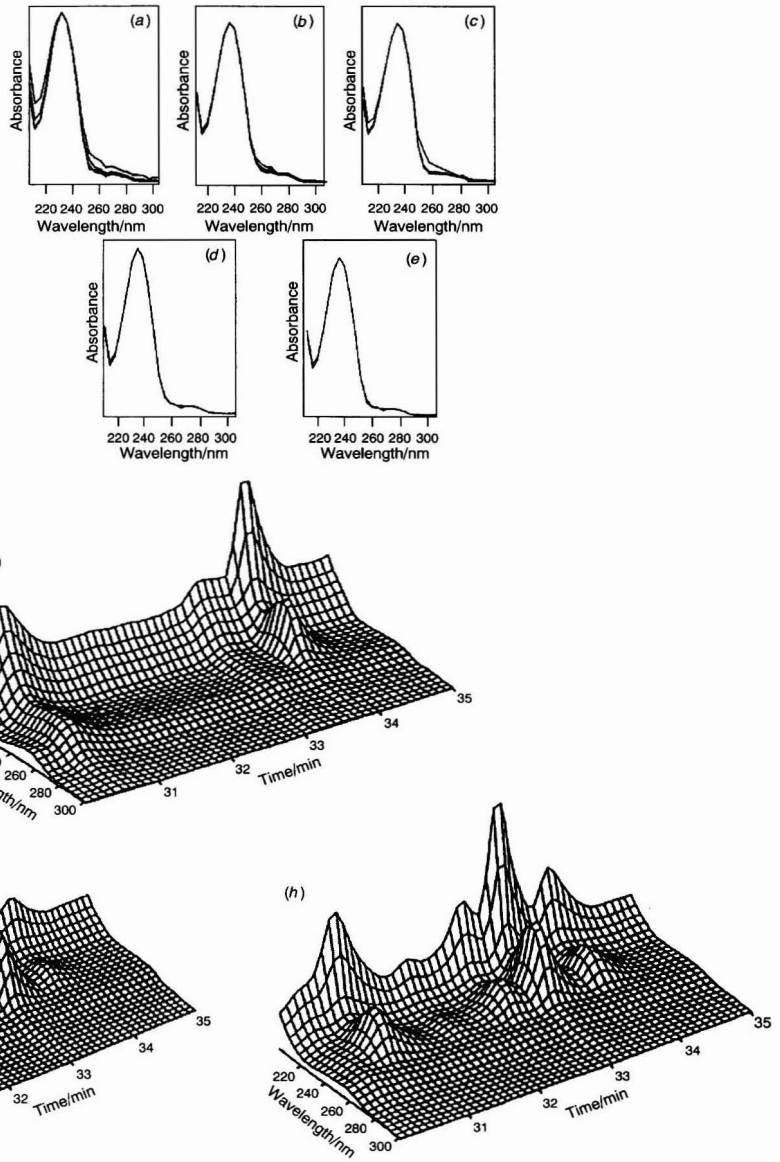

Fig. 2 Photodiode-array detection of derivatized myo-inositol standard, milk and supplemented infant formula extracts. Chromatographic conditions as described in Table 1. (*a*), (*b*) and (*c*): up-slope, apex and down-slope scan plots. (*a*) Inositol standard; (*b*) milk; and (*c*) supplemented infant formula; (*d*) and (*e*): peak apex spectral scan (normalized) *versus* standard. (*d*) Milk *versus* standard; and (*e*) infant formula *versus* standard; (*f*), (*g*) and (*h*): 3D isogram plot, swivel, 35, tilt, 20. (*f*) Inositol standard; (*g*) milk; and (*h*) supplemented infant formula

Other carbohydrates are potentially amenable to analysis by this technique, as demonstrated by earlier work.[18,19,23] In the present study, glucose, galactose, sorbitol, lactose and sucrose were also identified, with confirmatory characterization inferred from the disappearance of disaccharide peaks and concurrent growth in the corresponding monosaccharide peaks following acid hydrolysis. Minor, unidentified chromatographic artefacts produced in milk during such sample treatment, unfortunately interfere with inositol and therefore preclude a reliable HPLC estimation of its total concentration. In the event that this method should be extended to include bound inositol, additional techniques to fractionate the hydrolysate would need to be incorporated.

Evaluation of ultraviolet spectra using photodiode-array detection during validation studies, demonstrated peak purity and allowed positive identification of the aromatic isocyanate chromophore, but could not positively identify the attached sugar. However, confirmation of the inositol substrate was achieved with FAB-MS data, which revealed MH^+ and $(M + Na)^+$ ions in accordance with a fully derivatized C_6 sugar alcohol.

The purpose of this study was primarily to facilitate a chromatographic alternative to the microbial technique in the compliance monitoring of inositol-supplemented infant formulas. For these, as well as non-supplemented milks, the major portion of this carbohydrate is unbound (56–82%), as demonstrated by the separate microbial assays of free and total inositol (Table 2). This conclusion agrees with that of previous workers investigating other biological fluids and tissues[6,9] and rationalizes the analysis of inositol in its free form. The substantial agreement observed here between HPLC and microbial assay for free inositol in milk-based nutritional products, provides confidence in the proposed technique. The possible existence of a small positive bias in the latter approach at lower levels, may if real, reflect the less than total specificity of *S. uvarum* to this compound. There appears to be little published work relating to this sample type, although one recent study found similar levels of free myo-inositol in infant formulas, after enzymic fluorimetric analysis (30–90 mg per 100 g, dry basis).[34]

The technique was also applied to a study of free inositol levels in the milk of the cow, goat and human. Literature data are scarce regarding goats' milk, whereas levels in mature milk from humans have been variously reported to be 20–25 (free)[34] and 8–18 mg per 100 ml (total).[14] In comparison, mature milk from cows is reported to contain lower levels, *i.e.*, 3–8,[1] 2–5 (total),[14] and 2.5–3.7 mg per 100 ml (free).[17] The proportions of free myo-inositol in the milk of humans and cows obtained in the present study (8.8 and 2.1 mg per 100 ml, respectively) are in general agreement with cited literature data; an intermediate concentration (5.3 mg per 100 ml) was obtained for goats' milk. This latter value should provide useful data for the formulation of breast-milk substitutes based increasingly on goats' milk.

It seems pertinent also to note here that a progressive decrease in the concentration of myo-inositol with lactation period has been reported in the milk of both humans and cows,[14,34] whereas a study of the dog and cat, claimed an increasing trend with lactation.[16] It is intended that the technique proposed in the present work will be applied to the serial measurement of myo-inositol in milk during lactation in order to investigate these apparently conflicting reports.

Among mammalian milks, humans' milk is unique with respect to the contribution of its diverse complex oligosaccharides.[35,36] These are thought to be associated with stimulation of bifidus activity and protection in the neonate from enteropathic bacteria. That several late eluting oligosaccharides unique to humans' milk were observed in this study, makes the proposed scheme applicable to further study of these complex carbohydrates.

Finally, the method has also been shown to be useful in the analysis of vitamin premixes and other preparations containing inositol at pharmacological levels. The resulting chromatograms are free from the many complicating features present in milks, thereby facilitating a simple and rapid analysis under isocratic conditions.

Table 2 Comparative data for myo-inositol using the proposed HPLC method and a microbial technique

	myo-Inositol/mg per 100 g*		
	HPLC	Microbial	
Sample	Free	Free	Total
Skimmed milk powder	18.9 (1.9)	21.0 (2.1)	35.3 (2.8)
Skimmed milk powder	25.3 (2.0)	28.5 (2.8)	36.8 (3.5)
Whole-milk powder	14.1 (1.4)	14.2 (1.4)	25.5 (2.1)
Whole-milk powder†	17.0 (1.4)	21.9 (2.8)	34.0 (3.5)
Whole-milk powder†	18.0 (1.9)	21.0 (2.8)	32.0 (2.8)
Infant formula†	33.7 (2.7)	34.4 (2.8)	48.4 (3.5)
Infant formula†	23.4 (2.3)	25.2 (2.8)	38.0 (4.2)
Infant formula‡	38.3 (2.3)	37.2 (3.5)	48.3 (4.9)
Infant formula‡	65.2 (3.1)	62.9 (4.2)	76.7 (5.7)

* Means (and standard deviations) of duplicate assays.
† Vitaminized.
‡ Vitaminized and supplemented with myo-inositol.

Table 3 Free myo-inositol levels in the raw fluid milk of cows, goats and humans

Milk	myo-Inositol/ mg per 100 g*
Cow†	2.1 (0.28)
Goat†	5.3 (0.28)
Human‡	8.8 (0.42)

* Means (and standard deviations) of duplicate assays.
† Pooled herd milk.
‡ Pooled milk from three mothers in mid-lactation.

The authors thank Anchor Products for support during development of this work, J. Allen (Horticultural and Food Research Institute, New Zealand) for the FAB-MS studies, Dr. D. Dube (Bristol-Myers Squibb, Evansville, IN, USA) for the microbial analyses, and R. Indyk for manuscript preparation.

References

1 Cody, M. M., in *Handbook of Vitamins*, ed. Machlin, L. J., Marcel Dekker, New York, 2nd edn., 1991, pp. 567–572.
2 Michell, R. H., *Trends Biol. Sci.*, 1992, **17**, 274.
3 Chu, S. H., and Hegsted, D. M., *J. Nutr.*, 1980, **110**, 1209.
4 Woods, N. M., Cuthbertson, K. S. R., and Cobbold, P. H., *Nature (London)*, 1986, **319**, 600.
5 Hallman, M., Saugstad, O. D., Porreco, R. P., Epstein, B. L., and Gluck, L., *Early Hum. Dev.*, 1985, **10**, 245.
6 Holub, B. J., *Annu. Rev. Nutr.*, 1986, **6**, 563.
7 Eisenberg Jr., F., *J. Biol. Chem.*, 1967, **242**, 1375.
8 Nagasawa, T., Kiyosawa, I., Niyomura, M., and Toyoda, M., *Jpn. J. Zootech. Sci.*, 1969, **40**, 106.
9 Baker, H., DeAngelis, B., Baker, E. R., Khalil, M., Reddi, A. S., and Frank, O., *J. Micronutr. Anal.*, 1990, **8**, 223.
10 Weissbach, A., *Biochim. Biophys. Acta*, 1958, **27**, 608.
11 Dolhofer, R., and Wieland, O. H., *J. Clin. Chem. Clin. Biochem.*, 1987, **25**, 733.
12 MacGregor, L. C., and Matschinsky, F. M., *Anal. Biochem.*, 1984, **141**, 382.

13 Lewin, L. M., Szeinberg, A., and Lepkifker, E., *Clin. Chim. Acta*, 1973, **45**, 361.
14 Ogasa, K., Kuboyama, M., Kiyosawa, I., Suzuki, T., and Itoh, M., *J. Nutr. Sci. Vitaminol.*, 1975, **21**, 129.
15 Ford, C. W., *J. Chromatogr.*, 1985, **333**, 167.
16 Watanabe, T., Nagoa, E., Kuwahara, K., and Okonogi, S., *Nippon Nogei Kagaku Kaishi*, 1989, **63**, 857.
17 Troyano, E., Olano, A., Fernandez-Diaz, M., Sanz, J., and Castro, I. M., *Chromatographia*, 1991, **32**, 7–8, 379.
18 Bjorkqvist, B., *J. Chromatogr.*, 1981, **218**, 65.
19 Dethy, J.-M., Deveen, B. C., Janssens, M., and Lenaers, A., *Anal. Biochem.*, 1984, **143**, 119.
20 Petchey, M., and Crabbe, M. J. C., *J. Chromatogr.* (*Biomed. Appl.*), 1984, **307**, 180.
21 Lloyd, P., and Crabbe, J. C., *J. Chromatogr.*, (*Biomed. Appl.*), 1985, **343**, 402.
22 Kargacin, M. E., Bassell, G., Ryan, P. J., and Honeyman, T. W., *J. Chromatogr.*, 1987, **393**, 454.
23 Miwa, I., Kanbara, M., Wakazono, H., and Okuda, J., *Anal. Biochem.*, 1988, **173**, 39.
24 Lauro, P. N., Craven, P. A., and DeRubertis, F. R., *Anal. Biochem.*, 1989, **178**, 331.
25 Wang, W., Safar, J., and Zopf, D., *Anal. Biochem.*, 1990, **188**, 432.
26 Kinoshita, T., Kamitani, Y., Yoshida, J., Urano, T., Nimura, N., and Hanai, T., *J. Liq. Chromatogr.*, 1991, **14**, 1929.
27 Tomiya, N., Suzuki, T., Awaya, J., Mizuno, K., Matsubara, A., Nakano, K., and Kurono, M., *Anal. Biochem.*, 1992, **206**, 98.
28 Honda, S., *Anal. Biochem.*, 1984, **140**, 1.
29 Vidal-Valverde, C., Martin-Villa, C., Olmedilla, B., and Blanco, I., *J. Liq. Chromatogr.*, 1985, **8**, 75.
30 Ball, G. F. M., *Food Chem.*, 1990, **35**, 117.
31 Coquet, A., Veuthey, J. L., and Haerdi, W., *Chromatographia*, 1992, **34**, 651.
32 Rakotomanga, S., Baillet, A., Pellerin, F., and Baylocq-Ferrier, D., *Chromatographia*, 1991, **32**, 125.
33 Rakotomanga, S., Baillet, A., Pellerin, F., and Baylocq-Ferrier, D., *J. Pharm. Biomed. Anal.*, 1992, **10**, 587.
34 Pereira, G. R., Baker, L., Egler, J., Corcoran, L., and Chiavacci, R., *Am. J. Clin. Nutr.*, 1990, **51**, 589.
35 Neeser, J.-R., Golliard, M., and Vedovo, S. D., *J. Dairy Sci.*, 1991, **74**, 2860.
36 Bosch-Reig, F., Marcote, M. J., Minana, M. D., and Cabello, M. L., *Talanta*, 1992, **39**, 1493.

Paper 3/03542E
Received June 21, 1993
Accepted August 24, 1993

Speciation of Vanadium(v) and Vanadium(iv) With 4-(2-Pyridylazo)resorcinol by Using High-performance Liquid Chromatography With Spectrophotometric Detection

Suh-Jen Jane Tsai and Su-Jen Hsu

Department of Applied Chemistry, Providence University, Taichung Hsien, 433, Taiwan

By using 4-(2-pyridylazo)resorcinol (PAR) as the chelating reagent, vanadate and vanadyl ions were effectively separated by reversed-phase high-performance liquid chromatography with ultraviolet–visible detection at 540 nm. The optimum conditions for the determination of these metal ions were established. PAR chelates were eluted within 10 min with methanol–water (30 + 70 v/v) as the mobile phase containing acetate buffer (8.0×10^{-3} mol l^{-1}, pH 6.0) and PAR (3.0×10^{-4} mol l^{-1}). The retention times for V^{V} and V^{IV} were 4.91 and 9.01 min, respectively. The calibration graphs obtained for 100 µl samples were linear for 0.02–2.00 µg ml^{-1} vanadium. The detection limits were 0.2 and 0.1 ng per 100 µl sample volume for V^{V} and V^{IV}, respectively. The proposed method for the simultaneous speciation of vanadate and vanadyl ions was used to analyse a used vanadium-containing catalyst and good results were obtained in terms of precision and accuracy.

Keywords: Speciation; vanadium; 4-(2-pyridylazo)resorcinol; reversed-phase high-performance liquid chromatography; spectrophotometry

Introduction

Metal speciation often involves the determination of an element with a variety of physico-chemical status, such as differences in the oxidation state or being bound to different organic moieties.[1,2] The necessity for metal speciation has arisen from the unique characteristic of particular metal species in their occurrence, nutrition properties, toxicity, bioavailability, bioaccumulation, environmental pathways of elements and geochemical transport. Vanadium in trace amounts (ppb level) is beneficial to normal cell growth, being one of the so-called essential elements. However, toxicity arises when vanadium concentrations are increased to the ppm level. Vanadate ion is more toxic than vanadyl ion.[3]

In addition to the significance of the speciation of vanadium in biological and environmental studies, the concentration of vanadium in geological materials, heavy crude petroleum, sea-water, alloys and catalysts often requires accurate determination. Although many studies have been devoted to metal speciation, little work on the speciation of vanadate ion (VO_3^-) and vanadyl ion (VO^{2+}) has been reported. The precipitates of V^{V} and V^{IV} were collected at different pH values and then analysed by energy-dispersive X-ray fluorescence spectrometry with a limit of detection of 1.1–1.5 µg.[4] V^{III}–V^{II} equilibria in *N*-(hydroxyethyl)ethylenediaminetriacetic acid (HEDTA) solutions were studied by cyclic voltammetry and differential-pulse polarography.[5] Chromatographic separation was effective for metal species once a proper detector had been selected.[6,7] Lewis *et al.*[8] studied the speciation of trace metals by coupling ion chromatography with direct current plasma atomic-emission spectrometry (AES). The operating conditions for the chromatographic speciation of V^{V} and V^{IV} were optimized. The concentrations determined for both vanadate and vanadyl ions were 0.1 ppm (without preconcentration) and 0.05 ppm (with preconcentration). V^{V} and V^{IV} reacted differently with ethylenediaminetetraacetic acid (EDTA). Detection limits of 1.0 and 0.2 µg ml^{-1} were obtained for the EDTA chelates of V^{V} and V^{IV}, respectively, when they were separated by ion chromatography and detected with a conductivity detector.[9] Admixtures of V^{V} and V^{IV} had been determined spectrophotometrically by chelating with 2-hydroxyacetophenone oxime.[10] However, a two-column system consisting of chelating functional immobilized silica gels was employed for the preconcentration and speciation of V^{V} and V^{IV}. The detection limit was down to 60 pg ml^{-1} with inductively coupled plasma AES.[11]

4-(2-Pyridylazo)resorcinol (PAR), one of the most sensitive chromophores, chelates with a variety of metal ions.[12,13] It has the merit of forming water-soluble chelates with molar absorptivities of the order of 10^4 l mol^{-1} cm^{-1}. In this laboratory, PAR had been successfully applied to determine trace niobium(v) and tantalum(v) simultaneously on a C_{18} column.[14] As an anionic PAR chelate of pentavalent vanadium was found at pH 5.0–7.8, as reported by Yerramilli *et al.*,[15] and tetravalent vanadium (VO^{2+}) had been determined spectrophotometrically by chelating with PAR,[16] the applicability of PAR in the speciation of vanadium was further investigated.

This paper describes work on the speciation of vanadium. Vanadate and vanadyl ions were reacted with PAR by pre-column derivatization. The PAR chelates were separated and determined by reversed-phase high-performance liquid chromatography (HPLC) with ultraviolet–visible (UV/VIS) detection. The spectrophotometric and chromatographic characteristics have been studied. A rapid, simple, sensitive and accurate procedure for the direct simultaneous speciation of vanadate and vanadyl ions is proposed. The method was applied to measure vanadate and vanadyl ions in a used vanadium-containing catalyst to elucidate its practical application.

Experimental

Instrumentation

The chromatographic system consisted of a Waters Model 600 E system controller, a Waters U6K universal liquid chromatographic injector (2 ml injection loop), a Waters Model 740 data module and a Waters Lambda-Max Model 481 LC spectrophotometer. A Waters µBondapak C_{18} column (300 × 3.9 mm i.d.) coupled to a Waters guard column was used.

A Barnstead Nanopure II system was employed for water purification. A Radiometer PHM 85 precision pH meter and a combined electrode were used for pH measurements. The absorption spectra were obtained with a Shimadzu UV-260 UV/VIS recording spectrophotometer equipped with 1 cm quartz cells.

Reagents and Solutions

A V^{V} stock standard solution [vanadium standard solution, 1.000 g l^{-1} ± 0.3%, pH 9.5 (adjusted with ammonia solution), prepared from NH_4VO_3] was obtained from Fluka (Buchs, Switzerland). A V^{IV} stock standard solution was prepared from $VOSO_4 \cdot 5H_2O$ (Merck, Darmstadt, Germany). The precise concentration of vanadium was determined by flame atomic absorption spectrometry. PAR was used as the monosodium salt. Metal ion stock standard solutions (nitrates or chlorides) were prepared from atomic absorption standard solutions. Acetonitrile and methanol were of HPLC grade and were obtained from Mallinckrodt Specialty Chemicals (Paris, KY, USA). A used vanadium-containing catalyst was obtained from Chinese Petroleum (Kaoshing, Taiwan).

Procedure

The pre-column colour-developing process was performed as follows. A 2 ml volume of acetic acid–sodium acetate buffer solution (0.1 mol l^{-1}, pH 6.0) was mixed with 3 ml of PAR solution (2.5×10^{-3} mol l^{-1}), then 7.5 ml of methanol were added, followed by a volume of metal solution. The resultant sample solution was diluted to volume with distilled, de-ionized water (DDW) in a 25 ml calibrated flask. The resultant solution was set aside for 10 min to obtain complete chelation between metal ions and PAR.

An aliquot of the sample solution (typically 100 μl) was injected into the HPLC system. The mobile phase was a methanol–water (30 + 70 v/v) containing 8.0×10^{-3} mol l^{-1} acetate. The final pH was adjusted with either acetic acid or ammonia solution. Both sample and elution solutions were filtered through a 0.45 μm filter before injection. PAR chelates were detected at 540 nm with a flow rate of 1.0 ml min^{-1}.

Vanadium in the used catalyst sample was leached according to the following process. The used catalyst was dried at 104 °C for 18 h. After cooling, an accurately weighed amount of the catalyst (about 0.05 g) was mixed with 20 ml of 1% nitric acid in a poly(tetrafluorethylene) (PTFE) beaker. After stirring and gently heating the mixture for 8 h, it was filtered and diluted to 50 ml with 1% nitric acid in a calibrated flask. The catalyst solution was then ready for pre-column chelation. A volume of 1 ml of the catalyst solution was taken for each colour-developing process.

Results and Discussion

The speciation of vanadate and vanadyl ions was difficult. In order to establish the optimum chromatographic parameters, a series of studies were performed.

Absorption Characteristics and Chromatographic Behaviour of Vanadium Species

PAR and other chelating reagents were examined and the absorption characteristics of various vanadium chelates are given in Table 1. The molar absorptivity decreased in the sequence, PAR > alizarinsulfonic acid disodium salt > 4,5-dihydroxybenzene-1,3-disulfonic acid disodium salt (Tiron) > 1,5-diphenylcarbazide > cupferron > diantipyrylmethane(DAPM). Vanadium tended to undergo polymerization at analytical concentrations > 0.01 mol l^{-1} (about 500 μg ml^{-1}). This may cause erratic analytical results. However, polynuclear hydroxide complex formation could be prevented if a chelating reagent was added.[17] The absorption spectra of PAR chelates were identical. In fact, these spectra were overlapped (450–650 nm, λ_{max} = 540 nm) with comparable molar absorptivities, 6.4×10^4 and 4.8×10^4 l mol^{-1} cm^{-1} for V^{V}–PAR and V^{IV}–PAR, respectively. The colour-developing process took about 10 min and there was no pronounced variation in the absorption of PAR chelates within 2 h.

The stoichiometry of the red, water-soluble chelates was verified by the continuous-variation and molar-ratio methods. Both methods showed a 1:1 ratio of V and PAR, which was consistent with those reported in the literature.[15,16,18]

Table 2 gives the absorption characteristics of the metal chelates in acetate, tartrate, oxalate and citrate buffers (pH 6.0). Although chelation of vanadium with PAR could be done in tartrate buffer without a great decrease in sensitivity, solid salt was often found at the solvent draw-off valve of the HPLC system when tartrate was used. Therefore, the

Table 1 Absorption characteristics of vanadium complexes

Complexing reagent*	λ_{max}†/nm	Absorbance V^{V}	Absorbance V^{IV}
PAR	540	2.323	2.031
Alizarinsulfonic acid sodium salt	485	0.546	0.555
Tiron	310	0.435	0.395
1,5-Diphenylcarbazide	241	0.271	0.261
Cupferron	323	0.274	0.191
Diantipyrylmethane	ND‡	RL§	RL

* $c_{complexing\ reagent} = 3.0 \times 10^{-4}$ mol l^{-1}, $c_{metal} = 7.8 \times 10^{-5}$ mol l^{-1} in acetate buffer.
† Range = 200–800 nm.
‡ ND = not detectable.
§ RL = relatively low.

Table 2 Wavelengths of maximum absorption and molar absorptivities of PAR chelates in various buffer solutions

Buffer	V^{V}–PAR λ_{max}/nm	V^{V}–PAR Molar absorptivity/l mol^{-1} cm^{-1}	V^{IV}–PAR λ_{max}/nm	V^{IV}–PAR Molar absorptivity/l mol^{-1} cm^{-1}
Acetate	544	6.4×10^4	543	4.8×10^4
Tartrate	542	6.6×10^4	542	4.5×10^4
Oxalate	542	5.8×10^4	540	3.3×10^4
Citrate	544	6.1×10^4	542	3.0×10^4

Table 3 Absorbance of PAR chelates as a function of the concentration of acetate buffer

Concentration of acetate/mol l^{-1}	Absorbance* V^{V} chelate	Absorbance* V^{IV} chelate
2.0×10^{-3}	1.129	0.952
4.0×10^{-3}	1.157	0.952
6.0×10^{-3}	1.224	0.957
8.0×10^{-3}	1.268	0.958
1.0×10^{-2}	1.259	0.946
1.2×10^{-2}	1.257	0.945
1.6×10^{-2}	1.257	0.944
2.0×10^{-2}	1.256	0.943

* Absorbances are given as the means of five determinations. $c_{metal} = 2.0 \times 10^{-5}$ mol l^{-1}; $c_{PAR} = 3.0 \times 10^{-4}$ mol l^{-1}.

speciation was performed in acetate buffer (8.0×10^{-3} mol l^{-1}, as shown in Table 3).

The chromatographic behaviour of vanadium species was susceptible to the chromatographic parameters because vanadium had different ionic charges and molecular structures under different conditions. Although the PAR chelates were thermodynamically stable in the buffers used, there was no detectable signal of PAR chelates when oxalate and citrate were used as the buffer in the chromatographic separation. This implied that the kinetically labile PAR chelates might undergo hydrolysis or on-column degradation in the chromatographic separation. Therefore, the speciation was carried out in acetate buffer. The organic modifier was another parameter that needed to be considered. The addition of acetone, acetonitrile or methanol did not change the elution order. However, methanol was chosen on the basis of resolution and sensitivity. The methanol dependence of the capacity factor is shown in Fig. 1.

When the elution strength was increased, the retention time of PAR chelates was shortened. Vanadate and vanadyl chelates were eluted sequentially with retention times of 4.91 and 9.01 min, respectively. The vanadyl chelate was more sensitive than the vanadate chelate to the methanol content.

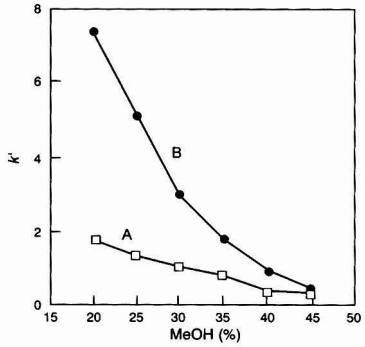

Fig. 1 Effect of the percentage of methanol in the mobile phase (pH 6.0) on k'. A, V^{V} chelate; and B, V^{IV} chelate. Optimum mobile phase: methanol–water (30 + 70); $c_{\text{acetate buffer}}$, 8.0×10^{-3} mol l^{-1}; c_{metal}, 5.0×10^{-5} mol l^{-1}, c_{PAR}, 3.0×10^{-4} mol l^{-1}. Flow rate, 1.0 ml min^{-1}; 540 nm

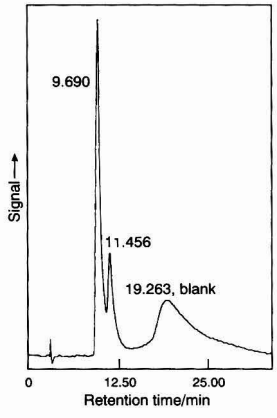

Fig. 2 Chromatogram obtained at pH 5.0. Elution conditions as given in Fig. 1 attenuation 32

This implied that the V^{IV} chelate was less polar and bonded more strongly to the non-polar C_{18} group. Hence it was more sensitive to the elution strength. Both capacity factors (k') converged at 45% methanol. A relatively long retention time of about 27 min was obtained using methanol–water (20 + 80 v/v). The resolution decreased as the methanol content increased. Serious overlap of V^{V}–PAR and V^{IV}–PAR was encountered using methanol–water (50 + 50 v/v). Based on the above observations, methanol–water (30 + 70 v/v) was chosen as the optimum eluent composition.

As the equilibra of PAR and vanadium species were dependent on the pH of the medium, further studies were performed to determine the optimum pH. PAR, denoted H_2R ($pK_{1,para}$ = 6.9 and $pK_{2,ortho}$ = 12.4[12]), is known to form V(R), V(HR) and $V(HR)_2$ complexes with V^{V} at pH 6.5 in phosphate buffer.[19,20] The deprotonation of HR^- occurred through complexing with metal ions. The chromatographic signal was not detectable at pH 4.0 as a result of the precipitation of $VO(OH)_2$.[18] Vanadium (IV)–PAR and V^{V}–PAR were not resolved at pH 5.0 whereas an excellent separation was obtained at pH 6.0. Representative chromatograms obtained at pH 5.0 and 6.0 are shown in Figs. 2 and 3, respectively.

The anionic vanadate ion (VO_3^-) and cationic vanadyl ion (VO^{2+}) reacted with the negative moiety of PAR and gave PAR chelates with different formal charges. Therefore, they were eluted sequentially as a result of the differences in their electrostatic interactions with the stationary phase and in their hydrophobic properties. Retention times of 14.90 and 48.11 min were obtained for V^{V}–PAR and V^{IV}–PAR, respectively, when the ion-pairing agent tetrabutylammonium bromide (TBABr) (1.0×10^{-3} mol l^{-1}) was included in the eluent. When the anionic vanadium–PAR complexes were paired with the TBA^+ cation, the interaction between the PAR complexes and C_{18} chains bonded on the silica stationary phase or the ion exchange between TBA^+ and a proton of a 'bare' silanol group was enhanced.[21] Consequently, longer retention times were required to elute the PAR chelates.

When the medium became more acidic, the colourless vanadate ion that originally existed in alkaline solution would be protonated and undergo the following reaction.[20]

$$HVO_3 + HR^- \rightleftharpoons VO_2R^- + H_2O$$

The blue vanadyl ion was stable in acidic solution. After complexing with PAR, $VO(H_2R)^{2+}$, $VO(HR)^+$ and VO(R) might be formed. As TBA^+ had a strong effect on the retention of vanadyl ion, as mentioned previously, the last species could be dominant under the elution conditions.

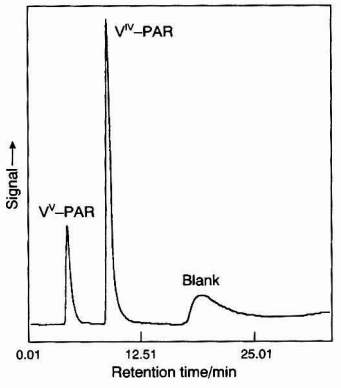

Fig. 3 Typical chromatogram obtained with the optimum conditions given in Fig. 1, attenuation 128

The optimum concentration of PAR in the pre-column derivatization was determined by monitoring the absorbance of chelates as a function of PAR concentration (0.50×10^{-4}–50.0×10^{-4} mol l^{-1}), and a concentration of 3.0×10^{-4} mol l^{-1} gave the maximum absorption. The addition of a complexing reagent to the eluent gave no noticeable variation in the chromatographic characteristics of PAR chelates. This indicated that metal chelates were kinetically inert throughout the entire chromatographic separation.[22]

The chromatographic performance was also susceptible to the flow rate of the eluent. By monitoring the retention time of chelates as a function of flow rate, the optimum flow rate was found to be 1.0 ml min^{-1}. The above experiments showed that the ionic compounds formed between PAR and vanadium species were well separated on an octadecyl-bonded silica (ODS) column with the optimum conditions established in this work.

Identification of Vanadium Species and Interference Studies

The two major peaks that occurred in the chromatograms could be the result of different coordination forms for one central ion instead of different species. Therefore, the vanadium species in the chromatograms were identified by the 'spike' method and an oxidation–reduction reaction. Hydrogen peroxide and $KMnO_4$ were used as oxidants and the reductants were $NH_2OH{\cdot}HCl$, $SnCl_2$, $N_2H_4SO_4$, ascorbic acid and HCHO. However, these reagents either caused precipitation or complicated the chromatograms, except for H_2O_2 and $NH_2OH{\cdot}HCl$. On adding H_2O_2 to the vanadyl solution, a peak corresponding to V^{V} was obtained as a result of the oxidation of vanadyl ions. A peak with the retention time of V^{IV} resulted when $NH_2OH{\cdot}HCl$ was added to a solution of vanadate. Fig. 4 gives the chromatograms obtained.

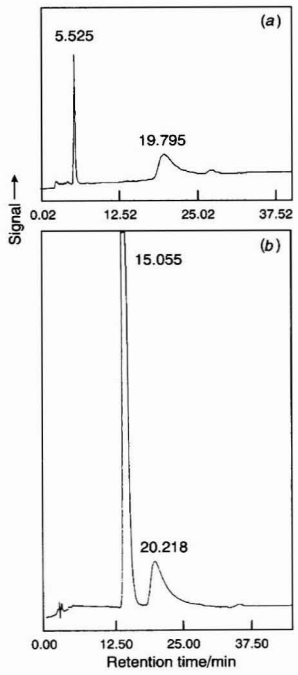

Fig. 4 Chromatograms obtained with the addition of oxidant and reductant. (*a*) 5.0×10^{-5} mol l^{-1} V^{IV} + 6.0×10^{-3} mol l^{-1} H_2O_2. (*b*) 5.0×10^{-5} mol l^{-1} V^{V} + 5.0×10^{-3} mol l^{-1} $NH_2OH{\cdot}HCl$

The potential interferences from foreign ions such as Mg^{II}, Co^{II}, Cu^{II}, Ni^{II}, Zn^{II}, Fe^{III}, Al^{III}, Ti^{IV}, Zr^{IV}, Hf^{IV}, Nb^{V}, Ta^{V}, Mn^{VI}, Cr^{VI}, Mo^{VI} and W^{VI} were investigated. The effect of foreign ions on the peak area of 1.02 μg ml^{-1} vanadium was indicated by the ratio of peak area of V–PAR solution to that of foreign ion-containing V–PAR solution. A summary of the results is given in Table 4. All of the foreign ions except Co^{II} and Zn^{II} had a negligible effect on the peak area of V^{IV}–PAR. Mg^{II}, Hf^{IV}, Nb^{V}, Ta^{V}, Mo^{VI} and W^{VI} did not show any pronounced effect (less than 10%) on the peak area of V^{V}–PAR with a mass ratio of up to 10. Among the foreign ions, PAR chelates of Cu, Co, Fe, Ti, Nb and Cr gave their own chromatographic peaks. These metal ions led to large variations in the peak area of PAR chelates except that of Nb.

Analysis of Real Samples

The calibration graphs obtained for 100 μl samples were linear for 0.02–2.00 μg ml^{-1} of vanadium. Good linearity of the calibration graphs was obtained over approximately two orders of magnitude for these chelates [amount of metal (ng) = $k \times$ peak area + b, where b = −(intercept × k) and k = 1/slope; the linear regression coefficients were 0.9997 and 0.9998 for V^{V}–PAR and V^{IV}–PAR, respectively]. The detection limits (signal-to-noise ratio = 3) were 0.2 and 0.1 ng for V^{V} and V^{IV}, respectively. The relative standard deviation of the retention times of these peaks under the same elution conditions was about 2% and that of the peak-area measurements was less than 10% (five replicate injections).

A used vanadium-containing catalyst was analysed by the proposed process to verify the applicability of the method.

Table 4 Interferences of foreign ions

Metal ion	Mass ratio*	Retention time/min	Ratio of peak area† *versus* V^{V}–PAR	Ratio of peak area† *versus* V^{IV}–PAR
V^{V}	1	4.91	1.00	1.00
V^{IV}	1	9.01	1.00	1.00
Mg^{II}	10		0.87	1.01
Co^{II}	10	17.1	1.48	0.25
	2		1.59	0.80
Cu^{II}	10	16.0	0.63	1.02
	2		0.87	0.97
Ni^{II}	10		0.71	0.84
	1		0.74	0.96
Zn^{II}	10		0.77	0.80
	1		0.87	0.98
Fe^{III}	10	38.0	0.20	1.12
	1		0.41	0.91
Al^{III}	10		0.70	0.85
	1		0.85	0.94
Ti^{IV}	10	3.21	0.71	0.97
	1		0.74	1.02
Zr^{IV}	10		0.61	0.98
	1		0.66	0.97
Hf^{IV}	10		0.99	1.01
Nb^{V}	10	3.45	1.03	1.06
Ta^{V}	10		0.99	0.98
Mn^{VI}	10		1.21	0.93
Cr^{VI}	10	2.81	0.15	1.04
	1		0.82	1.05
Mo^{VI}	10		0.95	1.04
W^{VI}	10		0.86	0.93
	1		0.93	0.97

* $c_{vanadium}$ = 1.02 ppm. Mass ratio = mass of foreign ion/mass of vanadium.

† Ratio of peak area = peak area of V–PAR in the presence of foreign ions/peak area of V–PAR in the absence of foreign ions.

The oxidation state of vanadium species was highly susceptible to the pre-treatment process and the pH of the medium. Any vigorous oxidant (such as concentrated HNO_3) was avoided in order to lessen the chance of the oxidation of vanadyl ions to vanadate ions. Therefore, 1% HNO_3 was chosen for leaching. The injection of 100 μl of the catalyst solution into the separation column produced a chromatogram with two well resolved peaks corresponding to V^V–PAR and V^{IV}–PAR, respectively, as shown in Fig. 5. The vanadium contents in the used catalyst determined from the calibration graphs were 2460 μg g^{-1} V^V and 29250 μg g^{-1} of V^{IV}. As the accurate content of vanadate and vanadyl ions in the used catalyst was not known owing to the inhomogenity of the solid sample, the accuracy of the proposed method was evaluated by the standard additions method. The vanadate and vanadyl contents found in 100 μl of catalyst solution were 9.85 ± 0.32 and 117 ± 4 ng, respectively. The recoveries obtained for V^V–PAR and V^{IV}–PAR were 96% and 103%, respectively.

Conclusions

The simultaneous speciation of vanadate and vanadyl ions was accomplished by reversed-phase HPLC on a C_{18} column. The proposed method requires minimum sample pre-treatment steps and the colour-developing step requires only about 10 min at ambient temperature, so a heating step is not necessary. After chelation with PAR, V^V–PAR and V^{IV}–PAR were well separated within 10 min with relatively good resolution. The successful application of the proposed method to the determination of vanadate and vanadyl ions in a used catalyst demonstrated the applicability of the proposed method.

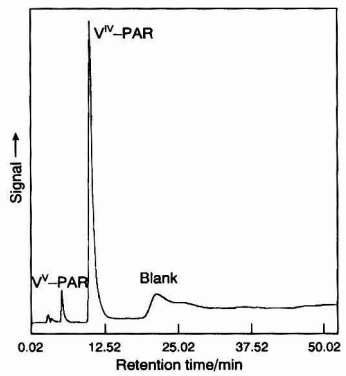

Fig. 5 Typical chromatogram of V^V–PAR and V^{IV}–PAR in a used catalyst. The operating conditions are as given in Fig. 1, attenuation 32. The injected amount of catalyst = 400 μg

The financial support of this work by a grant from the National Science Council of the Republic of China is gratefully acknowledged.

References

1 Fish, R. H., and Komlenic, J. J., *Anal. Chem.*, 1984, **56**, 510.
2 Fish, R. H., Komlenic, J. J., and Wines, B. K., *Anal. Chem.*, 1984, **56**, 2452.
3 Patel, B., Henderson, G. E., Haswell, S. J., and Grzeskowiak, R., *Analyst*, 1990, **115**, 1063.
4 Hirayama, K., and Leyden, D. E., *Anal. Chim. Acta*, 1986, **188**, 1.
5 Meier, R., and Werner, G., *Anal. Chim. Acta*, 1989, **219**, 281.
6 Chau, Y. K., *Analyst*, 1992, **117**, 571.
7 Robards, K., Starr, P., and Patsalides, E., *Analyst*, 1991, **116**, 1247.
8 Lewis, V. D., Nam, S. H., and Urasa, I. T., *J. Chromatogr. Sci.*, 1989, **27**, 468.
9 Komarova, T. V., Obrezkov, O. N., and Shpigun, O. A., *Anal. Chim. Acta*, 1991, **254**, 61.
10 Ramana Murthy, G. V., Sreenivasulu Reddy, T., and Brahmaji Rao, S., *Analyst*, 1989, **114**, 493.
11 Hirayama, K., Kageyama, S., and Unohara, N., *Analyst*, 1992, **117**, 13.
12 Anderson, R. G., and Nickless, G., *Analyst*, 1967, **92**, 207.
13 DiNunzio, J. E., Yost, R. W., and Hutchison, E. K., *Talanta*, 1985, **32**, 803.
14 Tsai, S. J. J., and Lee, Y., *Analyst*, 1991, **116**, 615.
15 Yerramilli, A., Kavipurapu, C. S., Manda, R. R., and Pillutla, C. M., *Anal. Chem.*, 1986, **58**, 1451.
16 Strelow, F. W. E., *Anal. Chem.*, 1987, **59**, 1907.
17 Kragten, J., *At. Spectrosc.*, 1981, **2**, 135
18 Marczenko, Z., *Separation and Spectrophotometric Determination of Elements*, Ellis Horwood, Chichester, 1986, p. 403.
19 Ming, X. Y., Wu, Y. H., and Schwedt, G., *Fresenius' J. Anal. Chem.*, 1992, **342**, 556.
20 Siroki, M., and Djordjevic, C., *Anal. Chim. Acta*, 1971, **57**, 301.
21 Miura, J., *Anal. Chem.*, 1990, **62**, 1425.
22 Main, M. V., and Fritz, J. S., *Anal. Chem.*, 1989, **61**, 1272.

Paper 3/03642A
Received June 25, 1993
Accepted September 2, 1993

Determination of 2,2,2-Trichloroethanol in Plasma and Urine by Ion-exclusion Chromatography

Hisaaki Itoh

Faculty of Pharmaceutical Sciences, Josai University, Sakado, Saitama 350-02, Japan

Shigero Ikeda

The Research Institute for Science and Technology, Ryukoku University, 67-Fukakusa, Fushimi, Kyoto 612, Japan

Norio Ichinose

Chemistry, Hamamatsu University School of Medicine, 3600-Handa-chyo, Hamamatsu 431-31, Japan

A simple and rapid chromatographic method has been developed for the determination of 2,2,2-trichloroethanol (TCEOH) and its glucuronide in plasma and urine. A glass column (150 × 6.6 mm i.d.) packed with Aminex A-5 cation-exchange resin (potassium form) following the slurry method was used as the analytical column, and an admixture of 10 mmol l^{-1} potassium sulfate and 10 mmol l^{-1} potassium hydroxide solution as the eluent (pH 12.2). Diluted plasma samples and urine samples were directly injected into the chromatograph through a 0.45 μm membrane filter without deproteinization. The amount of TCEOH conjugated to glucuronide was determined following treatment with β-glucuronidase (200 U) for 30 min at 37 °C. This allowed the concentration of free, total, and conjugated TCEOH to be determined. The calibration graph was rectilinear from 5 to 500 mg l^{-1} of TCEOH, with a detection limit of 3 mg l^{-1}, 2σ, being the signal-to-noise ratio. The analytical recovery of TCEOH, obtained by analysing spiked plasma and urine samples, was in the range 98.4–102% and the relative standard deviation was less than 3.5%.

Keywords: 2,2,2-Trichloroethanol; β-glucuronidase; plasma; urine; ion-exclusion chromatography

Introduction

Although 2,2,2-trichloroethanol (TCEOH) and trichloroacetic acid are not normal components of biological fluids, it is known that they are found in the plasma and urine of humans and animals exposed to certain chlorinated hydrocarbons such as trichloroethylene and 1,1,1-trichloroethane, which are used in industry as degreasing and cleaning agents.[1,2]

The Metabolism of trichloroethylene in humans and many animals has been elucidated by a number of workers.[3–12] Butler[3,4] systematically investigated the metabolic transformation of trichloroethylene in dogs; and Powell and coworkers[5,6] did this for human subjects. Because the final products of the metabolism of trichloroethylene, *i.e.*, trichloroacetic acid, TCEOH, and the glucuronide of the latter, are the same as those formed after the administration of 2,2,2-trichloroethane-1,1-diol, they postulated that 2,2,2-trichloroethane-1,1-diol is an intermediate in the metabolism of trichloroethylene. Cooper and Friedman[7] investigated the metabolic oxidation and reduction of 2,2,2-trichloroethane-1,1-diol to trichloroacetic acid and TCEOH, respectively. Furthermore, Leibman,[11] and Byington and Leibman[12] provided a complete *in vitro* pathway for the conversion of trichloroethylene to its major metabolites, TCEOH and trichloroacetic acid.

Many methods have been reported for the determination of trichloro compounds in biological samples.[8,13,14] Seto and Schultze[13] developed a method for the determination of trichloroethylene, trichloroacetic acid and TCEOH in bovine urine. In this method, the glucuronide of TCEOH in urine was hydrolysed and oxidized by oxidants to trichloroacetic acid, which is determined by means of colorimetry based on the development of a crimson colour in a boiling mixture of pyridine and strong alkali. Tanaka and Ikeda[14] reported a modified version of the method of Seto and Schultze, whereby using more drastic oxidation conditions, recoveries of TCEOH in the urine of human subjects, rabbits, guinea-pigs, and rats were largely improved. These and other methods employing the pyridine reaction, however, are tedious to perform and involve the use of harmful reagents.

Ion chromatography[15] is a remarkable technique that allows the determination of ionic species in samples having complex matrices with minimum, or at least reduced, sample preparation. A number of application studies have been reported for the determination of inorganic and organic ions in many environmental[16,17] and biological samples.[18,19] In 1989, Itoh[18] reported a simple and rapid method for the determination of trichloroacetic acid in human serum and urine by ion chromatography.

Ion-exclusion chromatography, one of the modes of ion chromatography, is also a useful technique for the separation of weak acids[15,20] (both organic and inorganic) and even small neutral species.[15] In this technique, typically a high capacity cation-exchange resin in the H^+ form and a dilute acid solution are used as stationary phase and eluent, respectively. Strong-acid anions are excluded from the resin according to the Donnan principle and elute at the void volume of the column. Weak-acid anions existing largely in the molecular form can distribute between the stationary and the mobile phase and their retention times are strongly correlated with their pK_a (K_a = acid dissociation constant).

This paper describes a simple and rapid method for the determination of TCEOH in plasma and urine samples by ion-exclusion chromatography with a high capacity cation-exchange resin in the K^+ form as the stationary phase and a mixed solution of potassium sulfate and potassium hydroxide as the eluent. The basic eluent in this system is used to ensure that acidic components such as carboxylic acids in samples are

entirely in their dissociated form, which is completely excluded from the resin and eluted at the void volume of the column.

Experimental

Apparatus

The chromatographic system consisted of a Dionex Model 2000i ion chromatograph (Dionex, Sunnyvale, CA, USA), a Model ERC-7510 refractive index detector (Erma, Tokyo, Japan), and a U-228 dual-pen recorder (Nippon Denshi Kagaku, Tokyo, Japan) and/or a C-R3A Chromatopac (Shimadzu, Tokyo, Japan). The column temperature was controlled by circulating water thermostated at 25 °C. An Omnifit glass column (150 × 6.6 mm i.d., Omnifit, Cambridge, UK) fitted with CRF-9 Teflon filters (pore size 10 μm, GL Sciences, Tokyo, Japan) was used. The column was packed with K^+ form cation-exchange resin, Aminex A-5 (particle size 13 ± 2 μm, degree of cross-linking 8%, exchange capacity 1.7 mequiv ml^{-1}, Bio-Rad Laboratories, Tokyo, Japan), by the slurry packing technique. The operating conditions are listed in Table 1.

Reagents and Materials

Distilled, de-ionized water was used throughout and was filtered through a 0.45 μm membrane filter (Tokyo Roshi Kaisha, Tokyo, Japan) before use. A TCEOH standard solution was prepared by dissolving TCEOH (Wako Pure Chemicals, Tokyo, Japan) in water and was standardized by colorimetry using the method of Tanaka and Ikeda.[14] An eluent was prepared by dissolving potassium sulfate (Wako Pure Chemicals) in water, mixing it with an aliquot of 1.0 mol l^{-1} potassium hydroxide solution, and then diluting the solution to 1000 ml with water. β-Glucuronidase, Type VII-A, was obtained from Sigma (St. Louis, MO, USA).

Plasma samples. A normal human-plasma sample was obtained from a healthy adult. Rat-plasma samples were collected from male Sprague Dawrey (SD) rats weighing 251–260 g 2 h after an oral administration of 53.0 mg of TCEOH dissolved in physiological salt solution. The plasma samples obtained were kept frozen at −20 °C until analysed.

Urine samples. A normal urine sample was obtained from a healthy adult who had had no known exposure to trichloroethylene in at least the 1 month prior to sampling. Four urine samples from trichloroethylene-exposed workers were also collected. Rat-urine samples were collected from five male SD rats weighing 243–261 g that had been exposed to trichloroethylene vapour for 1 h. The urine samples obtained were kept in a cold room (6 °C) or refrigerator until analysed.

Procedure

Analysis of free TCEOH

Dilute a plasma or urine sample three times with water. Filter this diluted solution through a 0.45 μm membrane filter (Abe Trading, Osaka, Japan) and inject the filtrate (50 μl) into the chromatograph.

Table 1 Operating conditions

Eluent	10 mmol l^{-1} potassium sulfate – 10 mmol l^{-1} potassium hydroxide
Column	Omnifit glass column (150 × 6.6 mm i.d.) packed with Aminex A-5 cation-exchange resin (particle size 13 ± 2 μm, K^+ form)
Column temperature	25 °C
Detector	Model ERC-7510 refractive index detector
Flow rate	1.0 ml min^{-1}
Sample loop	50 μl

Analysis of total TCEOH (free plus the glucuronide)

Place 500 μl of both a plasma or urine sample and 0.15 mol l^{-1} phosphate buffer solution (pH 6.8) in a test-tube and mix the contents for a few seconds by shaking. Then add 500 μl of β-glucuronidase (200 U). Incubate this mixed solution at 37 °C for 30 min. Filter the solution through a 0.45 μm membrane filter and inject the filtrate (50 μl) into the chromatograph.

Results and Discussion

Effects of the Concentration of Potassium Sulfate and Eluent pH

In order to determine the optimum chromatographic conditions, the effects of the concentration of potassium sulfate in the eluent and of pH of the eluent on the elution volumes of a number of alcohols and phenol were investigated.

Fig. 1 shows the effect of the concentration of potassium sulfate on the elution volumes of ten alcohols and phenol at pH 10.9. The change in the concentration of potassium sulfate in the eluent had little effect on the elution volumes of the alcohols and phenol; *i.e.*, with increasing potassium sulfate concentration, only a slight increase is observed in the elution volumes of the alcohols and phenol.

Fig. 2 shows the effect of eluent pH on the elution volumes of the alcohols and phenol; the concentration of potassium sulfate was kept constant at 10 mmol l^{-1}. It was found that the

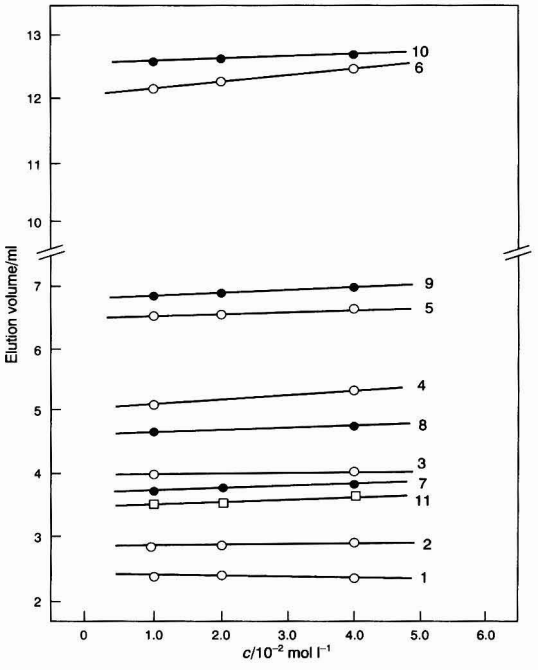

Fig. 1 Effect of the concentration (*c*) of potassium sulfate in the eluent (pH 10.9). All chromatographic conditions, except for the concentration of potassium sulfate and pH, are as shown in Table 1. 1, Ethanol; 2, propan-1-ol; 3, butan-1-ol; 4, propan-2-ol; 5, pentan-1-ol; 6, hexan-1-ol; 7, 2-chloroethanol; 8, 2-bromoethanol; 9, 2,2-dichloroethanol; 10, TCEOH; and 11, phenol

elution volumes of aliphatic alcohols remained unchanged in the entire range of eluent pH examined, and that those of the halogenated alcohols, especially TCEOH, were greatly affected by a change in the eluent pH (*i.e.*, a steep decrease in elution volume is observed above a pH of about 10). Further, the elution volume of phenol decreased dramatically with increasing eluent pH, until finally the column void volume was achieved at above pH 12.5.

This elution behaviour of the alcohols and phenol can be understood on the basis of the ion-exclusion mechanism. Under the experimental conditions, phenol (pK_a = 10.0) is present in equilibrium with the phenoxide ion, which is excluded from the strong cation-exchange resin particle due to Donnan membrane effects, hence, the increase in the ratio of phenoxide ion; conversely, the decrease in the ratio of the phenol molecule, the undissociated form, with increasing eluent pH results in the decrease in the elution volume. Similarly, the same interpretation based on the dissociation of alcohols, although their dissociation constants are unknown, holds for the decrease in the elution volumes of the halogenated alcohols.

Furthermore, the observed constant elution volumes of the aliphatic alcohols indicate that no dissociation takes place over the pH range examined.

Based on the above observation, the admixture of 10 mmol l^{-1} potassium sulfate and 10 mmol l^{-1} potassium hydroxide was selected as eluent (pH 12.2 ± 0.1). Fig. 3 shows an example of a chromatogram of a mixture of phosphate buffer and three halogenated ethanols.

Hydrolysis of the Conjugated TCEOH

In order to develop a simple and rapid method for the determination of both free and conjugated TCEOH, the conditions for the enzymic hydrolysis of glucuronide in biological samples were examined.

Both urine and plasma samples were treated with two different levels of β-glucuronidase (100 and 200 U) and incubated at 37 °C. Fig. 4 shows the relationships between incubation time and increase in the peak height for TCEOH

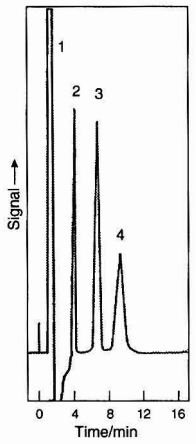

Fig. 3 Typical chromatogram of a mixture of phosphate buffer and three chlorinated ethanols. Detector range, ×0.25. All chromatographic conditions are as shown in Table 1. 1, Phosphate buffer (0.1 mol l^{-1}); 2, 2-chloroethanol (1.0 mmol l^{-1}); 3, 2,2-dichloroethanol (1.0 mmol l^{-1}); and 4, TCEOH (1.0 mmol l^{-1})

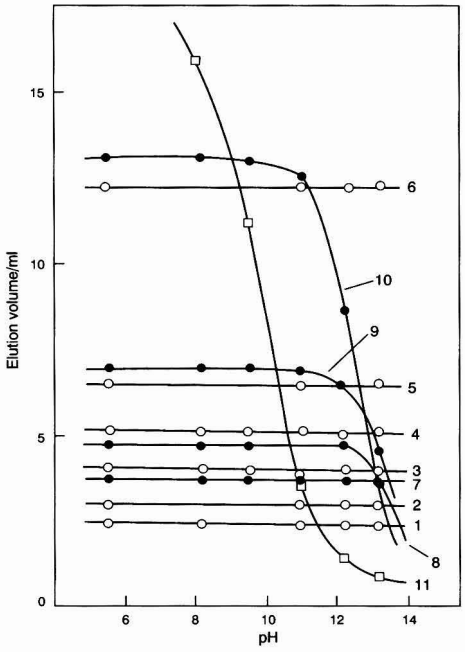

Fig. 2 Effect of the eluent pH on the elution volumes of ten alcohols and phenol. All chromatographic conditions, except for the concentration of potassium hydroxide in the eluent, are as shown in Table 1. 1–11, as in Fig. 1

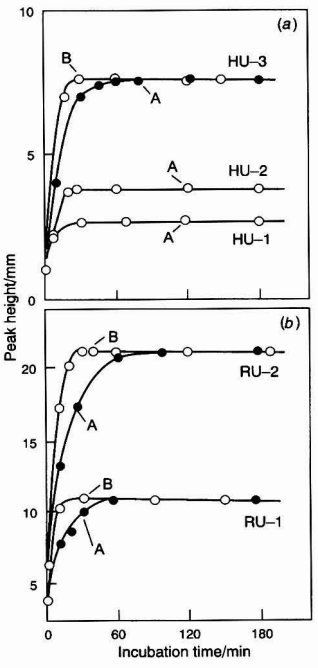

Fig. 4 Effects of the amount of β-glucuronidase and the incubation time. A, 100; and B, 200 U. (*a*) Human urine (HU-1, 2, and 3); and (*b*), rat urine (RU-1 and 2)

from urine samples. It was found that, regardless of rat and human urines, with 100 U of the enzyme, more than 90 min of the incubation time was required to attain the maximum peak height for TCEOH; with 200 U, on the other hand, the maximum peak height was obtained after 30 min. Similar results were also obtained for plasma samples. Hence, the conditions for the hydrolysis were chosen as described under Procedure.

Fig. 5 shows the chromatograms of a rat-urine sample (*a*) before and (*b*) after hydrolysis with 200 U of the enzyme.

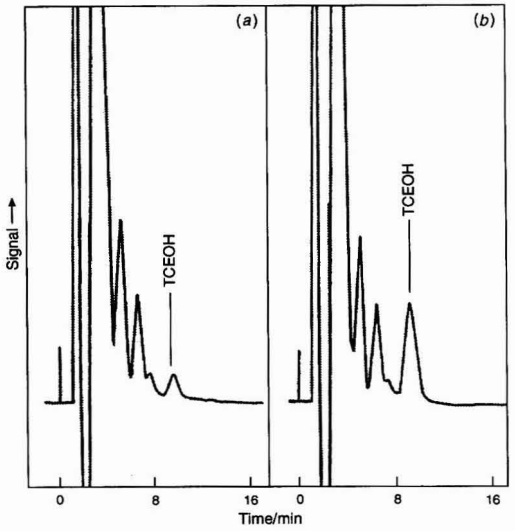

Fig. 5 Chromatograms of a rate-urine sample (*a*) before and (*b*) after hydrolysis with 200 U of β-glucuronidase. Detector range, ×0.5. All chromatographic conditions are as shown in Table 1. The elution positions of TCEOH are indicated

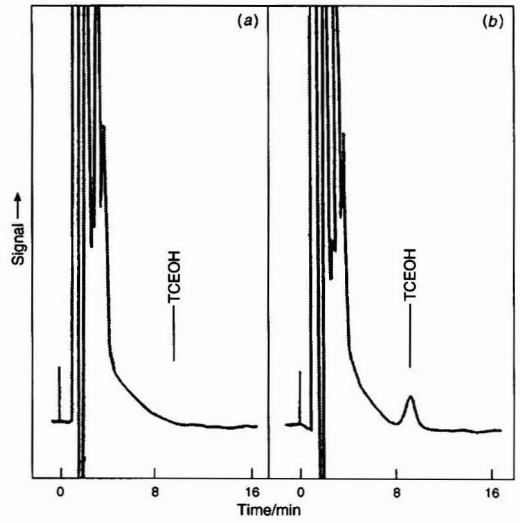

Fig. 6 Chromatograms of (*a*) a blank plasma and (*b*) a plasma sample spiked with 19.6 mg l^{-1} TCEOH. Detector range, ×0.25. All chromatographic conditions are as shown in Table 1. The elution positions of TCEOH are indicated

Calibration Graph and Detection Limits

The calibration graph was constructed for a standard TCEOH solution. Using the peak height, a rectilinear graph was obtained in the range 5–500 mg l^{-1} TCEOH. The detection limit (defined as twice the signal-to-noise ratio) for TCEOH

Table 2 Recovery and precision data of TCEOH in spiked human plasma and urine

Sample	Concentration/mg l^{-1}	*n*	s_r* (%)	Recovery (%)
Plasma	9.8	5	3.3	98.4
	19.6	5	1.3	101
	50.0	5	1.0	100
Urine	10.0	4	3.0	98.7
	50.0	4	2.6	102
	100	4	1.2	101
	150	4	0.8	98.6

* s_r = Relative standard deviation.

Table 3 Determination of TCEOH in plasma and urine

	Concentration ± *s**/mg l^{-1}		
Sample	Free	Total	Total†
Rat plasma—			
A	37.9 ± 1.0	93.4 ± 1.9	—
B	29.4 ± 0.8	107 ± 1	—
C	40.5 ± 0.9	119 ± 1	—
Human urine—			
A	26.4 ± 0.7	61.9 ± 1.2	63.5
B	6.9 ± 0.2	143 ± 2	138
C	3≥	71.5 ± 2.0	65.4
D	12.3 ± 0.4	54.8 ± 0.8	59.4

* Mean of five replicate determinations. *s* = Standard deviation.
† Results obtained by the pyridine reaction method.

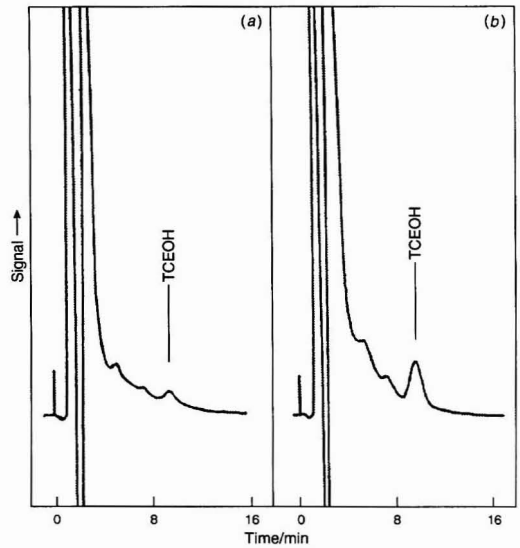

Fig. 7 Chromatograms of a rat-plasma sample (*a*) before and (*b*) after hydrolysis with 200 U of β-glucuronidase. Detector range, ×0.25. All chromatographic conditions are as shown in Table 1. The elution positions of TCEOH are indicated

was 3 mg l^{-1}. The relative standard deviation (s_r) for five replicate determinations of 10 mg l^{-1} of TCEOH was 1.8%.

Recovery and Precision

The recovery and precision of the method were determined by analysing plasma and urine samples from human subjects. The samples were spiked with known amounts of TCEOH. Fig. 6 shows the chromatograms of a blank plasma and a plasma sample spiked with 19.6 mg l^{-1} TCEOH. As shown in Table 2, the recoveries of TCEOH from plasma and urine ranged from 98.4 to 101 and 98.6 to 102% and the s_r values for TCEOH (n = 5 and 4) from 1.0 to 3.3 and 0.8 to 3.0%, respectively.

Determination of TCEOH in Plasma and Urine

The assay was performed on both three rat-plasma samples obtained 2 h after an oral administration of TCEOH dissolved in physiological salt solution, and four human-urine samples obtained from trichloroethylene-exposed workers. The analytical results are shown in Table 3. It was observed that the ratio of free to total TCEOH in human-urine samples varied widely. This is probably due to differences in the conditions (*i.e.*, time, concentration, *etc.*) of exposure to trichloroethylene and on individual variations in the metabolic rate of trichloroethylene. The analytical results obtained agreed well with those of the pyridine reaction method[14] (Table 3).

Figs. 7 and 8 show typical chromatograms of a rat-plasma and a human-urine sample, respectively, (*a*) before and (*b*) after hydrolysis with 200 U of the enzyme.

The proposed method can be used to determine rapidly and easily the concentration of free, total and conjugated TCEOH in plasma and urine, and can also be applied to the assay of TCEOH in other biological samples.

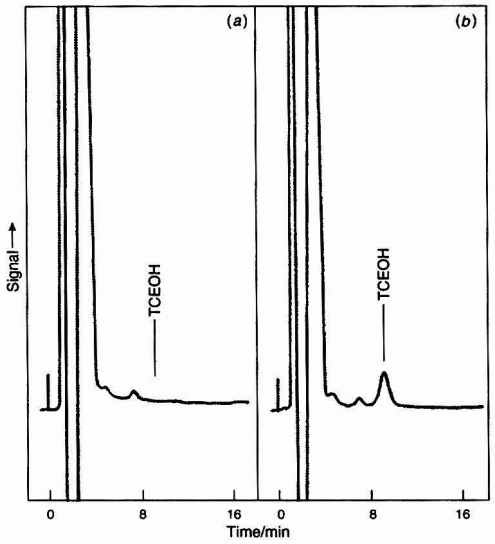

Fig. 8 Chromatograms of a human-urine sample (*a*) before and (*b*) after hydrolysis with 200 U of β-glucuronidase. Detector range, ×0.5. All chromatographic conditions are as shown in Table 1. The elution positions of TCEOH are indicated

References

1 Smith, G. F., *J. Ind. Med.*, 1966, **23**, 249.
2 *A Manual of Health Care of Workers Regularly Using Organic Solvents*, eds. Japan Industrial Safety and Health Association, Tokyo, 1983, ch. 1.
3 Butler, T. C., *J. Pharmacol. Exp. Ther.*, 1948, **92**, 49.
4 Butler, T. C., *J. Pharmacol. Exp. Ther.*, 1949, **95**, 360.
5 Powell, J. F., *Br. J. Ind. Med.*, 1945, **2**, 142.
6 Paykoç, Z. V., and Powell, J. F., *J. Pharmacol. Exp. Ther.*, 1945, **85**, 289.
7 Cooper, J. R., and Friedman, P. J., *Biochem. Pharmacol.*, 1958, **1**, 76.
8 Soucek, B., and Vlachová, D., *Br. J. Ind. Med.*, 1960, **17**, 60.
9 Friedman, P. J., and Cooper, J. R., *J. Pharmacol. Exp. Ther.*, 1960, **129**, 373.
10 Bartonicek, V., *Br. J. Ind. Med.*, 1962, **19**, 134.
11 Leibman, K. C., *Mol. Pharmacol.*, 1965, **1**, 239.
12 Byington, K. H., and Leibman, K. C., *Mol. Pharmacol.*, 1965, **1**, 247.
13 Seto, T. A., and Schultze, M. O., *Anal. Chem.*, 1956, **28**, 1625.
14 Tanaka, S., and Ikeda, M., *Br. J. Ind. Med.*, 1968, **25**, 214.
15 *Handbook of Ion Chromatography*, ed. Johnson, E. L., Dionex, Synnyvale, CA, 1986.
16 Mehra, H. C., Huysmans, K. D., and Frankenberger W. J., Jr., *J. Chromatogr.*, 1990, **508**, 265.
17 Hayakawa, K., Kato, A., Yamamoto, A., and Miyazaki, M., *Anal. Sci.*, 1992, **8**, 25.
18 Itoh, H., *Analyst*, 1989, **114**, 1637.
19 Grimble, G. K., *Anal. Proc.*, 1992, **29**, 468.
20 Turkelson, V. T., and Richards, M., *Anal. Chem.*, 1978, **50**, 1420

Paper 3/03815G
Received July 2, 1993
Accepted September 3, 1993

Thin-layer Chromatographic Spray Reagent for the Screening of Biological Materials for the Presence of Carbaryl

Vitthal B. Patil* and Murlidhar S. Shingare

Department of Chemistry, Marathawada University, Aurangabad-431 004, India

A spray reagent for the detection of the carbamate insecticide carbaryl was developed, consisting of 1% ammonium cerium(IV) nitrate in 20% v/v hydrochloric acid. This reagent reacts with the hydrolysis product of carbaryl, 1-naphthol, and forms a violet complex. Other carbamate insectides do not give similar coloured spots. Moreover, organophosphorus, organochlorine and pyrethroid insecticides and constituents of visceral extracts (amino acids, peptides, proteins, *etc.*) do not interfere. The sensitivity of the reagent is about 0.1 μg.

Keywords: Thin-layer chromatography; ammonium cerium(IV) nitrate; carbaryl; insecticide; biological material

Carbamate insecticides are being increasingly used domestically and in agriculture. The easy availability of these insecticides is reflected in an increasing number of criminal cases referred to forensic science laboratories concerning the misuse of carbamates.

A number of chromogenic spray reagents for the identification of carbamate insecticides by thin-layer chromatography (TLC) have been described. The most common are diazophenol (after alkaline hydrolysis),[1] Tollen's reagent[2] and alkaline Fast Blue B.[3] However, these reagents are normally used for the detection of phenolic compounds or cannabinoids and are also susceptible to biological impurities such as amino acids, proteins and peptides and hence are not specific. The spectrophotometric method reported by Appaiah *et al.*[4] for the detection of carbaryl in grains and formulations is not generally useful for biological samples owing to interference from constituents of viscera, co-extracted with the insecticides. Hence it was felt necessary to develop a specific and sensitive chromogenic spray reagent for the detection of carbaryl in biological materials by TLC.

This paper reports the use of 1% ammonium cerium(IV) nitrate in 20% v/v hydrochloric acid for the detection of the carbamate insecticide carbaryl and its hydrolysis product 1-naphthol.[5] 1-Naphthol reacts with the reagent to produce a violet colour. If 1% aqueous sodium nitrite solution is sprayed on the TLC plate, the intensity of the violet colour is enhanced.

Experimental

Reagents

All reagents were of analytical-reagent grade. Distilled water was used throughout.

Ammonium cerium(IV) nitrate reagent, 1%. A 1 g amount of ammonium cerium(IV) nitrate was dissolved in 100 ml of 20% v/v hydrochloric acid.

Sodium nitrite solution, 1%. A 1 g amount of sodium nitrite was dissolved in 100 ml of distilled water.

Sodium hydroxide solution, 10%. A 10 g amount of sodium hydroxide was dissolved in 100 ml of distilled water.

Procedure

A standard glass TLC plate was coated with a slurry of silica gel G (ACME) in water (1 + 2 m/m), to a thickness of 0.25 mm and the plate was activated at 110 °C for about 1 h. An amount of 1 μl of carbaryl in ethanol (1 mg ml^{-1}) was spotted on the plate, which was then developed in a previously saturated TLC chamber using hexane–acetone (4 + 1) as solvent up to a height of 10 cm.

The plate was removed from the chamber, dried in air and sprayed with 10% sodium hydroxide solution, followed by freshly prepared 1% ammonium cerium(IV) nitrate reagent. A violet spot was observed immediately on the TLC plate at R_F = 0.45. On spraying 10% sodium nitrite solution on the same plate, the intensity of the colour increased. The hydrolysis product of carbaryl, 1-naphthol, gives a similar colour reaction with the reagent at R_F = 0.54 without previous hydrolysis with sodium hydroxide. It was observed that commercial carbaryl in a formulation gave two spots with R_F values of 0.45 and 0.54, demonstrating that the commercial formulation sometimes contains 1-naphthol.

Extraction of Carbaryl Insecticide From Biological Material

Portions of about 100 g each of various types of visceral tissue (stomach, intestine, liver, spleen and kidney) containing carbaryl insecticide were individually minced in aqueous solution. Each sample was extracted in a separating funnel with 150 ml of diethyl ether, shaking the funnel for 2–3 min. The ether extract was transferred into an evaporating dish. The aqueous phase was re-extracted with 50 ml of diethyl ether (2–3 times). The extracts were combined and the solvent was evaporated at room temperature. The residue was dissolved in 1–2 ml of ethanol. A known volume (10 μl) of the solution was spotted on an activated TLC plate together with the standard solution of carbaryl insecticides. The plate was then developed as described under Procedure and sprayed with 10% sodium hydroxide solution followed by 1% ammonium cerium(IV) nitrate reagent and sodium nitrite solution.

Results and Discussion

A 1 mg amount of carbaryl was added to 100 g of minced visceral tissue, mixed well and kept for 1 d. The insecticide was then extracted with diethyl ether, the solvent evaporated at room temperature and the residue dissolved in 1 ml of ethanol. A 10 μl volume of this solution was spotted on a preactivated TLC plate together with 10 μl each of standard technical carbaryl solutions containing 80, 90, 100 and 110 mg

* Present address: Regional Forensic Science Laboratory, State of Maharashtra, Cantonment, Aurangabad-431 002, India.

of carbaryl per 100 ml of ethanol. The plate was then developed as described under Procedure and sprayed with 10% sodium hydroxide solution followed by 1% ammonium cerium(IV) nitrate reagent and 10% sodium nitrite solution. The intensity of the coloured spot for the visceral extract was compared with those obtained for the known standards and was found to correspond to the spot representing a concentration of 100 mg per 100 ml (average of three experiments). Hence the recoveries appeared to be better than 90%.

This reagent does not react with propoxur and carbofuran but does react with their hydrolysis products, giving reddish orange spots (sensitivity approximately 10 μg). Moreover, the following gave no reaction with this reagent and hence did not interfere: organophosphorus insecticides such as malathion, parathion, dimethoate, fenthion, fenitrothion, monocrotophos, methyl demeton, quinalphos, phosalone, ekatin, phorate, phosphamidon, dichlorvos and trichlorfon; organochlorine insecticides such as endrin, DDT, γ-HCH; and endosulfan and pyrethroid insecticides such as fenvalerate, cypermethrin and deltamethrin. The sensitivity of the reagent is approximately 0.1 μg per spot, observed after development.

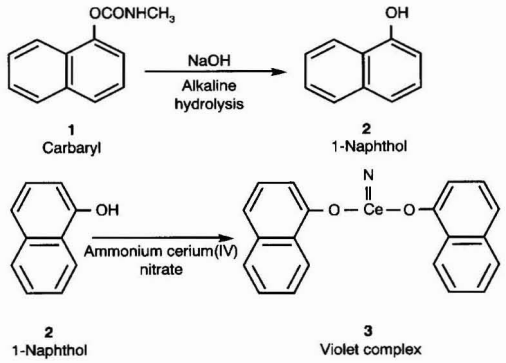

Fig. 1 Proposed reaction for formation of coloured complex

On alkaline hydrolysis, carbaryl gives 1-naphthol, which then reacts with ammonium cerium(IV) nitrate in acidic media to give the violet complex **3** as shown in Fig. 1.

The authors thank Professor D. B. Ingle, Head of the Department of Chemistry, Marathwada University, Aurangabad, and the Director, Forensic Science Laboratories, State of Maharashtra, Bombay, for their keen interest and valuable guidance in this work.

References

1 Randerath, K., *Thin-layer Chromatography*, Academic Press, New York, 1965, p. 176.
2 Kawale, G. B., and Jogalekar, V. D., *Curr. Sci.*, 1976, **45**, 57.
3 Tiwari, S. N., and Singh, R., *Brochure of the Autumn School of Forensic Science*, Chandigarh, India, 1979.
4 Appaiah, K. M., Ramakrishna, R., Subharao, K. R., and Kapur, O., *J. Assoc. Off. Anal. Chem.*, 1982, **65**, 32.
5 Ramulu, U. S., *Chemistry of Insecticides and Fungicides*, Oxford and IBH Publishing, Bombay, 1979, p. 188.

Paper 3/00121K
Received January 8, 1993
Accepted June 28, 1993

Experimental Correction for the Inner-filter Effect in Fluorescence Spectra

Mikael Kubista, Robert Sjöback, Svante Eriksson and Bo Albinsson*

Department of Biochemistry and Biophysics, Chalmers University of Technology, S-412 96 Gothenburg, Sweden

Recorded fluorescence intensity is in general not proportional to sample concentration owing to absorption of the incident and emitted light passing through the sample to and from the point inside the cell where the emission is detected. This well known inner-filter effect depends on sample absorption and on instrument geometry, and is usually significant even in samples with rather low absorption (the error is about 8% at an absorbance of 0.06 in a 1 cm square cell). In this work we show that a particular experimental set-up can be calibrated for the inner-filter effect from the absorption and fluorescence excitation spectra of a suitable standard. The calibration takes only a few minutes and provides correction with sufficient accuracy for most practical situations.

Keywords: Fluorescence; inner-filter effect; inner-filter correction

Introduction

Fluorescence spectroscopy has found wide application in analytical chemistry and biochemistry because of its extreme sensitivity and structural specificity. However, some experimental difficulties hinder its use as a quantitative tool. One such difficulty is that the recorded fluorescence intensity is not proportional to the concentration of the fluorophore owing to the so-called inner-filter effect.[1,2] This effect is due to the absorption of some of the incident light before it reaches the point in the sample at which luminescence is observed ('primary' inner-filter effect), and re-absorption of some of the emitted light before it leaves the cell ('secondary' inner-filter effect). Because of the inner-filter effect, the observed fluorescence intensity, I^{em}_{obs}, depends on the optical density of the sample at both excitation, $D(\lambda_{ex})$, and emission, $D(\lambda_{em})$, wavelengths (D = absorbance cm^{-1}), and is not a linear function of the fluorophore concentration, C:

$$I^{em}_{obs} \propto f[D(\lambda_{ex}),D(\lambda_{em})]C \approx f_p[D(\lambda_{ex})]\, f_s[D(\lambda_{em})]C \quad (1)$$

where factorization of the general correction function, $f[D(\lambda_{ex}),D(\lambda_{em})]$, assumes that the primary, $f_p[D(\lambda_{ex})]$, and secondary, $f_s[D(\lambda_{em})]$, inner-filter effects can be treated independently. This assumption is generally made, although its validity for strongly absorbing solutions has recently been questioned.[3]

Most corrections for the inner-filter effect for a right-angled cell geometry are based on the equations derived by Parker and Barnes:[4]

$$f_p[D(\lambda_{ex})] = \frac{10^{-D(\lambda_{ex})l_p}(10^{D(\lambda_{ex})\Delta l_p/2} - 10^{-D(\lambda_{ex})\Delta l_p/2})}{2.303D(\lambda_{ex})\Delta l_p} \quad (2)$$

where l_p is the distance from the point inside the cell at which luminescence is observed, Δl_p, the width of the excitation light beam, and $D(\lambda_{ex})$, the optical density of the sample at the wavelength of excitation (Fig. 1). The correction for the secondary inner-filter effect, $f_s[D(\lambda_{em})]$, is obtained by replacing $D(\lambda_{ex})$ with $D(\lambda_{em})$, and l_p and Δl_p, with l_s and Δl_s. Correction with these equations has been found to work well up to absorbances of about 2.[5,6] A disadvantage of this approach, however, is that the instrument parameters l_p, Δl_p, l_s, and Δl_s must be known, and the optical densities, $D(\lambda_{ex})$ and $D(\lambda_{em})$, of the sample must be measured.

An experimental approach to correct for the primary inner-filter effect that avoids some of these difficulties has been developed.[7,8] This so called 'cell-shift' method is based on the measurement of fluorescence intensities at two points in the cell along the incident beam, and gives high accuracy for absorbances up to 2.7.[9] The original approach was later modified to measure fluorescence intensities at two points along the diagonal of the cell, which also allows correction for the secondary inner-filter effect.[10] More sophisticated approaches to correct for the inner-filter effect, based on multiple detectors and fibre optics, have also been developed.[11,12]

The intention of this work was not to provide a new method for very accurate corrections of the inner-filter effect; the precision of those already cited is sufficient for most purposes. Instead, our aim was to provide a simple and easy approach for the calibration of a particular experimental set-up in a few minutes, using standard commercial instruments, which provides an accuracy sufficient for most practical situations. Our study was limited to the primary inner-filter effect, and is therefore only applicable to samples that do not absorb appreciably at the wavelength of emission. This is, however, the common situation.

Theory

If a sample does not absorb at the emission wavelength, the secondary inner-filter effect is negligible. The observed

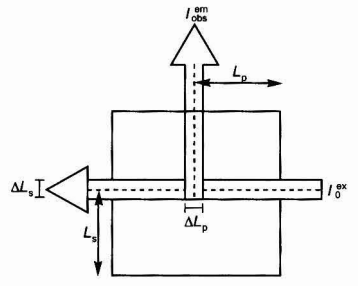

Fig. 1 Cross-section of a right-angled fluorescence cell. I^{ex}_0 = Intensity of the incident beam; I^{em}_{obs} = observed fluorescence intensity; l_p and l_s = distances from the point inside the cell at which luminescence is observed to the entry and exit cell walls, respectively; and Δl_p and Δl_s = widths of the emission and excitation light beams, respectively

* Present address: Department of Chemistry and Biochemistry, University of Colorado at Boulder, Boulder, Colorado 80309-0215, USA.

fluorescence intensity, when normalized with the intensity of the incident beam (quantum correction), is

$$I^{em}_{obs} \propto C\varepsilon(\lambda_{ex})\phi f_p[D(\lambda_{ex})] \quad (3)$$

where $\varepsilon(\lambda_{ex})$ is the molar absorptivity of the fluorophore, ϕ its fluorescence quantum yield, and $f_p[D(\lambda_{ex})]$ is the correction for the primary inner-filter effect, which depends on the absorbance of the sample at the wavelength of excitation. From eqn. (3), it immediately follows that the correction function can be determined experimentally by measuring the fluorescence intensities of a dilution series of a standard sample.[13]

Recalling that $C\varepsilon(\lambda_{ex}) = D(\lambda_{ex})$, eqn. (3) can be rewritten as

$$I^{em}_{obs} = \kappa D(\lambda_{ex}) f_p[D(\lambda_{ex})] \quad (4)$$

where κ is a proportionality constant, containing instrument parameters and also the fluorescence quantum yield of the fluorophore, which is assumed to be wavelength independent. As seen from eqn. (4), the fluorescence intensity does not depend directly on sample concentration, but only on sample absorption. As absorption generally also varies with wavelength, the correction function $f_p[D(\lambda_{ex})]$ can be determined using a single sample. By plotting the fluorescence intensity values recorded at different excitation wavelengths (at a fixed emission wavelength) *versus* the corresponding absorption values, the correction function for the entire interval from zero to maximum sample absorption can be determined. The approach requires that the absorption and fluorescence spectrophotometers are wavelength matched, and that the quantum correction of the spectrofluorimeter is appropriate. Further, the fluorophore used for calibration must have a wavelength-independent fluorescence quantum yield over a reasonable wavelength range. The calibration is then valid for the particular set-up, *i.e.*, for the type of cell used when placed at a certain position in the spectrofluorimeter.

Results

Fig. 2 shows fluorescence excitation spectra of 9,10-diphenylanthracene (DPA) in cyclohexane, measured in a 1 cm square cell, of samples with absorbances of 1.6, 0.2 and 0.02 at 392 nm. These spectra illustrate how serious the inner-filter effect can be. The excitation spectrum of the most dilute sample (C) shows negligible inner-filter effect and its shape is, within experimental error, identical with that of the absorption spectrum (D). This proves that the fluorescence quantum yield of DPA is constant in the wavelength region required for calibration. The spectrum of the sample of intermediate concentration (B) is broadened owing to a greater inner-filter effect at high absorption. For the most concentrated sample (A) the entire excitation spectrum is deformed: instead of a single maximum two maxima are observed, and a local minimum is found at the wavelength of the absorption maxima of the other samples. Here the inner-filter effect is so serious that the observed fluorescence intensity has begun to decrease with increasing absorption.

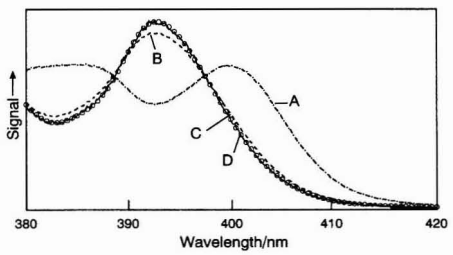

Fig. 2 Absorption and fluorescence excitation spectra of 9,10-diphenylanthracene in cyclohexane measured in a 1 cm square cell. Excitation spectra of samples with absorbances of A, 1.6, B, 0.2 and C, 0.02 at 392 nm. The absorption spectrum, D, was independent of concentration. Spectra are scaled to equal areas

Fig. 3(*a*) shows the fluorescence intensities of the most concentrated DPA sample plotted against the corresponding absorbances in the wavelength region 392–450 nm (the long wavelength side of the low energy absorption band). The non-linear behaviour of the plot is due to the inner-filter effect. The straight solid line (C) represents the fluorescence intensity that would have been observed in the absence of the inner-filter effect, and the plot can be used directly to correct experimental readings for the inner-filter effect: the ratio between the straight line and the curve, at the optical density at the excitation wavelength, is the appropriate correction factor.

For practical use it is desirable to express the correction function in functional form. The broken line (B) is the best fit to the function $D(\lambda_{ex})10^{-D(\lambda_{ex})l_p}$ with $l_p = 0.56$ cm. Here, $10^{-D(\lambda_{ex})l_p}$ is an approximation of the correction function described in equation (2) that is valid for small Δl_p. The good agreement between the fitted curve (B) and the experimental data (A) suggests that the approximation is adequate. The size of the emission bandpass affects the volume element from where luminescence is detected, and thus Δl_p. We found, however, that the same correction function is valid when bandpaths between 0.5 and 15 nm are used, suggesting that the value of Δl_p is not crucial, and that the same correction function can be used for all bandpaths.

Using the approximation $f_p[D(\lambda_{ex})] \approx 10^{-D(\lambda_{ex})l_p}$, eqn. (4) can be linearized as follows:

$$\log [D(\lambda_{ex})/I^{em}_{obs}(\lambda_{ex})] = l_p D(\lambda_{ex}) - \log \kappa \quad (5)$$

and l_p and $\log \kappa$ can be determined as the slope and intercept of a plot of $\log [D(\lambda_{ex})/I^{em}_{obs}(\lambda_{ex})]$ *versus* $D(\lambda_{ex})$ [Fig. 3(*b*)].

Once l_p is determined, fluorescence intensities recorded with the particular set-up can readily be corrected for the primary inner-filter effect:

$$I^{em}_{corr} = I^{em}_{obs} 10^{D(\lambda_{ex})l_p} \quad (6)$$

Discussion

We have presented a simple and easy way to determine the correction function for the primary inner-filter effect in

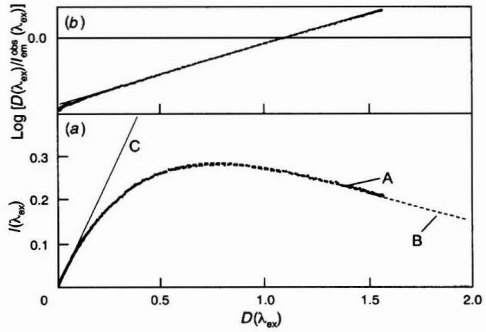

Fig. 3 (*a*) A, Plot of fluorescence intensities recorded at various excitation wavelengths *versus* the corresponding absorption intensities for DPA in cyclohexane; B, function $D(\lambda_{ex})10^{-D(\lambda_{ex})l_p}$ with l_p = 0.56 cm; and C, fluorescence intensities that would be observed in the absence of the inner-filter effect. The fluorescence intensities are scaled to give the proportionality constant $\kappa = 1$. (*b*) Plot of $\log [D(\lambda_{ex})/I^{em}_{obs}(\lambda_{ex})]$ *versus* $D(\lambda_{ex})$. The slope and intercept are l_p (0.56 cm) and $\log \kappa$, respectively. Data are from the wavelength ranges (*a*) 392–450 nm and (*b*) 392–415 nm. Cell length, 1 cm; $D(392) = 1.6$; λ_{em} = 505 nm

fluorescence spectroscopy. Using a fluorophore that has a wavelength-independent fluorescence quantum yield, the correction for the primary inner-filter effect for a particular experimental set-up can be determined by plotting the recorded fluorescence intensities at different wavelengths *versus* the corresponding absorbances. The correction is found to be well described by the function $10^{D(\lambda_{ex})l_p}$, where l_p is the depth in a right-angled measuring cell from where luminescence is measured, and $D(\lambda_{ex})$ is the total optical density of the sample at the excitation wavelength.

Scale of Error Induced by the Inner-filter Effect

The absolute error induced by the inner-filter effect is the deviation of the recorded fluorescence intensities from the straight line shown in Fig. 3(*a*). The absolute error is small at low absorbances, being essentially negligible below 0.06. It increases rapidly thereafter, becoming very large at high absorbances. However, the small absolute error at low absorbance may be misleading. In most instances, the relative error is more important:

$$(I^{em}_{corr} - I^{em}_{obs})/I^{em}_{obs} \approx 10^{-D(\lambda_{ex})l_p} - 1 \approx -2.303D(\lambda_{ex})l_p \quad (7)$$

where the latter approximation is valid within 10% at optical densities below 0.1 cm^{-1}. For our set-up, l_p = 0.56 cm, the relative error is roughly $1.3D(\lambda_{ex})$, therefore also being significant at low absorbance. At an absorbance of 0.06, where the absolute error is negligible, the relative error is about 8%.

In summary, correction for the primary inner-filter effect is, in most instances, desirable. In addition to being necessary for quantitative comparison of fluorescence intensities, it is required for comparison of excitation spectra recorded on different instruments. In the latter case, correction is particularly important because information about sample absorption, which is in general available, is insufficient for comparison purposes as the inner-filter effect also depends on the particular experimental set-up.

This work was supported by the Swedish Research Council for Engineering Sciences and by Magn. Bergvalls Stiftelse.

References

1 Parker, C. A., and Rees, W. T., *Analyst*, 1962, **87**, 83.
2 Parker, C. A., *Photoluminescence of Solutions*, Elsevier, Amsterdam, 1968, ch. 1, pp. 15–22; ch. 3, pp. 220–234.
3 Street, K. W., and Tarver, M., *Analyst*, 1988, **113**, 347.
4 Parker, C. A., and Barnes, W. J., *Analyst*, 1957, **82**, 606.
5 Holland, J. F., Tests, R. E., Kelly, P. M., and Timnick, A., *Anal. Chem.*, 1977, **49**, 706.
6 Christmann, D. R., Crouch, S. R., Holland, J. F., and Timnick, A., *Anal. Chem.*, 1977, **49**, 706.
7 Britten, A., Archer-Hall, J., and Lockwood, G., *Analyst*, 1978, **103**, 928.
8 Novak, A., *Collect. Czech. Chem. Commun.*, 1978, **43**, 2869.
9 Christmann, D. R., Crouch, S. R., and Timnick, A., *Anal. Chem.*, 1981, **53**, 2040.
10 Lutz, H.-P., and Luisi, P. L., *Helv. Chim. Acta*, 1983, **66**, 1929.
11 Yappert, H., and Ingle, B., *Anal. Spectrosc.*, 1989, **43**, 759.
12 Ratzlaff, E. H., Harfmann, R. G., and Crouch, S. R., *Anal. Chem.*, 1984, **56**, 342.
13 Lakowicz, J. R., *Principles of Fluorescence Spectroscopy*, Plenum Press, New York, 1983, ch. 2, pp. 43–47.

Paper 3/03606E
Received June 23, 1993
Accepted October 5, 1993

X-ray Fluorescence Analysis of Ferroalloys: Development of Methods for the Preparation of Test and Calibration Samples

Aurora G. Coedo, Maria Teresa Dorado, Carlos J. Rivero and Isabel G. Cobo
CENIM (CSIC), Gregorio del Amo 8, 28040 Madrid, Spain

Methods were developed with a view to evaluating various sample preparation systems for use with X-ray fluorescence techniques in order to determine the major and minor components of ferroalloys, which are used as alloy-forming elements in steel making. The methods were compared in terms of simplicity and rapidity and these parameters were assessed in relation to the accuracy and precision of the results. The samples were prepared in three formats: metal samples, by dilution with iron and remelting in an induction furnace; pellets, by direct compaction of the ground material, and beads, by alkaline melting of the pre-oxidized sample. The tests used to optimize these methods were conducted with commercial ferroalloys, previously characterized by employing wet chemical and spectroscopic methods. Reproducibility and precision studies were conducted on samples obtained using each of the three sample preparation systems. The precisions (relative standard deviations) of major element determinations were <0.8, <1.0 and <0.5% and those for minor elements were <5, <5 and <3% for metal samples, pellets and beads, respectively. The accuracy of the methods was checked by analysing reference materials of each type of ferroalloy.

Keywords: *Ferroalloy analysis; X-ray fluorescence spectrometry; sample preparation*

Introduction

Steel-making practice involves the addition of various elements into the bath. Such elements are generally incorporated in the form of ferroalloys, the most common being ferrochromium, ferromanganese, ferrosilicon, ferrovanadium, ferromolybdenum, ferrotungsten, ferroniobium, ferrophosphorus, ferrotitanium and ferroboron. A precise and accurate knowledge of the chemical composition of ferroalloys serves a dual purpose: economic, owing to the high cost of the principal components, and technological, owing to the influence exerted by the degree of definition of their composition on the manufacturing of the steels, when setting the tolerance limits and their properties.

Ferroalloys, with regard to their physical presentation (which is conditioned by the manufacturing process itself) are not suitable for direct analysis and a preliminary treatment is necessary. This step, *i.e.*, the sample preparation procedure, is one of the most critical phases of any analytical method.

In this study, the preparation of test samples was conducted with the following three procedures: obtaining metal samples, by diluting with iron and remelting in an induction furnace; formation of pellets, by directly compacting the sample previously ground to a certain grain size; and preparation of beads, by alkaline melting of the pre-oxidized sample. The calibration samples were prepared by the same system as used for the test samples, employing only one or two commercial ferroalloys of each of the types, by using different iron dilution ratios or different mixture proportions.

Experimental

General Operating Procedure

Scheme 1 shows the operating procedure followed in developing the working methods for the different types of ferroalloys.

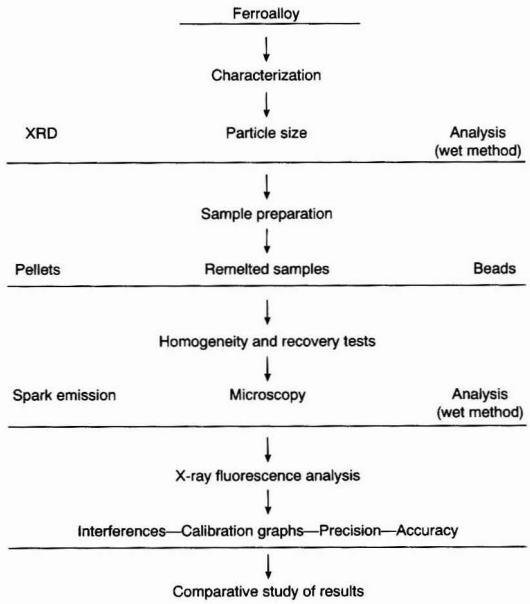

Scheme 1

Characterization of the Initial Materials

Two commercial ferroalloys with as extreme compositions as possible were selected to develop the methods for each type of ferroalloy, with a view to covering the ranges of concentrations included in the International Organization for Standardization (ISO) specifications for each type. The materials were carefully characterized and analysed using X-ray diffraction (XRD) techniques and wet analytical methods. In all instances, approximately 2 kg of material with a particle diameter of less than 5 cm were used. The diameter of the particles was decreased to approximately 10 mm using a jaw breaker and then to less than 2 mm with a steel disc mill.

Subsequently, the particle size was adjusted appropriately, depending on the sample preparation system used, with a tungsten carbide disc mill.

Sample Preparation

Metal samples

The test and calibration metal samples were obtained by melting the ferroalloy, previously mixed with iron, in a refractory crucible inside an induction furnace, provided with a direct reading automatic optical pyrometer. The molten metal was centrifuged and cast in an appropriate mould. Mullite–corundum refractory crucibles, of capacity approximately 20 ml, were used for the melting. To prevent the sample entering the pores of the uneven surface of the refractory, thus preventing it from melting, the inside walls of the refractory were covered with graphitized filter-paper. Once the components had been weighed to a precision of about 0.01 g and placed in the crucible, the latter was placed in the furnace stand so that when the inductor coils moved upwards, the crucible was concentric with them. The collector was placed perpendicular to the crucible, in order to receive the molten metal after the centrifugation process.

The collector was formed of a 'muzzle', made of the same heat-resistant material as the crucible, and a 'chill mould', consisting of two adjustable parts made from an alloy of 94% Cu and 6% Be. In line with the characteristics of the induction furnace and of the crucibles used, and also of the materials under study, the total mass of the remelted samples was 40 g. Hence, the amounts of ferroalloy plus iron added up to this total amount. The samples obtained were mushroom-shaped, with a cylindrical head of about 30 mm diameter and 8 mm thick, and a stem about 12 mm in diameter and 6 mm high.

Table 1 gives the values selected for the melting parameters of each type of ferroalloy studied.

Pellets

For pellet preparation, a portion of the material was milled to a grain size of less than 74 μm. In order for the materials to have as similar a grain size as possible, the material was not milled too much below this grain size, the aim being for most of the particles to be between 32 and 74 μm.

In order to avoid overheating the material, 10 g portions of ferroalloy were milled for 30 s periods, in 10 s fractions, until the indicated grain size was attained.

Test and calibration samples were prepared by mixing 8 g of the ferroalloy with 5 ml of 10% Elvacite (butyl methacrylate) in acetone, homogenizing manually until the acetone had evaporated completely. A layer of 8 g of boric acid was placed in an aluminium capsule 4 cm wide and 7 mm high, and then the 8 g sample with the binder was placed on top. A load of 40 ton cm^{-2} was exerted on the mixture for 20 s in a hydraulic press.

Beads

The process was performed manually, using a muffle furnace, and mechanically, with a bead machine. The following procedure was established: a small amount of alkaline flux and lithium tetraborate was placed in a platinum crucible, in such a way that the bottom and a few millimetres of the wall of the crucible were covered, and over it the sample and the oxidant were carefully mixed. During the oxidation phase, the sample mixture, flux and oxidant were heated progressively, without swirling, and when the flux began to melt it trapped the metal particles before the oxidation reaction started (hence contact between the reduced sample and the crucible was avoided). After oxidation, in a second step, the sample was fused with lithium tetraborate and during this step the crucible had to be oscillated to ensure complete homogenization of the mixture. The molten mass was poured on to nickel sheet 4.5 cm in diameter and 1 mm thick, or on to a platinum plate, preheated to dull red.

Table 2 lists the proportions of reactants and the oxidation and melting times and temperatures.

Results and Discussion

The industrial ferroalloys used to develop the methods and to obtain the samples for calibration were prepared and characterized in order to ensure homogeneous samples with as precise and accurate compositions as possible (it was essential to know their chemical composition with high precision in order to obtain accurate results from the corresponding calibration graphs). Wet chemical procedures[1–3] were used for the analysis, and standardized methods were applied when they were available. To determine the major elements (ferroalloy grade), inductively coupled plasma methods[4] were also employed in order to obtain results from two different techniques (classical and spectroscopic) and minimize the errors in the analytical results.

Metal Samples

The most important operational parameters in this system are the selection of the optimum dilution factor and the setting of the melting and casting temperatures.[5,6]

Table 1 Melting temperatures, melting times, casting temperatures, optimum dilutions (FeX + Fe) and maximum tolerated contents of alloying elements

Fe–X	Melting temperature/°C	Melting time/s	Casting temperature/°C	Optimum dilution	Maximum major element content (%)
Fe–Mo	1700	115	1500	15 + 25	30
Fe–Nb	1850	130	1850	12 + 28	24
Fe–V	1900	125	1700	12 + 28	25
Fe–Cr	1750	130	1650	12 + 28	30
FeCr–C	1550	120	1550	12 + 28	30
FeCrSi	1600	120	1600	8 + 32	12 (Si)
Fe–W	1900	112	1800	8 + 32	20
Fe–Si	1600	120	1400	6 + 34	15
FeSiMn	1400	115	1400	6 + 34	25 − Si + Mn
Fe–Mn	1400	115	1350	15 + 25	42
FeMn–C	1300	110	1150	15 + 25	36
Fe–P	1250	112	1100	6 + 34	5
Fe–Ti	1700	110	1500	4 + 36	10
Fe–B	1800	110	1450	0.75 + 39.25	2

Certain conditions governed the setting of the content of the maximum alloy-forming element in the samples, namely obtaining highly homogeneous samples that did not crack or break during casting or during the turning or polishing processes. At this point of the study, efforts were focused on defining a general system for melting all the ferroalloys, with specific guidelines for each particular instance. The over-all aim was to meet the following objectives: (a) maximum concentration of ferroalloy in the test sample to minimize analytical errors (greater sensitivity in determining the minor elements and greater accuracy in determining the main components); (b) a high percentage of recovered material; (c) ideal melting conditions for composition of the mixtures (the Fe–X binary phase equilibrium diagrams made it possible to pre-set the melting temperatures and to predict the possible phases that would appear in the samples); (d) good structural homogeneity, free from physical defects and with sufficient mechanical resistance to prevent them from breaking or deteriorating with time, and to withstand the sandpapering and polishing processes prior to analysis; (e) good chemical homogeneity in the distribution of both the major and minor components; and (f) short preparation time and ease of repeating similar tests.

Table 1 gives, in addition to the selected melting time and temperature parameters, the maximum major element contents that can be present in the samples without heterogeneity, breaking or fracture problems, and the optimum dilution factor. This last value was selected with a view to obtaining samples with major element contents below the established maxima (whatever the grade of the ferroalloy to be analysed), and covering any composition within the ISO specifications (in this way, for analysing any ferroalloy, it will suffice to prepare the test samples with this optimum dilution factor).

The calibration samples were prepared in the same way as the test samples from a single industrial ferroalloy. Iron dilutions were performed to different extents until the desired range of concentrations had been covered, taking into account the composition of the initial ferroalloy and the concentration range in which the alloying element is found in these materials.

Table 3 lists the major element contents of the industrial ferroalloys used to prepare the calibration samples and the maximum and minimum dilution factors used (these extreme dilution factors cover the whole range of concentrations desired) and the equivalent percentage (corresponding to a ferroalloy analysed from a test sample prepared with the optimum dilution factor).

Five intermediate dilutions were prepared between the minimum and maximum dilution factors for each type of ferroalloy tested, in order to have at least seven different compositions to establish accurately the calibration graphs. The test samples were prepared from 'optimum dilution', a dilution with which any ferroalloy grade can be analysed, within the same type, with the established calibration ranges. Three samples of each composition were prepared under identical working conditions, and six samples with the

Table 2 Oxidation times and temperatures (oxide beads)

Oxidation process reactants			Oxidation	
Reactant	Amount/g	Fe–X	Temperature/°C	Time/min
		Fe–Mo	650–700	4
		Fe–Nb	700–750	6
		Fe–V	700–750	6
FeX	0.2500*	Fe–Cr†	750–800	8
$Sr(NO_3)_2$	0.750*	Fe–Cr–Si	700–750	5
Na_2CO_3	2.000	Fe–W	700–750	6
$Li_2B_4O_7$	1.000	Fe–Si	650–700	4
NaI	0.020	Fe–Si–Mn	650–700	5
	‡	Fe–Mn†	800–850	5
		Fe–P	800–850	5
		Fe–Ti	650–700	6
		Fe–B	650–700	5

* The test samples and oxidizing reactive were used with a grain size of <100 μm.

† The test sample mass for samples with carbon contents >0.1% must be corrected in accordance with their losses through ignition:

$$\text{test sample mass/g} = \frac{0.2500 \times 100}{100 - \%C}$$

‡ Once oxidized, the sample was fused with 5.000 g of $Li_2B_4O_7$ at 1200 °C for 4 min.

Table 3 Major element contents, dilutions for calibration samples and percentage of major element equivalent to samples with the optimum dilution factor. The optimum dilution factor for each ferroalloy is indicated in Table 1

Commercial ferroalloy	Alloying element (%)	Dilution (X + Fe)		Major element in ferroalloy (%) (optimum dilution)	
		Minimum	Maximum		
Fe–Mo	70.70 ± 0.22	12 + 28	18 + 22	56.56	84.83
Fe–Nb	67.70 ± 0.20	8 + 32	14 + 26	45.13	78.97
Fe–V	78.01 ± 0.25	5 + 35	13 + 27	32.50	84.50
Fe–Cr	64.19 ± 0.18	8 + 32	18 + 22	42.80	96.30
Fe–Cr–C	66.60 ± 0.16	8 + 32	16 + 24	44.40	88.80
(Cr)*	32.34 ± 0.18			10.10	60.63
FeCrSi		2.5 + 37.5	15 + 25		
(Si)*	48.51 ± 0.16			15.5	90.95
FeSi	77.10 ± 0.25	0.5 + 39.5	7.5 + 32.5	6.42	96.45
(Mn)*	66.50 ± 0.25			39.06	100.00
FeSiMn		3.5 + 36.5	13 + 27		
(Si)*	16.60 ± 0.22			9.86	36.06
Fe–Mn	85.90 ± 0.11	13 + 27	17 + 23	74.45	97.33
Fe–Mn–C	76.00 ± 0.13	13.7 + 26.3	16.5 + 23.5	64.91	83.60
Fe–P	24.75 ± 0.16	4 + 36	7 + 33	16.46	28.87
Fe–W	76.20 ± 0.21	7 + 33	9 + 31	66.67	85.72
Fe–Ti	68.50 ± 0.16	1 + 39	5 + 35	17.72	85.62
Fe–B	18.26 ± 0.14	0.40 + 39.6	0.90 + 39.1	9.76	21.86

* % alloying element in the commerical ferroalloy considered.

'optimum dilution', with a view to conducting precision studies for verifying the repeatability of the sample preparation system.

The minor element calibration samples were also prepared to cover the ISO specifications. These elements were incorporated by adding the elements either from specifically prepared cast iron or from pure metals or the appropriate alloys. In any event, the set of samples obtained easily covered the ranges of concentrations in which the corresponding elements are normally present in the respective types of ferroalloys.

The total amount of sample recovered was in all instances above 99% (>39.6 g recovered from a total of 40 g).

The samples all had homogeneous structures, in accordance with the corresponding equilibrium diagrams of the component compounds.[7] They also had good chemical homogeneity, which was verified by spark emission spectrometry as follows. Four discharges were applied to each of the two samples of the extreme compositions (for each type of ferroalloy), at different points on the surface, and the emission of each element present, both major and minor, was measured. Then, to check the homogeneity in depth, two cuts were made in the samples, parallel to the surface and each 3 mm thick, and four discharges were applied to the surfaces exposed and the emissions were measured. The relative standard deviations (s_r) corresponding to the 12 measurements of each element in each sample were in all instances less than 1%, except for Al and Ti, for which the values were >10%.

Samples with the extreme compositions were employed to verify the propotions of the different elements. The determinations were made on the material in the form of chips, using wet analytical methods. These analyses revealed the correct incorporation of most of the components during the remelting process. The only exceptions were Al and Ti, because of the difficulties with the incorporation and homogeneous distribution of these two elements in the iron matrix. Their presence also hindered the determination of Si (an element that causes no difficulties when Al and Ti are absent) because they favoured the reduction of the silica of the crucible, producing silicon contamination in the sample. As the interaction between the crucible and the ferroalloy varied with the type of crucible and its porosity, tests were performed with other types of crucibles of different compositions. Circona (zirconium and aluminium silicate) crucibles react with the sample in the same way as the mullite–corundum crucibles, but they do not withstand such high temperatures as the latter and break more easily. Similar behaviour to that of the circona crucibles was noted with silica crucibles, which generally break before the melting has been completed. Consequently, the final tests were performed with mullite–corundum crucibles. All operating parameters were kept constant for each type of ferroalloy, to minimize and control the possible modifications of the molten mixtures.

With ferrochromes and ferromanganeses, the carbon contents were found to have an important influence on the X-ray fluorescence measurements of the major elements (Cr or Mn). These measurements increased in line with the carbon content, and it was necessary to correct the contents found for the major elements in terms of the sample carbon content.

To establish the corresponding corrections, two series of ferrochrome and ferromanganese samples were prepared, with a constant Cr and a constant Mn content, respectively, and variable carbon contents. With these samples, and the sets of samples prepared to establish the calibration graphs, both for the high-carbon materials and for materials with carbon contents of less than 0.1%, it was possible to define the correction factors. Once the corrections had been made, the results for all the samples prepared with constant Cr or Mn content and variable carbon contents (obtained from the calibration graph corresponding to samples with a carbon content of less than 0.1%) had $s_r < 0.5\%$.

Pellets

Although the advantages inherent in the melting of the samples are well known (with a view to eliminating matrix interferences), studies were conducted to evaluate the direct compaction sample preparation method with respect to speed of performance, ease of handling and absence of diluents. It must not be forgotten that in materials of this type, given that their origin is similar for each type of ferroalloy (because they came from a previous melting process), their mineralogical state was very similar and it was easier to correct for the matrix interferences, which then depended exclusively on the concentrations of interfering elements and not on the nature of the components. In this preparation system the grinding times and grain size were the parameters that had to be carefully set and monitored.[8]

The calibration samples were prepared by compacting mixtures, in five different proportions, of two ferroalloys, with the maximum available difference in compositions, to cover the whole range of possible concentrations within the specifications typical of each type of ferroalloy. Where the ISO specifications were not fully covered in this way, the ranges were completed with pellets prepared from reference materials, previously conditioned to the indicated grain size.

Table 4 lists the major element contents of the materials used to obtain the calibration samples for each type of ferroalloy. Samples corresponding to mixtures of the two corresponding industrial ferroalloys were inserted between the extreme contents of the calibration standards.

By using calibration samples that cover the whole range of concentrations desired, and all of them prepared from materials of similar grain size, matrix corrections can be made and suitable calibration graphs can be obtained for the direct analysis of these materials.

The stability of the compacted samples was checked by making measurements throughout the study. No significant variations were found that could be attributed to deterioration caused by the time that had elapsed since they were prepared.

Beads

Methods based on obtaining beads (oxide glasses) are widely used in the analysis of ferroalloys by X-ray fluorescence spectrometry because this system minimizes both the mineralogical influences and those due to the particle size and interelemental effects. Various methods have been described for obtaining beads with optimum characteristics for the analysis of ferroalloys by this sample preparation system.[9–13] The selection of the oxidant and of the oxidation and melting times and temperatures were the critical points of the system. The methods developed by Staats[11] and Petin *et al.*[12] were selected as the basis for this study. After tests to verify the reproducibility and precision, the ease of application and the times used, the oxidation system was simplified using $Sr(NO_3)_2$ at temperatures between 650 and 800 °C as the sole oxidizing agent. The tests were conducted using the same industrial ferroalloys as were used to develop the methods with remelted metal samples and compacted pellets. The bead calibration graphs were obtained from the beads prepared with five different proportions of two ferroalloys with the most extreme compositions available (the same as used for pellet calibration samples). If the initial ferroalloys did not cover the whole range of concentrations that appear in the ISO specifications, complementary samples were prepared by adding the corresponding elements in the form of oxides.

Between six and ten samples of scaled compositions were prepared to obtain each calibration graph.

To evaluate the behaviour of the different ferroalloys during the oxidation process, samples were prepared exclusively from oxides, with compositions similar to those of the industrial ferroalloys used to develop the methods. The comparative study of the results with both types of sample was used to assess the efficiency of the melting process and it showed that it is possible to make calibrations with primary materials, with well known stoichiometries, so minimizing the total errors.[14]

The beads obtained were highly stable with time. They were kept individually in plastic bags and inside desiccators (at a constant temperature) and were measured periodically throughout the study; the results revealed no changes that could be attributed to their deterioration.

A study was made of the deterioration suffered by the platinum crucibles due to the presence of elements in the metallic state (reduced) and to their reaction with the crucible walls, despite the fact that contact was minimized with the crucible loading system mentioned. It was concluded that when the process is performed manually (six platinum crucibles in normal laboratory use were employed) for all the ferroalloys studied (except for the ferrochrome), the mass losses of the platinum crucibles vary from 1 to 4 mg in each melting, hence these values depend on the characteristics of the samples and on the original state of the crucibles (depending on whether they have been attacked beforehand to a greater or lesser extent). The attacks were more significant with the ferrochromes, especially for the high-carbon ferrochromes. In any event, it must be stressed that, throughout the study (with a total of 1000 fusions), none of the

Table 4 Major element contents of samples employed for preparing calibration pellets

Fe–X	Sample	Major element content (%)	Fe–X	Sample	Major element content (%)
Fe–Mo	FeMo–PC	70.70	Fe–Nb	FeNb–AZMA	78.01
	FeMo–II	63.56		CRM–576	50.16
	IRSID–508	59.56			
	EUR–578	72.23			
Fe–Cr	FeCr–I–c	66.60	Fe–Mn	FeMn–c	76.00
	FeCr–T–c	58.39			
	CRM–507	70.30		FeMn	85.90
	CRM–554	74.60			
Fe–Cr–Si	FeCrSi–073	Cr: 32.34–Si: 48.51	Fe–Si–Mn	FeSiMn–c	Mn: 66.50–Si: 16.60
	FeCr–III	Cr: 64.19–Si: 1.05		FeSi–I	Si: 45.32–Mn: 0.48
Fe–V	FeV–9	78.01	Fe–W	FeW–7	76.20
	CRM–577	50.16		FeW–8	87.31
			Fe–Ti	FeTi–22	68.50
Fe–Si	FeSi–c	77.10		BCS–234/4	38.2
	FeSi–I	45.32	Fe–P	FeP–A	24.75
	FeSiMn–c	66.50		FeP–M	17.20

Table 5 Calibration parameters. Concentration = $D + E\,I$, where D = intercept on the ordinate/slope, E = 1/slope and I = intensity

	Remelted samples			Pellets			Beads		
Fe–X	D	E	s	D	E	s	D	E	s
Mo	−1.1250	0.2710	0.1000	11.2754	0.3244	0.1984	1.0302	0.4261	0.1088
Nb	0.3597	0.2519	0.1594	0.8219	0.2670	0.1999	1.1215	1.2635	0.1085
Cr	1.9054	0.2706	0.0679	42.2069	0.1887	0.2069	0.5690	1.5090	0.1326
V	1.3809	0.5220	0.1035	−99.315	0.9710	0.1890	−2.9702	3.1543	0.1044
W	0.4441	1.2768	0.0605	64.9524	0.3011	0.1393	−1.5216	1.8010	0.1209
Si	−0.0261	0.4045	0.0469	28.9502	0.1449	0.1308	0.2310	4.4745	0.1053
Mn	3.3734	0.3013	0.0750	−44.373	0.2537	0.1217	10.8171	1.1190	0.1205
P	0.4564	0.0216	0.0653	35.6223	0.3571	0.1156	0.7337	1.9660	0.1105
Ti	1.2698	0.4030	0.1607	−0.8672	0.1704	0.1501	−1.9005	3.2012	0.1396

Table 6 Precision tests

	X-ray fluorescence		
Test	Remelting	Pellets	Beads
Ten measurements on same sample [s_r (%)]	<0.20	<0.20	<0.10
Ten measurements on 6 samples [s_r (%)]	0.20–0.40	0.20–0.50	0.10–0.25
Major element tolerances (%)*	From ±0.25 to ±0.40	From ±0.30 to ±0.55	From ±0.15 to ±0.20
Minor element precision [s_r (%)]	<5 ex.Al–Ti	<5	<3

* $T = \pm t(s/\sqrt{n})$. The confidence intervals were calculated for a 95% confidence level and two determinations. The t and s values were obtained from ten measurements of each of the six samples with the same composition and prepared under the same operating conditions.

crucibles used had to be repaired. With the 'bead machine', only two crucibles were used. These were utilized simultaneously for making beads of other materials, and a total of around 250 fusions of ferroalloys were made; although the masses of the crucibles were not monitored, it was concluded that both were slightly attacked but were in perfect condition for use.

X-ray Analysis

All the series of calibration samples prepared (with the three systems employed), both for the alloying elements and for the minor elements, were measured by X-ray fluorescence spectrometry. Table 5 lists the calibration parameters corresponding to the alloying elements of each type of ferroalloy and the standard deviation (s) (dispersion of the experimental data in relation to the regression obtained from the theoretical values).

The reproducibility of these analytical systems was tested by measuring one sample ten times and also by measuring each of the six samples of each series ten times (prepared under the same conditions and with the same composition). The ranges of values obtained for the standard deviations are given in Table 6.

The accuracy of the procedures was checked by comparing various reference materials for each type of ferroalloy. The results agreed in all instances, within the levels of precision provided by the operating methods followed.

Conclusions

As a general conclusion, the levels of precision and accuracy attained in the analysis of ferroalloys by X-ray fluorescence spectrometry depend both on the sample preparation system followed and on the quality of the calibration samples used. The selection of the sample preparation system depends both on the laboratory facilities available and on the need for speed and precision. Complete series of calibration samples can be obtained from a single ferroalloy (in a metal sample system) or from two ferroalloys (pellet and bead systems) with the maximum difference of compositions available.

Major elements can be determined (from two measurements and for a confidence level of 95%) with confidence intervals from ±0.25 to ±0.40%, from ±0.30 to ±0.55% and from ±0.15 to ±0.20% using metal samples, pellets and beads, respectively. As regards the minor elements, the precisions ($n = 6$) were s_r <5, <5 and <3%, respectively.

In terms of the time taken to prepare the samples (with a particle size of <2 mm, that is, the size used in the remelting system) and ease of performance, the remelting and compaction systems are very easy to perform and take about 15 and 8 min per sample, respectively, whereas the beads system takes approximately 20 min and requires greater care.

In terms of cost, the compaction system involves no significant non-recoverable costs, whereas in the remelting and bead systems these costs can be considered to be similar (disposable crucibles for remelting and reactants and periodical recovery of the platinum crucibles for the beads).

This paper is part of a research project financially supported by the European Community for Coal and Steel (CECA), No. 7210-GD/932. We are grateful to Dr. G. Staats and Dr. J. Petin for their help concerning bead preparation.

References

1 *Standard Methods for Chemical Analysis of Ferroalloys, Annual Book of ASTM Standards*, E-31-85, ASTM, Philadelphia, PA, 1985, vol. 03.05, Sect. 3.
2 Soudan, P., *Techniques de l'Ingénieur*, 1990, *Metallurgie*, vol. 1, pt. 2, p. 266.
3 Cunningham, A., and Chanbasha, A. R., paper presented at British Steel BISRA Chemists' Conference, 1990.
4 Gómez Coedo, A., Dorado López, M. T., and Vindel Maeso, A., *Spectrochim. Acta, Part B*, 1986, **41**, 193.
5 Grimaldi, R., Meuci, A., and Randi, G., in *L'Analysi Strumentale delle Ferroleghe*, ed. Etas, G., Kompass, Milan, 1975.
6 Willay, G., *Rapport Exterieur IRSID RE. 1182*, May, 1985.
7 *Binary Alloy Phase Diagrams*, ed. Bayer, H. E., American Society for Metals, Metals Park, OH, 1986.
8 Ambrose, A. D., *The X-Ray Fluorescence Analysis of Iron Ore Sinter. A Study of Some Aspects of Specimen Preparation*, BISRA open report, MG/D/671/70.
9 Kawamura, K., *J. Iron Steel Inst. Jpn.*, 1974, **60**, 1892.
10 Wittman, A., Willey, G., and Seffer, R., *Préparation de Perles pour l'Analyse par FX*, Commission des Communautés Européennes, Luxembourg, 1979, EUR. 6288j.
11 Staats, G., *Arch. Eisenhüttenwes.*, 1974, **45**, 693.
12 Petin, J., Wagner, W., and Bentz, F., *Steel Res.*, 1985, **56**, 215.
13 Dirheimer, J. M., *Les fondants et l'Analyse des Alliages Metalliques. Fluxes and Analysis of Ferroalloys*, CCE–CETAS, Luxembourg, 1987.
14 Staats, G., *Fresenius' Z. Anal. Chem.*, 1993, **315**, 1.

Paper 3/02881J
Received May 20, 1993
Accepted July 5, 1993

Competitive Enzyme-linked Immunosorbent Assay for the Determination of Zinc Bacitracin in Animal Feedingstuffs*

C. Williams, I. Patel, C. J. Willer and N. T. Crosby
Laboratory of the Government Chemist, Queens Road, Teddington, Middlesex, UK TW11 0LY

Traditionally, bioassay has been the chosen technique for the determination of bacitracin compounds in animal feedingstuffs. However, detection and determination of this antibiotic have given problems when it is present at low levels. A competitive enzyme-linked immunosorbent assay (ELISA) by which it is possible to detect both bacitracin and zinc bacitracin at levels as low as 1 mg kg^{-1} in animal feeds is described. The ELISA technique has been used in this laboratory to monitor samples from a drug stability storage trial for the presence of zinc bacitracin. In addition, individual polypeptide components of zinc bacitracin have been separated by high-performance liquid chromatography. Fractions were collected and tested by the ELISA technique to assess the response between individual components and the primary antibody. The response was compared with known microbiological activity.

Keywords: Enzyme-linked immunosorbent assay; zinc bacitracin; animal feedingstuff

Introduction

The polypeptide antibiotic bacitracin produced by *Bacillus licheniformis* and *Bacillus subtilis*[1] is used extensively in the veterinary field as an animal-feed additive to promote growth and improve feed-conversion efficiency. Concentrations of the antibiotic in finished feeds range from 5 to 100 mg kg^{-1} depending on the age and species of animal.

Traditional bioassay methods of analysis are lengthy and sample numbers per assay are limited. In comparison, the enzyme-linked immunosorbent assay (ELISA) described offers the advantages of detection levels down to 1 mg kg^{-1} (Fig. 1) as well as shorter assay times, and, hence, increased sample throughput.

Zinc bacitracin is more stable than bacitracin, and is therefore preferred as an animal-feed additive. However, the monoclonal antibody used in this assay was raised against bacitracin as this was found to be more suitable for immunogen production than the zinc compound.

Bacitracin is a mixture of several similar polypeptides with components A and B known to be the most microbiologically active.[2]

The high-performance liquid chromatography (HPLC) method of Pavli and Sokolic[3] made it possible to separate the individual components of zinc bacitracin (Fig. 2). The individually separated components were then tested against the antibody (Fig. 3).

* Presented at SAC '92, an International Conference on Analytical Chemistry, Reading, UK, September 20–26, 1992.

Experimental

ELISA Principle

The antigen bacitracin conjugated to ovalbumin[4] is immobilized on plastic microtitre plate wells. Free antigen in the test sample or standard is added to the wells, followed by a limited amount of the first antibody. he free antigen competes with immobilized antigen for sites on the antibody and thus

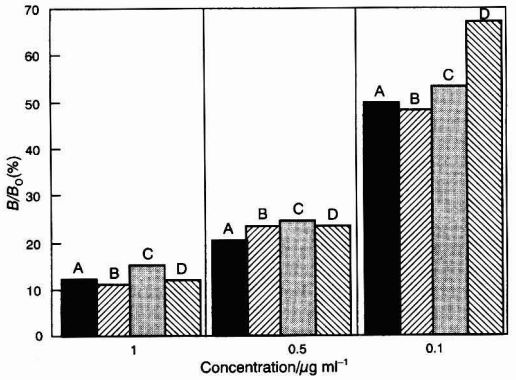

Fig. 1 Detection of bacitracin–zinc bacitracin at low levels in pig feed. A, Zinc bacitracin standard; B, premix standard (corrected for activity); C, sample spiked with bacitracin; and D, sample spiked with zinc bacitracin

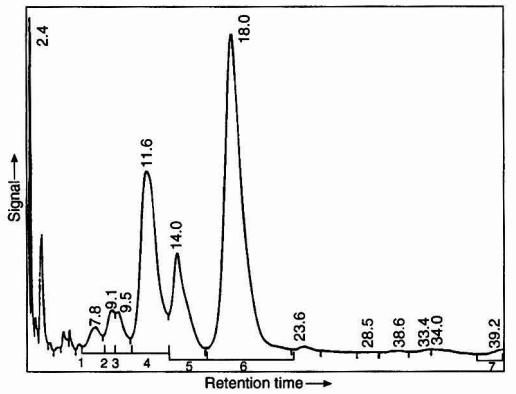

Fig. 2 Separation of the components of zinc bacitracin by HPLC. Fractions 1–7 are indicated. The figures marked against each peak are the corresponding retention times (min)

prevents immobilization of a certain fraction of the first antibody.

Separation of the first antibody–free antigen complex is achieved by inverting the microtitre plate to discard its contents, and then washing with phosphate-buffered saline–azide–Tween-80 (PBSTA).

The fraction of first antibody that has been immobilized by binding to the antigen in the plate coating is subsequently detected by the addition of an enzyme-labelled second antibody specific to the first antibody.

After incubation, the unbound second antibody is removed and the plate is washed.

A suitable substrate for the enzyme label is then added and the plate is incubated to allow colour development. The final colour end-point (absorbance), which is inversely proportional to the level of free antigen in the test sample or standard, is read on a photometer.

Materials and Method

Use analytical-reagent grade reagents and de-mineralized water throughout.

Phosphate-buffered saline + azide (PBSA). Use for the preparation of assay solutions unless otherwise instructed. Dissolve sodium azide (1 g), sodium chloride (8.5 g), disodium hydrogenorthophosphate (anhydrous, 16.05 g), and sodium dihydrogenorthophosphate (dihydrate, 5.85 g) in water and make up to almost 1 l, and adjust the pH to 7.2 with 1 mol l^{-1} sodium hydroxide. Make up to 1 l with water. Re-check the pH.

PBSA, pH 5.4. Use for sample extraction and dissolution of standards. Prepare as PBSA then adjsut the pH to 5.4 with 10 mol l^{-1} orthophosphoric acid.

PBSTA. Use for washing plates. Prepare as PBSA then add 0.5 ml of Tween 80.

Bovine serum albumin (BSA, Sigma A7030). Solution (1%) in PBSA pH 7.2. Use as a blocking solution to counteract the effects of non-specific binding.

Plate-coating solution. Bacitracin conjugated to ovalbumin prepared by the glutaraldehyde method.[4] Prepare by dissolving bacitracin–ovalbumin conjugate in PBSA, pH 7.2.

First antibody. Monoclonal antibody ascites produced by the fusion of spleen cells from immunized mouse with myeloma cell line to produce hybridoma. (The antibody used in this work was prepared by the University of Kent, Canterbury, UK.)

Second antibody (Sigma 0162). Alkaline phosphatase labelled anti-mouse, polyvalent, raised in goat. Dilute with PBSA, pH 7.2. Determine the dilution necessary so that after addition of substrate, colour development (maximum absorbance reading, 1.6–1.8) occurs within 20–30 min.

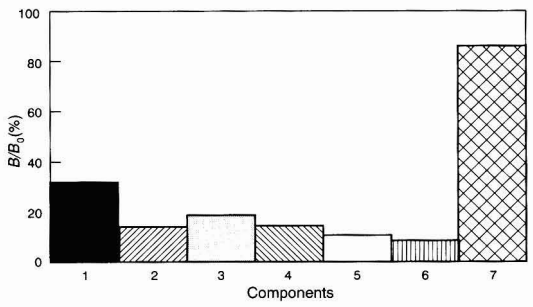

Fig. 3 ELISA on the separated components (1–7 in Fig. 2) of zinc bacitracin

Substrate. Prepare buffer by mixing the following reagents: glycine (0.5 mol l^{-1}, 5.00 ml); zinc chloride (0.1 mol l^{-1}, 0.25 ml); and magnesium chloride (0.1 mol l^{-1}, 0.25 ml). Pipette given volumes into a 25 ml calibrated flask, and make up to about 20 ml with water. Adjust the pH to 10.4 with 1 mol l^{-1} sodium hydroxide. Make up to volume with water. Add one tablet phosphatase substrate tablet (Sigma 104–105, 5 mg) to each 5 ml of substrate buffer before use.

Bacitracin (Sigma B0125).

Zinc bacitracin (Sigma B5150). Prepare stock solutions (1 mg ml^{-1}) and note the activity stated on the product label.

The following are also required: 150 ml stoppered conical flasks; 50 ml plastic conical centrifuge tubes with screw-tops (Falcon); Acrodisc filters (Gelman, 0.2 μm); Nunc Maxisorp plastic microtitre plates (Gibco); a Wrist-action shaker; a Titertek Multiscan plate reader (Labsystems); and a centrifuge.

Procedure

Antibody dilution curve

Before test samples or standards can be assayed it is essential to construct an antibody dilution curve. For competition to take place between immobilized antigen and free antigen the antibody must be in demand. The purpose of the antibody dilution curve is to determine the amount of first antibody that, in the absence of free antigen, will bind to 50% of the sites on the coated microtitre plate.

(1) Coat wells of microtitre plate with 50 μl of plate-coating solution. Determine the concentration of plate coating (1–10 μg ml^{-1}) by measuring the absorbance after different combinations of plate coating and first antibody have been incubated with the optimum concentration of second antibody conjugated to the enzyme label.

(2) Place the plate in a sealable polythene bag containing a few drops of de-mineralized water. Incubate the plate at 4 °C, at least overnight, or until required. (Coated plates can be stored for up to 4 weeks at 4 °C).

(3) Remove the plate from the bag and discard the plate contents. Wash the plate three times with PBSTA. Dry the plate by tapping it on absorbent tissue.

(4) Block each well with 200 μl of 1% BSA–PBSA. Cover the plate and leave it to incubate at room temperature for 2 h.

(5) Discard the blocking solution and wash the plate three times with PBSTA. Dry the plate on tissue.

(6) Prepare doubling dilutions of the first antibody using PBSA as diluent.

(7) Add 50 μl of PBSA to the plate wells. (Use this volume with standard solutions or sample extracts in the established assay.)

(8) Add 50 μl of the first antibody dilutions to PBSA in the wells, cover the plate and leave it to incubate at room temperature for 2 h.

(9) Discard the plate contents and wash the plate four times with PBSTA. Dry the plate on tissue.

(10) Add 50 μl of the second antibody to each well. Cover the plate and leave it to incubate overnight at 4 °C.

(11) Discard the plate contents, and wash the plate four times with PBSTA. Dry the plate on tissue.

(12) Add 150 μl of freshly prepared substrate to each well. Incubate the plate at room temperature until the colour of the enzyme–substrate complex develops and the absorbance reading of zero is between 1.6 and 1.8 (20–30 min). The maximum readings for both the PBSA blank and the negative sample extract blank should be between 0.1 and 0.15. Read the absorbance at 405 nm. Plot the absorbance (y) *versus* the first antibody dilution (x). From y at half the absorbance maximum obtain the first antibody dilution.

Competitive assay incorporating standards and test samples: extraction of zinc bacitracin from animal feedingstuffs

(1) Weigh 2 g of sample into a 150 ml conical flask. Add 20 ml of PBSA (pH 5.4) and place the flask on a wrist-action shaker for 30 min. Masses and volumes can be altered to give a final concentration of 0.5–1 μg ml^{-1} in the extract. Include the appropriate negative sample and use the extract to prepare calibration standards from 1 mg ml^{-1} stock solution [see step (4)].

(2) Transfer the contents of the flask to a 50 ml conical centrifuge tube. Centrifuge the contents for 15 min at 2000 rev min^{-1}. Filter a suitable volume of supernatant through a Gelman Acrodisc filter and retain the filtrate for analysis.

(3) Prepare standard solutions of bacitracin or zinc bacitracin from a 1 mg ml^{-1} stock solution. Use PBSA (pH 5.4) to dissolve the standards. Also prepare standards in the appropriate negative sample extract.

(4) Follow the procedure for the antibody dilution curve, but use 50 μl aliquots of standards or sample extracts for PBSA.

It is important to include blanks and zeros in each assay. Blanks should comprise 50 μl of PBSA or negative sample extract plus 50 μl of PBSA; no first antibody should be included. Zeros should comprise 50 μl of PBSA or negative sample extract plus 50 μl of first antibody.

Results

ELISA

As no antigen is present in the zero, there is no competition with immobilized antigen in the plate coating for sites on the first antibody. Therefore, total binding of the first antibody to antigen in the plate coating produces a high absorbance reading.

A decrease in absorbance shows that competition has taken place and indicates the presence of antigen in the test sample or standard.

Extensive investigation showed that PBSA (pH 5.4) was the most efficient extractant of zinc bacitracin from animal feeds. Calibration graphs of bacitracin in PBSA (pH 7.2) and zinc bacitracin in PBSA (pH 5.4) demonstrated parallelism. A similar response was seen for the standards of both bacitracin and zinc bacitracin in PBSA (pH 5.4).

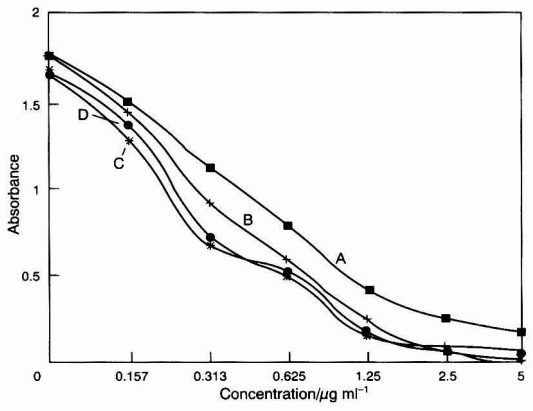

Fig. 4 Dose–response curves: A, premix 10% (4.2 U mg^{-1}); B, zinc bacitracin 1 (71 U mg^{-1}); C, zinc bacitracin 2 (69 U mg^{-1}); and D, bacitracin (73 U mg^{-1}). Plate coating, 3 μg ml^{-1}

No cross-reactivity was seen when the following commonly used veterinary medicinal additives were incorporated into the assay at normally prescribed concentrations: halofuginone; lincomycin; monensin; salinomycin; spiramycin; and virginiamycin.

Fig. 4 shows the dose–response curves for standards of bacitracin, zinc bacitracin from two different soruces, and zinc bacitracin premix (10% zinc bacitracin). All standards were prepared from stock solutions containing 1 μg ml^{-1} bacitracin and zinc bacitracin (*i.e.*, pharmaceutical grade zinc bacitracin from two different sources and premix) dissolved in PBSA (pH 5.4).

The decrease in absorbance at levels as low as 0.157 μg ml^{-1} indicates recognition of the antigen by the monoclonal antibody. The lower activity of the premix is also apparent. The activity of each 0.157 μg ml^{-1} standard was as follows: bacitracin (Sigma), 0.0115 U ml^{-1}; zinc bacitracin (Sigma), 0.0111 U ml^{-1}; zinc bacitracin 2, 0.0108 U ml^{-1}; and premix, 0.0066 U ml^{-1}.

The results in Fig. 4 were obtained from the mean of eight absorbance readings for each standard concentration. The relative standard deviations ranged from 1 to 10%.

The capacity of the assay to detect the presence of both bacitracin and zinc bacitracin in feeds at concentrations lower than the minimum prescribed level of 5 mg kg^{-1} (=0.5 μg ml^{-1} in the sample extract) can be seen in Fig. 1. Negative pig-feed samples were spiked at levels of 10, 5 and 1 mg kg^{-1}. At concentrations as low as 0.1 μg ml^{-1} in the sample extract (= 1 mg kg^{-1}) some matrix interference can be seen, but there is still a lower absorbance reading, indicating the presence of the antigen. The similarity in activity of both forms of bacitracin is also illustrated.

Absorbance readings for the negative sample extracts (zeros) were comparable to those obtained for the PBSA zeros (Table 1), indicating that the feed components had not interfered with the ELISA.

Five feedingstuffs supplemented with zinc bacitracin were assayed; the results obtained by ELISA compared well with those from bioassay (Table 2). These findings also show that the recovery of zinc bacitracin from feedingstuffs by the described extraction method is satisfactory.

Further evidence to support the recovery is given in Table 3.

Table 1 Effect of sample matrix

PBSA zero	Absorbance	Negative feed extract (zero)	Absorbance
Assay 1	1.769	Assay 1 pig feed	1.678
Assay 2	1.629	Assay 2 pig feed	1.543
Assay 3	1.961	Assay 3 pig feed	1.834
Assay 4	1.797	Assay 4 layer feed	1.571
Assay 5	1.687	Assay 5 layer feed	1.779

Table 2 Results from recovery experiment 1

	Concentration/mg kg^{-1}		
Feed (declared zinc bacitracin content)	ELISA (day 1)	ELISA (day 2)	Bioassay
Pig feed (10 mg kg^{-1})	9	7	12*
Pig feed (20 mg kg^{-1})	18	20	17
Pig feed (50 mg kg^{-1})	41	36	47
Layer feed (20 mg kg^{-1})	21	25	17
Layer feed (50 mg kg^{-1})	42	46	44

* This value was obtained from commercially available ELISA.

HPLC Conditions for the Separation of Zinc Bacitracin

A Shimadzu HPLC system was used under the following operating conditions: ultraviolet detector (wavelength, 220 nm); column (Zorbax C8; 5 μm; length, 250 mm; i.d., 4.6 mm); mobile phase [490 ml methanol–acetonitrile (50 + 50) were added to 510 ml 0.05 mol l^{-1} potassium dihydrogenphosphate, and the pH of the final solution was adjusted to 6.8]; flow rate (1 ml min^{-1}); and injection volume (200 μl).

Zinc bacitracin (1 mg) was dissolved in acid mobile phase (99% mobile phase + 1% concentrated orthophosphoric acid). Fractions 1–7 (Fig. 2) were collected, the organic components of the mobile phase were removed by evaporation under nitrogen, and the remaining fraction solutions contained in 0.05 mol l^{-1} potassium dihydrogenphosphate were included in the ELISA method. The responses of the individual components are shown in (Fig. 3). Fractions 4, 5 and 6 correspond to bacitracin components B_1, B_2 and A, respectively, which are known to be the most microbiologically active.[2] The response of these components in the ELISA demonstrates activity as shown by the low B/B_0 (%) values (i.e., bound/unbound %), indicating the presence of antigen and its recognition by the monoclonal antibody. Fraction 7 was found to be comparatively inactive.

Table 3 A negative pig feed was spiked at 5 mg kg^{-1} with a 100 μg ml^{-1} standard solution of zinc bacitracin (activity, 71 U mg^{-1}), zinc bacitracin powder (activity, 71 U mg^{-1}), and premix (10% zinc bacitracin; activity, 4.2 U mg^{-1}). These spiked samples were assayed with a manufacturer's sample supplemented at 20 μg kg^{-1} with zinc bacitracin (activity, 42 U mg^{-1}). Extracts were prepared from each sample to give an expected final concentration of 0.5 μg ml^{-1} zinc bacitracin

Sample reference	Absorbance
Zinc bacitracin standard (0.5 μg ml^{-1})	0.600
Negative feed (spiked with 100 μg ml^{-1} standard solution)	0.583
Negative feed (spiked with zinc bacitracin powder)	0.551
Premix standard (0.5 μg ml^{-1})	0.805*
Negative feed (spiked with premix)	0.810*
Supplemented feed	0.866*

* The lower activity of the premix and the zinc bacterial supplemented feed is shown by the higher absorbance readings.

Discussion

Because of antibody specificity, it can be seen from the results that it is possible to use the described ELISA method to detect the presence of the antibiotic zinc bacitracin at levels as low as 1 mg kg^{-1} in animal feedstuffs. Given the 96 well composition of a microtitre plate it is possible to analyse in a shorter time a greater number of standards, samples, and controls than the conventional assay allows. Another advantage of this ELISA method is the rapid and simple extraction procedure, which does not entail excessive sample extract dilution, and hence reduces errors.

Similar responses are seen for pharmaceutical grades of bacitracin and zinc bacitracin, and zinc bacitracin premix, which is the form in which the antibiotic is usually added to feeds.

The inclusion of the components of zinc bacitracin in the ELISA method following separation by HPLC was useful in its demonstration of individual component activity within the assay. These findings are supported by the assessment of microbiological activity determined by other workers.

The authors thank the DTI's National Measurement Systems Policy Unit for funding this work.

References

1 Brewer, G. A., in *Analytical Profiles of Drug Substances*, ed. Florey, K., Academic Press, New York, London, 1980, vol. 9, pp. 1–69.
2 Bell, R. G., *J. Chromatogr.*, 1992, **590**, 163.
3 Pavli, V., and Sokolic, M., *J. Liq. Chromatogr.*, 1990, **13**, 303.
4 Avrameas, S., *Immunochemistry*, Pergamon Press, 1969, vol. 6, pp. 53–66.

Paper 3/013041
Received March 5, 1993
Accepted September 7, 1993

Development of an Enzyme-linked Immunosorbent Assay for Isoproturon in Water

M. F. Katmeh, G. Frost, W. Aherne* and D. Stevenson†
Robens Institute, University of Surrey, Guildford, Surrey, UK GU2 5XH

A competitive enzyme-linked immunosorbent assay (ELISA) suitable for the determination of the urea herbicide isoproturon [3-(4-isopropylphenyl)-1,1-dimethyl urea] in water has been developed. A derivative of isoproturon [3-(4-isopropylphenyl)-1-carboxypropyl-1-methyl urea] has been synthesized and linked to thyroglobulin using the *N*-hydrosuccinimide reaction. The immunogen was used to immunize two sheep, which both responded by producing specific antibodies to isoproturon with little cross-reactivity to various structurally related and unrelated pesticides. The enzyme label was prepared by coupling the hapten to horseradish peroxidase using the above reaction. The coated-antibody competitive ELISA, which has a sensitivity of 0.03 μg l^{-1}, permits the direct determination of isoproturon in various water matrices and can facilitate the monitoring of water quality in drinking-water supplies.

Keywords: *Isoproturon; antibody production; enzyme-linked immunosorbent assay; urea herbicide; water analysis*

Introduction

Increased public awareness of possible harmful effects of toxic chemicals in the environment has led to a greater demand for analytical methods capable of determining low levels of pesticides. These in particular have received much attention by the European Community (EC) and the EC maximum admissible concentration (MAC) for single pesticides in drinking water has been set at 0.1 μg l^{-1} (0.1 ppb).[1]

Analysis for pesticide residues has conventionally been achieved by chromatographic techniques such as high-performance liquid chromatography, gas chromatography and mass spectrometry. While these methods are highly specific and generally achieve adequate limits of detection, sample preparation procedures are often time consuming and limit sample handling capacity. The need to develop more cost-effective methods for monitoring occupational and environmental exposure and the quality of water supplies has led to the development of pesticide immunoassays.[2] Immunoassays have been developed for a variety of pesticides including atrazine,[3] simazine,[4] paraquat[5,6] and 2,4-D [(2,4-dichlorophenoxy)acetic acid].[7]

Isoproturon [3-(4-isopropylphenyl)-1,1-dimethyl urea] (Fig. 1) is a urea herbicide commonly used in the UK to control broad leaf weeds and grasses, particularly in the cultivation of cereals. It has been detected in drinking-water supplies in the UK[8] at concentrations greater than 0.1 μg l^{-1} (the MAC for single pesticides in drinking water). This concentration of isoproturon cannot be easily measured by traditional and approved techniques such as those of chromatography,[9] and such methods may not be ideally suited to the task of rapid and frequent monitoring of large numbers of samples.

As an alternative, quantitative enzyme-linked immunosorbent assay (ELISA) offers high specificity, sensitivity, simplicity and suitability for the analysis of a large number of samples in a short period of time.[10–12] Recently, Liegeois and co-workers[13,14] described ELISA methods suitable for detecting 1 μg l^{-1} of isoproturon in aqueous and soil samples. In this paper, the development of a direct, competitive ELISA procedure, with a limit of detection of 0.03 μg l^{-1} (below the MAC level) and which provides a simpler and more reliable assay than the indirect ELISA system, is described.

Experimental

Materials and Equipment

Unless stated otherwise, all chemicals were of AnalaR grade from BDH (Poole, Dorset, UK). Phosphate-buffered saline (PBS), pH 7.4 (0.15 mol l^{-1}), containing 0.05% v/v of Tween 20 (Sigma, Poole, Dorset, UK), was used as the washing buffer for the assay. Barbital solution (0.07 mol l^{-1}), pH 9.6 (14.4 g l^{-1} sodium barbitone), was used for coating the antibodies on to the solid support. Horseradish peroxidase (HRPO) was purchased from Biozyme (Blaenavon, Gwent, UK). Other chemicals used were *N*-hydroxysuccinimide, dicyclohexylcarbodiimide (DCC) and dimethylformamide (DMF), obtained from Sigma. A standard stock solution (1 mg ml^{-1}) of isoproturon in methanol was prepared from a stock powder (Greyhound Chemicals, Birkenhead, UK) and stored at 4 °C. Immulon 2 flat-bottomed polystyrene microtitre plates (Dynatech, Billinghurst, Sussex, UK) were used as the solid support. Colour development from the ELISA reaction was measured with a Multiskan bichromatic microtitre plate reader [Labsystems Group (UK), Basingstoke, Hampshire, UK].

Synthesis of 3-(4-Isopropylphenyl)-1-carboxypropyl-1-methyl Urea

The first stage of the synthesis, involving the formation of (4-isopropyl)phenyl isocyanate **2**, was carried out with triphosgene as a convenient and less hazardous replacement

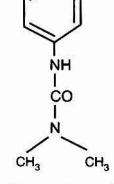

Fig. 1 Chemical structure of isoproturon [3-(4-isopropylphenyl)-1,1-dimethyl urea]

* Present address: Institute of Cancer Research, Drug Development Section, 15 Cotswold Road, Belmont, Sutton, Surrey, UK SM2 5NG.
† To whom correspondence should be addressed.

or the monomer, Triphosgene [bis(trichloromethyl)carbonate; 0.85 g, 2.86 mmol] was weighed into a two-neck flat-bottomed flask (150 ml) fitted with a reflux condenser and an addition funnel mounted on a suitable hot-plate stirrer. Dry toluene (6 ml) was added and the solution was stirred with a magnetic stirrer. A solution of (4-isopropyl)phenylamine **1** (1.14 g, 8.4 mmol) in dry toluene (7 ml) was added dropwise, and the funnel was washed out with dry toluene (5 ml). The mixture was gently refluxed, and all the solids slowly dissolved with the evolution of HCl gas ($CaCl_2$ guard tube). Heating was continued for 2 h, and the flask and contents were left overnight at room temperature.

For the second stage, the intermediate isocyanate solution **2** was evaporated to remove toluene, and the viscous residue was added dropwise to a stirred solution of *N*-(methylamino)butyric acid hydrochloride (1.3 g, 8.5 mmol) and sodium hydroxide (0.74 g, 18.5 mmol) in water (10 ml) in a 50 ml conical flask. The solution was stirred for 2 h at room temperature at which time the pH was 11. A small amount of fine precipitate was filtered off, washed with water (7 ml) and combined with the main precipitate. The filtrate was acidified with 2 mol l^{-1} HCl to pH 3, and the resulting precipitate was filtered off on a Whatman (Maidstone, Kent, UK) No. 50 paper (Buchner funnel) and washed with water until the filtrate was pH 5. The product 3′-(4-isopropylphenyl)-1-carboxypropyl-1-methyl urea **3** was dried in vacuum over $CaCl_2$ to 725 mg. Examination by thin-layer chromatography (ethyl acetate–hexane, 4 + 1) showed one major spot only. The reaction sequence of the hapten **3** is shown in Fig. 2.

Isoproturon–Protein Conjugate

The isoproturon hapten **3** was conjugated to bovine thyroglobulin using the *N*-hydroxysuccinimide active ester reaction.[15] The whole reaction was carried out at room temperature. Hapten 8817 (100 μmol) was dissolved in 0.5 ml of dry re-distilled DMF. Similarly, 100 μmol of *N*-hydroxysuccinimide and 300 μmol of DCC was each dissolved in DMF (0.25 ml). The above three solutions were mixed together overnight at room temperature (needle crystals of dicyclohexylurea were formed). Thyroglobulin (0.1 μmol, 68 mg) was dissolved in 1 ml of distilled water, then 20 μmol of the active ester, assuming complete reaction (after crystals were spun down), was added to the protein solution, and the reaction mixture was stirred overnight (a heavy precipitate was formed). The conjugate used had a nominal molar ratio (thyroglobulin : active ester) of 1 : 200. Finally, the conjugate was dialysed against distilled water (3 × 1 l) for 48 h. The concentration of the protein in the retentate was adjusted to 5 mg ml^{-1}, and the solution was stored at 4 °C in the presence of sodium azide (0.1% of final concentration).

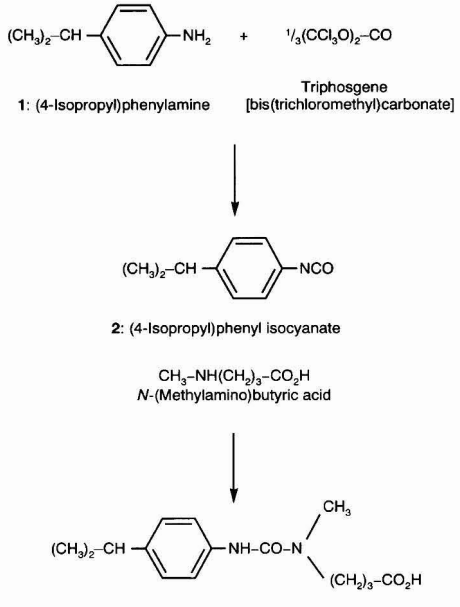

Fig. 2 Reaction sequence for synthesizing hapten **3**

Immunization Procedure

Two mature Suffolk sheep were immunized by conventional procedures. Thyroglobulin conjugate (5 mg) and 0.1 ml of BCG (bacillus Calmette–Guerin) vaccine (Evans Health Ltd., Leatherhead, Surrey, UK) in 1 ml of sterile water was emulsified with 2 ml of non-ulcerative freunds adjuvant and injected intramuscularly into the hind legs and back. The animals were boosted approximately 2 months later with half the primary dose containing no BCG. A further five boosting doses were administered at appropriate intervals, which resulted in a significant immune response. Blood was collected from the jugular vein 10 d after each immunization and at appropriate intervals (*i.e.*, boostings, were made every 4–5 months, and blood collections were made every two weeks). After allowing the blood to clot, the serum was separated and stored at 4 °C with the addition of sodium azide (0.1%).

Purification of Antisera

A radioimmunoassay (RIA), using ^{14}C-isoproturon radiolabel (Ciba-Geigy plc, Whittlesford, Cambridge, UK) and dextran-coated charcoal was used to screen the antisera for the presence of specific antibodies. The immunoglobulin G (IgG) fraction from antisera with the highest titres, as determined by RIA, were obtained by DEAE ion-exchange chromatography. The antiserum was diluted 1 + 10 in 0.01 mol l^{-1} phosphate buffer (pH 6.4) and applied to a diethylaminoethyl (DEAE) Zetaprep 15 Disk (Pharmacia, Uppsala, Sweden), and the IgG fraction was eluted with the same buffer. Fractions (10 × 5 ml) were collected from the cartridge, and the absorbance of each fraction was measured at 280 nm. The four most concentrated fractions were pooled. The concentration of immunoglobulin in the partially purified isoproturon antibodies was found to be 1.29 mg ml^{-1} (A 1% 280 nm = 1.40[16]). The purified immunoglobulin was stored at 4 °C with the addition of thiomersal solution (0.1% final concentration).

Preparation of Peroxidase Isoproturon Label

The isoproturon hapten was also conjugated to HRPO, by using the *N*-hydroxysuccinimide active ester method at a nominal molar ratio (HRPO hapten) of 1 : 20. The enzyme conjugate was de-salted on a Sephadex G-15-120 column after being left overnight in the dark at room temperature.

Competitive ELISA

The final assay protocol is described below.

A microtitre plate was coated with 200 μl per well (0.65 μg ml^{-1}) of partially purified (by ion exchange) isoproturon antibody (sheep 1 BIVa) diluted in 0.07 mol l^{-1} sodium barbitone, pH 9.6 (Fig. 3). The plate was incubated overnight at 4 °C in a moist chamber and washed three times using a wash-bottle containing 0.15 mol l^{-1} PBS (pH 7.4) containing

0.05% v/v in Tween 20 (PBST). Standard solutions (100 μl per well) of isoproturon in the range 0–100 ng ml^{-1} (six standards), made up in tap-water, were applied to the plate followed by the addition of HRPO-labelled isoproturon (1 + 3999), diluted in PBS buffer containing 2.5% of normal sheep serum, 100 μl per well, to bring the total volume to 200 μl per well. The plate was incubated in a shaker incubator (Amerlite, Amersham, Buckinghamshire, UK) for 1 h at 37 °C. After incubation the plate was washed four times with PBST, and 200 μl per well of chromagen–substrate (20 mg of tetramethylbenzidine dissolved in 1 ml of DMF to make up the sub-stock solution, then, as required, 100 μl of the sub-stock solution dissolved in 20 ml of citrate buffer (pH 5) and 10 μl of H_2O_2) was placed in all the wells. After a further 30 min incubation the reaction was stopped by the addition of 1 mol l^{-1} HCl (50 μl per well). The plate was read using the Labsystems Multiskan plate reader at 450 nm, and the standard curves were evaluated off-line using a four-parameter logistic plot (RiaCalc, Wallac, Milton Keynes, UK).

Results

Antiserum Production

The response of the animals to the isoproturon–thyroglobulin immunizations were monitored by RIA using ^{14}C-isoproturon label and dextran-coated charcoal. Both sheep produced an adequate immune response, but unfortunately, one animal died at an early stage. The remaining animal produced high-titre antisera, as illustrated in Fig. 4. The high-titre antiserum collected from Sheep 1, 9 d after the fourth boost, was eventually used to establish the assay procedure described below.

Optimization of Reagents

The dilution of the coating antibody and isoproturon label were the first conditions that required optimization, and, therefore, a checkerboard experiment was set up in which various dilutions of the coating antibody were titrated against various dilutions of the enzyme-labelled isoproturon. A 1 + 1999 (0.65 μg ml^{-1}) dilution of the antibody and 1 + 3999 dilution of the isoproturon label were chosen for the assay development since they were shown to yield high absorbance

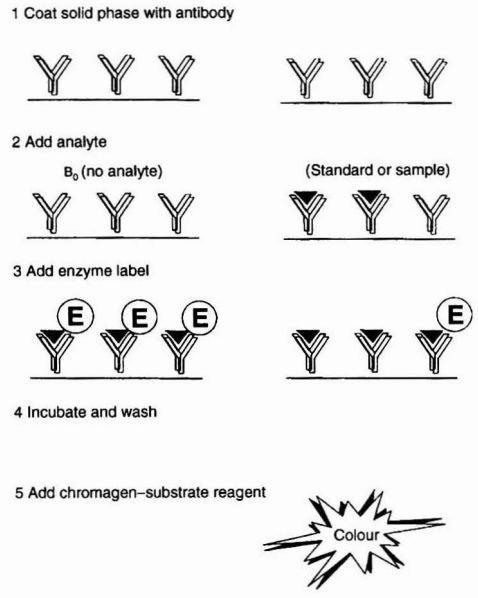

Fig. 3 Diagrammatic representation of competitive ELISA protocol for the phenyl urea herbicide isoproturon

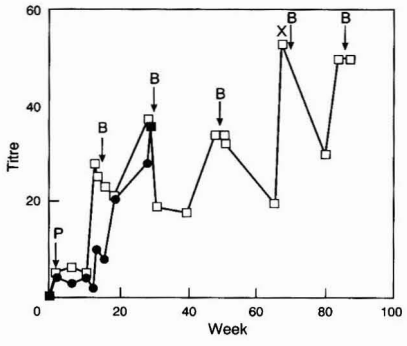

Fig. 4 Immune response in two sheep (sheep 1, □, and sheep 2, ●) immunized with the isoproturon hapten conjugated to bovine thyroglobulin. The antiserum from sheep 1 collected 66 weeks following the initial injection (×) was utilized for further assay development. (Points marked P = prime and B = boost)

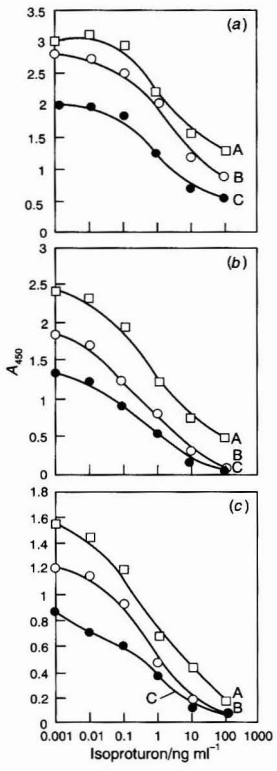

Fig. 5 Optimization of the dilutions of isoproturon coating antibody and enzyme label for the calibration graph (A, antibody dilution 1 + 999; B, antibody dilution 1 + 1999; and C, antibody dilution 1 + 3999). Label dilution: (*a*) 1 + 19999; (*b*) 1 + 39999; and (*c*) 1 + 79999

readings, a wide dynamic range and good sensitivity for the standard curve (Fig. 5). The effects of different types of microtitre plates, temperatures and incubation times on the antibody–antigen reaction were also investigated. The polystyrene microtitre plate incubated overnight at 4 °C showed better reproducibility and higher absorbance than any other conditions examined. Therefore, the conditions described in the methods section were used to validate the assay.

Assay Validation

The mean of six isoproturon standard curves, prepared in tap-water and obtained using the isoproturon–ELISA method described, is shown in Fig. 6. The sensitivity of the assay, defined as the concentration equivalent to a three standard deviation (s) fall from binding at B_0 (the binding measured in the absence of isoproturon), was 0.03 μg l^{-1}, well below the EC admissible concentration for pesticides in drinking water. The intra-assay relative standard deviation (s_r) shown in Fig. 6 ranged from 1 to 5% across the standard curve compared with the inter-assay s_r, which ranged from 1 to 15%, as shown in Table 1. Table 2 shows the degree of reactivity of isoproturon antibody with various herbicide compounds. Although not all urea herbicides have been tested for cross-reactivity, the antibody demonstrates remarkably high specificity towards isoproturon.

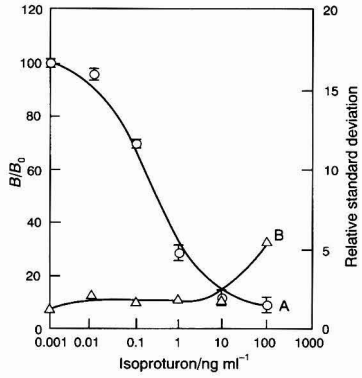

Fig. 6 Intra-assay variation for isoproturon calibration graph. A, Mean of six standards (error bas show standard deviation; B, relative standard deviation.

Table 1 The precision of the isoproturon ELISA within and between assays by using a mean of six standard curves

Isoproturon standard/ ng l^{-1}	Within-assay variation		Between-assay variation	
	Mean B/B_0 (s)	s_r (%)	Mean B/B_0 (s)	s_r (%)
10	96 (1.98)	2.1	94 (1.39)	1.5
100	70 (0.98)	1.4	65.5 (5.6)	8.54
1000	29 (0.22)	0.76	25 (3.7)	15

Table 2 Specificity of isoproturon antiserum towards a selection of herbicides

Compound	Cross-reaction (%)
Isoproturon	100
Chlorotoluron	0.187
Chlorbromuron	0.085
Metoxuron	0.1
Chlorsulfuron	<0.001
Metamitron	
2,4-D	
MCPA	
Atrazine	
Simazine	
Mecoprop	
Propyzamide	
Paraquat dichloride	
Terbutryn	
MCPB	

Determination of Isoproturon in Tap-water

The effect of matrices was investigated by comparing standard curves prepared with different solutions (distilled water, tap-water and PBS). Although Fig. 7 shows no significant matrix effect between the three sets of standards plotted as B/B_0, tap-water was chosen for diluting standards as it is the matrix most closely resembling that of drinking-water supplies in general. However, when spiking 200 pg ml^{-1} of isoproturon into river water and water obtained from an ornamental lake, the

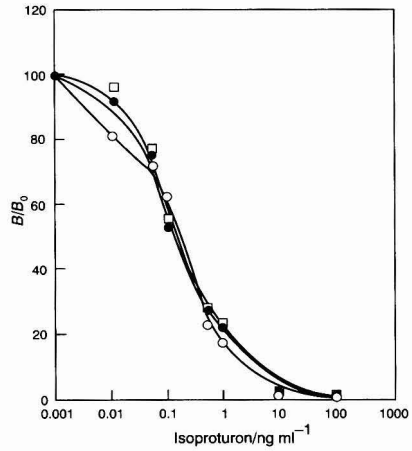

Fig. 7 Effect of different matrices on the isoproturon calibration graph using ELISA protocol. Standards were prepared in tap water (□); distilled water (●); phosphate buffered saline (○)

Table 3 The recovery of isoproturon from different water sources by using ELISA

Isoproturon added/pg ml^{-1}	Amount determined/ pg ml^{-1}	s_r (%) (n = 5)	Recovery (%)
From tap-water			
(day 1) 100	184	5.9	96
200	184	1.1	92
800	651	1.2	81
From tap-water			
(day 2) 100	84	10.1	84
200	162	9.1	81
800	736	3.2	92
From tap-water			
(day 3) 100	108	7.3	108
200	187	5.9	94
800	814	4.7	102
From river water			
River A: 200	162	0.8	81
River B: 200	169	3.1	85
River C: 200	163	2.4	82

recoveries were 215 and 186%, respectively. Enhanced recovery could be due to the presence of organic matter in the river samples interfering with the antigen–antibody binding reaction. Since we have previously observed improved recovery of pesticides from biological fluids,[17] the effect of adding normal sheep serum to the enzyme-labelled isoproturon solution was investigated. The addition of serum to the assay medium slightly increased the sensitivity of the standard curve, but did not significantly change the precision of the assay. However, reproducible and quantitative recovery of isoproturon from water obtained from various sources (*e.g.*, river- and tap-water) was possible. Tap-water samples spiked with isoproturon solution showed recoveries ranging from 80 to 110%, and river-water samples spiked with isoproturon solution showed recoveries ranging from 80 to 85% (Table 3).

Discussion

A rapid, sensitive and easy to perform ELISA for the urea herbicide isoproturon has been described. In the first instance the assay was optimized for high sensitivity in order to meet the requirements of the EC MAC of 0.1 μg l^{-1} for individual pesticides, although with suitable modifications other applications such as biological monitoring and occupational exposure studies would also be possible.

The high specificity of the antibodies described here was achieved by covalently coupling thyroglobulin protein with a carboxyl group synthesized on the secondary amino group of the hapten. It is known that the specificity of the antiserum is directed primarily towards the part of the molecule most distant from the point of attachment [*i.e.*, the isopropylphenyl group of the hapten **3**, Fig. 2]. The cross-reactivity of the antiserum with a range of related and unrelated pesticides was low. The closely related urea herbicide chlorotoluron showed virtually no cross-reactivity.

The ELISA assay for isoproturon was reliable and robust from day to day and by using standards prepared in tap-water (previously shown to have no effect on the antibody–antigen reaction) a limit of detection three times less than the MAC (0.03 μg l^{-1}) was achieved.

Water samples from a variety of sources are likely to exhibit a wide range of pH and ionic strength, and often contain suspended solids. Initial experiments showed that differences in matrix effects between standards and samples resulted in non-quantitative and variable recovery of isoproturon from authentic water samples. Previous experience has shown improved recovery of atrazine and paraquat from biological samples,[17] and the addition of normal sheep serum (at a final concentration of 2.5%) to the enzyme conjugate was found to overcome the matrix effects seen with ground water; quantitative recovery of isoproturon was then obtained. It may be appropriate to apply this simple modification to other immunoassays for water pollutants if matrix effects are found to result in significant errors.

Immunoassays have an important role to play in environmental analysis. The antibodies described here have been used to develop a rapid and sensitive method for monitoring water supplies for the presence of isoproturon. In conclusion, the assay provides a feasible alternative method for the determination of this herbicide in water supplies. At present, the possibility of adapting semi-quantitative 'field assays' for isoproturon is under investigation in our laboratory.[18]

This work was supported by the Health and Safety Executive.

References

1 EC Directive relating quality of water intended for human consumption (80/778/EEC), *Off. J. Eur. Commun.*, L229/11.
2 van Emon, J. M., Seiber, J. N., and Hammock, B. D., *Anal. Methods Pestic. Plant Growth Reg.*, 1989, **27**, 217.
3 Bushway, R. J., Perkins, B., Savage, S. A., Lekousi, S. J., and Ferguson, B. S., *Bull. Environ. Contam. Toxicol.*, 1988, **40**, 647.
4 Hardcastle, A., Aherne, G. W., and Marks, V., *J. Biolum. Chemilum.*, 1988, **2**, 209.
5 Niewola, Z., Walsh, S. T., and Davis, G. E., *Int. J. Immunopharmacol.*, 1983, **3**, 211.
6 Niewola, Z., Benner, J. P., and Swaine, H., *Analyst*, 1986, **111**, 399.
7 Knopp, D., Nuhr, P., and Dobberkan, H. J., *Arch. Toxicol.*, 1985, **58**, 27.
8 Lees, A., and McVeigh, K., *An investigation of Pesticide Pollution in Drinking Water in England and Wales*, Friends of the Earth, London, 1988.
9 Thurman, E. M., Meyer, M., Pomes, M., Perry, C. A., and Schwab, A. P., *Anal. Chem.*, 1990, **62**, 2043.
10 Newsome, W. H., *J. Agric. Food Chem.*, 1985, **33**, 528.
11 Feng, P. C. C., Wratten, S. T., Horton, S. R., Sharp, C. R., and Logusch, E. W., *J. Agric. Food Chem.*, 1990, **38**, 159.
12 Kaufman, B. M., and Clower, M., Jr., *J. Assoc. Off. Anal. Chem.*, 1991, **74**, 239.
13 Liegeois, E., Dehon, Y., de Brabant, B., Copin, A., and Portetelle, D., in *Proceedings of an International Symposium on Environmental Biotechnology*, Ostende, 1991, p. 69.
14 Liegeois, E., Dehon, Y., de Brabant, B., Perry, P., Portetelle, D., Copin, A., *Sci. Total Environ.*, 1992, **123/124**, 17.
15 Anderson, G. W., *J. Am. Chem. Soc.*, 1963, **86**, 1839.
16 Little, J. K., and Donahue, H., in *Methods in Immunology and Immunochemistry*, eds. Williams, C. A., and Chase, M. A., Academic Press, New York, 1967, vol. 2, 343 pp.
17 Hardcastle, A., Saleem, E., and Aherne, G. W., in *Proceedings of ACB National Meeting*, eds. Martin, S. M., and Hallaran, S. P., Association of Chemical Biochemists, London, 1990, p. 2.
18 Hardcastle, A., Aherne, G. W., Thorpe, G., in *Watershed/The Future for Water Quality in Europe*, eds. Wheeler, D., Richardson, M. L., and Bridges, J., Pergamon Press, Oxford, 1989, vol. 2, p. 293.

Paper 3/01325A
Received March 8, 1993
Accepted August 2, 1993

Integrated Optical Immunosensor for *s*-Triazine Determination: Regeneration, Calibration and Limitations

Frank F. Bier,* Ralf Jockers† and Rolf D. Schmid

GBF—Gesellschaft für Biotechnologische Forschung mbH, Department of Enzyme Technology, Project Group Biosensors, Mascheroder Weg 1, D-38124 Braunschweig, Germany

Grating couplers, as an example of an integrated optical transducer, were investigated for label-free immunosensing in a flow-through system. The detection of pesticides by a competitive assay format was demonstrated using a triazine (terbutryn) as an example. Long-term stability and reproducibility were achieved by immobilizing the hapten, which in this instance was a derivative of the pesticide to be determined. Hence, the lifetime of the sensor does not depend on the stability of the antibody but is limited only by the quality of the immobilization. Regeneration of the sensor surface was achieved using proteinase supported by acidic washing; it was observed directly and could therefore be optimized. In consequence, calibration, usually critical in immunosensing, was possible. Non-specific binding was determined to be 10% and could be decreased by addition of bovine serum albumin. The detection limit found for terbutryn was 15 μg l^{-1} in the arrangement used; strategies for enhancement of sensitivity are discussed.

Keywords: Immunosensor; integrated optics; grating coupler; competitive assay; s-triazine

The combination of the recognition capability of antibodies with the transducing potential of optical, and especially integrated optical, systems should lead to a suitable and sensitive analytical tool. This notion has stimulated much work in recent years on biosensors using optical transduction principles and their application to immunosensing. Examples are the surface plasmon resonance (SPR), interferometry and grating couplers (for a review, see ref. 1); all these transducers work without any label attached to the ligands. Additionally, much effort has gone into the development of integrated optics to miniaturize transducing devices. However, until now no immunosensor has reached the market. The main obstacles to the adaptation of immunochemistry to immunosensors, especially if label-free techniques are used, are that the antibodies, when immobilized, usually lose binding capacity by the immobilization procedure; non-specific binding cannot easily be distinguished from the specific binding; and regeneration, *i.e.*, release of the antigen–antibody binding, is most often incomplete or impossible owing to the lability of the antibody. Regeneration, however, is necessary for calibration, with the exception of batch calibration for disposable sensors, a method described by Badley *et al.*[2] However, industrial production facilities are required for this type of calibration; these facilities are usually not available in scientific laboratories. Therefore, several attempts have been made to facilitate the release of antigen–antibody binding or to regenerate antibody-coated surfaces.[3,4]

In hapten determination, the problem of regeneration and calibration can be overcome by immobilization of the hapten or a suitable derivative. This has been shown recently with the example of pesticides in a fluorescence-based system.[5] For the use of fluorescence, however, expensive equipment is necessary, which, additionally, is limited in its miniaturization capability. Furthermore, labels have to be introduced for fluorescence detection, which increase assay costs and often decrease the affinity of the antibody for the antigen. These arguments have stimulated work on integrated optical transducers, which are inherently capable of working without any label.

One example of integrated optical transducers, is grating couplers, introduced by Tiefenthaler and Lukosz.[6,7] Until now, reports dealing with affinity binding on grating couplers, *e.g.*, of IgG and anti-IgG, have not reported regeneration and thus calibration was not performed.[8]

In this paper, we report the regeneration and calibration of a label-free immunosensor. The binding of a monoclonal antibody against the *s*-triazine terbutryn is demonstrated using an immobilized derivative of this compound and competition with free analyte is shown. We also demonstrate the effect of non-specific binding on the performance of the sensor.

Pesticides are of great analytical interest as they have been found in ground and drinking waters in recent years. Much effort has gone into developing reliable methods for the detection of pesticides in water destined for human usage. The immunoassay, most often used in the format of an enzyme-linked immunosorbent assay (ELISA), has been shown to be a highly sensitive method for the detection of pesticides in different kinds of water samples and soil extracts.[9–11] In this study we used a monoclonal antibody as a model against terbutryn, which is a herbicide of the *s*-triazine group. The study gives insight into the development of an immunosensor.

Experimental

Reagents

The following reagents were used: aminopropyltriethoxysilane (APTS) (Aldrich, Steinheim, Germany); *N,N*-dimethyldodecylamine *N*-oxide (LDAO) (Fluka, Neu-Ulm, Germany); proteinase K from *Tritirachium album* (Serva, Heidelberg, Germany); bovine serum albumin fraction V (BSA) (Boehringer Mannheim, Mannheim, Germany); terbutryn [2-(1′,1′-dimethylethylamino)-4-ethylamino-6-methylthio-1,3,5-triazine] (Labor Dr. Ehrenstorfer, Augsburg, Germany) [in some experiments terbutryn purchased from Riedel-de Haën (Seelze, Germany) was used]; and 2-aminohexyl-amino-4-ethylamino-6-isopropylamino-1,3,5-triazine (AHA), synthesized by reaction of atrazine [2-chloro-4-

* To whom correspondence should be addressed. Present address: MDC—Max-Delbrück-Centrum für Molekulare Medizin, AG Biosensoren, Robert-Rössle-Strasse 10, D-13122 Berlin-Buch, Germany.

† Present address: Institut Cochin de Génétique Moléculaire, Laboratoire d'Immuno-Pharmacologie Moléculaire, 22 Rue Méchain, F-75014 Paris, France.

ethylamino-6-(1′-methylethylamino)-1,3,5-triazine] with hexyldiamine (A. Bückmann, GBF Braunschweig, Germany). All other chemicals used were of analytical-reagent grade. The monoclonal antibody K1F4 is of the mouse IgG1 subclass. The hybridoma cell line used for the antibody production was kindly provided by Professor B. Hock (Technical University of Munich, Munich, Germany); it is described in detail in ref. 12. The antibody was purified by ion-exchange chromatography with S- and Q-Sepharose (H. Steingass, GBF).

The buffers used were 0.15 mol l^{-1} phosphate-buffered saline (pH 8.0) (PBS) supplemented with 0.08% LDAO, and 0.1 mol l^{-1} glycine–HCl (pH 1.5) (elution buffer).

Proteinase K was diluted in PBS to final concentrations of 2 and 10 μg ml^{-1}.

Terbutryn was dissolved in pure ethanol at 1 mg ml^{-1} and diluted in PBS to the final concentration.

Preparation of Sensor Surfaces and Immobilization of Triazine Derivatives

The grating couplers used were planar SiO_2–TiO_2 monomode waveguides with an embossed grating (2400 lines mm^{-1}) (ASI, Zürich, Switzerland). Prior to silanization, the sensor surface region of the grating was cleaned overnight with dry toluene. In some experiments, preparation of the sensor surface was carried out with a short immersion (5 s) in chromic acid. The cleaned surface was silanized with 10% v/v APTS in dilute HCl (pH 3.4) at 75 °C for 2 h, washed with water and dried at 100 °C. AHA was immobilized with glutaraldehyde (as described in detail in ref. 5) using a modified method closely related to that described in ref. 13. In summary, the silanized waveguide was immersed in 1% v/v glutaraldehyde in 0.1 mol l^{-1} phosphate buffer for 1 h at room temperature, washed with water, immersed in 0.2 and 0.5 mg ml^{-1} solutions of aminohexylatrazine in PBS for 2 h each, followed by the addition of 1 volume of Tris–HCl (pH 7.5) and standing for 1 h at room temperature, washed with PBS, immersed in 0.1 mmol l^{-1} NaOH containing 10 mg ml^{-1} $NaBH_4$ for 30 min at room temperature (to reduce Schiff's base) and finally washed and stored in PBS at 4 °C.

Experimental Set-up

Flow system

The grating coupler waveguides were placed in a suitable flow-through cell connected to a simple flow system (constructed to minimize flow paths). The flow system consists of a 3/2-way valve for buffer/elution buffer and a multi-channel valve for the samples. A peristaltic pump was used to force all the reagents through the flow cell. A schematic diagram of the system is given in Fig. 1. The flow system was constructed to perform completely automatically. To avoid the production of air bubbles in the narrow incubation cell a detergent was added to the buffer. Using 0.08% of LDAO as detergent no influence on the antibody binding was observed.

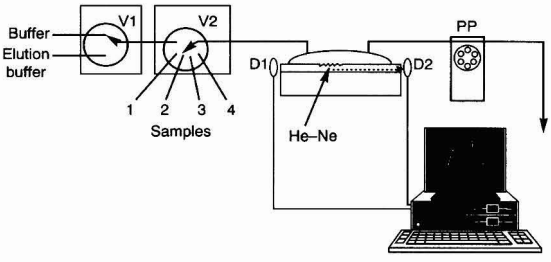

Fig. 1 Grating coupler integrated into a flow system and connected to a computer-aided data collection and data processing unit. V1 is a 3/2-way valve, switches between buffer and elution buffer; V2, a multiport valve for the introduction of different samples; D1 and D2 are photodiodes to measure the incoupling light, which comes from the laser source (He–Ne, 632.8 nm, polarized); PP, peristaltic pump

Grating coupler

The grating coupler was read out with a grating coupler system GCS-1 (ASI, Zürich, Switzerland). The change in refractive index on the sensor surface due to antibody binding was observed by measuring the incoupling angle.[7] From the measured change of the incoupling angle the effective refractive index, n_{eff}, of the guided mode was calculated:

$$n_{eff} = n\sin\alpha + l(\lambda/\Lambda)$$

where n is the refractive index of air, α the angle of incidence, l the refraction order, λ = 632.8 nm the wavelength of the incident light (He–Ne) and Λ the grating number. Solving the mode equation,

$$\phi_m = (2m/tF)(n_F^2 - n_{eff,m}^2)^{-1/2} + \phi_F$$

[eqn. (3.4) in ref. 7], where m is the mode number, n_F the refractive index of the guiding film and ϕ_F the overall phase shift due to the interfaces of the guiding film with its surroundings, for at least two modes, an apparent waveguide thickness, tF, was calculated with the assumption that the refractive index of the guiding film was constant. The details of the calculations are given in ref. 14. The calculations were carried out automatically during the measurement using ASI software.

Assay Procedure

The complete measuring cycle was as follows: (1) washing with PBS (5 min, baseline); (2) incubation with antibody (20 or 30 min); (3) washing with PBS (5 min, signal); and (4) regeneration by (a) washing with elution buffer (5 min), (b) washing with PBS (5 min), (c) incubation with proteinase (10 min), (d) washing with PBS (5 min) and (e) washing with elution buffer (5 min). In some experiments the times of steps 4(a), (b) and (d) were decreased to 1 min or even omitted, and that of step 4(c) was decreased to 5 min by using a higher proteinase concentration (10 μg ml^{-1}) without loss of regeneration capability.

The difference in signal readout before (step 1) and after (step 3) incubation was taken as the system response, measured as the difference in apparent waveguide thickness (tF in nm).

In competition experiments, free analyte and antibody were mixed at least 1 h before incubation on the waveguide.

Results and Discussion

Immobilization

The hapten was coupled directly to the silanized sensor surface, without the use of a protein carrier. This was achieved by adapting standard techniques known from protein chemistry[13] using a hapten derivative with a spacer arm and an amino group as the active site. The spacer between the sensor surface and the hapten consists of six carbons. The coupling of AHA was found to be very stable, as the sensor could be cleaned with ethanol and stored dry without loss of activity.

Covalent binding of a suitable hapten derivative has to be established. The derivative should have a spacer separating the hapten molecule from the surface to increase the accessibility of the hapten by the antibody binding sites, a notion strongly supported by the work of Tiefenauer and Andres.[15] In our example, the spacer was a hexyl group, long enough to allow binding of the antibody to the immobilized

hapten. The coupling by the amino group of the spacer to the modified surface with free aldehyde groups was carried out by the usual protein chemistry that results in a Schiff's base, which was subsequently reduced. The specificity for the binding of the antibody to the coated surface and the high regeneration capability (see below) provide strong evidence for the covalent coupling of the hapten derivative. It should be pointed out that this method of direct coupling of a hapten or hapten derivative to a sensor surface may be used for any type of hapten detection.

Regeneration

Studies were made of the regeneration of the sensor surface. With grating couplers it is possible to detect label-free (and in real time) binding and release of antibodies, as shown in Fig. 2. The results shown were achieved with the modified surface using the monoclonal antibody at a concentration of 1.2 μg ml^{-1} (following A in Fig. 2). With 8 mol l^{-1} urea, sometimes described as a regeneration solution for antibody binding, no release of antibody was observed. Glycine–HCl buffer (pH 1.5) does release the bound antibody partially but is insufficient for regenerating the sensor surface, as was observed by residual binding (details are shown in Fig. 2 in ref. 5). Complete regeneration was achieved by incubation with 10 μg ml^{-1} proteinase (start of incubation indicated as C in Fig. 2). The sensor surface is now completely reactivated without loss of activity, as could be seen during subsequent measurements (see Fig. 3). It is possible for regeneration to be performed in this manner more than 600 times over a 2 month period; this is demonstrated by the data shown in Fig. 3: Fig. 3(*a*) shows a sequence of measurements taken on the fifth day after immobilization and Fig. 3(*b*) shows data taken on day 78 after immobilization with the same sequence.

Also with prolonged acidic washing at pH 1.0 (10 min), complete regeneration was observed. However, during this procedure the baseline of the sensor had a tendency to drift. After several incubation–regeneration cycles with low-pH solution (pH 1.0), the apparent waveguide thickness decreases slightly, indicating some interaction of the SiO_2–TiO_2 film with protons (data not shown).

After regeneration had been confirmed, a series of measurements using various amounts of antibody were possible; the results are summarized in Fig. 4. The calibration graph is shown in the range 0.2–6 μg ml^{-1}. The values are averaged from 3–5 measurements and the error bars indicate the standard deviation (*s*) of *tF*; it is in the range 0.04–0.05 nm.

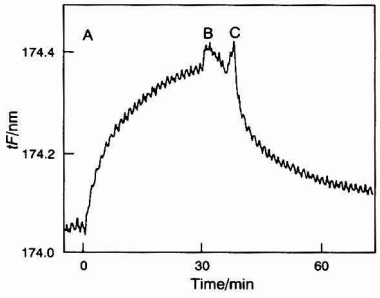

Fig. 2 Real-time monitoring of binding and release of antibodies observed with a grating coupler modified by covalently bound AHA. Apparent thickness of the waveguide *tF* (nm) was observed during a time period of 75 min. Incubation of the monoclonal antibody K1F4 in a concentration of 6 μg m^{-1} started at A and was stopped at B by washing with buffer solution; at C incubation of proteinase K (100 μg ml^{-1}) was started

Using 2*s* as the significance criterion, the detection limit is 0.5 μg ml^{-1} of antibody. Between 0.2 and 2 μg ml^{-1} a linear regression line can be calculated (dashed line in Fig. 4). However, with higher antibody concentrations deviations from linearity are observed.

Non-specific Binding

Non-specific binding was investigated either by competitive binding experiments (see below for details) and by addition of

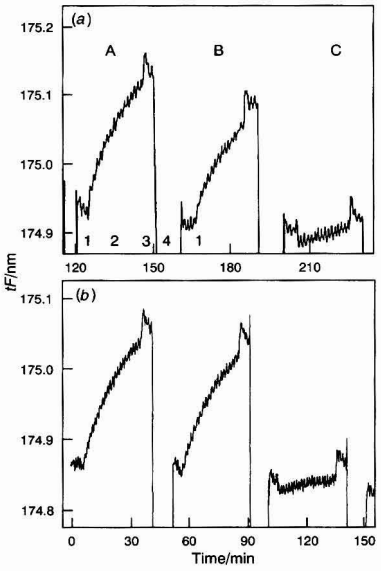

Fig. 3 Competition curves: Real-time monitoring of binding and its inhibition of triazine specific antibodies to AHA modified grating couplers. Apparent thickness of the waveguide is observed during the assay procedure (the steps numbered at the bottom of part (*a*) are for the first binding event, as described in the text). The binding events shown are: A, binding of monoclonal antibodies (K1F4, 1.2 μg ml^{-1}); B, reduction of binding in the presence of 10 μg ml^{-1} of terbutryn; and C, nearly complete suppression of binding by an overdose of terbutryn (1 mg l^{-1}). (*a*) Performance of the sensor at day 5 after immobilization, and (*b*) at day 78, showing the same sequence

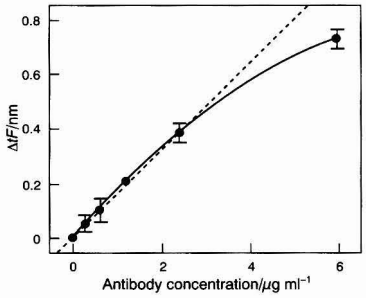

Fig. 4 Standard curve of binding of the monoclonal antibody K1F4 on the sensor surfaces coated with AHA. The change of apparent thickness of the waveguiding film (*tF*/nm) induced by binding of different antibody concentrations is shown. Solid line = 2nd order regression over the whole range, broken line = 1st order regression from 0 to 2 μg ml^{-1}

BSA. In the competitive experiments binding was decreased with increasing terbutryn concentration (see Figs. 3 and 6), indicating that binding to the grating coupler was mainly induced by specific binding; however, residual binding of 10% was observed. Fig. 5 shows the effect of adding various amounts of BSA (0.1–1000 μg ml^{-1}) to 1.2 μg ml^{-1} specific antibody (K1F4): the signal increased significantly if more than 10 μg ml^{-1} of BSA were added. The signal obtained by binding of 1.2 μg ml^{-1} of antibody without being supplemented with BSA is taken as 100% and the increase due to BSA is given in per cent as the additional signal (left-hand scale and filled circles in Fig. 5). Non-specific binding with increasing BSA concentration was observed only when more than 10 μg ml^{-1} were added.

In competitive experiments, however, binding is inhibited more effectively in the presence of small amounts of BSA: if the (mass) concentration of BSA was of the same order of magnitude as the antibody concentration, inhibition occurred more effectively, resulting in only 5% residual binding. This is also shown in Fig. 5 (right-hand scale, open triangles), the residual binding occurring in the presence of an excess of terbutryn (1000 μg ml^{-1}) being plotted against BSA concentration. The 100% value in this case is the signal of 1.2 μg ml^{-1} of K1F4 antibody binding without any terbutryn.

Calibration

Using the monoclonal antibody from clone K1F4, competition between bound and free analyte can be demonstrated. Fig. 3 shows (A) binding; (B) reduction of binding by 10 μg l^{-1} terbutryn and (C) nearly complete suppression of binding by an overdose of terbutryn (1 mg l^{-1}). A calibration graph for terbutryn is shown in Fig. 6. The data shown were obtained using 1.2 μg ml^{-1} of antibody. The system response *versus* the logarithm of terbutryn concentration displays a sigmoidal curve. The standard deviation of five independent measurements is 0.05 nm (10% of the reference signal). The 50% value was 100 μg l^{-1} of terbutryn and the detection limit was found to be 15 μg l^{-1}.

The linear range covers only one order of magnitude (20–200 μg l^{-1}), which we think is caused by the small sensing field, *i.e.*, the focus of the incident laser beam on the grating, which is less than 1 mm^2. Devices performing in this way are applicable to monitoring the pass over of a predefined threshold.

The detection limit of 15 μg l^{-1}, however, is too high for the application of this sensor for drinking water monitoring. For example, it is required to detect amounts of pesticides down to 0.1 μg l^{-1} by the European Drinking Water Act.[16]

Sensitivity with regard to the analyte is limited by the detection limit of the sensor with regard to the antibody binding. The detection limit for antibody binding using the grating coupler was 0.5 μg ml^{-1}, which was higher than with systems employing labels such as fluorescence. With a fibre-optic fluorescence immunosensor we found an antibody concentration of 0.03 μg ml^{-1} as the detection limit, using the same immunochemical system as described here.[5] In consequence, the sensitivity, with regard to the analyte, is increased by more than one order of magnitude by using a fluorescence label. Despite this drawback, integrated optics provide great potential for miniaturization and automation, both of which are useful in both pollution monitoring and other applications; it is therefore worthwhile looking at enhancement strategies. There are possibilities in all three fields of biochemical sensor development.

The transducer. The sensitivity of the grating coupler can be enhanced by using a waveguide with a higher refractive index to provide a more efficient evanescent wave.[1] Such waveguides are now available[17] and will be investigated in the near future.

Chemical modification of the surface. Recently it has been shown that the use of weaker binding derivatives as competitors on the sensor surface can enhance the sensitivity of immunosensors based on a competitive assay format.[18] Additionally, an optimization of the amount of bound competitors may help to alter the sensitivity.

The biological component. More sensitive antibodies, *i.e.*, antibodies with a higher affinity to the analyte, have been developed recently.[19]

Conclusion

Immunosensors for the detection of *s*-triazines using an immobilized hapten derivative can be regenerated and thus calibrated. Non-specific binding was found to be low. We have shown that it was possible to use this approach for integrated optical transducers working without a label. Binding and release of anti-*s*-triazine antibody to the modified grating coupler was monitored in real time. The linear range was found to be fairly narrow, covering only one order of magnitude (20–200 μg l^{-1} terbutryn); the analysis time is about 30 min per sample using the assay format described here. Sensors of this type are designated to monitor the pass over of a given threshold. Application of the approach discussed here to drinking water will depend on the success of enhancement strategies.

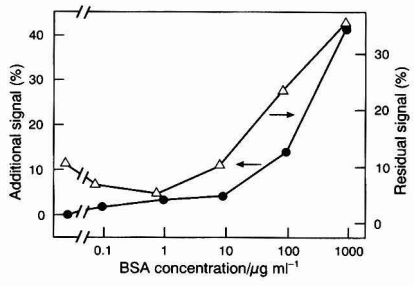

Fig. 5 Unspecific binding of BSA to the AHA modified grating coupler. Additional binding of BSA, which was added to 1.2 μg ml^{-1} antibody (100% antibody without BSA); residual binding in presence of an overdose of terbutryn with added BSA (100% binding of antibody without any terbutryn

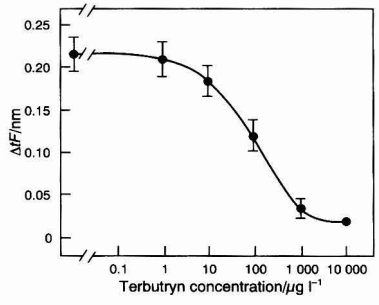

Fig. 6 Calibration graph of the modified grating coupler for terbutryn. The change of apparent thickness of the waveguiding film (tF/nm) induced by binding of antibody (K1F4, 1.2 μg ml^{-1}) and the suppression of binding by different concentrations of terbutryn is shown

The authors thank Professor Dr. B. Hock and Dr. T. Giersch (Technical University of Munich), who supported this work by providing the cell line K1F4. They also thank H. Steingass (GBF) for the gift of purified antibodies. The excellent technical assistance of A. Steiner and C. Standfuss is gratefully acknowledged.

References

1 Lukosz, W., *Biosensors Bioelectron.*, 1991, **6**, 215.
2 Badley, R. A., Drake, R. A. L., Shanks, I. A., Smith, A. M., and Stephenson, P. R., 1987, *Philos. Trans. R. Soc. London, Ser. B*, 1987, **316**, 143.
3 Boltieux, J.-L., Biron, M.-P., Desmet, G., and Thomas, D., *Clin. Chem. (Winston-Salem N.C.)*, 1989, **35**, 1026.
4 Bright, F. V., Betts, T. A., and Litwiler, K. S., *Anal. Chem.*, 1990, **62**, 1065.
5 Bier, F. F., Böcher, M., Stöcklein, W., Bilitewski, U., and Schmid, R. D., *Sens. Actuators B*, 1992, **7**, 509.
6 Tiefenthaler, K., and Lukosz, W., *Opt. Lett.*, 1984, **10**, 137.
7 Tiefenthaler, K., and Lukosz, W., *J. Opt. Soc. Am.*, 1989, **B6**, 209.
8 Nellen, P. M., and Lukosz, W., *Biosensors Bioelectron.*, 1991, **6**, 209.
9 Van Emon, J. M., Seiber, J. N., and Hammock, B. D., in *Analytical Methods for Pesticides and Plant Growth Regulators Advanced Analytical Techniques*, ed. Sherma, J., Acad. Press, New York, 1989, vol. 17, p. 217.
10 Hock, B., and Immunoassay Study Group, *Anal. Lett.*, 1991, **24**, 529.
11 Wittmann, C., and Hock, B., *Nachr. Chem. Tech. Lab.*, 1991, **39** (11), M1–M4.
12 Giersch, T., and Hock, B., *Food Agric. Immunol.*, 1990, **2**, 85.
13 Weetall, H. H., *Methods Enzymol.*, 1976, **44**, 134.
14 Tiefenthaler, K., 1992 in *Advances in Biosensors*, ed. Turner, A. P. F., JAI Press, London, vol. 2, p. 261.
15 Tiefenauer, L. X., and Andres, R. Y., *J. Steroid Biochem.*, 1990, **35**, 633.
16 *EEC Drinking Water Directive*, 80/778/EWG, No. L229, Commission of the European Communities, Brussels, 1980, p. 11.
17 Kunz, R. E., Du, C. L., Edlinger, J., Pulker, H. K., and Seifert, M., *Sans. Actuators A*, 1991, **25–27**, 155.
18 Jockers, R., Bier, F. F., and Schmid, R. D., *J. Immunol. Methods*, 1993, **163**, 161.
19 Hock, B., personal communication.

Paper 3/00736G
Received February 8, 1993
Accepted August 27, 1993

pH Indicator Based Ammonia Gas Sensor: Studies of Spectral Performance Under Variable Conditions of Temperature and Humidity

Radislav A. Potyrailo,* Sergiy P. Golubkov, Pavlo S. Borsuk and Petro M. Talanchuk

Analytical Instruments Research Department, R&D Institute of Special Instruments, Kyiv Polytechnic Institute, Kyiv-56, 252056, Ukraine

Evgeniy F. Novosselov

Department of Chemistry, Kyiv Polytechnic Institute, Kyiv-56, 252056, Ukraine

Polymer–dye films, incorporating immobilized Bromocresol Purple pH indicator, can be used for ammonia gas sensing under the temperature and humidity variations that can occur during field operating conditions. To reveal the spectral features of the polymer–dye films, comparative spectral studies of the indicator dissolved in water and immobilized on the polymer matrix were performed. The modified absorption band of the immobilized indicator base form indicates the formation of an indicator–polymer ionic complex. Variations in the temperature (20–40 °C) and relative humidity (50–85%) of the monitored ammonia gas produced noticeable distortions of the short-wavelength wing of the band profile and also of its peak. The long-wavelength wing of the band profile was relatively stable under these conditions and demonstrated a good correspondence to the Gaussian-shaped curve.

Keywords: *Ammonia gas sensor; field operating conditions; Bromocresol Purple; absorption band*

Introduction

One of the ways of solving the pollution monitoring problem of gases and liquids is the use of optical chemical sensors based on the principle of photometric detection of reversible changes in the absorption spectra of chromogenic reagents, when exposed to specific chemicals.[1,2] Ammonia is one of the gases excreted in poultry and livestock farming and is widely used in microelectronics technology and in the chemical and food industries. Because of the toxic properties of ammonia in both gaseous and aqueous forms, its detection is often required.[3] pH-sensitive acid–base indicators are highly specific for ammonia determination. Exposure to ammonia increases the pH of an indicator based sensor. The resulting pH change is measured as light absorbance of the base form of the indicator and is related to the ammonia concentration in the sample. This allows for a simple instrument design.

Several approaches have been reported for preparing optical ammonia sensors based on pH indicators. They may be entrapped in the pores of plastic optical fibre obtained by heterogeneous cross-linking polymerization[4] or doped into the silicone polymer cladding of an optical fibre.[5] The indicator solution may be placed behind a gas-permeable microporous membrane made of poly(tetrafluoroethylene)[6] or in a semi-permeable microporous poly(propylene) hollow fibre.[7] A simpler way to fabricate a sensor for monitoring ammonia gas concentration levels down to 3 mg m^{-3} is to immobilize a pH indicator on a polymer support to form a polymer–dye film.[8] A practical problem limiting the development of pH indicator-based ammonia sensors is the dependence of the sensor response on temperature and humidity fluctuations of the detected gas.[9–13] Although numerous examples of pH indicator applications in ammonia sensors,[4–7,14–16] and spectral studies of immobilized pH indicators for analytical applications[17–20] have been reported, no work has been published with detailed analyses of changes in the absorption spectra of pH indicators immobilized on polymer supports when exposed to ammonia with different temperatures and humidities.

This paper presents results of the investigation of the influence of the polymer on the absorption spectra of polymer–dye films employed in fibre-optic[12] and portable[8] ammonia gas analysers. Differences in the absorption spectra of Bromocresol Purple (BCP) indicator, dissolved in water and immobilized on poly(methylphenylsiloxane) (PMPS) film, are discussed. The detailed analysis of changes in the polymer–dye film absorption spectra when exposed to ammonia gas of different temperatures and humidities was performed.

Theoretical Background

Light absorption of a pH indicator over the visible region of the spectrum is characterized by the electronic absorption spectrum of the indicator molecules. They contain single and double chemical bonds forming a conjugated chain. The absorption spectrum of the indicator accounts for electron oscillations in the conjugated chain of the molecule with chromophoric and auxochromic groups of atoms. In a simple molecule with one chromophoric group, light absorption obeys the Gaussian-shaped curve of probability distribution as follows:[21]

$$A = A_{max} \exp[-\log 2\,(\lambda - \lambda_{max})^2/(0.5\,\Delta\lambda)^2] \qquad (1)$$

where A_{max} and A are absorbance values at the peak of the absorption band and at the point of interest, respectively, λ_{max} and λ are the wavelengths at these points and $\Delta\lambda$ is the absorption bandwidth at the $0.5A_{max}$ level. If wavenumbers (ν/cm^{-1}) are plotted on the abscissa, the absorption band has a symmetrical profile. When wavelengths (λ/nm) are plotted on the abscissa, the curve is asymmetric, slightly stretched to shorter wavelengths.

In the indicator employed, the whole system of the conjugated chain is excited under the influence of light, in

* Present address: Department of Chemistry, Indiana University, Bloomington, IN 47405, USA.

contrast to the excitation of single electrons in simple molecules. Deviation of the absorption band shape from the Gaussian-shaped curve is possible owing to different factors: influence of the conjugated chain of the molecule, overlap of the absorption bands in the molecular spectrum and influence of the solvent.[22] Moreover, in contrast to indicator solutions that possess a homogeneous structure, polymer–dye films have the heterogeneous structure of indicator–polymer systems. The formation of ionic indicator–polymer complexes in the film extends the conjugated chain of indicator molecules resulting in a deviation of the absorption band shape from that exhibited by the indicator solution.

pH indicators exist in two forms, acidic and basic, depending on the pH of the sample. The reversible colour change of the indicators is due to the change from one form into another, accompanied by changes in the indicator conjugated chain. When an indicator, being a weak organic acid, is dissolved in water in the presence of a known amount of ammonia, the equilibrium between the acidic and basic forms is given by

$$HInd + NH_4^+ + OH^- \rightleftharpoons Ind^- \cdots NH_4^+ + HOH \quad (2)$$

where HInd denotes the acidic form of the indicator and Ind^- denotes the basic form of the indicator that results after a hydrogen ion, H^+, has dissociated from the molecule.

Polymers employed in the formation of solid chemical-sensitive films exhibit a certain sensitivity to water vapour in the ambient air.[9,23] When the indicator is immobilized on a polymer matrix, in particular on siloxane as used in our approach, the water molecules adsorb on its surface immediately after formation of the film. They saturate the ≡Si–O^- and ≡Si^+ groups of the siloxane matrix forming Si–OH groups. Chemically bound water molecules form a permanent hydrated surface layer about 10^{-7}–10^{-6} cm thick, in contrast to a temporary hydrated surface layer, formed by physical adsorption. The thickness of the latter is around 10^{-5} cm and depends on the water content of the air, *i.e.*, relative humidity and temperature.[24]

When the indicator immobilized on the siloxane matrix (Y) is exposed to ammonia gas with a certain level of relative humidity, the equilibrium between the acidic and basic form is given by

$$[Y\cdots IndH]\cdot n_1H_2O_{ad} + n_2NH_3 + n_3H_2O(air) \rightleftharpoons [Y\cdots Ind^-\cdots n_4NH_4^+]\cdot n_5H_2O_{ad} + n_6H_2O(air) \quad (3)$$

where n_i are coefficients dependent on the relative humidity and temperature of the ammonia gas and $_{ad}$ signifies adsorbed water.

The principal reaction in either an aqueous solution [eqn. (2)] or dye film [eqn. (3)] involves an acid–base neutralization in which the weakly acidic indicator donates a proton to the weakly basic ammonia, thus turning the indicator from the acidic into the basic form. The ionic nature of the ammonia–indicator reaction illustrated that the water content in the dye film could influence the reaction sensitivity. This was found to be one of the most important effects to be considered in that the amount of water incorporated into the dye film at the time of reaction had a profound effect on the reaction sensitivity and sensor response.[14] The temperature and humidity of the gas monitored affect this amount of water in the film. An increase in temperature decreases the amount of water and increases both the ionization constant of water and the ammonia dissociation constant. These changes result in a smaller sensor response.[11] Humidity changes produce the reverse effect. Temperature and humidity changes affect not only the measured absorbance of the immobilized indicator *via* the change in the dissociation constant of the indicator, but also the shape of the absorption curve and its peak position *via* the changes in polarization and length of the conjugated chain of the indicator–polymer complex and deviations in the strength of this ionic complex itself.

When ionic charges appear in the indicator molecule, *i.e.*, when the polarity increases at the ends of its conjugated chain, the absorption band of the acidic form of the indicator diminishes and, at the same time, the absorption band of the basic form of the indicator intensifies. The value of the absorption peak shift in the transition of the indicator from the acidic to the basic form, $\Delta\lambda_{max}^{acid-base}$, is considered acceptable for photometric applications when it exceeds 100 nm.[21]

Experimental

Sensor Design

Fig. 1 shows a schematic diagram of the ammonia sensor design. A miniature gas cell (dead volume about 2 ml) is fabricated as an aluminium block with holes for gas flow and for mounting a light-emitting diode (LED), sensing and reference silicon photodiodes and a transducer holder. Several quartz slides (6 × 6 × 0.5 mm) coated with BCP–PMPS films are mounted consecutively in the holder in front of the sensing photodiode. The output signal of the reference photodiode is not affected by variations in the ambient parameters. This sensor design was applied in a portable ammonia gas analyser for the determination of ammonia concentrations in the range 3–200 mg m^{-3}. A detailed description of its electronics package and instrument performance under conditions of constant gas temperature and humidity has been given previously.[8]

Reagents

All chemicals were of analytical-reagent grade from Khimreactyv (Ukraine). The indicator selected was BCP, which belongs to the sulfonphthalein class, and which can be used for precise ammonia determinations at relatively low concentrations. Sulfonphthaleins exhibit high molar absorptivities of their basic form, are generally stable at room temperature and resistant to photochemical degradation on exposure to visible radiation.[22] Polymethylphenylsiloxane was selected as a support matrix for BCP because of its high gas permeability, low interaction between polymer chains and inherent hydrophobic and film-creating properties.[25] For spectral studies dye films were coated on flat quartz slides 25 mm wide and 2 mm thick. Prior to coating with dye films, the slides were etched for 3 min in a buffered HF solution to provide better contact between the dye film and the glass surface. Films were spun on the slides at 2000–2500 rpm by applying a drop of a solution of

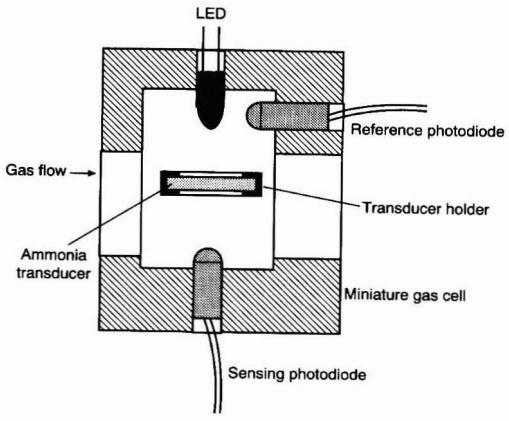

Fig. 1 Schematic configuration of the ammonia sensor

PMPS and BCP in toluene (an inert solvent). The solvent was evaporated at room temperature for 24 h and then at 80 °C for 4 h. During this process, a light-yellow BCP–PMPS film was formed on the glass surface. The indicator molecules were immobilized on the polymer support through the weak chemical binding, and these formed ionic indicator–polymer complexes.

A test solution of BCP in water was prepared at a concentration of 10 mol l^{-1}. After scanning the spectrum of the solution using the experimental set-up described below, a few drops of 1% ammonia solution were added to the solution. Spectrum scanning was repeated and then a few drops of 2 mol l^{-1} hydrochloric acid were added.

Instrumentation

The light from a grating monochromator (MDR-23; LOMO, Russia), excited by an incandescent lamp, was passed through a sample chamber containing the polymer–dye film in a gas cell, and the emerging radiation was detected by a photomultiplier tube. The optical arrangement was interfaced to a PC (MS0507; Electronica, Russia) by scanning and processing software (KSVU-23; LOMO). Data were collected from 350 to 700 nm with 1 nm resolution. Different ammonia concentrations were prepared by passing dry high-purity nitrogen at a measured flow rate not exceeding 20 ml min^{-1} over 10% ammonia solution and diluting it with a measured amount of air at a constant relative humidity. Ammonia concentrations in the gas mixtures were determined by drawing a sample of gas mixture and conducting chemical analysis using Nessler's reagent. Various relative humidity levels for different ammonia gas concentrations were used, ranging from 50 to 85%. A hygrometer was mounted on-line to measure the relative humidity. The gas temperature was varied over the range 20–40 °C by a resistive heater that was wound around the quartz substrate. The temperature was measured by a thermocouple. Pure air was pumped over the polymer–dye film for recovery after the interaction with ammonia. All experiments were conducted at ambient temperature (20 °C) and atmospheric pressure. The numerical values of experimental and calculated data are presented in Table 1.

Results and Discussion

General Spectral Differences

Fig. 2 shows typical absorption spectra of BCP indicator, A, dissolved in water, B, in the presence of hydrochloric acid, C, in the presence of ammonia solution, D, immobilized on a PMPS film in pure air and E, in ammonia gas. Indicator dissolved in water possesses two absorption bands (A). The band peak at around 430 nm corresponds to the acidic form and the band peak at around 590 nm to the basic form of the indicator, illustrating an equilibrium between two forms in aqueous solution. After the addition of hydrochloric acid, the equilibrium shifts to the formation of the extra acidic form of the indicator (B). After addition of ammonia solution, most of the indicator molecules are in the basic form (C). When BCP indicator immobilized on a PMPS matrix is exposed to pure air, it exhibits an absorption spectrum similar to its acidic form when in aqueous solution owing to the acidic properties of the polymer matrix (D). The polymer contains no amphoteric electrolytes such as water, so the indicator is in the acidic form. When the BCP–PMPS film is exposed to ammonia gas, the indicator turns into the basic form (E).

Polymer Effect

The absorption band of the basic form of the indicator was chosen for analytical measurements because its peak absorption is greater than that of the acidic form, and hence provides a better optical sensitivity to ammonia concentration changes. The effect of PMPS or water on the absorption band of the dye film or indicator solution, exposed to ammonia (gas concentration 200 mg m^{-3}, temperature 20 °C, 70% relative humidity or 1% ammonia solution, respectively) is indicated in Fig. 3 by the 20 nm shift in the peak position towards longer wavelengths and broadening of the absorption band of the dye film, contrasted with the absorption band of the indicator solution.

The observed shift indicates the formation of an ionic indicator–polymer complex. BCP molecules were bound to PMPS through hydrogen bonding. Polymer molecules affect the conjugated chain of the indicator molecules. The greater shift towards longer wavelengths in the BCP–PMPS film (20 nm) when compared with the 5 nm shift in the dye film based

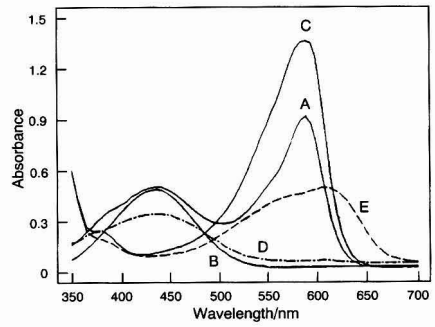

Fig. 2 Absorption spectra of BCP indicator: A, dissolved in pure water; B, in the presence of hydrochloric acid; C, in the presence of ammonia solution; D, immobilized on polymer film in pure air; and E, in ammonia gas

Table 1 Numerical values of experimental and calculated data

	Peak position of absorption bands					Absorption band of basic form of the indicator		
pH indicator system	λ_{max}^{acid}/nm	Red shift/nm	λ_{max}^{base}/nm	Red shift/nm	$\Delta\lambda_{max}^{acid-base}$/nm	Total width*/nm	Half-width of long-wavelength wing†/nm	Broadening of long-wavelength wing/nm
BCP–H_2O	430	10	590	20	161	60	19	1.8
BCP–PMPS	440		610		170	124	34	

* Determined from Figs. 3 and 4 at the 0.5 A_{max} level.
† Determined in the spectral region from 650 to 670 nm.

on Bromothymol Blue (BTB) pH indicator and the same polymer film reported previously[12] indicates the greater chemical link between BCP and PMPS molecules.

This chemical binding also results in broadening of the absorption band. The broadening of the band indicates that the indicator–polymer system is more labile than the indicator–solution system. The half-width of the absorption band of the BCP–PMPS film is 1.8 times greater than that for the BCP solution in water and 1.2 times greater than that for BTB systems.[12] This indicates a faster dynamic response for sensors based on BCP–PMPS films, which is of great importance for real-time ammonia monitoring employing optical chemical sensors of this type.

The correspondence of the shape of the absorption bands to the Gaussian profile was examined in order to perform further compensation for measurement errors occurring due to sensor applications in conjunction with polychromatic light sources such as $Ga_{0.7}Al_{0.3}As$ LEDs with peak emission wavelengths of 662–665 nm and bandwidths of 18 nm at the 0.5 level. These LEDs were applied in fibre-optic[12] and portable[8] ammonia gas analysers. A region of the absorption curve that corresponds to the Gaussian profile will be presented as a straight line in the plot of λ *versus* $[\log(A_{max}/A)]^{1/2}$ as follows:

$$[\log(A_{max}/A)]^{1/2} = [(\log 2)^{1/2}/0.5\Delta\lambda]\ (\lambda - \lambda_{max}) \quad (4)$$

The slope of the line determines the half-width of the absorption band as follows:

$$0.5\Delta\lambda = (\log 2)^{1/2}/\tan\alpha \quad (5)$$

where α is an angle between the line and the positive direction of the abscissa. The point of intersection of the line with the abscissa determines the exact value of λ_{max}. Fig. 4 shows the absorption bands of the basic form of BCP in water and in the dye film when both were exposed to ammonia (1% ammonia solution or ammonia gas at a concentration of 200 mg m^{-3}, temperature 20 °C, 70% relative humidity). We set $\lambda_{max} = 0$ to indicate a real position of the absorption peak.

The treatment of the curves showed that the absorption band is asymmetric. Points along the short- and long-wavelength wings of the absorption curves do not retain the same slope, taking into consideration that $\tan(180°-\alpha) = -\tan\alpha$. The points on the long-wavelength wings keep within straight lines in the required spectral region of the LED emission band from 650 to 670 nm. The short-wavelength wings of both curves are distorted. We consider that this distortion is due to the influence of the conjugated chain of the indicator molecules and polymer molecules bound to them. The absorption band of the acidic form of the indicator also affects the short-wavelength wing. The value of the absorption peak shift in the indicator transition from acidic to basic form $\Delta\lambda_{max}^{acid-base}$, in the BCP–PMPS film of around 170 nm compares with 161 nm for the BCP solution in water. This is acceptable for spectrophotometric applications.

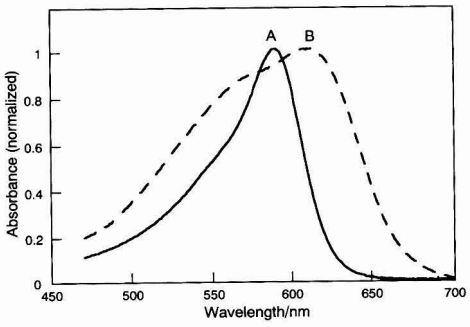

Fig. 3 Absorption band of the basic form of BCP indicator: A, dissolved in water; and B, immobilized on polymer film

Effects of Temperature and Humidity

Temperature and humidity affect the peak value of the absorption band, and hence the instrument performance. This complex effect is discussed elsewhere.[26] In this section we examine the effect of temperature and humidity on the absorption curve profile. Fig. 5 shows the changes in the profile of the respective portion of the absorption spectra with changes in temperature and ammonia concentration. Temperature variations in the range of interest (20–40 °C) do not produce a shift of the absorption peak position. Changes in concentration and temperature of ammonia gas do not noticeably affect the shape of the long-wavelength wing of the absorption curve and its peak. With increasing ammonia concentration a decrease in the absorption band half-width is observed only for the short-wavelength wing of the absorption curve. The half-width of this absorption curve also depends on temperature. With constant ammonia concentration the half-width increases with increase in temperature. Owing to the significant distortion of the short-wavelength absorption curve, an accurate value of its half-width for different concentrations and temperatures of ammonia gas was not determined. The broadening of the absorption band with

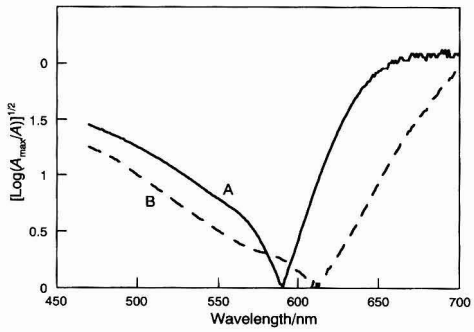

Fig. 4 Shape correspondence of the absorption band of BCP indicator to the Gaussian-shaped curve: A, dissolved in water; and B, immobilized on polymer film

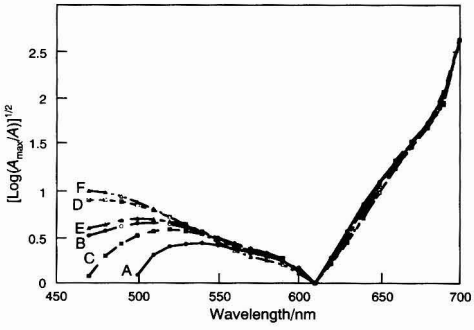

Fig. 5 Profile change of the absorption band of the BCP–PMPS film with changing of temperature and ammonia concentration at relative humidity 65%: A, 50 mg m^{-3} NH_3, 40 °C; B, 200 mg m^{-3} NH_3, 40 °C; C, 50 mg m^{-3} NH_3, 30 °C; D, 200 mg m^{-3} NH_3, 30 °C; E, 50 mg m^{-3} NH_3, 20 °C; and F, 200 mg m^{-3} NH_3, 20 °C

increasing temperature and decreasing ammonia concentration is accounted for by changes in the dissociation constant of the indicator–polymer ionic complex with variations in temperature and ammonia concentration.

The sensor response is also dependent on the relative humidity of the gas being monitored. The peak value of the absorption band decreases with decreasing relative humidity from 85 to 50% for ammonia gas of concentration 200 mg m^{-3} at 20 °C, as illustrated in Fig. 6. Humidity changes also affect the shape of the absorption curve. In Fig. 7 the same portion of the absorption spectrum has been normalized to an absorbance of 1 to display the difference in absorption curves shape with changes in relative humidity. The strong absorption band peak at 610 nm has a weak shoulder at around 580 nm. This composite band reflects the effects of two distinct absorption bands that cannot be separated. The 580 nm peak decreases from its initia level of 0.96 to 0.85 with a decrease in relative humidity from 85 to 50%. It can be assumed that this absorption band appears as a result of the complex interaction of indicator molecules immobilized on the polymer support with H_3O^+ ions. The relative humidity of the gas mixture affects not only the peak values of two inseparable peaks but also the peak positions. This is illustrated by a 10 nm shift of the 610 nm peak towards shorter wavelengths with an increase in relative humidity from 50 to 85%. We consider that this shift is due to the water saturation of the indicator–polymer matrix at high relative humidity levels. The change in position of the 580 nm peak was not satisfactorily determined because of the significant overlap of the peaks.

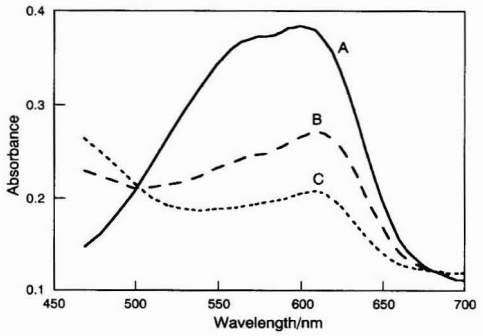

Fig. 6 Peak value of BCP–PMPS film absorption band as a function of relative humidity of ammonia gas sample at concentration of 200 mg m^{-3} and temperature 20 °C: A, at 85%; B, at 65%; and C, at 50% relative humidity

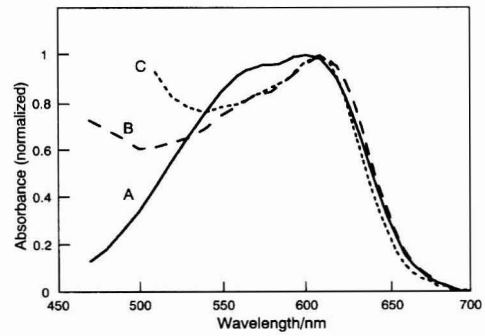

Fig. 7 Shape change of BCP–PMPS film absorption band as a function of relative humidity of ammonia gas sample at concentration of 200 mg m^{-3} and temperature 20 °C: A, at 85%; B, at 65%; and C, at 50% relative humidity

Conclusions

The results of this study indicate that the immobilization of a pH indicator on a siloxane polymer support modifies the spectral properties of the indicator, in particular the position and shape of the absorption band of its basic form. Temperature and humidity variations of ammonia gas mixtures produce noticeable effects on the absorption band profile. Although temperature variations in the range of interest (20–40 °C) do not influence the absorption peak position, they do change the bandwidth of the absorption band. This bandwidth also exhibits a dependence on ammonia concentration. Humidity changes produce distortion of the peak profile and shift of the peak position towards shorter wavelengths with increasing humidity level. The only region of the absorption band that does not exhibit noticeable profile distortion with temperature and humidity changes is its long-wavelength wing. This region also demonstrates a good correspondence to the Gaussian-shaped curve. The distortions of the curve profile in its peak and short-wavelength wing are a source of error in sensor response when employing dye films for transmittance measurements using polychromatic light sources such as LEDs. The contribution of this term can be avoided if only the long-wavelength wing is used. The results of this study have been recently employed in the development of a model of steady-state response of an ammonia gas sensor. The model was experimentally evaluated under variable temperature and humidity conditions.[26]

References

1 Potyrailo, R. A., and Golubkov, S. P., *Sensor Rev.*, 1992, **12**, No. 2, 22.
2 Arnold, M. A., *Anal. Chem.*, 1992, **64**, 1015A.
3 *Air Pollution Control, Part III, Measuring and Monitoring Air Pollutants*, ed. Strauss, W., Wiley-Interscience, New York, 1978.
4 Zhou, Q., Kritz, D., Bonnell, L., and Sigel, G. H., Jr., *Appl. Opt.*, 1989, **28**, 2022.
5 Blyler, L. L., Jr., Lieberman, R. A., Cohen, L. G., Ferrara, J. A., and MacChesney, J. B., *Polym. Eng. Sci.*, 1989, **29**, 1215.
6 Arnold, M. A., and Ostler, T. J., *Anal. Chem.*, 1986, **58**, 1137.
7 Berman, R. J., and Burgess, L. W., in *Chemical, Biochemical, and Environmental Fiber Sensors*, eds. Lieberman, R. A., and Wlodarczyk, M. T., *Proceedings of SPIE 1172*, The Society of Photo-Optical Instrumentation Engineers, Bellingham, Washington, 1989, pp. 206–214.
8 Golubkov, S. P., Vasilenko, N. A., Potyrailo, R. A., Kovtun, V. S., Borsuk, P. S., in *Environmental and Process Monitoring Technologies*, ed. Vo-Dinh, T., *Proceedings of SPIE 1637*, The Society of Photo-Optical Instrumentation Engineers, Bellingham, Washington, 1992, pp. 227–232.
9 David, D. J., Willson, M. C., and Ruffin, D. S., *Anal. Lett.*, 1976, **9**, 389.
10 Giuliani, J. F., Bey, B. P., Jr., Wohltjen, H., Snow, A., and Jarvis, N. L., in *Digest of Technical Papers, International Conference on Solid-State Sensors and Actuators, Transducers' 85*, Institute of Electrical and Electronics Engineers, New York, 1985, pp. 74–76.
11 Rhines, T. D., and Arnold, M. A., *Anal. Chem.*, 1988, **60**, 76.
12 Potyrailo, R. A., Golubkov, S. P., and Borsuk, P. S., in *International Conference on Optical Fibre Sensors in China, OFS(C)'91*, ed. Culshaw, B., *Proceedings of SPIE 1572*, The Society of Photo-Optical Instrumentation Engineers, Bellingham, Washington, 1991, pp. 434–438.
13 West, S. J., Ozawa, S., Seiler, K., Tan, S. S. S., and Simon, W., *Anal. Chem.*, 1992, **64**, 533.
14 Smock, P. L., Orofino, T. A., Wooten, G. W., and Spencer, W. S., *Anal. Chem.*, 1979, **51**, 505.
15 Giuliani, J. F., Wohltjen, H., and Jarvis, N. L., *Opt. Lett.*, 1983, **8**, 54.

16 Çağlar, P., and Narayanaswamy, R., *Analyst*, 1987, **112**, 1285.
17 Kirkbright, G. F., Narayanaswamy, R., and Welti, N. A., *Analyst*, 1984, **109**, 1025.
18 Bacci, M., Baldini, F., and Bracci, S., *Appl. Spectrosc.*, 1991, **45**, 1508.
19 Boisde, G., Blanc, F., Machuron-Mandard, X., *Int. J. Optoelectron.*, 1991, **6**, 407.
20 Gauglitz, G., and Reichert, M., *Sens. Actuators B*, 1992, **6**, 83.
21 Babko, A., and Pilipenko, A., *Photometric Analysis: General Principles and Working Tools*, Mir, Moscow, 1971 (in English).
22 *Indicators*, ed. Bishop, E., Pergamon Press, Oxford, 1972.
23 Giuliani, J. F., Jarvis, N. L., and Snow, A. W., in *Fundamentals and Applications of Chemical Sensors*, eds. Schuetzle, D., and Hammerle, R., *ACS Symp. Ser.*, No. 309, American Chemical Society, Washington, DC, 1986, ch. 19, pp. 320–329.
24 Jebsen-Marwedel, H., and Bruckner, R., *Glastechnische Fabrikationsfehler*, Springer, Berlin, 1980.
25 Golubkov, S. P., Potyrailo, R. A., Novosselov, E. F., and Borsuk, P. S., in *Proceedings of First International Soviet Fibre Optics Conference, ISFOC '91, Leningrad, USSR, March 25–29, 1991*, eds. Kady, J., Mahoney, P., and Polishuk, P., Information Gatekeepers, Boston, 1991, vol. 1, pp. 330–334.
26 Pokyralio, R. A., in *Optical Methods for Chemical Process Control*, ed. Farquharson, S., and Leener, J. M., *Proceedings of SPIE 2069*, The Society of Photo-Optical Instrumentation Engineers, Bellingham, Washington, 1993, pp. 76–84.

Paper 3/01534C
Received March 17, 1993
Accepted August 24, 1993

Ion-selective Field-effect Transistor and Chalcogenide Glass Ion-selective Electrode Systems for Biological Investigations and Industrial Applications*

Yuri G. Vlasov, Eugene A. Bychkov and Andrey V. Bratov

Department of Chemistry, Saint Petersburg University, Saint Petersburg 199034, Russia

In this paper the fabrication and application of two different modern potentiometric solid-state chemical sensors, namely, chalcogenide glass ion-selective electrodes and field-effect transistor-based sensors, are described. Examples of their use in industry, waste water analysis and biomedical treatment are discussed.

Keywords: *Solid-state chemical sensor; chalcogenide glass ion-selective electrode; ion-selective field-effect transistor; biology sensitive field-effect transistor; sensor application*

Introduction

During the last two decades, various types of chemical sensors have been developed, including conventional ion-selective electrodes (ISEs) with membranes and sensors based on new physical, chemical and biological principles and modern technology. The systems include ion-selective field-effect transistors (ISFETs) and other FET-based sensors (GasFETs and BioFETs), optical sensors [opt(r)odes], acousto-electronic devices and biosensors utilizing enzyme and immunological reactions or bio-organism activity. Even so, despite the extensive research and development of new chemical sensors, there is a lag between such investigations and exploitation of the devices in analytical applications through commercial availability. All three directions of chemical sensor development are closely connected to one another, and analytical achievements are able to influence both research and commercial progress in the field.

ISFETs and chalcogenide glass ion-selective electrodes (CGISEs), the subject of this paper, belong to the large group of potentiometric sensors that can be classified as shown in Fig. 1. This classification is an improved version of chemical sensor classification proposed earlier.[1] In the first instance, this classification divides the sensors into three groups according to the chemical species sensed, namely, electrons, ions and molecules. Then come the different types of sensors according to both the mechanism of operation and construction style, namely, electrodes of the first and second kinds, oxidation–reduction systems, ISEs, ISFETs, GasFETs and BioFETs. Finally, there are the types of membranes used in chemical sensors.

Considering the variety of potentiometric chemical sensors and the history of their development, it can be recognized that the conventional ISEs, including the pH glass electrode developed in the period 1906–1967, are now commercially available. The sensors considered in this paper are relatively new, and the first report on CGISEs was published by Baker and Trachtenberg[2] in 1969 while Bergveld[3] introduced ISFETs in 1970. ISFETs have since been extensively investigated by many research groups in many countries, while CGISEs were the focus of studies by Vlasov and co-workers[4,5] in Russia. Despite this effort, only a few companies in Japan, USA, The Netherlands, Switzerland and Russia have started commercial production of pH-ISFETs, and the only place where CGISEs are produced commercially is our Laboratory of Chemical Sensors at St. Petersburg University, Russia. Nevertheless, ISFETs and CGISEs have many advantages, which should make them very attractive for wide application in chemical analyses. The principal advantages of these sensors are:

ISFETs—small size; completely solid-state design; low output resistance; application of integrated circuit (IC) microelectronic technology for their fabrication; low cost of mass production; possibility of developing multisensors on one chip to make them especially convenient for biomedical application and microanalysis.

CGISEs—a new generation of ISEs of the highest possible reliability and lifetime in aggressive, strong acid and corrosive media. These have long-term stability with steady potential during continuous measurements, all-solid state design, high sensitivity and low detection limits. There is no necessity for preliminary treatment of the sensor before measurements; they are especially convenient for industrial and environmental control applications.

The aim of this paper is to describe some of our results on the development of CGISEs and ISFETs and their application in technological and biological investigations.

Experimental

Chalcogenide Glass Preparation

The details of experimental methods of the preparation of chalcogenide glasses have been described elsewhere.[6,7] The main features of their fabrication consist of glass formation from melted pure substances in evacuated silica ampoules (800–1200 K) followed by quenching in air or water. The homogeneity and amorphous state were confirmed by X-ray diffraction, while surface properties were studied by X-ray photoelectron spectroscopy, Auger electron spectroscopy, secondary-ion mass spectrometry and radioisotope methods.

Sensor Fabrication

CGISEs

Electrode membranes were prepared by cutting discs (6–10 mm in diameter) from the glasses, followed by polishing and sealing into plastic tubes. Solid inner contacts were obtained by deposition of a silver layer on the inner side of the

* Presented at the International Symposium on Electroanalysis in Biomedical, Environmental and Industrial Sciences, Loughborough, Leicestershire, UK, April 20–23, 1993.

membrane and attaching a wire by micro-adhesive. CGISEs for the determination of various ions in solutions have been developed (Table 1).

ISFETs

Different ISFET designs were used and were fabricated on p-type (10–40 Ω cm) silicon wafers of <100> orientation. The ISFET channel length was 20 μm and the width varied in the range 0.5–2 mm. The gate region was formed by a thermally grown SiO_2 layer (70–100 nm), and pH-sensitive films consisted of ZrO_2 or Ta_2O_5. The fabrication processes for these devices have been presented in more detail elsewhere.[8] All the sensors were prepared using standard planar technology, and epoxy resin was used for encapsulation.

pH–ISFETs with ZrO_2 and Ta_2O_5 gate films showed a linear pH dependence in the range 1–13 with sensitivities of 56 ± 0.3 and 57 ± 1 mV pH^{-1}, respectively. It was found that the pH sensitivity is independent of the solution ionic strength in the range 10^{-3}–1 mol l^{-1}.

The pH-ISFET structure described above was used for fabricating various FET-based sensors with different membranes.

Results and Discussion

Sensor Application

The application of chemical sensors depends on their properties and design. In this paper, two different types of sensors are considered. All solid-state CGISEs have the size of conventional ISEs (diameter 7–10 mm, length 150 mm) and, owing to their chemical and mechanical stability and long lifetime, they are especially convenient for industrial and environmental applications. Because of IC microelectronics technology, ISFETs have a small size (1–2 mm), low resistance, solid-state design and low cost and can be very convenient for medical and biological applications. The market for the sensors depends on whether customers (in industry, medicine and biotechnology) are aware of the possibilities of their application.

Application of CGISEs in Industry

Electrolysis baths and nuclear-power stations

Copper-CGISEs have been used in plants producing ultrapure metallic nickel, the quality of which depends on its impurities (copper and others). The monitoring of trace concentrations of copper (0.5–4.0 mg l^{-1}) was carried out in nickel electrolysis baths (70–80 g l^{-1} of nickel) at 75 °C. It was, therefore, possible to detect copper in technological solutions in the presence of a 10^6-fold excess of nickel. The mean operation periods for the copper-CGISE during the continuous measurements were from 1–3 months. The period for conventional commercial crystalline ISEs was 2–3 d.

In order to improve the reliability and safety of nuclear-power stations, it is necessary to monitor corrosion processes

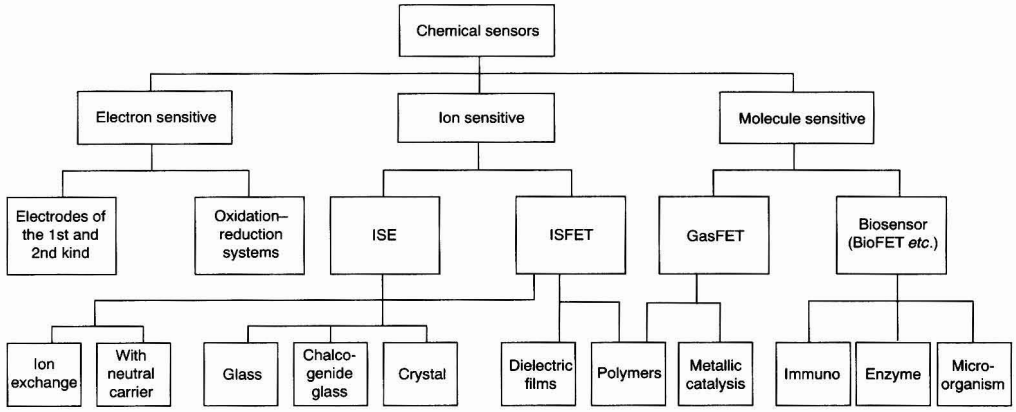

Fig. 1 Classification of potentiometric chemical sensors

Table 1 Chalcogenide glass ion-selective sensors

Determined ion (X)	Membrane composition	Sensitivity/ mV pX^{-1}	Detection limit/ 10^{-7} mol l^{-1}	pH
Ag^+	Ag–As–S Ag–As–Se	59	5	Up to 6 mol l^{-1} HNO_3
Cu^{2+}	Cu–Ag–As–Se	29	1	Up to 1 mol l^{-1} HNO_3
Pb^{2+}	PbI_2–Ag_2S–As_2S_3 PbS–Ag_2S–As_2S_3 PbS–AgI–As_2S_3	29	1	2–6
Cd^{2+}	CdS–Ag_2S–As_2S_3 CdI_2–Ag_2S–As_2S_3	28	1	1–7
Fe^{3+}	$Ge_{28}Sb_{12}Se_{60}$(Fe)	58	500	1–2
Br^-	AgBr–Ag_2S–As_2S_3*	59.5	5	2–10
Tl^+	Tl-chalcogenide glass	59	50	0–5†
Hg^{2+}	Hg-chalcogenide glass	28	5	0–6†

* Glassy/crystalline membrane.
† pH region depends on solution concentration.

in technological equipment over long periods. It is highly desirable to carry out determinations of copper and iron in working waters with the minimum of pre-treatment procedures. The actual problem seems complex because of the low concentration levels of copper (approximately 3–6 μg l^{-1} and even lower) and iron (≥10–15 μg l^{-1}) in high-purity water. The possible application of ISEs in this field meets two serious obstacles. (*i*) Membrane materials of commercially available electrodes are not sufficiently chemically stable to ensure long-term measurements under the above mentioned conditions because of, *e.g.*, partial membrane dissolution and perceptible surface deterioration (and, consequently, electrode response). (*ii*) A considerable part of the copper and iron are present in such water in the form of colloids, associates, complexes, *etc.*, rather than in the form of free ions.

All these problems were solved as a result of investigations of CGISE application and the development of a special method of ion determination. Copper-CGISEs were used as chemical sensors for the determination of copper and iron. A high chemical durability of the sensing membrane in corrosive media, as well as at low concentration limits, allows the determination of the copper ion content in the range of approximately 3–100 μg l^{-1} under real conditions in a nuclear-power plant. We applied a simple and reliable analytical procedure has been developed for converting copper and iron into ionic form. It includes acid treatment, pH adjustment and addition of a complexing agent. The measurements of the steady-state potential of the electrode were carried out according to a rigid schedule within 2 mins. Iron concentrations as low as 15 μg l^{-1} can be determined by this method. The whole determination of copper and iron takes 10–15 min and can be repeated immediately for a prescribed period of time.

CGISEs for industrial waste water treatment

CGISEs have been used to control waste water treatment with sodium sulfide, sodium carbonate, sodium hydroxide or calcium hydroxide, both in simulated waste water solutions prepared from copper, lead or nickel nitrate and nitric acid, or in real industrial processes in some factories equipped with commercial waste water treatment systems in which commercial pH glass electrodes are used.

The sensors were tested in simulated waste water prepared from 1 mmol l^{-1} $Cu(NO_3)_2$, $Ni(NO_3)_2$ or $Pb(NO_3)_2$ acidified with HNO_3 to pH 3; simulated waste water treatment includes heavy metal precipitation by Na_2S, NaOH, Na_2CO_3 and $Ca(OH)_2$.

Fig. 2 shows an example of the simulated waste water treatment monitored by means of the CGISE and pH electrode. The solution composition before treatment was 1 mmol l^{-1} copper nitrate acidified to pH 3 with nitric acid. Addition of sodium sulfide results in precipitation of copper sulfide with a corresponding decrease in potential for both the CGISE and pH electrode. It should be noted, however, that the potential difference is approximately 600 mV for the CGISE and only approximately 200 mV for the pH electrode. Moreover, a shift in the response curve for the CGISE towards lower reagent addition volume is observed. These results indicate that the CGISE sensor is much more sensitive than the pH electrode to the change in copper concentration in waste water.

Fig. 3 shows a typical recording of copper concentration during industrial waste water treatment. The recorded copper levels correlated with measurements by atomic absorption spectrometry. The CGISE exhibits a fast and reproducible response to the changes in copper concentration from 20 to 0.04 mg l^{-1} during treatment; pH values were in the range 3.2–4.3. Separate experiments were performed to observe sensor response at higher (up to 1000 mg l^{-1}) and lower (0.04–1.0 mg l^{-1}) copper concentrations. In all instances, the CGISE displayed reliable response to the changes in copper concentration during treatment.

These examples show that CGISEs can be usefully applied to control and operate the treatment of waste water containing heavy metal ions in industry. They are much more sensitive than a conventional pH electrode to changes in heavy metal ion concentration during the treatment.

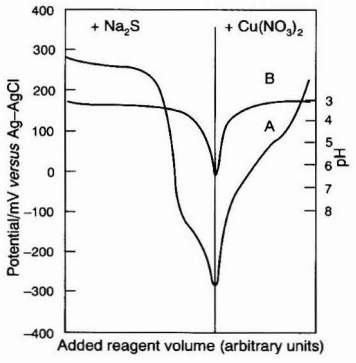

Fig. 2 Comparison of the response of pH-glass electrode and Cu-CGISE in waste water treatment monitoring. A, Chalcogenide glass sensor; and B, pH electrode. Solution composition before treatment, 1×10^{-3} mol l^{-1} $Cu(NO_3)_2$–HNO_3

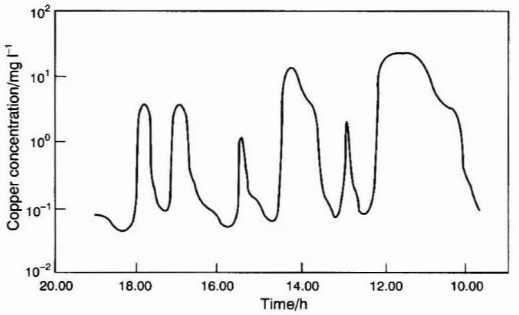

Fig. 3 Use of a Cu-CGISE in the continuous control of waste water treatment of microelectronic plants

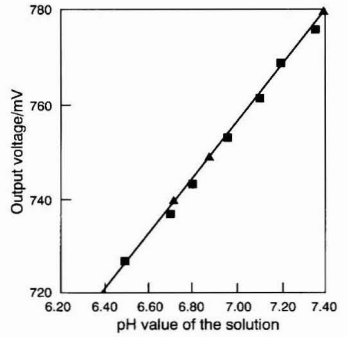

Fig. 4 pH response of ZrO_2-ISFET in whole heparinized blood titrated with small amounts of NaOH and HCl. ■ = Experimental points; ▲ = buffer solutions

pH-ISFET for Blood Investigation

It has already been shown[9,10] that pH-ISFETs with Si_3N_4 and Al_2O_3 gate films can be used for continuous monitoring of whole blood pH. In this work, the characteristics of ZrO_2- and Ta_2O_5-ISFETs were investigated in plasma, whole blood and blood enriched with blood cells (*e.g.*, erythrocytes).

Fig. 4 presents the ZrO_2-ISFET response obtained in heparinized whole blood titrated with small amounts of HCl or KOH (0.1 mol l^{-1}) *versus* the pH value of the sample measured by a glass pH electrode. Over the physiologically meaningful pH range, the sensor exhibits a linear pH response. It must be noted that to stabilize the sensor's characteristics after initial contact with blood samples, it must be pre-soaked in the sample for 15–20 min. The response time to rapid pH changes in blood was slightly higher than in standard buffer solutions ($\tau_{98\%} \approx 1$ min). This can be attributed to the high (0.1 mol l^{-1}) sodium ion concentration in blood. The stability of the sensor characteristics during contact with blood was controlled by testing the output voltage in a standard buffer solution. After 5 h of measurements, fluctuations did not exceed ±1 mV. Measurements of pH carried out on plasma, whole blood and blood enriched with blood cells showed no visible differences in sensor behaviour. The experimental data obtained are presented in Table 2. Values of pH measured with ISFETs were based on two calibration points (pH 6.88 and 7.42).

pH-ISFETs with Ta_2O_5 gate films also exhibited a linear pH response in blood samples, but their response time was much higher (2–5 min) in comparison with ZrO_2-ISFETs. It is presumed that the large response-time values in this instance are due to the formation of an adsorbed protein layer that has its own buffer capacity.

It was found that contact with blood results in a shift of the calibration graph for the ISFETs along the voltage axis. While in plasma the difference between the pH measured with a glass electrode with a Ta_2O_5-ISFET was 0.05–0.1 unit, and in blood enriched with blood cells the error was 0.3–0.4 pH unit. In buffer solution, the sensor output value returned to its initial value after 5–10 min. These effects are probably associated with adsorption of proteins at the Ta_2O_5-ISFET gate.

Table 2 Direct pH measurements performed in whole blood with a ZrO_2-gate ISFET

Glass electrode	6.75	7.36	7.24	7.10	6.95	6.75	6.51
ISFET	6.73	7.37	7.23	7.09	6.93	6.74	6.55

Table 3 Comparative pH measurements in gastric juice

Glass electrode	4.49	1.12	3.28	4.12	2.02	1.20	1.82
Antimony electrode	4.34	1.98	3.40	4.20	2.18	1.80	2.01
Ta_2O_5-ISFET	4.50	1.13	3.24	4.09	2.03	1.22	1.84

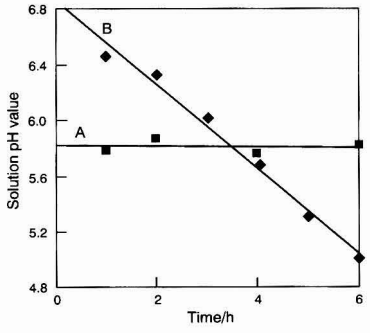

Fig. 5 Kinetics of pH changes measured with Ta_2O_5-ISFET in glucose solution containing *Staphylococcus aureus* with (A) and without (B) addition of Cu_2SO_4 (10^{-4} mol l^{-1})

pH-ISFETs in Gastroenterological Measurements

Usually, special probes with miniature glass pH electrodes or antimony–antimony oxide electrodes are used for *in vivo* pH measurements in gastroenterological investigations. The former electrodes suffer from a high output impedance; the latter have a non-linear pH response and can easily be contaminated by various organic compounds. Experimentation has shown that ISFETs can successfully be used for this purpose. The experimental data obtained from comparative pH measurements on gastric juices performed with a glass electrode, an antimony electrode and with Ta_2O_5-ISFETs are summarized in Table 3.

pH-ISFETs for Microbiological Investigation

The activity of micro-organisms can be investigated by chemical sensors, and micro-organisms can be used for the fabrication of new types of biosensors.[11,12]

A pH-sensitive ISFET with a Ta_2O_5 gate film has been studied, the ISFET having been used for continuous pH measurements in small (0.2 ml) volumes of solutions of different substrates containing the micro-organism *Pseudomonas aeruginosa* or *Staphylococcus aureus*. The kinetics of pH changes in the solutions under investigation have been determined for a 6 h interval (Fig. 5). The pH changes are associated with decomposition of the substrate by bacterial enzymes.

Various toxic substances can affect the behaviour of micro-organisms and hence lead to a decrease in their enzymic activity. This work has shown that the presence of metal ions (Cu^{2+}) in the substrate solution has a pronounced effect on the kinetics of pH changes (Fig. 5). The possible application of this effect to the construction of a biosensor for toxic compound registration is obvious.

pK- and pCa-ISFETs

pK and pCa are important medical and biological parameters. Among materials that can be used for the preparation of ion-sensitive membranes for ISFETs for such measurements, only a few are of an inorganic nature that can be deposited using standard microelectronic processes. The commonly used material for the sensitive membranes of ion sensors is plasticized poly(vinyl chloride) (PVC) containing an appropriate ionophore. Unfortunately, PVC has poor adhesion to ISFET gate insulators and this leads to problems when processes of membrane formation are involved. The promising approach in this direction is the use of polymers with photo-initiated cross-linking, so that photo-lithographic processes for membrane formation can be applied.

The main requirement for a polymer membrane matrix is that it must hold a large amount (up to 60%) of plasticizer, which is necessary for proper function of the ionophore in the membrane. Moreover, it must have good adhesion to the ISFET surface.

In this work, polymers based on esters of methacrylic acid with the common formula

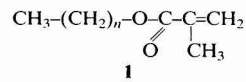

1

were used. The size of the polymer network, and subsequently its stiffness, was regulated by the length of the hydrocarbon chain (n = 4–9 on average) and the amount of additional cross-linking agent

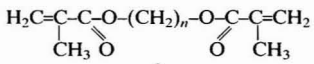

2

A mixture of **1** and **2**, together with plasticizer, was applied by spin coating on a silicon wafer to yield ISFETs, and polymerization was effected under ultraviolet (360 nm) radiation. Benzoyl peroxide and benzophenone were used as initiator and photo-sensitizer, respectively. It was found that the polymer obtained can hold up to 40% of various plasticizers that are commonly used in conventional ion-selective membrane compositions, and good adhesion to the ISFET-gate oxide surface was achieved.

Fig. 6 shows the response of K- and Ca-sensitive ISFETs with membranes formed by the standard photo-lithography technique and containing 39% of plasticizer (dinonyl adipate and dioctylphenyl phosphonate, respectively) and the ionophore valinomycin for potassium and bis(octylphenyl)phosphoric acid for calcium. The sensors exhibited sensitivities of 26 mV $(pCa)^{-1}$ and 55 mV $(pK)^{-1}$, less than 2 min response times and lifetimes of more than 20 d.

Biosensor for Urea Determination

For the fabrication of an enzyme biosensor (EnFET) for urea determination, ZrO_2-ISFET and an albumin membrane with immobilized urease were used.[13] The membrane was placed in a special holder mechanically attached to the gate region of the sensor.[13] In this instance, the membrane can be easily changed after a decrease in enzyme activity. The measurements of urea concentration were carried out in phosphate buffer (10 mmol l^{-1}, pH 7.4) solutions. The response time of the urea sensor was about 2 min and the calibration graph (Fig. 7) was linear in the concentration range 0.02–1.0 mmol l^{-1} urea. The sensor response remained stable (±5 mV) during all the experiments (10 d).

EnFETs for Inhibitor Determination

EnFETs can be used to determine inhibitors (compounds that cause a decrease in the rate of enzyme reaction) by reacting with the enzyme or enzyme–substrate intermediate to form a corresponding complex. Cholinesterase derivatives are widely used to detect various inhibitors, including toxic compounds such as pesticides. Results obtained with an ISFET sensitive to acetylcholine by Gotoh *et al.* have been reported;[14] we have asterisked the characteristics of butyrylcholinesterase-based EnFETs[15] whereby the possibility of sensor application for the detection of inhibitors was also shown.

Butyrylcholinesterase (BCE) catalyses the reaction

$$\text{Butyrylcholine} \xrightarrow{\text{BCE}} \text{Choline} + \text{Butyric acid}$$

which provides butyric acid and thereby changes the pH value in the membrane. An EnFET membrane was formed from a gelatine solution, prepared in phosphate buffer (0.01 mol l^{-1}, pH 7.5), containing butyrylcholinesterase on a Ta_2O_5-ISFET gate.

The influence of irreversible inhibitors on EnFET parameters was studied using two pesticides, dimethyldichlorovinyl phosphate (DDVP) and diisopropyl fluorophosphate (DFP). The EnFET characteristics were assessed in substrate solution (10^{-3} mol l^{-1}); the EnFET was then immersed in a solution containing a specific amount of inhibitor (10^{-6}–10^{-2} mol l^{-1}) for a strictly determined period of time (2–15 min). After that, the sensor was rinsed and its characteristics in the substrate solution were assessed again. Experimental data are shown in Fig. 8. Each point on the curve represents the result obtained with an EnFET with a freshly prepared membrane. The output voltage of different sensors was reproducible with an accuracy within 10%. If the percentage inhibition is lower than 30–40%, the EnFET can be used more than once. Detection limits of 5×10^{-5} mol l^{-1} for DFP and 10^{-6} mol l^{-1} for DDVP were observed.

Conclusion

New types of chemical sensors, such as CGISEs and ISFETs, can be applied in many branches of industry, medicine and biology and for environmental control.

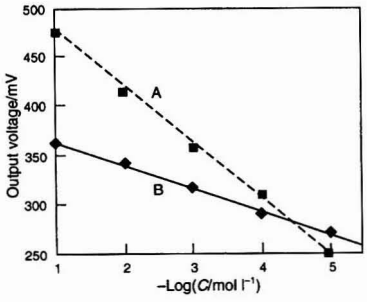

Fig. 6 Response of A, pK- and B, pCa-ISFET with photocurable polymer membranes

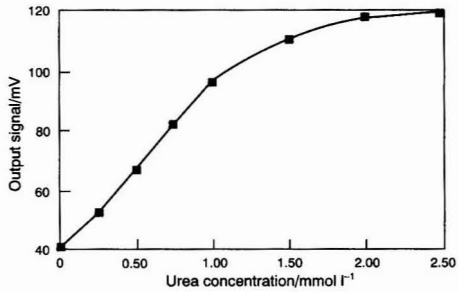

Fig. 7 Chemical response of the urea EnFET sensor. Conditions: phospate buffer, 10 mmol l^{-1}, pH 7.4

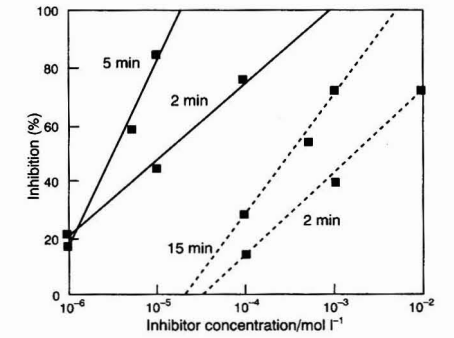

Fig. 8 EnFET sensitivity to the irreversible inhibitors DFP (solid line) and DDVP (broken line). Conditions: substrate concentration, 1×10^{-3} mol l^{-1}; phosphate buffer, 1×10^{-4} mol l^{-1}; KCl, 0.1 mol l^{-1}; and pH 7.5

The authors thank the research staff of the Laboratory of Chemical Sensors at St. Petersburg University for their participation and contributions to the research programme described in this paper.

One of us (Yu. G. V.) thanks the Royal Society for a Kapitza Fellowship tenable at the University of Wales, Cardiff which made possible the presentation of this paper.

References

1 Vlasov, Yu. G., *Zh. Anal. Khim.*, 1992, **47**, 114.
2 Baker, C. T., and Trachtenberg, J., *U.S. Office Saline Water Res. Dev. Progr. Rep.*, 1969, **469**, 35.
3 Bergveld, P., *IEEE Trans. Biomed. Eng.*, 1970, **17**, 70.
4 Vlasov, Yu. G., and Bychkov, E. A., *Ion-Sel. Electrode Rev.*, 1987, **9**, 5.
5 Vlasov, Yu. G., Bychkov, E. A., and Legin, A. V., *Sens. Actuators B*, 1992, **10**, 55.
6 Vlasov, Yu. G., and Bychkov, E. A., *Anal. Lett.*, 1989, **22**, 1125.
7 Vlasov, Yu. G., Moskvin, L. N., Bychkov, E. A., and Golikov, D. V., *Analyst*, 1989, **114**, 185.
8 Vlasov, Yu. G., Bratov, A. V., and Tarantov, Yu. A., *Zh. Prikl. Khim. (Leningrad)*, 1988, **61**, 767.
9 Schepel, S. J., de Rooij, N. F., Koning, G., Oeseburg, B., and Zijlstra, W. G., *Med. Biol. Eng. Comput.*, 1984, **22**, 6.
10 Sibbald, A., Covington, A. K., and Carter, R. F., *Clin. Chem. (Winston-Salem, N.C.)*, 1984, **30**, 135.
11 Gaisfeld, W. C., Richardson, N. J., Haggett, B. G. D., and Rawson, D. M., *Biochem. Soc. Trans.*, 1991, **19**, 15.
12 Bennetto, H. P., Box, J., Delaney, G. M., Mason, J. R., Roller, S. D., Stirling, S. L., and Thurston, C. V., in *Biosensors*, eds. Turner, A. P. F., Karube, I., and Wilson, G. S., Oxford University Press, Oxford, 1987, pp. 291–314.
13 Vlasov, Yu. G., Laurenavichus, V. A., Tarantov, Y. A., and Bratov, A. V., *Zh. Anal. Khim.*, 1989, **44**, 1651.
14 Gotoh, M., Tamiya, E., Momoi, M., Kagawa, Y., and Karube, I., *Anal. Lett.*, 1987, **20**, 857.
15 Vlasov, Yu. G., Bratov, A. V., Levichev, S. S., and Tarantov, Yu. A., *Sens. Actuators B*, 1991, **3**, 283.

Paper 3/03545J
Received June 21, 1993
Accepted July 7, 1993

Amperometric Biosensor for Phenols Based on a Tyrosinase–Graphite–Epoxy Biocomposite

Joseph Wang, Lu Fang and David Lopez

Department of Chemistry and Biochemistry, New Mexico State University, Las Cruces, NM 88003, USA

A new biocomposite, based on the incorporation of the enzyme tyrosinase into a graphite–epoxy resin matrix, was used for the effective biosensing of phenolic compounds. The enzyme retains its bioactivity on confinement in the epoxy resin environment. This renewable (polishable) and rigid bioprobe offers convenient quantification for various phenolic substrates. The fast response (steady-state time = 25 s) accrues from the close proximity of the enzyme and graphite sites. The influence of various experimental variables was explored for optimum biosensing performance. Flow-injection monitoring of phenolic compounds at a rate of 50 samples h^{-1} yielded a detection limit of 1×10^{-6} mol l^{-1} and a relative standard deviation of 1.4% ($n = 40$).

Keywords: Phenol; biosensor; tyrosinase; graphite epoxy resin

Introduction

Considerable attention has been given to the reliable quantification of phenols in complex environmental, food, pharmaceutical and industrial matrices. Amperometric biosensors, based on the enzyme tyrosinase, have proved to be very useful for this task.[1–5] Mushroom tyrosinase (known also as polyphenol oxidase) is a copper-containing mono-oxygenase that converts phenolic substances to the corresponding quinones.[6] The liberated quinone species can be electrochemically reduced to allow convenient low-potential detection of the phenolic analytes. Previous avenues to the fabrication of phenol biosensors have involved the incorporation of tyrosinase within a carbon paste matrix[3,5] or its immobilization on various graphite electrodes.[1,2,4] Tyrosinase-containing plant tissues have also been employed for fabricating bioprobes for phenols.[7]

The objective of the present study was to develop a renewable and robust phenol biosensor based on a tyrosinase biocomposite. Earlier work conducted in this laboratory involved a commercially available epoxy resin bonded graphite for preparing polishable enzyme electrodes.[8–11] Successful biosensors for glucose,[8] alcohol,[9] bilirubin[10] and hydrogen peroxide[11] have been developed based on the incorporation of appropriate enzymes within graphite–epoxy resin matrices. Also, Algeret and co-workers[12,13] have recently described various glucose bioelectrodes based on graphite–epoxy resin composites. Analogous preparations of chemically modified electrodes have also been reported.[14–16] The polishable (reusable) nature, mechanical stability and fast response of graphite–epoxy resin bioelectrodes makes them very attractive for many practical applications. The following sections describe the fabrication, characterization and advantages of a polishable biosensor for phenols based on the immobilization of tyrosinase within a graphite–epoxy resin composite.

Experimental

Apparatus

Amperometric and voltammetric experiments were performed with a Bioanalytical Systems (BAS) Model CV-27 voltammetric analyser, in connection with a BAS *x–y–t* recorder. Batch experiments employed a 10 ml cell (Model VC-2, BAS). The working electrode, reference electrode (Ag–AgCl, Model RE-1, BAS) and platinum wire auxiliary electrode joined the cell through holes in its Teflon cover. A magnetic stirrer and a stirring bar provided convective transport during amperometric measurements. The flow injection system consisted of a carrier reservoir, a Rainin Model 5041 injection valve (20 μl sample loop), interconnecting PTFE tubing and a large volume wall-jet detector. The flow of the carrier solution was maintained by gravity.

Electrode Preparation

The biosensor was prepared from an epoxy resin bonded graphite (grade RX, Dylon, Cleveland, OH, USA) as described for other biocomponents.[8,9] Tyrosinase was first crushed to fine particles, then added to the 1 + 1 resin–accelerator mixture (5% m/m), and mixed thoroughly for 15 min. A portion of this mixture was packed into the end of a 3 mm i.d. glass tube. Electrical contact was established *via* a copper wire. The electrode was then cured at room temperature for 48 h. The surface was polished with a 320 grit silicon carbide paper. Residual polishing material was removed by thoroughly rinsing with doubly distilled water. The polishing procedure was repeated before each experiment. Between experiments the biocomposites were stored at 4 °C.

Reagents

Tyrosinase [EC 1.14.18.1, from mushroom, 6300 U mg^{-1} (1 U = 16.67 nkat)] and catechol were purchased from Sigma. Aldrich provided the *p*-cresol and *p*-chlorophenol, and phenol was obtained from Fisher. All solutions were prepared daily in the 0.05 mmol l^{-1} phosphate buffer solution (pH 6.7), which also served as supporting electrolyte. These solutions were prepared using doubly distilled water.

Procedure

All measurements were performed at room temperature. Amperometric biosensing proceeded under batch and flow-injection conditions, at a stirring rate of 300 rev min^{-1} and a flow rate of 2.0 ml min^{-1}, respectively. The desired working potential was then applied, and transient currents were allowed to decay to steady-state values before amperometric monitoring.

Results and Discussion

Fig. 1 shows cyclic voltammograms for the blank and *p*-cresol solutions (broken and solid lines, respectively) recorded at (*a*) the plain and (*b*) the tyrosinase-containing graphite–epoxy electrodes. In the absence of biocatalytic activity, the unmodified electrode is not responsive to the presence of the phenolic compound (within the potential window examined). In contrast, a well defined cathodic peak, starting at +0.02 V and reaching a maximum at −0.15 V, is observed at the biocomposite surface. Such a peak corresponds to the reduction of the enzymically liberated quinone species. These (and all subsequent) data illustrate that the tyrosinase maintains its biocatalytic activity within the graphite–epoxy matrix, and that such a matrix does not suffer from resistive (ohmic) effects. Indeed, the peak potential for the quinone product is similar to that obtained at other carbon surfaces.

The behaviour shown in Fig. 1 can be exploited for the effective biosensing of phenolic compounds. Fig. 2 shows a typical response of the 5% m/m tyrosinase biocomposite to successive 2×10^{-6} mol l^{-1} increments of the phenol concentration. The graphite–epoxy bioelectrode responds rapidly to the change in the substrate concentration, producing a steady-state response within 25 s. Such a fast response is attributed to the close proximity of the enzyme and graphite sites and to the absence of an external membrane barrier. High sensitivity is indicated by the well defined response for low (μmol l^{-1}) concentrations of the substrate. The signal-to-noise characteristics (S/N = 3) indicate a detection limit of 5×10^{-7} mol l^{-1}. The data of Fig. 2 yielded a linear calibration plot, with a slope of 43 nA l μmol^{-1} (correlation coefficient, 0.999). Deviations from linearity were observed at higher concentrations (see subsequent data below). As expected, no response was observed for analogous measurements at the 'enzyme-free' surface (not shown).

Various experimental parameters affecting the amperometric response were evaluated to optimize the analytical performance. Fig. 3 shows the effect of A, the operational potential and B, the pH on the response of the tyrosinase bioprobe. In accordance with the cyclic voltammetric data (Fig. 1), cathodic detection of the substrate starts at +0.1 V; a rapid increase in the reduction current is observed between +0.10 and −0.20 V, with a decrease at higher potentials. The response also increases rapidly with increasing pH between pH 4.5 and pH 6.0, and decreases sharply for solutions with pH higher than 6.7. A broad optimum pH range of 5–8 was reported for the free enzyme.[17] All subsequent biosensor work was hence carried out at −0.2 V in a pH 6.7 buffer. This low potential detection minimizes potential interferences from common electroactive species.

Fig. 4 displays the amperometic response of the tyrosinase biocomposite to successive standard additions of 1×10^{-5} mol l^{-1} of: (*a*) catechol; (*b*) *p*-chlorophenol; (*c*) *p*-cresol; and (*d*) phenol. The sensor responds rapidly to these concentration increments of the various substrates, and offers convenient quantification at the μmol l^{-1} level. The corresponding calibration plots are shown in Fig. 5. As expected for

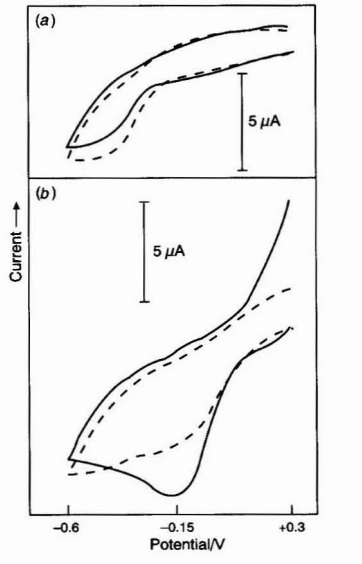

Fig. 1 Cyclic voltammograms for 1×10^{-2} mol l^{-1} *p*-cresol at graphite–epoxy electrodes containing (*a*) 0% and (*b*) 5% m/m tyrosinase. Scan rate, 20 mV s^{-1}; solution, 0.05 mol l^{-1} phosphate buffer (pH 6.7). Broken line, blank; and solid line, *p*-cresol solution

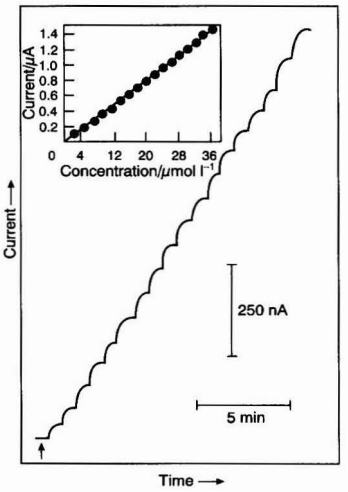

Fig. 2 Current–time recording obtained at the 5% m/m tyrosinase-containing graphite–epoxy electrode on increasing the phenol concentration in 2×10^{-6} mol l^{-1} steps. Solution, 0.05 mol l^{-1} phosphate buffer (pH 6.7); operating potential, −0.20 V; stirring rate, 300 rev min^{-1}

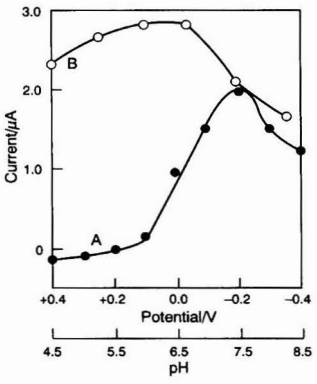

Fig. 3 Effect of A, applied potential and B, solution pH on the response to 1×10^{-5} mol l^{-1} catechol. Other conditions, as in Fig. 2

biocatalytic sensors, the response increases non-linearly with the substrate concentration. The trend in sensitivity (*p*-cresol > catechol > *p*-chlorophenol > phenol) differs in part from that reported for other tyrosinase electrodes,[18] and indicates changes in the selectivity pattern induced by the hydrophobic environment of the graphite–epoxy resin.

A 4% decrease in the response was observed for 10 successive batch measurements of 1×10^{-5} mol l^{-1} phenol at an unpolished surface (not shown). This decrease is attributed to slow surface fouling by the reaction product. This passivation effect can be greatly minimized under flow-injection conditions (see subsequent data) or eliminated by surface polishing. Indeed, unlike early phenol biosensors, the biocomposite approach offers a unique way to restore (regenerate) reproducibly the original response. Tyrosinase retains its biocatalytic activity on confinement in the epoxy resin matrix over long periods. Only 3 and 10% decreases in the response were observed over 10 and 20 d, respectively (under dry storage at 4 °C). Such stability may be attributed in part to a 'protective' action of the epoxy resin matrix (analogous to that reported for non-aqueous environments[19]).

Graphite–epoxy resin based biocomposites hold great promise for monitoring flowing streams. Various flow systems, based on liquid chromatography and flow injection, are often used for on-line monitoring of phenolic compounds in various matrices. Fig. 6(*a*) displays the flow-injection response (at −0.20 V) of the tyrosinase detector for 20 µl solutions of increasing phenol concentration (10–110 µmol l^{-1}, A–K). The biocomposite detector exhibits well defined peaks and offers convenient quantification of these µmol l^{-} concentrations. The favourable signal-to-noise characteristics result in a low detection limit of 1×10^{-6} mol l^{-1} (based on S/N = 3). Hence, 1.9 ng can be detected in the 20 µl sample. The flow-injection response is proportional to the phenol concentration [see inset (Fig. 6); slope, 2.22 nA l µmol^{-1}; and correlation coefficient, 0.998). The wide linear range (*versus* analogous batch measurements, *e.g.*, as shown in Fig. 5) is attributed to the dilution (dispersion) effect of the flow-injection system. The tyrosinase bicomposite also exhibits attractive dynamic properties, with a rapid increase and decrease of the current. The peak half-width (≈25 s) allows an injection rate of 50 samples h^{-1}. The flow-injection response is also highly reproducible [Fig. 6(*b*)]. This prolonged series of 40 repetitive injections of 5×10^{-5} mol l^{-1} phenol solution yielded a relative standard deviation of 1.4% (mean, 143 nA; range, 140–147 nA). The response properties shown in Fig. 6 make the tyrosinase biocomposite very attractive for monitoring phenolic compounds in chromatographic effluents. In particular, the new detector would add a new dimension of selectivity (based on biorecognition) to chromatographic detection. A dual-electrode operation (based on enzyme-modified and plain electrodes) should greatly enhance the information obtained from the amperometric monitoring of phenols. The tyrosinase biocomposite should be advantageous for chromatographic separations with mobile phases rich in

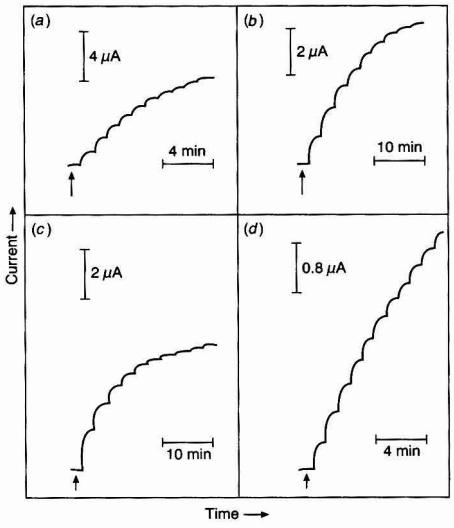

Fig. 4 Amperometric response for successive additions of 1×10^{-5} mol l^{-1} catechol (*a*), *p*-chlorophenol (*b*), *p*-cresol (*c*) and phenol (*d*). Conditions, as in Fig. 2

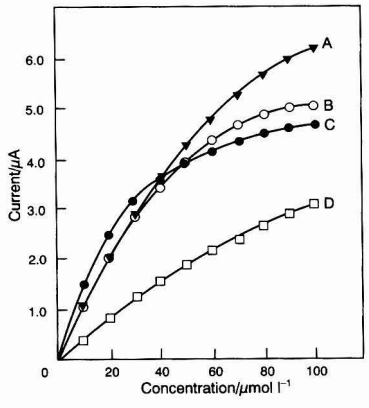

Fig. 5 Dependence of the steady-state current on the concentration of: A, catechol; B, *p*-chlorophenol; C, *p*-cresol; and D, phenol. Conditions, as in Fig. 4

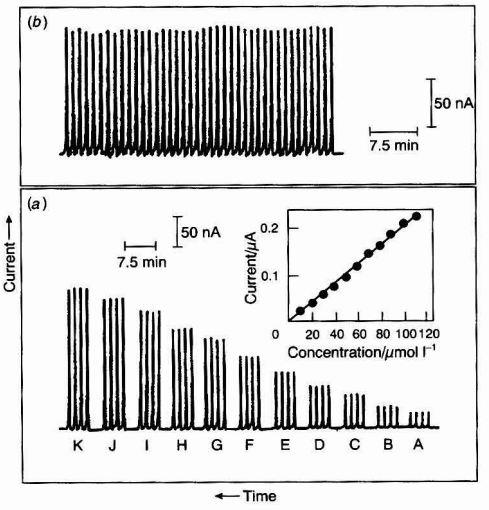

Fig. 6 (*a*) Flow-inection response to phenol solutions of increasing concentration from 1×10^{-5} to 1.1×10^{-4} mol l^{-1} (A–K). (*b*) Flow-injection response to repetitive injections of a 5×10^{-5} mol l^{-1} phenol solution. Flow rate, 2.0 ml min^{-1}; sample volume, 20 µl. Potential and solution, as in Fig. 2

organic media (as often required for phenolic compounds). This is owing to the inherent activity of tyrosinase in non-aqueous environments,[20] and the compatibility of graphite–epoxy resins with such media.[15]

In summary, the experiments described above illustrate an attractive approach for the fabrication of renewable and robust phenol biosensors. Tyrosinase maintains its enzymic activity on confinement in the composite matrix, with typical polishing procedures resulting in fresh biosurfaces. This coupling of a class-selective enzyme with the versatility of the graphite–epoxy strategy results in the effective biosensing of phenolic compounds. Monitoring of the total phenol content and of individual compounds should be accomplished in connection with flow-injection and liquid-chromatographic systems, respectively. Various additives may be incorporated in the biocomposite matrix to enhance the analytical performance further. In addition, metallized graphites[21] could be used for preparing biocomposites with 'built-in' electrocatalytic action. Other enzymes, cofactors and mediators could be incorporated within the graphite–epoxy resin matrix to give reagentless and robust biosensors for other important substrates.

This work was supported by the National Institutes of Health (Grant No. GM 08136-19).

References

1 Hall, G., Best, D., and Turner, A. P. F., *Anal. Chim. Acta*, 1988, **213**, 113.
2 Connor, M. P., Sanchez, J., Wang, J., Smyth, M. R., and Mannino, S., *Analyst*, 1989, **114**, 1427.
3 Bonakdar, M., Vilchez, J., and Mottola, H., *J. Electroanal. Chem.*, 1989, **266**, 47.
4 Ortega, F., Cuevas, J., Centenera, J., and Dominguez, E., *J. Pharm. Biomed. Anal.*, 1992, **10**, 789.
5 Wang, J., Fang, L., and Lopez, D., in *Biosensors*, in the press.
6 Rodriquez, M., and Flurkey, W., *J. Chem. Educ.*, 1992, **69**, 767.
7 Wang, J., and Lin, M. S., *Anal. Chem.*, 1988, **60**, 115.
8 Wang, J., and Varughese, K., *Anal. Chem.*, 1990, **62**, 318.
9 Wang, J., Gonzalez-Romero, E., and Ozsoz, M., *Electroanalysis*, 1992, **4**, 539.
10 Wang, J., and Ozsoz, M., *Electroanalysis*, 1990, **2**, 647.
11 Wollenberger, U., Wang, J., Ozsoz, M., Gonzalez-Romero, E., and Scheller, F., *Bioelectrochem. Bioenerg.*, 1991, **26**, 287.
12 Cespedes, F., Martinez-Fabregas, E., Bartoli, J., and Algeret, S., *Anal. Chim. Acta*, 1993, **273**, 409.
13 Cespedes, F., Martinez-Fabregas, E., and Algeret, S., *Electroanalysis*, in the press.
14 Shaw, B., and Creasy, K., *Anal. Chem.*, 1988, **60**, 1241.
15 Wang, J., Golden, T., Varughese, K., and El-Rayes, I., *Anal. Chem.*, 1989, **61**, 508.
16 Wring, S., Hart, J., and Birch, B., *Anal. Chim. Acta*, 1990, **229**, 63.
17 Horowitz, N., Fling, M., and Horn, G., in *Methods in Enzymology*, eds. Tabor, H., and Tabor, C., Academic Press, New York, 1970, vol. XVIIA, pp. 615–620.
18 Ortega, F., Dominguez, E., Jönsson-Pettersson, G., and Gorton, L., *J. Biotechnol.*, in the press.
19 Zaks, A., and Klibanov, A. M., *Science*, 1984, **224**, 1249.
20 Wang, J., Lin, Y., and Chen, Q., *Electroanalysis*, 1993, **5**, 23.
21 Wang, J., Naser, N., Angnes, L., Wu, H., and Chen, L., *Anal. Chem.*, 1992, **64**, 1285.

Paper 3/03749E
Received June 30, 1993
Accepted August 5, 1993

Voltammetric Determination of Dopamine in the Presence of Ascorbic Acid at Over-oxidized Polypyrrole–Indigo Carmine Film-coated Electrodes

Zhiqiang Gao,* Beshen Chen and Minxian Zi

Department of Chemistry, Henan University, Henan, Kaifeng, 475001, China

Over-oxidized polypyrrole films doped with indigo carmine (PPy–IC) offer substantial improvements in voltammetric sensitivity and selectivity towards dopamine. This polymer coating attenuates the voltammetric response of ascorbic acid while the oxidation peak current of dopamine is enhanced by over one order of magnitude compared with that at the bare electrode. The high sensitivity and selectivity for dopamine appears to be mainly due to the charge discrimination and the analyte accumulation. The detection limit is dependent on both film thickness and preconcentration time. At a 0.25 μm thick PPy–IC film-coated electrode, for a 2 min preconcentration time, the detection limit is 10^{-8} mol l^{-1}, over two orders of magnitude lower than at a bare glassy carbon electrode. The concomitant ascorbic acid shows no interference although its concentration is as high as 0.1 mmol l^{-1}. The effects of various experimental parameters on the voltammetric response of dopamine were also investigated. The attractive permselective and preconcentrating properties of the PPy–IC films make them valuable for *in vivo* electrochemistry.

Keywords: Dopamine; polypyrrole; indigo carmine; voltammetry; film-coated glassy carbon electrode

Introduction

There has been considerable interest in using voltammetric electrodes for *in vivo* monitoring since the first *in vivo* voltammograms were obtained in the 1970s[1] and a number of publications have appeared subsequently.[2–12] It has been possible to detect oxidizable neurotransmitters present in active brain tissues.[2] Electrochemistry has been combined with pharmacological stimulation methods to provide information about basic biology and transmitter diffusion on a real-time basis. However, attempts to measure neurotransmitters, particularly dopamine (DA), in the brain with voltammetric electrodes require the use of several strategies to improve the qualitative and quantitative aspects of these measurements. The main problem associated with measuring levels of this monoamine *in vivo* is the very low DA concentration (10^{-8}–10^{-6} mol l^{-1}) and the large excesses of interfering anions such as ascorbic acid (AA) (about 0.1 mmol l^{-1}).[2] Unfortunately, at most solid electrodes, AA is oxidized at potentials similar to those of DA, resulting in an overlapped voltammetric response, hence complicating the interpretation of the data.

The ability to measure DA selectively in the presence of AA has been a major target of electroanalytical research. Considerable efforts have been devoted towards improving the sensitivity and selectivity of DA against AA. The characteristics of the carbon substrate may be favourably altered through electrochemical pre-treatment of the electrode. This can have the effect of lessening the oxidative overpotential for AA, thus increasing the resolution of its oxidation signal from that of DA, thereby minimizing electrocatalytic complications.[13,14] However, this type of surface modification has been reported to diminish in effectiveness with time under certain circumstances;[15] thus, polymer films, including Nafion,[16–18] stearic acid,[19,20] poly(estersulfonic acid)[21] and poly(*N*-vinylpyrrolidone)[22] have been explored as electrode modifiers to achieve similar results. Among them, Nafion, a perfluorosulfonated polymer, has been the most intensively studied polymer as a coating for electrochemical sensors, particularly in the determination of DA. The attraction of this polymer arises from the charge repulsion between the anionic sulfonate groups in the polymer film and negatively charged interferents in the solution. In addition, hydrophobic cations such as DA have been demonstrated to be accumulated in Nafion films through ion-exchange equilibrium.[16,23] AA can also be removed by coupling with enzymatic reactions.[24] New polymers with attractive permselective properties are desirable for the further development of voltammetric sensors for DA.

This paper describes the analytical advantages and characteristics of a novel polymeric coating based on polypyrrole (PPy) film polymerized in indigo carmine solution (PPy–IC). We have demonstrated recently[25] that electrodeposition of polypyrrole was easily achieved in saturated indigo carmine (IC) solution. Owing to the bulky volume of the IC molecule, it is immobilized in PPy films. However, when the PPy film is subjected to potential cycling between −1.0 and 0.4 V in an alkaline medium, the conjugated structure of PPy is destroyed and IC molecules are expelled from the film, which leads to a negatively charged porous film on the electrode surface, yielding permselectivity based on charge repulsion. The discriminative properties of PPy–IC-coated electrodes were studied in detail in this work.

Experimental

Reagents and Apparatus

Dopamine in the hydrochloride form was obtained from Aldrich and indigo carmine and analytical-reagent grade L-ascorbic acid were purchased from Merck and all were used as received. Pyrrole obtained from Merck was purified by double distillation and stored at low temperature protected from light. All other chemicals were of analytical-reagent grade and were used as received. Working solutions of DA and AA were prepared daily with distilled, de-ionized water, which was previously deoxygenated with high-purity nitrogen. Phosphate buffer solution (0.1 mol l^{-1}, pH 7.4) was used as the supporting electrolyte. The dissolved oxygen was removed by

* Present address: Department of Materials and Interface, Weizmann Institute of Science, Rehovot, 76100, Israel.

bubbling with high-purity nitrogen and a nitrogen atmosphere was maintained throughout.

Voltammetric experiments were performed with a Metrohm E506 Polarecord. In some cases a PAR Model 174A polarographic analyser was used. A conventional three-electrode system was used throughout. The working electrode was a PPy–IC film-coated glassy carbon electrode (area 0.2 cm^2) (Metrohm), the auxiliary electrode was a platinum wire and a saturated calomel electrode (SCE) was used as the reference electrode. All potentials given in this paper are referred to the SCE. Experiments were performed at room temperature.

Preparation of PPy–IC Film-coated Glassy Carbon Electrodes

Before PPy film deposition, the electrode was polished with 0.3 and 0.05 μm alumina slurries, rinsed with water and polished thoroughly with a clean and wet cloth. It was then pre-treated, according to the procedure described by Anjo *et al.*,[26] using polarization at 1.2 V in 0.1 mol l^{-1} NaOH solution for 5–10 min. Subsequently, the electrode was placed in a 0.1 mol l^{-1} pyrrole-saturated IC solution, which was previously de-oxygenated with high-purity nitrogen for at least 20 min and kept in a nitrogen atmosphere. Electropolymerization was achieved by constant-current electrolysis (1–2 mA cm^{-2}). The film thickness was controlled, based on the amount of charge passed.[27] When the PPy film deposition process was finished the electrode was transferred into 0.1 mol l^{-1} phosphate–0.1 mol l^{-1} NaOH solution (pH 12–13) for potential cycling between 0.4 and −1.0 V, until the voltammetric activity of the film had been lost completely. The potential scan rate used was in the range 20–50 mV s^{-1}. The electrode was ready for use after the final wash with water.

Voltammetric Determination of DA with PPy–IC Film-coated Electrodes

The preconcentration–voltammetric determination–renewal scheme was used in all experiments. For the preconcentration step, the film-coated electrode was immersed under open-circuit conditions in 25 ml of 0.1 mol l^{-1} phosphate buffer–0.1 mmol l^{-1} AA solution (pH 7.4) containing DA. After a given period of time an anodic potential scan was conducted from −0.2 V to a final potential of 0.4 V which was maintained for several minutes to ensure complete oxidation of the previously preconcentrated DA prior to the next measurement.

Results and Discussion

Voltammetric Behaviour of PPy–IC Film at Different pH Values

The effect of pH on the voltammetric response of the PPy–IC film was studied first, in order to determine the optimum range over which the film is permselective. As shown in Fig. 1, in 1.0 mol l^{-1} HCl the electrochemistry of the film is reversible and the film is highly stable, withstanding thousands of cyclic potential scans without a significant decrease in its voltammetric activity. However, the film shows no permselective properties in this medium. It was found that the formal potential of the film ($E^{\circ\prime}$) exhibits a strong pH dependence. At pH <9.0, $E^{\circ\prime}$ shifts by about 53 mV per pH unit, which indicates that one proton per electron is involved in the redox process of the film. In contrast, at pH >9.0, $E^{\circ\prime}$ is no longer pH dependent and the film loses its typical redox response quickly when scanning at pH >10. In addition, during the potential scans, a blue layer is observed near to the electrode surface (pH <13), which clearly shows that the entrapped IC is repelled from the film. Once the voltammetric activity has been lost, a cationic permselective film is obtained. The rate of de-activation of the film depends on the pH of the electrolyte solution. Increasing the pH of the electrolyte accelerates the deactivating process, probably because the decrease in activity is caused by the nucleophilic attack of OH^- on the pyrrole units, and the hydroxyl groups are then oxidized to carbonyls.[28] However, a higher base concentration usually results in non-uniform film properties, especially when thick films are used, and the film shows poor adherence to the glassy carbon surface. In this work, the PPy films were always treated in 0.1 mol l^{-1} phosphate–0.1 mol l^{-1} NaOH solution at pH 12–13.

Cyclic Voltammetry of DA and AA at PPy–IC Film-coated Electrodes

Cyclic voltammograms for the oxidation of DA and AA in 0.1 mol l^{-1} phosphate buffer (pH 7.4) at a bare glassy carbon electrode were studied first. As illustrated in Fig. 2, the voltammogram of DA shows a quasi-reversible character. The anodic peak potential is 0.16 V and the peak current for the oxidation of 0.2 mmol l^{-1} DA is 84.0 μA cm^{-2} at 40 mV s^{-1}.

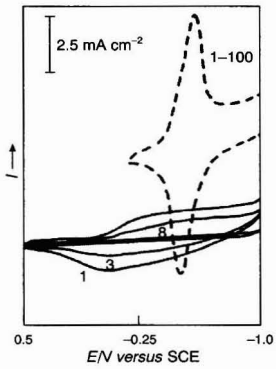

Fig. 1 Cyclic voltammograms of PPy–IC film-coated electrodes at different pH values. Film thickness 0.5 μm, potential scan rate 100 mV s^{-1}. Broken line, 1.0 mol l^{-1} HCl (pH 0) and solid line, 0.1 mol l^{-1} phosphate–0.1 mol l^{-1} NaOH solution (pH 12.0); cycle numbers are indicated

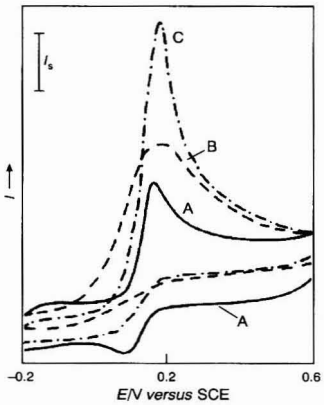

Fig. 2 Cyclic voltammograms of DA and AA at bare glassy carbon electrodes. 0.1 mol l^{-1} phosphate buffer (pH 7.4), potential scan rate 40 mV s^{-1}. A, 0.2 mmol l^{-1} DA; B, 1.6 mmol l^{-1} AA; and C, 0.2 mmol l^{-1} DA + 1.6 mmol l^{-1} AA. Current sensitivity I_s for DA is 40 μA cm^{-2} and for AA and AA + DA is 100 μA cm^{-2}

The reproducibility of the anodic peak current is fairly good; for example, for six determinations, the anodic peak currents vary from 83 to 86 μA cm^{-2} with a relative standard deviation of about 4.5%, and the peak potentials remain unchanged from electrode to electrode. This indicates little loss in sensitivity at a base pre-treated glassy carbon electrode with repeated scans, suggesting that there is no electrode fouling due to the oxidative process. In addition, it was confirmed that the background current of a base pre-treated glassy carbon electrode is much lower than that of an untreated or acid pre-treated electrode.[26] On the other hand, the cyclic voltammogram of AA at the glassy carbon electrode shows a totally irreversible process. Usually the anodic peak is drawn out and not well defined. The peak potential can vary by as much as 100 mV in either direction depending on the history of the electrode surface. The cyclic voltammogram of the combination of DA and AA is also shown in Fig. 2, which indicates no sign of peak separation at the bare electrode.

As shown in Table 1, the anodic peak current is much higher than the sum of the peak currents of DA and AA in separated solutions, and the reduction wave of DA is not apparent with increasing AA concentration. An explanation for this effect was given by Tse *et al.*[29] in early work. In the presence of AA, the oxidized species of DA would be reduced back to DA, and therefore a catalytic EC process would occur in the solution. Evidence for this can also be found in the literature with the strong reducing nature of AA in biological situations. The enhancement of the anodic peak current depends on both the concentration ratio of AA : DA and the pH of the solution. The largest anodic peak current is obtained at an AA concentration over 12 times higher than the DA concentration. The anodic peak current is increased by about 350% compared with that for the same concentration of DA alone. Furthermore, the largest enhancement is only observed in the pH range 7–9. The above results suggest that the sensitivity of DA might be improved by adding AA to the sample solution. Indeed, the detection limit is down to micromolar levels in the presence of 0.05 mmol l^{-1} AA.

The cyclic voltammograms for both DA and AA at a PPy–IC film-coated glassy carbon electrode are shown in Fig. 3. Similarly to that obtained with the bare glassy carbon electrode, the electrochemistry of DA at the film-coated electrode is also a quasi-reversible process. Owing to the cation-exchange properties of the film, the ratio of the cathodic-to-anodic peak currents of DA is increased. Some positive shifts (<20 mV) in anodic peak potentials are observed. The most significant point of Fig. 3 is that the film-coated electrode decreases the sensitivity for AA whereas it increases that for DA.

Table 1 Effect of AA on the anodic peak current of the catalytic process in 0.1 mol l^{-1} phosphate buffer–0.2 mmol l^{-1} DA solution (pH 7.4). Potential scan rate, 40 mV s^{-1}

AA/mmol l^{-1}	i_{pa}(AA)*/ (μA cm^{-2})	i_{pa}(AA + DA)/ (μA cm^{-2})	i_{pa}(cat)†/i_{pa}(DA) (%)
0.0	0.0	84.0	100
0.2	34.0	115	96
0.4	68.0	164	114
0.8	136	310	208
1.2	206	422	257
1.6	270	510	286
2.0	345	605	309
2.4	413	700	342
2.8	478	770	349
3.2	545	841	352

* i_{pa}(AA) was obtained in the absence of DA under the same experimental conditions.

† i_{pa}(cat) = i_{pa}(AA + DA)–i_{pa}(AA).

The sensitivity enhancement is more evident if one examines the linear sweep voltammograms in Fig. 4. The voltammetric response of DA at the bare glassy carbon electrode gives a reproducible diffusion-controlled anodic peak at 0.16 V (see Fig. 2). At the film-coated electrode, however, the DA response is now a symmetrical peak voltammogram, no longer controlled primarily by solution mass transport but typical of that for a surface process.[32] An analysis of the log i_{pa} (i_{pa} = anodic peak current) *versus* log v^x (v = potential scan rate) plot was carried out in order to determine the exponents (x) of the potential scan rate as a function of DA concentration in the solution and the film thickness. With decreasing DA concentration x increases from 0.5 towards 1, which is expected for a surface process.[32] As the PPy–IC film is in its negatively charged state, it is more likely that this change in slope is due to the contribution of the preconcentrated DA in the film. For a 2 min preconcentration at micromolar concentration levels, the anodic current at the film-coated electrode is over one order of magnitude higher than that at the bare glassy carbon electrode. At very low concentrations, *e.g.*, 10^{-7} mol l^{-1}, the contribution of the solution diffusion process is negligibly small compared with the surface process, and therefore the anodic peak current is entirely controlled by the preconcentrated DA in the film. On the other hand,

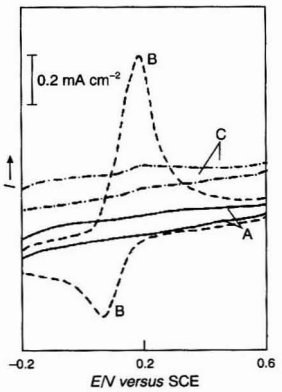

Fig. 3 Cyclic voltammograms of DA and AA at PPy–IC film-coated glassy carbon electrodes. Film thickness 0.5 μm, 0.1 mmol l^{-1} phosphate buffer (pH 7.4), potential scan rate 40 mV s^{-1}, preconcentration time 60 s. A, Blank buffer solution; B, 0.5 mmol l^{-1} DA; and C, 2 mmol l^{-1} AA

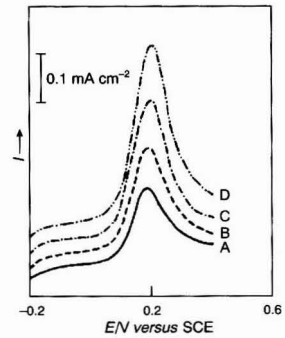

Fig. 4 Effect of preconcentration time on the voltammetric response of DA at a PPy–IC film-coated glassy carbon electrode. Film thickness 0.5 μm, 0.1 mmol l^{-1} phosphate buffer + 10 μmol l^{-1} DA (pH 7.4), potential scan rate 40 mV s^{-1}. A, 30; B, 60; C, 120; and D, 300 s

although the voltammogram does not correspond to this, a totally surface process and some solution-diffusion contributions are undoubtedly present at high concentrations. However, a large part of the increased sensitivity for DA at the film-coated electrode seems clearly to be the result of DA preconcentration. It should be mentioned that this only occurs with relatively thin films. The diffusion process of DA within the film will play some role when thick films are used (see below). The film-coated electrode, pre-soaked in dilute DA solution, is rinsed with distilled water and placed in blank buffer solution, gave two well defined redox peaks, which will disappear completely after a few cyclic potential scans. Such behaviour is further evidence for DA being accumulated into the film.

Previous work on over-oxidized PPy films by Brajter-Toth and co-workers[33,34] have shown that PPy films, after over-oxidation treatment, shows anion-excluding properties. However, the voltammetric responses of cations, *e.g.*, DA, Methyl Viologen and $Ru(NH_3)_6^{3+}$, are also suppressed. The current sensitivities for cations are never higher than that at the bare glassy carbon electrode, no matter what solution is employed for the over-oxidation of the PPy film. In contrast, the PPy–IC film shows a significant enhancement of current sensitivities towards cations. The explanation for this is evident if one considers the volume of counter ions. Similarly to normal PPy films, the potential cycling of the PPy–IC film in an alkaline medium results in the formation of negatively charged groups on the backbones of PPy,[28] and the counter ion, IC, is rejected from the film. The bulky volume of IC can then account for the permselectivity differences. Over-oxidized PPy–IC films would be expected to have much larger pores than the normal over-oxidized PPy films doped with inorganic anions. It seems that the permselectivity of PPy films can be controlled by a judicious choice of the counter ions, providing the basis for the analytical usefulness of the over-oxidized PPy film-coated electrodes. Optimization of the counter ions should be based on both sensitivity and selectivity considerations.

In order to develop a practical procedure for the determination of DA, after each measurement the film must return to its 'analyte-free' state. However, after the first anodic scan the preconcentrated DA in the film is not completely oxidized and, therefore, will affect the subsequent measurements. This effect is more pronounced at high concentrations of DA. Different methods for effective renewal of the film had to be evaluated. It was found that renewal of the film is easily accomplished by soaking the film-coated electrode in 0.1 mol l^{-1} phosphate buffer solution (pH 7.4) for about 2 h. The renewal process could be greatly accelerated by applying a sufficiently positive potential to the electrode. In practical work, the electrode was polarized at 0.4 V for 1 min after each determination at concentrations lower than 0.1 mmol l^{-1}. At higher DA concentrations, the film can only be partly renewed and therefore the electrode cannot be used in practical work at DA concentrations higher than 1.0 mmol l^{-1}. The reproducibility and stability of the renewed electrode were examined in ten parallel determinations. For a 0.5 μmol l^{-1} DA solution with a preconcentration time of 2 min, the relative standard deviation was 6.0%; usually the electrode can be used for about 2 h without significant decreases in sensitivity and selectivity. After running for 1 d, the magnitude of the voltammetric response for DA decreases by about 25%, but exactly the same shape of the voltammogram is maintained, with no shifts in peak potentials. The instability of the film seems to be a result of changes in film structure rather than the commonly observed poisoning effect of catecholamines at solid electrode surfaces.[35,36] Further work is in progress to study the detailed structure of the film and the interaction with cationic species by employing Fourier transform infrared and other spectroscopic techniques.

The effect of film thickness on sensitivity, selectivity and detection limit is demonstrated in Fig. 5. The current sensitivity (for 10 μmol l^{-1} DA) increases with increasing film thickness. For fairly thick films, the anodic peak current drops again [Fig. 5(*a*)]. There are three reasons for the higher current sensitivity at the moderate-thickness film-coated electrode. The first involves the preconcentration capacity (*i.e.*, the number of negative charges in the film). For a very thin film, the saturation effect will be unavoidable with high analyte concentrations. If this happens, the concentration of analyte in the film will become virtually constant. Hence only small currents can be detected with very thin films. The preconcentration capacity increases linearly with increasing film thickness, therefore, an increment of current sensitivity would be expected. Furthermore, the current sensitivity observed for different film thicknesses is strongly affected by the analyte concentration and the preconcentration time. For instance, in 0.1 μmol l^{-1} DA solution the highest current sensitivity is observed with a 0.2 μm PPy–IC film within 10 min of preconcentration. However, as can be seen in Fig. 5(*a*), at the 10 μmol l^{-1} level, the highest sensitivity is obtained with a 0.5 μm PPy–IC film.

The second explanation for the decrease of current sensitivity at very thick film-coated electrodes concerns the film volume by assuming a constant surface area and a constant flux of analyte into the film, regardless of the film thickness. As all the films are exposed to the same solution for the same preconcentration time, the thick and thin films imbibe the same number of moles of analyte. However, because the volume of thin films is much smaller, the concentration of analyte in the film is higher. Hence it would be expected to show greater sensitivity.

The validity of the constant-diffusion hypothesis can be checked by comparing the anodic peak currents. If constant diffusion occurs, the anodic peak currents of DA in PPy–IC films should be inversely proportional to the film thickness, *i.e.*, the peak current at a 0.5 μm thick film-coated electrode should be ten times higher than that at a 5.0 μm thick film-coated electrode. In fact, the anodic peak current at a 0.5 μm thick film-coated electrode is only about three times higher, indicating that the diffusion rate cannot be constant and the average flux of DA into thick films is faster than that into thin films. The decrease in flux into thin films is due to the accumulation of an appreciable amount of DA in the film, which will decrease the concentration gradient from a constant value to a smaller, time-dependent value. In addition, with increasing film thickness, the effective surface area is probably increased, resulting in an enhancement of the preconcentration efficiency.

The last possibility for this is that, as shown in Fig. 5(*a*), the voltammetric response of DA at thick film-coated electrodes exhibits a typical diffusion-controlled process.[32] At thick film-coated electrodes, the dominant process is the diffusion of analyte through the film. An electron-exchange process takes place at the glassy carbon/PPy–IC film interface, thus any change in the film thickness will result in a change in diffusion pathways for DA. As expected, the diffusion process of DA within the film becomes more and more important and the sensitivity will be lowered with increasing film thickness. Similar behaviour was observed at a Nafion film-coated electrode.[37]

It was also found that better selectivity and sensitivity can be achieved when a longer preconcentration time is used. This is not surprising as longer preconcentration allows a larger amount of DA to be accumulated in the film (Fig. 4). Obviously, the sensitivity and selectivity are dependent on the interplay of film thickness and preconcentration time. As shown in Fig. 5(*b*) at a fixed preconcentration time, the selectivity increases rapidly with increasing film thickness and

finally a virtually constant value is reached. For practical purposes, when the AA concentration is lower than 0.2 mmol l^{-1} which is the normal concentration level in the mammalian brain, the selectivity with a 0.25–1.0 μm thick PPy–IC film-coated electrode is adequate for DA determination in the range 0.1–10 μmol l^{-1}. A better detection limit is observed with a 0.2–0.5 μm thick film-coated electrode. At very thin film-coated electrodes, a large background current arises from the oxidation of AA that is capable of diffusing through the film, which causes serious problems for DA determination. However, owing to the increase in charging current with thick film-coated electrodes, the lowest detectable concentration is only about 0.5 μmol l^{-1} [Fig. 5(*b*)].

Voltammetric Determination of DA With a Large Excess of AA

Fig. 6 shows linear-sweep voltammograms obtained at the film-coated electrode. The analyte solution is 0.1 mol l^{-1} phosphate buffer (pH 7.4) containing 0.1 μmol l^{-1} DA and 0.1 mmol l^{-1} AA. The DA : AA concentration ratio is similar to that of biological systems, *e.g.*, mammalian brain tissues. After immersion of the film-coated electrode in the solution for 2 min the uppermost voltammograms are obtained. The peak current is due to the oxidation of DA, although the bulk concentration of AA is three orders of magnitude higher than that of DA. A small effect is observed with further increases in AA concentration up to 0.3 mmol l^{-1}. Neither a large background current nor a pronounced catalytic current is observable at the film-coated electrodes.

The calibration graphs for DA in 0.1 mol l^{-1} phosphate buffer–0.1 mmol l^{-1} AA solution (pH 7.4) are shown in Fig. 7. These graphs also indicate a number of important points concerning the effect of film thickness on the sensitivity, detection limit and linear response range. In agreement with the above discussion, the moderately thick film gives a high sensitivity and low detection limit. Note that with line A, the anodic peak current becomes virtually independent of DA concentration above 10 μmol l^{-1}. This is due to the saturation effect.[38] For line B, the current sensitivity is much lower than that for line A, but it yields a longer linear response range. With very thin film-coated electrodes (<0.1 μm) the detection limit is greatly decreased owing to the contribution of AA oxidation.

The reproducibility of a single 0.5 μm thick PPy–IC film-coated electrode was determined from a series of repetitive linear-sweep voltammetric analyses of a 1.0 μmol l^{-1} DA–0.1 mmol l^{-1} AA mixture in 0.1 mol l^{-1} phosphate buffer (pH 7.4). For a 2 min preconcentration time, the mean anodic peak current is 23.0 μA cm^{-2} with a range of

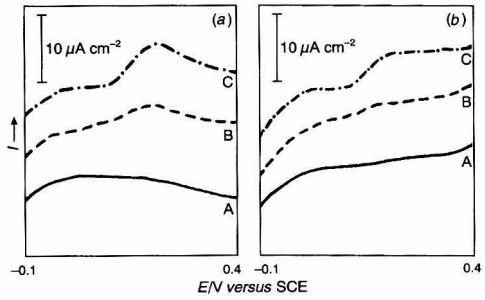

Fig. 6 Voltammetric responses of DA with a large excess of AA at (*a*) 0.2 μm and (*b*) 0.5 μm PPy–IC film-coated glassy carbon electrodes. Preconcentration time 120 s, potential scan rate 40 mV s^{-1}. A, 0.1 mol l^{-1} phosphate buffer (pH 7.4), B, 0.1 mol l^{-1} phosphate buffer + 0.1 mmol l^{-1} AA (pH 7.4) and C, 0.1 mol l^{-1} phosphate buffer + 0.1 mmol l^{-1} phosphate buffer + 0.1 mmol l^{-1} AA + 0.1 μmol l^{-1} DA (pH 7.4)

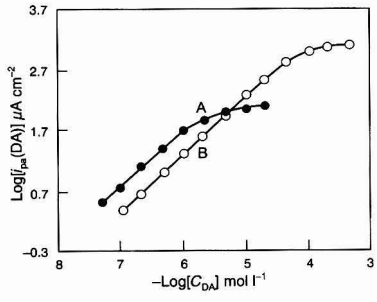

Fig. 7 Calibration graph for DA at PPy–IC film-coated glassy carbon electrodes. Film thickness: A, 0.1 μm and B, 0.6 μm; other conditions are as for Fig. 6

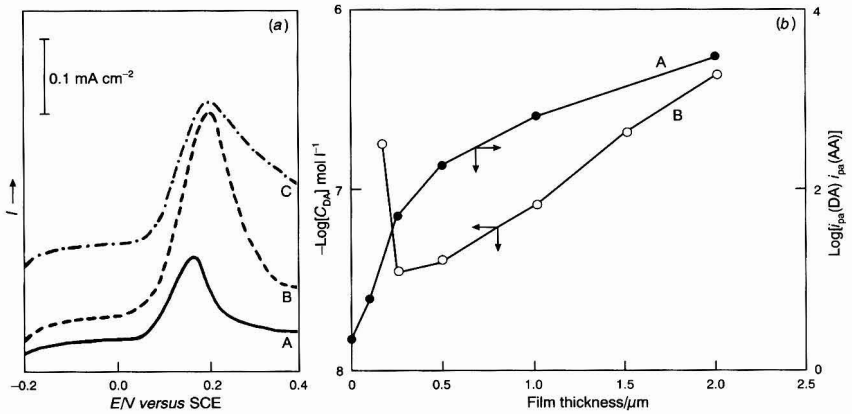

Fig. 5 Effect of film thickness on the sensitivity, selectivity and detection limit of DA. 0.1 mmol l^{-1} phosphate buffer (pH 7.4), preconcentration time 120 s, potential scan rate 40 mV s^{-1} (*a*) 10 μmol l^{-1} DA; A, 0.15 μm, B, 0.5 μm and C, 1.5 μm thick PPy–IC films. (*b*) Dependence of A, selectivity and B, detection limit on film thickness

21.5–24.0 μA cm^{-2}, and a relative standard deviation of 6.0%, indicating a satisfactory method for practical applications, especially for *in vivo* electrochemistry. However, because of the complicated nature of the electropolymerization process, it was very difficult to obtain a highly reproducible film thickness, although great care was taken in the film preparation. For ten measurements with 0.6 μm thick PPy–IC films at micromolar concentration levels, the lowest relative error of voltammetric responses was about 15%. This value, however, is still much better than for previously reported ion-exchange film-coated electrodes prepared by solvent evaporation or the spin-coating method. This is obviously due to the more precise control of the thickness of PPy–IC films by controlling the charge used during polymerization.

This work clearly demonstrates that the determination of DA in the presence of AA is facilitated with PPy–IC film-coated electrodes, as AA oxidation is almost entirely eliminated and the contribution from catalytic chemical reactions is also minimized.

In conclusion, the experiments described above have indicated that the transport properties and preconcentration characteristics of PPy–IC films make them suitable for voltammetric sensing. In particular, the enhanced selectivity obtained as a result of excluding anionic species could be very valuable for *in vivo* electrochemistry. With its low cost and ease of preparation, the PPy–IC film appears to open up new opportunities for further sensor development.

References

1 Adams, R. N., *Anal. Chem.*, 1976, **48**, 1126A.
2 Wightman, M. R., May, L. J., and Michael, A. C., *Anal. Chem.*, 1988, **60**, 769A.
3 *Voltammetry in the Neurosciences: Principles, Methods, and Applications*, ed. Justice, J. B., Jr., Humana Press, Clifton, NJ, 1987.
4 Broderick, P. A., *Electroanalysis*, 1990, **2**, 241.
5 Marsden, C. A., Joseph, M. H., Kurk, Z. L., Maidment, N. T., O'Neill, R. D., Schenk, J. O., and Stamford, J. A., *Neuroscience*, 1988, **25**, 289.
6 Lennart, S., Peter, C. W. H., Kenn, J., and Joergen, E. A., *Brain Res.*, 1993, **609**, 36.
7 Wrightman, M. R., and Zimmerman, J. B., *Brain Res. Rev.*, 1990, **15**, 135.
8 Zimmerman, J. B., and Wightman, R. M., *Anal. Chem.*, 1991, **63**, 24.
9 Abe, T., Lau, Y. Y., and Ewing, A. G., *Anal. Chem.*, 1991, **63**, 24.
10 Chien, J. B., Wallingford, R. A., and Ewing, A. G., *J. Neurochem.*, 1990, **54**, 633.
11 Broderick, P. A., *Neurosci. Lett.*, 1988, **95**, 275.
12 Hafizi, S., Kruk, Z. L., and Stamford, J. A., *J. Electroanal. Chem.*, 1990, **283**, 125.
13 Gonon, F. G., Buda, M., Cespuglio, R., Jouvet, M., and Pujol, J.-F., *Nature (London)*, 1980, **280**, 902.
14 Gonon, F. G., Navarre, F., and Buda, M., *Anal. Chem.*, 1984, **56**, 573.
15 Gonon, F. G., Cespuglio, R., Buda, M., and Pujol, J.-F., *Methods in Biol. Amines Res.*, 1983, 165.
16 Nagy, G., Gerhardt, G. A., Oke, A. F., Rice, M. E., Adams, R. N., Moore, R. B., III, Szentirmay, M. N., and Martin, C. R., *J. Electroanal. Chem.*, 1985, **188**, 85.
17 Kristensen, E. W., Kuhr, W. G., and Wrightman, R. M., *Anal. Chem.*, 1987, **59**, 1752.
18 Capella, P., Ghasemzadeh, B., Mitchell, K., and Adams, R. N., *Electroanalysis*, 1990, **2**, 175.
19 Gelbert, M. B., and Curran, D. J., *Anal. Chem.*, 1986, **58**, 1028.
20 Blaha, C. D., and Lane, R. F., *Brain Res. Bull.*, 1983, **10**, 861.
21 Wang, J., and Lin, M. S., *Electroanalysis*, 1980, **10**, 861.
22 Coury, L. A., Jr., Huber, E. W., Birch, E. M., and Heineman, W. R., *J. Electrochem. Soc.*, 1989, **136**, 2603.
23 Szentirmay, M. N., and Martin, C. R., *Anal. Chem.*, 1984, **56**, 1898.
24 Wang, J., Naser, N., and Ozsoz, M., *Anal. Chim. Acta*, 1990, **234**, 315.
25 Gao, Z., Bobacka, J., Lewenstam, A., and Ivaska, A., *Electrochim. Acta*, in the press.
26 Anjo, D. M., Kahr, M., Khodabakhsh, M. M., Nowinski, S., and Wanger, M., *Anal. Chem.*, 1989, **61**, 2603.
27 Diaz, A. F., and Castillo, J. I., *J. Chem. Soc., Chem. Commun.*, 1980, 397.
28 Beck, F., Braun, P., and Oberst, M., *Ber. Bunsenges. Phys. Chem.*, 1987, **91**, 967.
29 Tse, D. C. S., McCreery, R. L., and Adams, R. N., *J. Med. Chem.*, 1976, **19**, 37.
30 Stein, L., and Wise, C. D., *Science*, 1971, **171**, 1032.
31 Navon, A. J., *Insect Physiol.*, 1978, **29**, 39.
32 Bard, A. J., and Faulkner, L. R., *Electrochemical Methods*, Wiley, New York, 1980, p. 213.
33 Freund, M. S., Budalbhai, L., and Brajter-Toth, A., *Talanta*, 1991, **38**, 95.
34 Witkowski, A., Freund, M. S., and Brajter-Toth, A., *Anal. Chem.*, 1991, **63**, 622.
35 Sternson, A. W., McCreery, R., Feinberg, B., and Adams, R. N., *J. Electroanal. Chem.*, 1973, **46**, 313.
36 Hawley, M. D., Tatawawadi, S. V., Piekarski, S., and Adams, R. N., *J. Am. Soc. Chem. Soc.*, 1967, **89**, 447.
37 Whiteley, L. D., and Martin, C. R., *Anal. Chem.*, 1987, **59**, 1746.
38 Guadalupe, A. R., and Abruña, H. D., *Anal. Chem.*, 1985, **57**, 142.

Paper 3/03540I
Received June 21, 1993
Accepted August 3, 1993

Determination of Uranium by Liquid Scintillation and Cerenkov Counting

R. Blackburn and M. S. Al-Masri*

Department of Chemistry and Applied Chemistry, University of Salford, Salford, UK M5 4WT

Three radiometric methods for the determination of uranium in aqueous samples, involving the use of a liquid scintillation counter, have been studied and compared. Uranium is separated and purified by coprecipitation with iron(III) hydroxide followed by an anion-exchange process. The purified uranium in the eluate (0.1 mol l^{-1} HCl) can either be collected and stored and the Cerenkov radiation from the in-growth of the high-energy β-emitter ^{234}Pa counted, or the uranium can be extracted from the chloride eluate into diethylhexylphosphoric acid in toluene containing appropriate scintillation materials and counted by a liquid scintillation technique. Alternatively, uranyl chloride can be converted into uranyl nitrate, which is then dissolved in 1 ml of 1,4-dioxan, and the solution is subsequently mixed with scintillation solution and counted. In the liquid scintillation methods, both ^{234}U and ^{238}U can be determined, but, by using the Cerenkov method, ^{238}U is measurable in isolation. Several variants of the chemical-separation procedure have been studied in relation to their effect on quenching, sensitivity and accuracy. The background count rates observed were 0.04, 0.075 and 0.213 counts s^{-1} for the 1,4-dioxan, extraction and Cerenkov techniques, respectively; the lower limit of detection was taken as 3σ of the background. Chemical yields were in the range 80–90%.

Keywords: Extractive scintillator; 1,4-dioxan; Cerenkov counting; ^{234}U; ^{238}U; ^{234}Pa

Introduction

Determination of uranium is important in any programme of uranium mining and ore processing and is also important in environmental safety monitoring and geochemical studies. Several radiometric methods for the determination of uranium have been used. α-Spectroscopy is considered to be a very precise, versatile and sensitive method for α-emitters such as uranium, but preparation of the counting samples is laborious and time consuming, and correction factors are needed for self-absorption and geometry. Liquid scintillation methods have been widely used for α-emitters,[1,2] and uranium has been determined in several types of samples, *e.g.*, fertilizers,[3,4] phosphate rocks,[5,6] geological samples,[7] water samples[8,9] and environmental samples associated with uranium mining and milling.[10] In most of these methods, uranium is introduced into the counting vial by extracting it with solvents such as TBP (tributyl phosphate), TOPO (trioctylphosphine oxide) and dehpa (diethylhexylphosphoric acid], which are miscible with scintillation solution. Emulsifying agents have been used for both aqueous[8] and organic samples[11] immiscible with scintillation solution. The advantages of liquid scintillation methods [especially with pulse-shape analysis (PSA)] are low background (and, therefore, a lower limit of detection) and near 100% efficiency. To offset these advantages, the methods for uranium suffer from poor resolution of α-peaks and from colour-quenching problems as uranium forms yellow complexes with the scintillation solution.

In this work, we have examined and compared three methods where uranium is separated from the water sample by coprecipitation and an anion-exchange separation process. Two of these methods involve liquid scintillation. The first is based on extraction of uranium from the ion-exchange eluate, with use of dehpa in toluene containing the scintillation materials. In the second, uranium in the chloride eluate is converted into uranyl nitrate, which is dissolved in 1 ml of 1,4-dioxan, and the resulting solution is mixed with scintillation solution and counted. The third (non-scintillation) method is based on measurement of the Cerenkov radiation generated from the high-energy β-emitting nuclide ^{234}Pa, which is a daughter of ^{234}Th, itself a daughter of ^{238}U.

Experimental

Materials and Equipment

1,4-Dioxan, iron(III) chloride carrier solution and other chemicals were of analytical-reagent grade, and de-ionized water was used throughout. The extractive scintillator was prepared by dissolving 0.4 g of POPOP [1,4-bis-(5-phenyloxazol-2-yl)benzene], 4 g of PPO (2,5-diphenyloxazole), 0.5 g of bis-MSB [1,4-bis-(2-methylstyryl)benzene], 32 g of naphthalene and 70 g of dehpa in scintillation-grade toluene (1 l total volume). The scintillation solution for counting 1,4-dioxan solutions, used to dissolve uranyl nitrate, was prepared in exactly the same way except that the naphthalene content was increased to 200 g. Three standard uranyl nitrate solutions were prepared from uranium of natural isotopic composition. Two of these (1000 and 50 μg ml^{-1}) were in diluted nitric acid (1%) solution and the third was in 1,4-dioxan (282.26 μg ml^{-1}).

Counting was carried out by means of a Packard (Downers Grove, IL, USA) Tri-Carb 1900 CA liquid scintillation analyser with PSA.

Radiochemical-separation Procedure

The radiochemical-separation procedure described here is well established[9,12] and consists of two parts, *viz.*, coprecipitation of uranium (together with any thorium, plutonium and protactinium present) on ferric hydroxide, and separation of uranium from these and other elements by ion exchange.

Coprecipitation

The aqueous sample (0.5–1 l for environmental water samples) is acidified with 5 ml of HCl, and 1 ml of iron(III) chloride solution containing 20 mg of Fe^{3+} is added. The sample is thoroughly mixed and boiled gently. At this stage,

* Present address: Atomic Energy Commission of Syria, Damascus, P.O. Box 6091, Syria.

ammonia solution (6 mol l^{-1}) is added dropwise until iron(III) hydroxide is precipitated.

The mixture is boiled for a further 10 min and set aside for 30 min to cool.

The product is filtered, and the precipitate and filter-paper are transferred into a beaker containing 25 ml of 8 mol l^{-1} HCl. The filter-paper is removed and washed with 5 ml of 8 mol l^{-1} HCl. The solution is then ready for ion-exchange separation.

Ion-exchange separation

The column material, borosilicate, is prepared by slurrying the anion-exchange resin (Dowex 1X-4, Cl^- form, 100–200 mesh) with 8 mol l^{-1} HCl and pouring the slurry into a column of 13 mm bore to form a resin bed of length 100 mm.

The sample is loaded on to the column at a flow rate of 5 ml min^{-1}. After loading, the column is washed with 40 ml of 8 mol l^{-1} HCl to remove thorium. Protactinium is eluted with 50 ml of 4–5 mol l^{-1} HCl, and iron (and plutonium, if present) is eluted with 50 ml of a freshly prepared mixture consisting of 1 ml of 47% HI per 9 ml of 8 mol l^{-1} HCl.

The column is then washed with 50 ml of 8 mol l^{-1} HCl, and uranium is eluted with 45 ml of 0.1 mol l^{-1} HCl. This eluate is used for all three methods investigated.

Regeneration of the column is carried out by passage of 30 ml of 1% $NaHSO_3$ solution in 6 mol l^{-1} HCl, followed successively by 50 ml of 6 mol l^{-1} HCl, 25 ml of water and 50 ml of 8 mol l^{-1} HCl.

Preparation of Sample for Counting

Extraction method

Uranium is extracted from the eluate (0.1 mol l^{-1} HCl) by shaking for 5 min with 10 ml of the extractive scintillator in a 50 ml separatory funnel. After a single extraction (virtually 100%), the organic layer is transferred into a 22 ml counting vial and counted. Since the fluorescence conversion efficiency for α-particles is lower than that for β-particles, in the approximate ratio 1 : 10,[13] the peak associated with a 4.0 MeV α-particle appears at approximately 400 keV. In the Tri-Carb 1900 CA liquid scintillation counter, ^{234}U and ^{238}U are counted in the region 190–400 keV.

1,4-Dioxan system

The eluate is evaporated to dryness, and the residue is dissolved in 3 ml of 4 mol l^{-1} nitric acid. The nitrate solution is gently evaporated to dryness by means of an infrared lamp, and the uranyl nitrate is dissolved in 1 ml of 1,4-dioxan. This solution is mixed with 9 ml of toluene-based scintillator solution and counted; ^{234}U and ^{238}U are counted in the region 230–450 keV.

Cerenkov method

After completing the elution of uranium from the column, the time is recorded, since this is the beginning of the build-up of the daughters ^{234}Pa and ^{234}Th. The eluate is evaporated to 15 ml and transferred into a 22 ml plastic counting vial. After allowing a suitable period for ^{234}Pa build-up (depending on the initial concentration of uranium) the Cerenkov signal is counted with use of the ^3H channel of the liquid scintillation counter.

Results and Discussion

Extraction Scintillation Method

The extraction of uranium(VI) from hydrochloric acid solution has been studied[14] and was re-investigated here with a view to its application to the determination of uranium by liquid scintillation counting. The variation of uranium count rate (^{234}U and ^{238}U) with hydrochloric acid concentration is shown in Fig. 1. The extractant becomes more strongly coloured (yellow) at molarities greater than 0.8 mol l^{-1} and the count rate is decreased. Liquid scintillation counting as a means for the determination of uranium and ascertaining its distribution between the phases can, therefore, produce incorrect results since uranium could be extracted at high concentration, but, because of the colour and chemical quenching effects, the organic extract would be less efficiently counted. It is also possible that there are two different compounds formed, as suggested in an earlier study.[14] Because any variation in the acidity of the aqueous sample leads to a change in the extent of extraction, the acidity must be identical for both the sample and standards. Variations in dehpa concentration seem to have little quenching effect on the system, and this is in agreement with results obtained earlier[15] where dehpa was considered to be the least effective quencher (after TBP) among the various solvents used for α-counting. In addition, the effect of naphthalene concentration on the counting system indicates that there is no necessity to use this compound in the extractive scintillator.

1,4-Dioxan Scintillation Method

Uranyl chloride is converted into uranyl nitrate since the latter is more soluble in 1,4-dioxan and more stable. Its preparation must be performed by gentle evaporation under a lamp or in a hot water-bath as uranyl nitrate can decompose if dried on a hot-plate. The amount of 1,4-dioxan required is determined by the solubility of uranyl nitrate in this solvent (0.291 g g^{-1} of 1,4-dioxan).[16] The spectrum for ^{234}U and ^{238}U, counted in a scintillator solution containing 0.2 ml of 1,4-dioxan, is shown in Fig. 2, and the effect of 1,4-dioxan concentration on the ^{234}U and ^{238}U α-peak positions is shown in Fig. 3; higher concentrations of the solvent, shift the peak maxima to lower energy. This shift can be reversed by increasing the naphthalene concentration in the scintillation solution. Naphthalene used with 1,4-dioxan acts as an intermediate secondary solvent[17] and also restores some of the scintillator

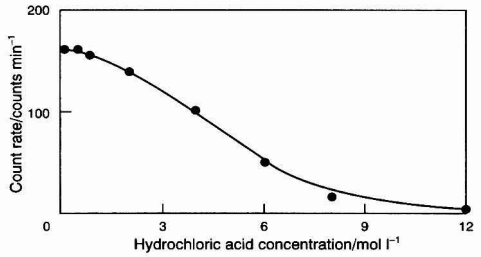

Fig. 1 Effect of HCl concentration on uranium extraction

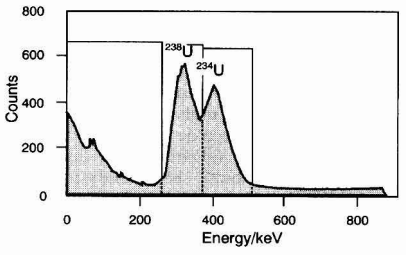

Fig. 2 ^{234}U, ^{238}U and their daughters spectrum

efficiency; the addition of 200 g of naphthalene to 1 l of toluene increases the count rate by 6.23%.

Cerenkov Method

Assuming a complete separation by the ion-exchange system, ^{234}U, ^{238}U and ^{235}U are the only isotopes present in the eluate and all are α-emitters. These do not produce a Cerenkov signal and nor do the immediate short-lived daughters of ^{234}U and ^{235}U. The only isotope that grows in after separation and produces Cerenkov radiation is ^{234}Pa, the daughter of ^{238}U *via* ^{234}Th, which has a maximum β-energy of 2.29 MeV with a branching ratio of 98%. Secular equilibrium between ^{234}Pa and ^{238}U takes about 4 months to establish, and attainment of complete equilibrium is time consuming. However, the sample can be counted at any convenient known time after separation, and a correction can be made; the time delay can be short or long, according to the uranium concentration to be measured.

Several factors affecting Cerenkov counting efficiency have been studied. Sample volume has little effect on the counting efficiency because the β-energy of ^{234}Pa is very high. Variation in acid concentration from 0.1 to 8 mol l^{-1} HCl leads to an increase of 21.57% in the Cerenkov count rate, owing to the increase in the refractive index of the counting medium.

Comparison of Methods

PSA was used in both the liquid scintillation methods to discriminate between the general β-and γ-radiation background and the β-activities of daughters, which build up after separation. A spectrum for ^{234}U, ^{238}U and their daughters in 1,4-dioxan is shown in Fig. 2. Another α-peak (for ^{235}U) is located between those for ^{234}U and ^{238}U, but it is not apparent partly due to the poor resolution (FWHM, Full Width at Half Maximum, of 21%) of both the extraction and 1,4-dioxan methods, and the very low activity of ^{235}U present in the sample. The use of PSA decreases the background signal in the counting region, thereby enhancing the sensitivity. Background count rates were 0.04, 0.075 and 0.213 counts s^{-1} for the 1,4-dioxan, extraction and Cerenkov methods, respectively. The lower limit of detection can be taken as 3σ of the background count rate. Other reported liquid scintillation methods yield background count rates that are higher[9] and lower[3,6] than those found in this study. PSA is not essential for the Cerenkov method where the counts are collected in the ^{3}H counting channel and, therefore, any counter, modern or otherwise, can be used.

Studies[1,2,8] have shown that there is 100% detection efficiency for the α liquid scintillation process, a value confirmed in this work. The Cerenkov detection efficiency determined here, by using standard uranium solutions, was found to be 62.35%, which is a high value compared with those of other α-measurement methods.

The radiochemical-separation procedure described here is widely used before determination of uranium by α-spectrometry, where good separation of other ions is necessary, as they affect the preparation of the thin α-source. Such a restriction does not apply when liquid scintillation counting is to be used, but the presence of even trace amounts of Fe^{3+} in the eluate does cause severe colour quenching and would normally necessitate the complete removal of this species from the column before elution of uranium. However, an alternative procedure is to elute the uranium and Fe^{3+} together and reduce the Fe^{3+} to Fe^{2+}, which is not extracted into the scintillation solution. This procedure allows one to use ^{59}Fe, a γ-emitting radionuclide, as a tracer for uranium; the iron is recovered and counted in the reduced aqueous form after uranium extraction.

In the 1,4-dioxan method the presence of both Fe^{2+} and Fe^{3+} causes severe quenching and, therefore, the uranium eluate must be separated from any trace of iron by the normal method. The presence of iron is not a problem in Cerenkov counting as this is not subject to chemical quenching, and any colour quenching by Fe^{3+} can be avoided by addition of 0.1 g of ascorbic acid. The effect on the Cerenkov count rate of adding ascorbic acid to samples containing Fe^{3+} is shown in Fig. 4. Clearly, ^{238}U can be eluted with Fe^{3+} and, provided that the latter is reduced to Fe^{2+}, there is no need to separate uranium and iron. Iron-59 can, in principle, be used as a tracer for uranium separation, as with the extraction–liquid scintillation method, but as it generates its own Cerenkov signal, corrections are necessary and its use is not recommended.

The conventional separation step for protactinium is not necessary for the Cerenkov method since the β-emitting ^{234m}Pa is short lived (1.17 min) and decays very quickly. The other naturally occurring protactinium isotope ^{231}Pa is an α-emitter and does not produce Cerenkov radiation. In principle, ^{231}Pa can cause some interferences with the liquid scintillation methods, but it is present in natural samples only at very low levels.

A disadvantage of the liquid scintillation–extraction technique is that only a limited amount of uranium can be introduced into the counting vial because of the coloration of the scintillator by a yellow uranium complex that causes serious colour quenching. The effect of uranium concentration on all three counting systems is shown in Fig. 5, and it is clear that the maximum amount of uranium for the extraction method is about 300 μg if a linear relationship between count rate and uranium concentration is desired. For the 1,4-dioxan and Cerenkov methods, the relationship between count rate and uranium concentration is linear at all concentrations investigated. The extraction method can be used for samples (environmental samples) of low uranium content without any quenching problems related to uranium complexes, whereas the 1,4-dioxan and Cerenkov methods can be used for both low- and high-content uranium samples (*e.g.*, nuclear waste). The only problem with the Cerenkov method for low-activity

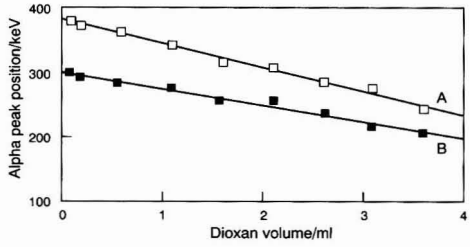

Fig. 3 Variation of alpha peak position with dioxan volume. A, ^{234}U; B, ^{238}U

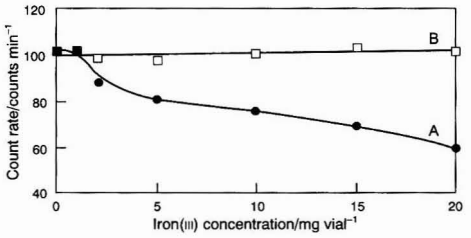

Fig. 4 Variation of Cerenkov count rate with A, Fe^{3+} and B, Fe^{2+} concentration

samples is the need for long storage times to allow build-up of sufficient activity of ^{234}Pa.

Interference encountered with liquid scintillation methods from the build-up of daughters was examined. The count rate of a newly prepared uranium sample in the region of interest (^{234}U and ^{238}U) increases by 1.6%, 17 h after elution. This is not a problem if the sample is counted immediately after elution. There is no interference encountered with the Cerenkov method.

The over-all chemical recovery for uranium was found to be between 80 and 90% in all the methods, which is comparable with that of other currently used methods; even higher recoveries were observed for the Cerenkov-based method.

Conclusion

The determination of uranium by two liquid scintillation methods and one Cerenkov-based method have been studied and compared. The choice of method depends on several factors, *viz.*, the aim of the analysis, the sensitivity and accuracy required, the uranium concentration in the sample, and the time available for analysis. By using both the Cerenkov technique and the extraction scintillation method, a smaller number of separation steps is required; moreover, in both procedures, uranium can be determined without separation from iron, an essential requirement in other published methods.[5,9,12] However, for the Cerenkov method a time-consuming storage step is required to allow ^{234}Pa to grow. Cerenkov and 1,4-dioxan liquid scintillation methods are applicable to samples of higher uranium content, such as phosphate rocks, fertilizers, nuclear fuels, and environmental samples relating to uranium mining and milling, but the extraction method is easier and more applicable to samples (*e.g.*, natural waters) of low uranium concentration.

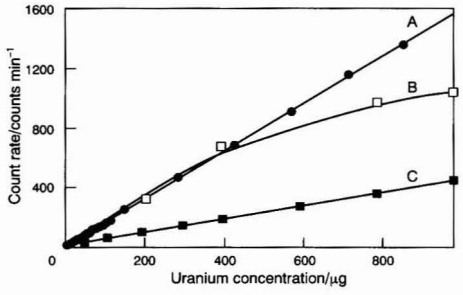

Fig. 5 Variation of count rate with uranium concentration. A, Dioxan method; B, extraction method; and C, Cerenkov method

We are grateful to the Syrian Atomic Energy Commission for financial support to M. S. A.-M.

References

1 McDowell, W. J., in *Liquid Scintillation Counting; Recent Applications and Development*, eds. Pens, C. T., Horrocks, D. L., and Alpen, E. L., Academic Press, New York, 1980, p. 315.
2 Yang, D., Yongiun, Z., and Mobins, S., *J. Radioanal. Nucl. Chem.*, 1991, **147**, 177.
3 McDowell, W. J., Farrar, D. T., and Billings, M. R., *Talanta*, 1974, **21**, 1231.
4 Bouwer, J. E., McKlveen, J. W., and McDowell, W. J., *Health Phys.*, 1978, **34**, 345.
5 McDowell, W. J., and Weiss, J. F., *Health Phys.*, 1977, **32**, 73.
6 Bouwer, E. J., McKlveen, J. W., and McDowell, W. J., *Nucl. Technol.*, 1979, **42**, 102.
7 Abuzeida, M., Arebi, B. H., and Zolatarev, Y. A., *J. Radioanal. Nucl. Chem.*, 1987, **116**, 285.
8 Horrocks, D. L., *Nucl. Instrum. Methods*, 1974, **117**, 589.
9 Pluta, I., Tomza, I., and Pluta, T., *Nucl. Geophys.*, 1990, **4**, 489.
10 Cooper, M. B., and Wilks, M. J., Liquid scintillation counting of alpha-emitting nuclides of the Uranium Series, in: *Annual Review of Research Projects*, ed. Keam, D. W., ART/TR-060, Australian Radiation Laboratory, Yallamie, Vic., 1983, pp. 118–121.
11 Sezginer, N., *Turkish J. Nucl. Sci.*, 1984, **11**, 62.
12 Krieger, L. H., and Whittaker, L. E., *Prescribed Procedures for Measurement of Radioactivity in Drinking Water, EPA-600/4-80-032*, US Environmental Protection Agency, Cincinnati, OH, 1980, pp. 96–102.
13 Selinger, H. H., *Int. J. Appl. Radiat. Isot.*, 1960, **8**, 29.
14 Bhanushali, R. D., Negi, S., and Ramakrishna, V. V., The extraction of U(VI) from hydrochloric acid by D2EHPA and mixtures of D2EHPA and HTTA in *Radiochemistry and Radiation Chemistry Symposium*, Dept. of Atomic Energy, Bombay 22–26 Feb., 1988, 3 pp.
15 McDowell, W. J., and Coleman, C. F., *Anal. Lett.*, 1973, **6**, 795.
16 Palei, P. N., *Analytical Chemistry of The Elements, Uranium*, ed. Vinogradov A. P., Ann Arbor–Humphrey Science Publishers, MI, London, 1970, p. 10.
17 Dyer, A., *Liquid Scintillation Counting Practice*, Heyden, London, 1980, p. 23.

Paper 3/05153F
Received August 26, 1993
Accepted October 12, 1993

Solubility of Barium(II) Taurodeoxycholate

Emilio Bottari

Dipartimento di Chimica, Università 'La Sapienza', P.le A. Moro 5, 00185 Rome, Italy

Maria Rosa Festa

Dipartimento di Scienze Animali, Vegetali e dell'Ambiente, Via Cavour 50, 86100 Campobasso, Italy

The solubility of barium(II) taurodeoxycholate was studied as a function of taurodeoxycholate ion concentration at 25 °C and in 0.100, 0.200, 0.300, 0.400, 0.500, 0.600 and 0.750 mol l^{-1} $N(CH_3)_4Cl$ as a constant ionic medium. For this purpose the total concentration of barium(II) was determined by means of atomic absorption spectrometric and polarographic measurements in solutions equilibrated with solid barium(II) taurodeoxycholate and at known hydrogen ion concentration. An attempt was also made to determine the free concentration of barium(II) ions by measuring the electromotive force (e.m.f.) of galvanic cells involving a barium(II) membrane electrode. The free concentration of hydrogen ion was measured by use of a glass electrode. The results of solubility and e.m.f. measurements could be explained by assuming the presence of associated species between barium(II) and taurodeoxycholate with different ratios depending on the concentration of the ionic medium. The solubility product and the association constants were determined for all the ionic medium concentrations. On the basis of the results, a relationship between solubility and free concentration of taurodeoxycholate ions can be deduced.

Keywords: Bile salts; micelles; solubility product; barium(II) taurodeoxycholate; taurodeoxycholate ion measurement

Introduction

Among the cholanic acids found in human and animal bile, sodium deoxycholate and its salts conjugated with glycine and taurine represent a very important class of bile salts because of their biological behaviour. They are able to solubilize cholesterol and lecithin[1–4] and these properties can probably be attributed to their capacity to form micellar aggregates.[5] The most important physico-chemical properties of such compounds have been illustrated by Small[5] and Carey.[6]

To explain the structure, size and shape of aggregates relative to sodium deoxycholate (NaDC), sodium glycodeoxycholate (NaGDC) and sodium taurodeoxycholate (NaTDC), important studies have been performed. From data obtained by applying different experimental approaches (such as nuclear magnetic resonance, NMR, calorimetric measurements, circular dichroism, X-ray analysis, SAXS and extended X-ray absorbtion fine structure spectroscopy, EXAFS), a helical structure was assumed.[7–14] In addition to the knowledge of the structure, size and shape of the aggregates, their behaviour in aqueous solutions and the influence of ionic medium, pH and concentration play an important role.

By taking into account the complexity of the aggregates formed in solutions, it seems of crucial importance to investigate these systems over a wide range of concentrations of the reagents and to measure the maximum possible number of parameters at equilibrium.

A suitable method for measuring the free concentration of glycodeoxycholate was reported[15] and applied to the determination of the aggregation number of aqueous micellar solutions of NaGDC in order to establish the prevailing species.[16]

This method was based on the different solubility of lead(II) glycodeoxycholate in the absence and presence of sodium ions.

The aim of this work was to investigate the possibility of applying a similar method in order to study NaTDC solutions. For this purpose we sought a slightly soluble salt of taurodeoxycholic acid (TDC) so that by comparing its behaviour in aqueous solution in the absence and presence of sodium ions, fundamental information on the interactions between sodium and TDC could be obtained. This paper reports the dependence of the solubility of barium(II) taurodeoxycholate on the concentration of taurodeoxycholate ions.

As it is necessary to determine the solubility over a wide concentration range of the reagents, in order to minimize the variation of the activity coefficients in spite of the change in concentration of the reagents, the method using a constant ionic medium, proposed by Biedermann and Sillén,[17] was adopted. All the measurements were performed at 25 °C and in the ionic medium $N(CH_3)_4Cl$. Data were obtained at different concentrations of $N(CH_3)_4Cl$ so that the behaviour of barium(II) taurodeoxycholate found for each concentration of ionic medium in the absence of sodium ions could be compared with that obtained in the presence of sodium ions.

Experimental

Apparatus

Solubility measurements were performed in a thermostated room at 25.0 ± 0.2 °C and e.m.f. measurements were performed using a thermostat set at 25.00 ± 0.05 °C.

For the determination of solubility, a Pye Unicam PU 9200X flame atomic absorption spectrometer and a Metrohm Model 646 VA processor connected with a Metrohm Model 647 stand for polarographic measurements were used.

E.m.f. measurements were performed as described previously.[15] A Philips IS561-Ba/SP barium electrode was used.

Other details concerning e.m.f. and polarographic measurements were similar to those described previously.[15,16]

Reagents

Hydrochloric acid, tetramethylammonium chloride and tetramethylammonium hydroxide were prepared and analysed as described previously.[18]

A stock standard solution of barium(II) chloride was prepared by dissolving, in doubly distilled water, the compound from Carlo Erba that had been recrystallized twice from water. To the stock standard solution was added a small amount of HCl (approximately 1×10^{-4} mol l^{-1}). The total content of barium(II) was determined gravimetrically as

sulfate, while H, the analytical excess of hydrogen ions with respect to the ionic medium, was determined according to Gran.[19]

Solid barium(II) taurodeoxycholate was prepared by adding a large excess of $BaCl_2$ to a stirred and warm (about 50 °C) solution of sodium taurodeoxycholate (Sigma), recrystallized from acetone–water. The precipitate obtained was kept in contact with the supernatant solution for at least 1 week and subsequently filtered through a Gooch crucible (G5) and then washed until barium(II) was absent and then dried at 120 °C. In order to determine the stoichiometric composition of the solid, a sample was analysed for total barium(II) content according to Anderegg *et al.*[20] Another sample was checked by thermal analysis and it started to decompose at about 350 °C.

The results of both analyses showed that the ratio between barium(II) and taurodeoxycholate in the solid is 1:2 and the compound contains (9/2)H_2O per mole of barium(II) taurodeoxycholate. As the results of several analyses agreed to within ±0.2%, this formula was assumed for the solid. It was stored in a silica-gel desiccator and its composition, periodically checked, remained constant for several months.

Tetramethylammonium taurodeoxycholate [$N(CH_3)_4TDC$] was prepared by mixing a slight excess of taurodeoxycholic acid (donated Prodotti Chimici e Alimentari SpA Basoluzzo) with a stirred tetramethylammonium hydroxide (RP, Carlo Erba) solution. The mixture obtained was filtered and by adding a large excess of acetone (RP, Carlo Erba) solid tetramethylammonium taurodeoxycholate was obtained. The solid was filtered through a Gooch crucible (G5) and dried at 70 °C.

A standard solution of $N(CH_3)_4TDC$ was prepared by dissolving a known amount of the prepared solid in a measured volume of water. The concentration was checked by evaporating a weighed amount of solution at 120 °C until constant mass was obtained. The value of H was determined according to Gran.[19]

Method

To determine the solubility of barium(II) taurodeoxycholate (S) and to find the relationship between the solubility and the free concentration of TDC ions, it was necessary to know the behaviour of barium(II) taurodeoxycholate in the selected ionic media. The constant ionic medium method, proposed by Biedermann and Sillén,[17] was adopted so that a wide concentration range could be investigated. The general composition of solutions T′ was the following: H mol l^{-1} in H^+, B mol l^{-1} in Ba^{II}, A mol l^{-1} in TDC^-, $(X - 2B - H)$ mol l^{-1} in $N(CH_3)_4^+$, $(X - A)$ mol l^{-1} in Cl^-, where TDC^-, B and A indicate the total concentration of barium(II) and taurodeoxycholate, respectively, and X represents the concentration of the ionic medium (0.100, 0.200, 0.300, 0.400, 0.500, 0.600 and 0.750 mol l^{-1}). To each solution T′ was added an excess of solid barium(II) taurodeoxycholate, $Ba(TDC)_2 \cdot (9/2)H_2O$, and the mixture was shaken until equilibrium was reached at 25 °C.

Periodic checks had shown that a time of 40 h was sufficient to reach equilibrium. In a constant ionic medium the activity coefficients can be assumed to be constant in spite of the variation of the concentrations of the reagents and, consequently, activities can be replaced by concentrations in all calculations.

Equilibrated solutions were analysed for the free concentration of barium(II), b, and hydrogen ions, h, by measuring the e.m.f. of the following galvanic cells:

$$(-)\ \text{RE}|\text{solution T}|\text{Ba E}\ (+) \qquad \text{(I)}$$

$$(-)\ \text{RE}|\text{solution T}|\text{GE}\ (+) \qquad \text{(II)}$$

where RE, Ba E and GE are reference, barium(II) and glass electrodes, respectively, and solution T is the same solution T′ saturated with solid barium(II) taurodeoxycholate.

After the determination of b and h, each solution T was centrifuged at 4000 rev min^{-1} and filtered and, after suitable dilution, the total concentration of barium(II) ions, B, was determined by means of atomic absorption spectrometry and differential-pulse polarography (DP50). The total concentration of barium(II) in solution T corresponded to the solubility, S.

From the material balance of barium(II), by taking into account the mass action law, we can write

$$S = B = b + \sum_{q}\sum_{p'}\sum_{r'} q\,\beta_{q,p',r'}\,b^q\,h^{p'}\,a^{r'} \qquad (1)$$

where $q \geqslant 1$, p' has any value and $r' \geqslant 1$, h is the free concentration of H^+ and a is the free concentration of taurodeoxycholate ions.

As all the measurements were carried out in solutions where the solid was present, it was difficult to obtain information on the nuclearity of the species containing barium(II) and we were not able to determine q and the values of $\beta_{q,p',r'}$. On this basis, it was possible to obtain only the ratio between barium(II) and taurodeoxycholate in solutions so that eqn. (1) can be rearranged as follows:

$$S = b + \sum_{p}\sum_{r} \gamma_{p,r}\,b\,h^p\,a^r \qquad (2)$$

where $\sum_{r}\sum_{p} \gamma_{p,r} = \sum_{q}\sum_{p'}\sum_{r'} \beta_{q,p',r'}\,b^{q-1}$, is constant in solutions equilibrated with the solid. The material balance of taurodeoxycholate, by taking into account the mass action law, can be written as follows:

$$A = a + \sum_{p}\sum_{r} r\,\gamma_{p,r}\,ba^r\,h^p \qquad (3)$$

In eqn. (3), protonated species of taurodeoxycholate could be neglected on the basis of e.m.f. measurements of cell II carried out in the absence of barium(II) and as a function of H ($0 \leqslant H \leqslant 0.020$ mol l^{-1}) and A ($0.005 \leqslant A \leqslant 0.025$ mol l^{-1}).

By combining eqn. (2) and eqn. (3), the first approximated free concentration of TDC^- can be calculated:

$$a = A - (S - b) \qquad (4)$$

The parameters S, a and h constitute the basis of the successive elaboration in order to obtain K_S and the predominating values of p, r and $\gamma_{p,r}$.

From the e.m.f. measurements with cell I, it was difficult to obtain accurate b values. The barium electrode was extremely sensitive to the concentration of the ionic medium and to $-\log h$.

The e.m.f. of cell I (in millivolts) at 25 °C can be expressed as follows:

$$E_{Ba} = E^0_{Ba} + Y \log b \qquad (5)$$

where the liquid junction potential is neglected by taking into account the $-\log h$ range investigated and E^0_{Ba} is a constant determined in the absence of taurodeoxycholate in the first part of each series of measurements. The value of Y is strongly dependent on the concentration of the medium and on the value of $-\log h$ of the solution. However, it decreased on increasing the concentration of $N(CH_3)_4Cl$. The too small value of Y does not allow a good response to be obtained relative to b, so we assume that b values are not refined data.

Results

Several series of values of $\log S(\log a)$ were obtained for the different values of the concentration of the ionic medium. From eqn. (2) and from the knowledge of a (eqn. 4), we can write

$$\log (Sa^2) = \log K_S + \log (1 + \sum_{p}\sum_{r} \gamma_{p,r}\,h^p\,a^{r-2}) \qquad (6)$$

In Fig. 1 as an example the values of $-\log (Sa^2)$ are plotted *versus* $-\log a$ for 0.100 mol l^{-1} $N(CH_3)_4Cl$. As the points all

fall together independent of the h value, the solubility is independent of h and $p = 0$. As the maximum slope of the trend of the points in Fig. 1 is more than 2, it can be assumed that r is greater than 2. Eqn. (5) can be normalized[21] in the form

$$y = \log (1 + u^2 + \alpha u^3)$$

where $\log (Sa^2) - y = \log K_S$, $\log u = \log a + (1/2)\log \gamma_2$ and $\log \gamma_3 = \log \alpha + (3/2)\log \gamma_2$. By superimposing the experimental points on the family of normalized curves, the two plots are shifted parallel to the two axes until the best fit is obtained and then the values of $\log K_S$, $\log \gamma_2$ and $\log \gamma_3$ can be obtained. In Fig. 1 there is good agreement between the curve and the points.

A similar treatment is performed also for the experimental data obtained at ionic medium concentrations of 0.200 and 0.300 mol l^{-1}. In Table 1 the values of K_S, γ_2, and γ_3 obtained are given.

The points obtained at $N(CH_3)_4Cl$ concentrations of 0.400, 0.500, 0.600 and 0.750 mol l^{-1} cannot be explained by assuming the formation of species with ratios of 1:2 and 1:3 between barium(II) and TDC. In Figs. 2 and 3, the experimental data obtained at 0.500 and 0.600 mol l^{-1} are plotted as $-\log (Sa^2)$ *versus* $-\log a$ and in the maximum slope never exceeds 2, hence the maximum value assumed by r is 2 and as a consequence eqn. (5) can be written as

$$\log (Sa^2) = \log K_S + \log (1 + \gamma_2 a^2)$$

The points on Figs. 2 and 3 are superimposed on a normalized curve[21] of the equation $y = \log (1 + u^2)$, where $\log (Sa^2) - y = \log K_S$ and $u = a\sqrt{\gamma_2}$. At the position of the best fit the values of K_S and γ_2 are obtained. In Table 1 the values obtained for each selected ionic medium concentration are collected. In Figs. 2 and 3 the normalized curves at the position of best fit are drawn and point agreement is good.

As the first approximation value of the free concentration of taurodeoxycholate, a, was calculated by means of eqn. (4), where the b values are considered not to be refined data, the values of K_S, γ_2 and γ_3 obtained could be taken as first approximation values. However, refined values, obtained by an iterative treatment of the data, gave values of the constants almost identical with those in Table 1. Independently, the experimental S, A, h and b values were treated with a program written for a personal computer.[22] Values of K_S, γ_2 and γ_3 coincident with those in Table 1 were obtained. The value of the solubility product at zero ionic strength was $-\log K_f^\circ = 8.07 \pm 0.10$.

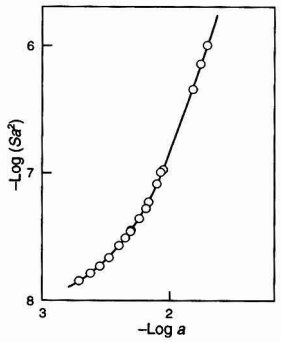

Fig. 1 Experimental points obtained at 0.100 mol l^{-1} $N(CH_3)_4Cl$. The normalized curve at the position of best fit is also shown

Table 1 Values of K_S, γ_2 and γ_3 for barium(II) taurodeoxycholate at 25 °C at different concentrations of the ionic medium $N(CH_3)_4Cl$

Ionic medium concentration/mol l^{-1}	$-\log K_S$	$\log \gamma_2$	$\log \gamma_3$
0.10	7.92	4.54	6.91
0.20	7.25	4.26	6.49
0.30	6.85	3.94	5.97
0.40	6.75	4.46	—
0.50	6.42	4.40	—
0.60	6.29	3.44	—
0.75	6.10	3.40	—

Discussion

Table 1 shows the behaviour of barium(II) taurodeoxycholate in aqueous solution in the presence of the solid $Ba(TDC)_2$. The values of K_S, γ_2 and γ_3 found at seven different concentrations of $N(CH_3)_4Cl$ as ionic medium and at 25 °C are given. It can be seen that the values of $-\log K_S$ decrease with increasing ionic medium concentration. This trend indicates that the solubility of $Ba(TDC)_2$ increases with increasing concentration of $N(CH_3)_4Cl$.

The presence of the ionic medium plays an important role in two different respects, first with regard to the variation of the activity coefficients of the reagents. The activity coefficients can be assumed to be constant for each concentration of the ionic medium, but they alter when the concentration of the ionic medium is changed. From Table 1, it is evident that the value of $-\log K_S$ changes more from 0.100 to 0.300 mol l^{-1} than from 0.300 to 0.750 mol l^{-1} $N(CH_3)_4Cl$.

Ellilä[23] found that the $\log k_a$ value of acetic acid changes depending on the ionic strength and the activity coefficient decreases up to about 0.3 mol l^{-1} NaCl more than it does from

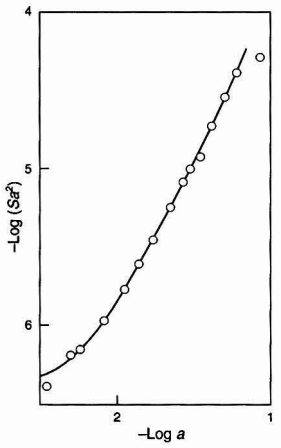

Fig. 2 Experimental points obtained at 0.500 mol l^{-1} $N(CH_3)_4Cl$. The normalized curve at the position of best fit is also shown

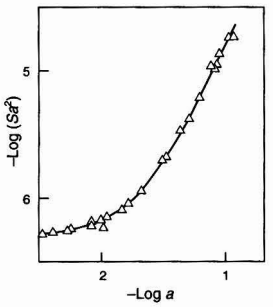

Fig. 3 Experimental points obtained at 0.600 mol l^{-1} $N(CH_3)_4Cl$. The normalized curve at the position of best fit is also shown

0.3 to 1 mol l^{-1}. Näsänen[24] found the same effect on the constant of the complex formation between aluminium(III) and catechol disulfate. The second effect is due to the probable association between taurodeoxycholate and tetramethylammonium ions coming from the ionic medium. This effect increases with increasing concentration of the ionic medium.

The changes in log γ_2 and log γ_3 also involve both variations in the activity coefficients and the association between $N(CH_3)_4^+$ and TDC^-. The value of log γ_2 is higher at 0.400 than at 0.300 mol l^{-1}, but at 0.300 mol l^{-1} $N(CH_3)_4Cl$ the species $Ba(TDC)_3$ is still present, whereas it disappears at 0.400 mol l^{-1} with an increase in the value of log γ_2. It seems reasonable to suggest that at higher concentrations of $N(CH_3)_4Cl$ the association between $N(CH_3)_4^+$ and taurodeoxycholate prevails with respect to the formation of $Ba(TDC)_3$.

Taking into account the main aim of this work, it is desirable to find a simple correspondence between solubility and free concentration of taurodeoxycholate ions. For glycodeoxycholate,[15] e.m.f. measurements with galvanic cells containing the electrode Pb, $Pb(GDC)_2$/GDC were conveniently used for this purpose.

For taurodeoxycholate, the response of the barium electrode under the selected experimental conditions and in solutions saturated with $Ba(TDC)_2$ is considered not to be reliable for obtaining a, the free concentration of TDC^-. From eqn. (1) and by taking into account the results in Table 1, we can write

$$S = b + \gamma_2 ba^2 + \gamma_3 ba^3 \quad (7)$$

for the data obtained at 0.100, 0.200 and 0.300 mol l^{-1} $N(CH_3)_4Cl$ and

$$S = b + \gamma_2 ba^2 \quad (8)$$

for the other concentrations.

Eqn. (7) and (8) can be written as follows:

$$\log S = \log K_S + \log \gamma_2 + \log (1 + \gamma_2^{-1} a^{-2} + \gamma_3 \gamma_2^{-1} a) \quad (9)$$

and

$$\log S = \log K_S + \log \gamma_2 + \log (1 + \gamma_2^{-1} a^{-2}) \quad (10)$$

respectively. Both eqns. (9) and (10) show that for the studied system at the selected ionic medium concentrations, log S is only a function of $-\log a$. Knowing the values of K_S, γ_2 and γ_3, theoretical curves for each concentration of the ionic medium can be calculated and drawn corresponding to the experimental points.

Figs. 4 and 5 give two examples of plots of log S *versus* $-\log a$ for 0.200 and 0.400 mol l^{-1} $N(CH_3)_4Cl$, respectively. The good agreement between the experimental points and calculated curves supports the validity of our results and provides the opportunity to obtain $-\log a$ from only a knowledge of $-\log S$ (determined experimentally) in solutions where $Ba(TDC)_2$ solid is present.

In this way it is possible to apply eqns. (9) and (10), expressing the relationship between the solubility of $Ba(TDC)_2$ and the free concentration of taurodeoxycholate, to the study of aqueous micellar solutions of sodium taurodeoxycholate at a constant concentration of $N(CH_3)_4Cl$ as the ionic medium.

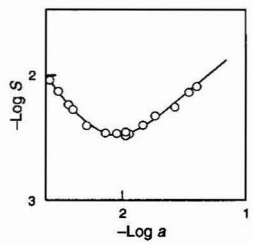

Fig. 4 Solubility of barium(II) taurodeoxycholate as a function of the free concentration of TDC^- at 0.200 mol l^{-1} $N(CH_3)_4Cl$. The curve was calculated using the K_S, γ_2 and γ_3 values in Table 1

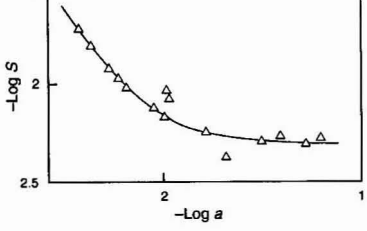

Fig. 5 Solubility of barium(II) taurodeoxycholate as a function of the free concentration of TDC^- at 0.400 mol l^{-1} $N(CH_3)_4Cl$. The curve was calculated using the K_S and γ_2 values in Table 1

This work was supported by the National Research Council of Italy (CNR), Progetto finalizzato Chimica Fine II, and by the Ministero dell'Università e della Ricerca Scientifica e Tecnologica (MURST), Italy.

References

1 Small, D. M., Burges, M., and Dervichian, D. G., *Nature (London)*, 1966, **211**, 816.
2 Admiral, W. H., and Small, D. M., *J. Clin. Invest.*, 1968, **47**, 1043.
3 Carey, M. C., and Small, D. M., *J. Clin. Invest.*, 1978, **61**, 998.
4 Masoro, E. J., *Physiological Chemistry of Lipids in Mammals*, Saunders, Philadelphia, 188–194.
5 Small, D. M., in *The Bile Acids*, eds. Nair, P. P., and Kritchevsky, D., Plenum Press, New York, 1971, ch. 8, pp. 249–356.
6 Carey, M. C., in *Sterols and Bile Acids*, eds. Danielsson, H., and Sjovall, J., Elsevier North-Holland Biomedical Press, Amsterdam, 1985, pp. 345–403.
7 Conte, G., Di Blasi, R., Giglio, E., Porretta, A., and Pavel, N. V., *J. Phys. Chem.*, 1984, **88**, 5720.
8 Campanelli, A. R., Ferro, D., Giglio, E., Imperatori, P., and Piacente, V., *Thermochim. Acta*, 1983, **67**, 223.
9 D'Alagni, M., Forcellese, M. L., and Giglio, E., *Colloid Polym. Sci.*, 1985, **263**, 160.
10 Esposito, G., Zanobi, A., Giglio, E., Pavel, N. V., and Campbell, I. D., *J. Phys. Chem.*, 1987, **91**, 83.
11 Giglio, E., Loreti, S., and Pavel, N. V., *J. Phys. Chem.*, 1988, **92**, 2858.
12 Campanelli, A. R., Candeloro De Sanctis, S., Giglio, E., and Scaramuzza, L., *J. Lipid Res.*, 1987, **28**, 483.
13 D'Alagni, M., Giglio, E., and Petriconi, S., *Colloid Polym. Sci.*, 1987, **265**, 517.
14 Chiessi, E., D'Alagni, M., Esposito, G., and Giglio, E., *J. Inclus. Phenom.*, 1991, **10**, 453.
15 Bottari, E., and Festa, M. R., *Ann. Chim. (Rome)*, 1990, **80**, 217.
16 Bottari, E., and Festa, M. R., unpublished work.
17 Biedermann, G., and Sillén, L. G., *Ark. Kemi*, 1953, **5**, 425.
18 Bottari, E., and Festa, M. R., *Ann. Chim. (Rome)*, 1980, **76**, 405.
19 Gran, G., *Analyst*, 1952, **77**, 661.
20 Anderegg, G., Flaschka, H., Sallmann, R., and Schwarzenbach, G., *Helv. Chim. Acta*, 1953, **37**, 113.
21 Sillen, L. G., *Acta Chem. Scand.*, 1956, **10**, 186.
22 Bottari, E., Curzio, G., Coccitto, T., Festa, M. R., and Jasionowska, R., *Ann. Chim. (Rome)*, 1988, **78**, 635.
23 Ellilä, A., *Ann. Acad. Sci. Fenn., Ser. A*, 1953, No. 51.
24 Näsänen, R., *Acta Chem. Scand.*, 1951, **5**, 1293.

Paper 3/01990J
Received April 6, 1993
Accepted June 15, 1993

Photometric Titration of Small Amounts of Cationic Surfactants in an Aqueous Medium

Shoji Motomizu and Yun-hua Gao

Department of Chemistry, Faculty of Science, Okayama University, Tsushimanaka, Okayama 700, Japan

Kouji Uemura and Shinsuke Ishihara

Kyoto Electronics, Shinden, Kisshoin, Minamiku, Kyoto-shi 601, Japan

A photometric titration method for cationic surfactants with tetrabromophenolphthalein ethyl ester (TBPE) as an indicator was developed. In the presence of a non-ionic surfactant (Triton X-100), TBPE was dissolved in an acidic aqueous medium, giving a yellow colour in the acidic form (TBPE·H). When a bulky cation (Q^+) was added, TBPE·H reacted with Q^+ to form an ion associate (Q^+·$TBPE^-$), and the colour changed from yellow to blue. This colour reaction was used for the detection of the end-point. Direct and indirect titration methods for the determination of cationic surfactants were examined. Dodecylbenzenesulfonate ion (DBS^-) was used as a titrant for cationic surfactants in the direct titration. The colour changed from blue to yellow at pH 3.6, and absorbance changes were monitored with a fibre-optic sensor with a 630 nm interference filter. Benzyldimethyltetradecylammonium (zephiramine) ion was found to be the preferred titrant in the indirect titration. The titrant was added to a solution of cationic surfactant containing a known excess amount of anionic surfactant DBS^- at pH 3.6. Cationic surfactants at concentrations from 5×10^{-6} to 1×10^{-3} mol dm^{-3} could be determined.

Keywords: Photometric titration; cationic surfactant; tetrabromophenolphthalein ethyl ester; dodecylbenzenesulfonate; zephiramine

Introduction

Various types of cationic surfactants are widely used as fabric softeners, hair rinses, corrosion inhibitors and antimicrobial agents. The determination of cationic surfactants at concentrations of several millimolar or more is often necessary in process and quality control and in waste water control. In such instances, two-phase titration methods have been widely used.[1–3]

El-Khateeb and Abdel-Moety[4] reported a method for determining low levels of cationic surfactants that do not require any extraction of ion associates. The method was based on the addition of cationic surfactants to a solution of an anionic dye, resulting in a change in intensity of the dye colour. However, the calibration graph was only linear over the range 0.5×10^{-3}–3×10^{-3} mol dm^{-3}.

In a previous paper,[5] we reported an automated method for the determination of anionic surfactants at micromolar concentrations in an aqueous medium using a photometric detector. This paper presents a photometric titration method for the determination of cationic surfactants by using an indicator system based on the chromogenic reaction of tetrabromophenolphthalein ethyl ester (TBPE) with a titrant (Q^+).

Experimental

Reagents

Tetrabromophenolphthalein ethyl ester solution. A 1×10^{-3} mol dm^{-3} TBPE solution was prepared by dissolving 70 mg of TBPE (potassium salt) (Wako) in 100 cm^3 of ethanol.

Titrant. Benzyldimethyltetradecylammonium chloride (zephiramine; $Zeph^+Cl^-$) (Dojindo Laboratories) was dried to constant mass under reduced pressure (about 400 Pa) before use and the dried salt was dissolved in distilled water to give a 1.25×10^{-3} mol dm^{-3} stock standard solution.

Cationic surfactants. Distearyldimethylammonium chloride ($DSDMA^+Cl^-$) (Tokyo Kasei Kogyo) was dried to constant mass under reduced pressure (about 400 Pa) before use and the dried salt was dissolved in ethanol to give a 1.25×10^{-2} mol dm^{-3} stock standard solution. Other quaternary ammonium salts (listed in Table 1) were dried under reduced pressure in a similar manner to zephiramine and the dried salts were dissolved in distilled water.

Anionic surfactants. Sodium dodecyl sulfate (LS, 99.9%) and sodium linear dodecylbenzenesulfonate (DBS, 99.0%) were purchased from Wako and sodium di-2-ethylhexylsulfosuccinate (SSS, 96.3%) from Kanto Chemical (Tokyo, Japan). These anionic surfactants were dried at 50 °C to constant mass under reduced pressure before use. They were dissolved in distilled water to give a 2×10^{-3} mol dm^{-3} stock standard solution, and were used after accurate dilution.

Non-ionic surfactant, Triton X-100 (TX-100). A 50 cm^3 volume of TX-100 (Rohm & Haas) was dissolved in hot distilled water. The solution was cooled and sufficient distilled water was added to bring the volume to 500 cm^3.

Buffer solutions. Sodium monochloroacetate–monochloroacetic acid buffer solution (1 mol dm^{-3}, pH 2.2–4.0) and sodium acetate–acetic acid buffer solutions (1 mol dm^{-3}, pH 4.0–4.6) were used to adjust the pH of reaction solutions to 2.2–4.6.

Apparatus

Absorbance changes were measured with a Kyoto Electronics AT-310J automatic titrator with an APB-310 auto piston burette and a fibre-optic sensor. pH values were measured with a Corning Ion Analyzer 250 with a combined electrode. Beakers of 50 cm^3 were used, and solutions in the beakers were stirred continuously with a magnetic stirrer bar during titration.

Standard Procedure

Direct titration

A 25 cm^3 volume of sample solution containing cationic surfactant at concentrations up to 2×10^{-4} mol dm^{-3} was placed in a 50 cm^3 beaker and 1 cm^3 each of 0.50% TX-100, 2.5

$\times 10^{-4}$ mol dm^{-3} TBPE and 1 mol dm^{-3} monochloroacetate buffer solution (1 mol dm^{-3}, pH 3.6) were added. The mixture was titrated with DBS^- (5.0×10^{-4} mol dm^{-3}) with the continuous recording of the absorbance until the colour changed from blue to yellow. The absorbance changes were monitored with a fibre-optic sensor with a 630 nm interference filter. End-points were read from the inflection points using differential curves.

Results and Discussion

Comparison of Direct Titration With Indirect Titration

The titration is based on the reaction of cationic surfactants with anionic, normally long-chain anionic surfactants to form associates. With the ionic charges neutralized, the ion associates formed have non-polar character, and are much more hydrophobic than each free ion. Therefore, the ion associates often precipitate in an aqueous medium. In the proposed titration system, because of the presence of non-ionic surfactants, the ion associates can form mixed micelles with TX-100 and are solubilized in the aqueous medium.

In the direct titration, the standard solution of an anionic surfactant, *e.g.*, DBS, was used as a titrant.

The reaction of sample ions with the titrant is

$$CS^+ + DBS^- \rightleftharpoons (CS^+ \cdot DBS^-)_m \quad (1)$$

and the chromogenic reaction at the end-point is

$$(CS^+ \cdot TBPE^-)_m + H^+ + DBS^- \rightleftharpoons (CS^+ \cdot DBS^-)_m + (TBPE \cdot H)_m \quad (1')$$

where subscript m denotes the species in a micelle phase and TBPE·H, $CS^+ \cdot TBPE^-$ and $CS^+ \cdot DBS^-$ are the protonated species of TBPE and the ion associates of CS^+ with $TBPE^-$ or DBS^-, respectively.

Indirect titration with $Zeph^+$ is based on the following reaction:

$$(CS^+ \cdot DBS^-)_m + \underset{\text{(excess)}}{DBS^-} + Zeph^+ \rightleftharpoons (CS^+ \cdot DBS^-)_m + (Zeph^+ \cdot DBS^-)_m \quad (2)$$

and the chromogenic reaction at end-points is

$$(TBPE \cdot H)_m + Zeph^+ \rightleftharpoons (Zeph^+ \cdot TBPE^-)_m + H^+ \quad (2')$$

Results obtained by using the direct and indirect titration methods are given in Table 1. The assay percentages were determined on the basis of the assumption that the purity of the vacuum-dried zephiramine is 100.00%. This assumption may be considered practically correct from the results previously examined in our laboratory by a colloid titration.[6,7] It was found that neither the direct nor the indirect titration method was suitable for cationic surfactants with an alkyl chain consisting of less than 12 carbon atoms. For cationic surfactants with very strong hydrophobicity, such as $DSDMA^+$, positive errors occurred in the direct titration. This is because the ion associate of the indicator with an analyte ion, $DSDMA^+ \cdot TBPE^-$, is very stable and the substitution reaction of $TBPE^-$ in the $DSDMA^+ \cdot TBPE^-$ ion associate with the titrant DBS^- is difficult. More reasonable results were obtained for cationic surfactants, except for $TDTMA^+$ and $DDTMA^+$, by the indirect titration. In subsequent experiments, the indirect titration method was examined in detail.

Table 1 Results obtained with the direct and indirect titration methods. TBPE, 5×10^{-6} mol dm^{-3}; TX-100, 0.02%; pH, 3.6

Cationic surfactant (quaternary ammonium ion, Q^+)	CS^+ abbreviation	Assay (%)	
		Direct*	Indirect†
Tetradecylbenzyldimethylammonium chloride	$Zeph^+$	100.00	100.00
Cetylbenzyldimethylammonium chloride	$CBDMA^+$	102.33	100.44
Distearyldimethylammonium chloride	$DSDMA^+$	113.20	103.55
Stearyltrimethylammonium chloride	$STMA^+$	101.53	100.44
Cetyltrimethylammonium chloride	$CTMA^+$	102.02	100.78
Tetradecyltrimethylammonium bromide	$TDTMA^+$	84.00	90.18
Dodecyltrimethylammonium chloride	$DDTMA^+$	12.67	36.63
Decyltrimethylammonium bromide	$DTMA^+$	—‡	4.19
Benzethonium chloride	Hyamine	100.53	96.93
Cetylpyridinium chloride	CPy^+	101.72	100.24
Dodecylpyridinium chloride	$DoPy^+$	—‡	55.67

* Titrant, 5×10^{-4} mol dm^{-3} DBS^-; sample, 25 cm^3 of 1×10^{-4} mol dm^{-3} analyte (CS^+).

† Titrant, 5×10^{-4} mol dm^{-3} $Zeph^+$; sample, a mixture of 10 cm^3 of 1×10^{-4} mol dm^{-3} analyte (CS^+) and 15 cm^3 of 2×10^{-4} mol dm^{-3} DBS^-.

‡ End-points were not found.

Effect of Amounts of TBPE Indicator and Non-ionic Surfactants

As described previously,[5] a 5×10^{-6} mol dm^{-3} solution of TBPE was used for the determination of anionic surfactants in the standard procedure of direct titration with the titrant $DSDMA^+$, and the concentration of TX-100 was found to be the most important parameter to obtain clear end-points in the automated photometric titration.

In this work, 5×10^{-6} mol dm^{-3} of TBPE was adopted, and an experiment with various TX-100 concentrations up to 0.10% in the solution was carried out. When less than 0.01% v/v TX-100 was present in the solution, the solution was turbid owing to the precipitation of both TBPE·H and the ion associate formed. With increasing amount of TX-100, the solution became clearer. The colour change at the end-points, however, became less sharp and the reproducibility of the end-points became worse with increasing amount of TX-100. In Fig. 1, some examples of titration curves are shown. From these results, 0.02% v/v TX-100 was adopted as a compromise in the standard procedure in this work.

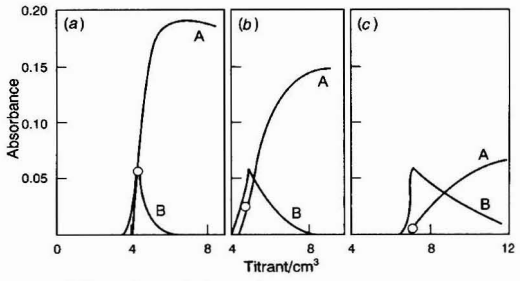

Fig. 1 Effect of non-ionic surfactant concentration on titration curves. A, Absorbance curve; B, differential curve; circle indicates end-point. TBPE, 5.0×10^{-6} mol dm^{-3}; titrant, 5×10^{-4} mol dm^{-3} $Zeph^+$; sample, 10 cm^3 of 1.0×10^{-4} mol dm^{-3} $STMA^+$ with 15 cm^3 of 2×10^{-4} mol dm^{-3} DBS^- (pH 3.6). TX-100: (*a*) 0.02, (*b*) 0.04, (*c*) 0.10%

Selection of Quaternary Ammonium Salts Used as Titrants for Indirect Titration

Some of the quaternary ammonium salts listed in Table 1 were examined as titrants in the indirect titration. A comparison of titrants is shown in Table 2. From these results, all five titrants can react with cationic surfactant analytes with stronger hydrophobicity or an alkyl group larger than $C_{14}H_{29}$. However, analytes with shorter alkyl chains such as $DDTMA^+$, $DTMA^+$ or $DoPy^+$ could be determined with such titrants. Fig. 2 shows the titration curves for $CBDMA^+$ as analyte obtained with $Zeph^+$, $DSDMA^+$ and $Hyamine^+$ as titrants. The absorbance increase was in the order $DSDMA^+ > Zeph^+ > Hyamine^+$. This result shows that the more hydrophobic the titrant, the clearer is the end-point. Therefore, the more hydrophobic titrant seems better. However, when the solutions of less hydrophobic or less reactive analytes were titrated with a hydrophobic titrant such as $DSDMA^+$ in the indirect titration, the following substitution reaction will occur before the end-points:

$$CS^+{\cdot}DBS^- + DSDMA^+ \rightleftharpoons DSDMA^+{\cdot}DBS^- + CS^+ \quad (3)$$

This substitution reaction results in a negative error. Therefore, $DSDMA^+$ is not desirable as a titrant when the reactivity of CS^+ is less than that of $DSDMA^+$. In the standard procedure of the indirect titration, $Zeph^+$ was adopted as a compromise with respect to its high purity and suitable reactivity. Good reproducibility of the titration was achieved with $Zeph^+$, as is shown in Table 2.

Effect of pH of Solution on the Chromogenic Reaction

The acid dissociation constant of TBPE·H is known to be about 4.2, and therefore it is difficult to exchange the titrant $Zeph^+$ for the H^+ of TBPE·H at pH <3.2. Fig. 3 shows examples of the titration curves of $Zeph^+$. When the pH of the sample solutions is <3.2, the colour change becomes less sharp and the end-point is too late, which results in a decrease in accuracy and precision. Conversely, at pH >4.2, where TBPE easily dissociates, the end-point comes too soon, and the precision and reproducibility are lower than those at pH near 3.5. From these results, titrations in the pH range 3.2–4.0 are recommended, and in this work pH 3.6 was adopted.

Selection of Anionic Surfactants as Reagent Reacting With Analytes

Anionic surfactants, such as DBS^-, SSS^- and LS^-, were examined as the reagent reacting with analytes. In the presence of 0.02% TX-100, precipitation occurred in the vicinity of the end-point in the titration with $Zeph^+$ when SSS^- and LS^- were used. This is probably because TX-100, DBS^- and $Zeph^+$ all possess benzene rings and the ion associates formed are easy to dissolve, whereas SSS^- and LS^- do not possess benzene rings. Fig. 4 shows the titration curves in the presence of 0.025% TX-100. It is obvious from such titration curves that a better result was obtained by using DBS, but not by using LS^-.

Determination Ranges for Cationic Surfactants

Tables 3 and 4 show the data for the calibration graphs of CPy^+, Hyamine, $STMA^+$ and $Zeph^+$ as analytes at

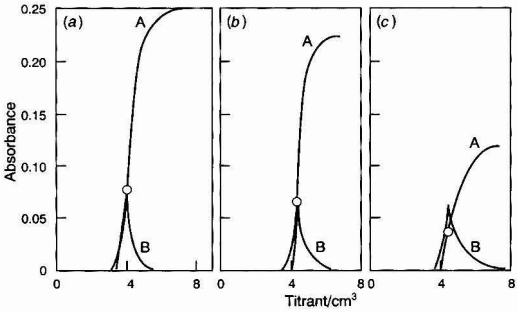

Fig. 2 Titration curves for the titration of $CBDMA^+$ (analyte) with $DSDMA^+$, $Zeph^+$ and Hyamine as titrant. A, Absorbance curve; B, differential curve; circle indicates end-point. Sample, 10 cm^3 of 1.0 × 10^{-4} mol dm^{-3} analyte $CBDMA^+$ with 15 cm^3 of 2 × 10^{-4} mol dm^{-3} DBS^- (pH 3.6). TX-100, 0.02%; TBPE, 5 × 10^{-6} mol dm^{-3}. Titrant: (*a*) $DSDMA^+$; (*b*) $Zeph^+$; (*c*) Hyamine

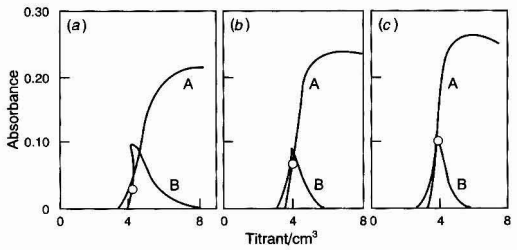

Fig. 3 Effect of pH on titration curves. A, Absorbance curve; B, differential curve; circle indicates end-point. TBPE, 5.0 × 10^{-6} mol dm^{-3}; titrant, 5 × 10^{-4} mol dm^{-3} $Zeph^+$; sample, 10 cm^3 of 1.0 × 10^{-4} mol dm^{-3} $Zeph^+$ with 15 cm^3 of 2 × 10^{-4} mol dm^{-3} DBS^-; TX-100, 0.02%. (*a*) pH 3.2; (*b*) pH 3.6; (*c*) pH 4.0

Table 2 Comparison of titrants in indirect titration method. TBPE, 5 × 10^{-6} mol dm^{-3}; TX-100, 0.02%; pH, 3.6; Titrant, 5 × 10^{-4} mol dm^{-3} Q^+; sample, mixture of 10 cm^3 of 1 × 10^{-4} mol dm^{-3} analyte (CS^+) and 15 cm^3 of 2 × 10^{-4} mol dm^{-3} DBS^-. Results are mean values of three replicate assays (%); the ± values are the largest deviations from the mean values

Analyte (CS^+)	Titrant (Q^+)				
	$DSDMA^+$	$Zeph^+$	$CTMA^+$	Hyamine	$TDTMA^+$
$Zeph^+$	100.00	100.00	100.00	100.00	100.00
$CBDMA^+$	99.02 ± 0.45	100.44 ± 0.06	99.68 ± 0.05	98.12 ± 0.55	97.86 ± 0.26
$DSDMA^+$	100.52 ± 0.53	103.55 ± 0.39	99.45 ± 1.07	104.29 ± 0.19	105.77 ± 0.05
$STMA^+$	96.65 ± 0.05	100.44 ± 0.05	97.06 ± 1.29	97.65 ± 0.55	103.77 ± 0.28
$CTMA^+$	95.61 ± 0.12	100.78 ± 0.20	102.02 ± 0.26	98.35 ± 0.30	104.28 ± 0.59
$TDTMA^+$	92.72 ± 0.24	90.18 ± 0.40	98.62 ± 0.34	94.44 ± 0.12	100.88 ± 0.31
$DDTMA^+$	19.76 ± 1.55	36.63 ± 2.2	36.08 ± 0.19	37.31 ± 0.97	47.74 ± 0.63
$DTMA^+$	2.68 ± 0.60	4.19 ± 0.61	7.32 ± 0.88	1.51 ± 0.52	8.56 ± 0.30
Hyamine	88.54 ± 0.43	96.93 ± 0.50	99.91 ± 0.97	98.96 ± 0.60	106.93 ± 0.02
CPy^+	103.39 ± 0.93	100.24 ± 0.16	103.40 ± 0.51	97.65 ± 1.10	104.23 ± 0.62
$DoPy^+$	35.55 ± 0.28	55.67 ± 1.64	45.28 ± 0.68	74.14 ± 0.52	76.31 ± 0.16

concentrations up to 2×10^{-4} mol dm^{-3}, obtained at pH 3.6 with 5×10^{-4} mol dm^{-3} Zeph$^+$ as the titrant. The four regression curves were almost identical over this concentration range. In practical analyses, the calibration graph of Zeph$^+$ was used as a standard. Table 4 also shows the data for the calibration graph of Zeph$^+$ at higher concentrations. The calibration graph gave a completely linear response and good reproducibility even at higher concentrations. It can be seen from the tables that the proposed method is suitable for concentrations of cationic surfactants up to 1.25×10^{-3} mol dm^{-3}, and the limit of the determination is about 5×10^{-6} mol dm^{-3} of cationic surfactants.

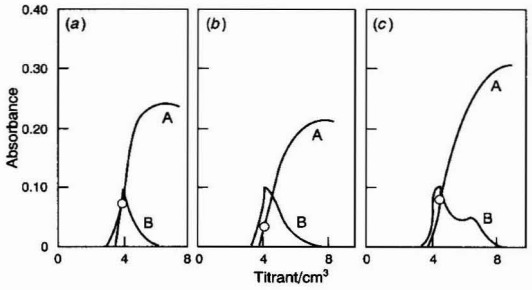

Fig. 4 Effect of anionic surfactants (AS$^-$) on titration curves. A, Absorbance curve; B, differential curve; circle indicates end-point. Sample: 10 cm^3 of 1×10^{-4} mol dm^{-3} TDTMA$^+$ with 15 cm^3 of 2×10^{-4} mol dm^{-3} AS$^-$; titrant, 5×10^{-4} mol dm^{-3} Zeph$^+$; TX-100, 0.025%; TBPE, 5.0×10^{-6} mol dm^{-3}. (*a*) DBS$^-$, (*b*) SSS$^-$, (*c*) LS$^-$

Table 3 Linearity of calibration graphs. Titrant, 5×10^{-4} mol dm^{-3} Zeph$^+$; sample, mixture of 10 cm^3 of analytes (CS$^+$) and 15 cm^3 of 2×10^{-4} mol dm^{-3} DBS$^-$

[CS$^+$]/ 10^{-4} mol dm^{-3}	Titrant/cm^3		
	A*	B*	C*
0	6.402 ± 0.005	6.402 ± 0.005	6.402 ± 0.005
0.125	6.180 ± 0.012	6.203 ± 0.006	6.198 ± 0.009
0.250	5.960 ± 0.005	5.957 ± 0.009	5.939 ± 0.025
0.500	5.407 ± 0.011	5.431 ± 0.030	5.400 ± 0.009
1.000	4.406 ± 0.020	4.382 ± 0.009	4.376 ± 0.007
1.500	3.389 ± 0.008	3.369 ± 0.005	3.345 ± 0.024
2.000	2.404 ± 0.012	2.364 ± 0.008	2.210 ± 0.003
Regression curves:†	$y = 6.402 - kx$		
	$k = 2.01 \times 10^4$	$k = 2.02 \times 10^4$	$k = 2.03 \times 10^4$

* Analyte (CS$^+$): (A) CPy$^+$; (B) STMA$^+$; (C) Hyamine$^+$.

† y = Volume of titrant (cm^3); x = concentration of CS$^+$ (mol dm^{-3}); k = slope of regression curve.

Table 4 Linearity of calibration graphs of the analyte Zeph$^+$ at lower and higher concentrations. At lower concentrations: titrant, 5×10^{-4} mol dm^{-3} Zeph$^+$; sample, mixture of 10 cm^3 of Zeph$^+$ and 15 cm^3 of 2×10^{-4} mol dm^{-3} DBS$^-$; TX-100, 0.02%; pH 3.6; TBPE, 5×10^{-6} mol dm^{-3}. At higher concentrations: titrant, 2.0×10^{-3} mol dm^{-3} Zeph$^+$; sample, mixture of 10 cm^3 Zeph$^+$ and 15 cm^3 of 1.25×10^{-3} mol dm^{-3} DBS$^-$; TX-100, 0.12%; other conditions as for lower concentrations

[Zeph$^+$]/ 10^{-4} mol dm^{-3}	Titrant/cm^3	[Zeph$^+$]/ 10^{-3} mol dm^{-3}	Titrant/cm^3
0.00	6.402 ± 0.007	0.00	9.762 ± 0.007
0.05	6.367 ± 0.030	0.01	9.693 ± 0.003
0.10	6.250 ± 0.003	0.025	9.683 ± 0.001
0.50	5.424 ± 0.033	0.31	8.091 ± 0.021
1.00	4.397 ± 0.011	0.62	6.360 ± 0.020
1.50	3.374 ± 0.020	1.24	3.055 ± 0.040
2.00	2.323 ± 0.001		
Regression curve*	$y = 6.402 - kx$		$y = 9.762 - kx$
	$k = 2.04 \times 10^4$		$k = 5.39 \times 10^3$

* y, x and k as in Table 3.

Application of the Indirect Titration Method to the Determination of Synthetic Cationic Surfactants

Several synthetic products containing cationic surfactants were analysed by the proposed method, after being dissolved in water. The results obtained were compared with those obtained by other methods (Table 5). Table 6 shows the carbon numbers in the alkyl chain of the practical samples listed in Table 5. With samples 1 and 2, good agreement between the proposed method and the Epton or STB method was obtained at high concentrations of the analyte. With sample 3, however, a relatively large deviation occurred between the proposed method and the $K_3Fe(CN)_6$ method. Some of this deviation is probably due to the surfactants with short alkyl chains and some to the methods adopted for nominal contents.

In order to examine the cause of the deviations, the standard cationic surfactants with short alkyl chains were

Table 5 Determination of synthetic cationic surfactants by the indirect titration method

Sample No.	Other methods: nominal (%)	Proposed method: assay (%)*	
		A†	B†
1	78‡	75.10 ± 0.10	76.18 ± 0.18
2	51§	45.64 ± 0.00	48.73 ± 0.10
3	24¶	10.98 ± 0.08	18.30 ± 0.04

* Percentage assays were calculated using the apparent formula masses given in Table 6.

† Analyte concentrations: (A) 5×10^{-4}–1×10^{-5} mol dm^{-3}; (B) about 10^{-3} mol dm^{-3}.

‡ Epton method.[3]

§ STB method.[8]

¶ $K_3Fe(CN)_6$ method.[9]

Table 6 Carbon numbers in alkyl chain of cationic surfactants examined in Table 5

No.	Main substance	Formula mass	Alkyl chain composition (%)			
			C_8–C_{10}	C_{12}	C_{14}	C_{16}–C_{18}
1	DSDMA$^+$ Cl$^-$	563			4	96
2	Benzalkonium (Cl$^-$)	354		58	35	7
3	DDTMA$^+$ Cl$^-$	264	14	50	19	17

Table 7 Reaction percentage of cationic surfactants with short alkyl chains. Conditions as in Table 4

Sample	Found (%)	
	A*	B*
Zeph$^+$	100.00	100.00
TDTMA$^+$	90.18	100.00
DDTMA$^+$	36.63	74.91
DTMA$^+$	4.19	9.92
DMBDoA$^{+\dagger}$	88.62	93.81

* (A) Low concentrations, about 10^{-5} mol dm^{-3}; (B) high concentrations, about 5×10^{-4} mol dm^{-3}.

† Dimethylbenzyldodecylammonium ion.

titrated with $Zeph^+$ at high and low concentrations. The results obtained are given in Table 7. When the alkyl chain length of the cationic surfactants decreases to 12 carbon atoms, the reaction percentage becomes low even at high concentrations. From these results, it can be seen that the reason for the low assay with sample 3 is its short alkyl chain.

These results indicate that the shorter the length of the alkyl chain in surfactants, the less is the formation of ion associates, and the formation of ion associates at higher concentrations of analytes proceeds more than that at low concentrations of analytes.

Conclusion

A photometric titration method for cationic surfactants in an aqueous medium was developed. The colour change at the end-points was very clear. By using the proposed titration method, cationic surfactants with alkyl chains containing more than 14 carbon atoms can be determined at micromolar levels.

The authors are grateful to the Japan Science Society for financial support with a Sasakawa Scientific Research Grant.

References

1 Eptons, S. R., *Trans. Faraday Soc.*, 1948, **44**, 226.
2 *International Standard*, ISO 2871, International Organization for Standardization, Geneva, 1988.
3 *Japanese Industrial Standard*, JIS K 3362, Japanese Standards Association, Tokyo, 1990.
4 El-Khateeb, S. Z., and Abdel-Moety, E. M., *Talanta*, 1988, **35**, 813.
5 Motomizu, S., Oshima, M., Gao, Y. H., Ishihara, S., and Uemura, K., *Analyst*, 1992, **117**, 1775.
6 Tôei, K., and Kawada, K., *Bunseki Kagaku*, 1972, **21**, 1510.
7 Tôei, K., and Kohara, T., *Anal. Chim. Acta*, 1976, **83**, 59.
8 Cross, J. T., *Analyst*, 1965, **90**, 315.
9 Longman, G. F., *The Analysis of Detergents and Detergent Products*, Wiley, London, 1975, p. 255.

Paper 3/04244H
Received July 20, 1993
Accepted September 1, 1993

CUMULATIVE AUTHOR INDEX

JANUARY–MARCH 1994

Book Reviews

Mass Spectrometry. Volume 1. Clinical and Biomedical Applications
Edited by Dominic M. Desiderio. *Modern Analytical Chemistry*. Pp. xiv + 354. Plenum. 1993. Price US$69.50. ISBN 0-306-44261-2.

Today, mass spectrometry is characterized by a huge sphere of application: from atoms to intact biopolymers, from archaeology to zoology. This particular book recognizes that biochemical mass spectrometry is one area that has seen more than its fair share of major advances in recent years. For instance, some years ago peptide chemists would chemically derivatize their unknown and rather short peptides prior to electron or chemical ionization for sequence determination. Then, in the early 1980s, larger peptides would be examined by fast atom bombardment mass spectrometry. Now, intact proteins with molecular masses of over 200 000 Da are addressed by electrospray ionization (ESI) or matrix-assisted laser desorption ionization (MALDI). The area is clearly ripe for reviewers.

An impressive list of 15 contributors has been assembled to produce chapters on the principles and applications of ESI, ESI and tandem mass spectrometry for the analysis of biomolecules, and the use of mass spectrometry for the study of muscle relaxants, neuropeptides, neurotransmitters, cannabinoids, inherited metabolic disorders, acylcarnitines, and platelet-activating factor. Unfortunately, MALDI hardly features in this volume. The book is amply referenced to 1991, but there is only a smattering of references to papers published in 1992. It ends with a nine-page subject index.

'Readers could use the book to update and extend their knowledge to some of the modern mass spectrometric approaches to problems in clinical and biochemical science'.

Mann and Fenn provide the opening chapter on the basics of ESI, and Smith, Loo and Edmonds follow it with a review of the application of ESI to biomolecules (actually, only polypeptides and proteins are covered). Both sets of authors are well practised at this type of article. The latter chapter contains useful sections on higher-order structure of polypeptides and on ESI–tandem mass spectrometry. The introduction of new methods for biochemical analysis is always to be encouraged but some of the attendant jargon is less welcome as these overviews illustrate (*e.g.*, 'sprayability' and 'adducted species'). Also, on pages 4–6, the reader will find a bewildering array of acronyms: FD, EH, TS, AS, ES, IEM, IS, AES, SIMS, FIB and ADIE. Jargon and acronyms excepted, these chapters are clear and effective but they are not sufficiently didactic for true newcomers to mass spectrometry.

The application-led chapters begin with an evaluation of mass spectrometry for the determination of pharmacokinetic properties of the charged neuromuscular blocking agents, mainly concerning chemical ionization following thermal *N*-demethylation, and fast atom bombardment. In well reasoned and authoritative accounts, the editor, Faull, and Harvey describe the quantitative analysis of neuropeptides, chiefly by fast atom bombardment, and the determination of neurotransmitters and cannabinoids, respectively. Largely, the latter two reviews concern gas chromatography–mass spectrometry (GC–MS).

In two truly clinical sections, the role of mass spectrometry in diagnosis and characterization of metabolic disorders is described. The first concerns the analysis of urine by GC–MS for organic acids, while the second covers the detection of acylcarnitines in blood spots, predominantly by fast atom bombardment tandem mass spectrometry. A brief final chapter discusses GC–MS and fast atom bombardment of platelet-activating factor. Usefully, several of the contributions on applications include some material on sample handling and competing or complementary analytical methods.

The book contains some inconsistencies between different contributions and a few minor errors (for example, the labelling of Fig. 1.4A/B is not in accord with the accompanying text). I would recommend this book only to those with a good grasp of the basic aspects of mass spectrometry (electron ionization, GC–MS and so on). Such readers could use the book to update and extend their knowledge to some of the modern mass spectrometric approaches to problems in clinical and biochemical science. As a book of this size cannot be comprehensive, its value to a reader depends on that individual's interests. If they reside in structural protein chemistry, physiology, metabolism and neuronal systems, then this volume will be a helpful purchase.

M. E. Rose

Surface Analysis Techniques and Applications
Edited by D. R. Randell and W. Neagle. Pp. vi + 174. Royal Society of Chemistry. 1990. Price £37.50. ISBN 0-85186-597-6.

This slim volume is a collection of papers given at a meeting with the same title organized by various bodies within the Royal Society of Chemistry and the Institute of Physics. The aim of the meeting was to provide an overview of the current status of surface analysis methodology for the non-expert and this aim has been carried over into the philosophy of the book of the meeting. There are 12 chapters ranging between 10 and 26 pages in length and a surprisingly good subject index. This latter feature is, I suspect, the only contribution the editors could make, apart from hustling the speakers to provide the material, as the book has been produced from camera ready copy.

This book is one of the ugliest camera ready copy books I have seen and illustrates all the worst features of this form of production. There is no consistency in font, spacing, justification or reference format. There are hand-written Greek symbols and many of the diagrams and figures are too small or too faint. The reproduction of the photographs is, however, excellent.

The order of the chapters is a little odd. I like Miller's chapter on 'Industrial Applications of Surface Characterization', but it should have been the first chapter not the fifth (the editors have essentially considered it to be the first of the applications chapters). The book is a little unbalanced, due possibly to the editors having to work with the material submitted. While the short chapter by Hercules, 'Surface Analytical Techniques—An Overview'), is rightly placed before the applications chapters; it is too short. Curiously enough, it dwells more on the difficulties of obtaining reliable information than it does on how information may be obtained in the first place. The book lacks a good introductory chapter (which should have been written by the editors?—just who is getting the royalty payments on this book?). I am continually disappointed by texts on surface analysis that fail to point

out, right at the beginning, that it is possible to get a lot of really useful information without the need for detailed spectral interpretation by means of the 'before and after' approach. That is, obtain the spectra by whatever technique is going to be appropriate before, and then after, some diagnostic experiment has been performed. What is required is that the differences between the two spectra be interpreted in the light of likely changes in the surface resulting from the experiment (treatment, or whatever). Maybe this is just too naive and simplistic.

'one of the ugliest camera ready copy books I have seen'.

The imbalance in the book is because there are not enough chapters explaining the basic principles of the techniques. Following on from the introductory overview chapter, the techniques of surface enhanced Raman spectrometry, ellipsometry and secondary ion mass spectrometry get separate chapters but then there is a bunch of applications chapters (industrial, corrosion processes, fracture studies, glasses) before a mixed chapter on the 'Applications of Electron Microprobe Analysis, Auger Microprobe Analysis and X-ray Diffraction to the Examination of a Metallized Surface'. There is then a basic principles chapter ('Electron Microscopy and Surface Analysis') and finally two chapters from instrument manufacturers dealing with a high resolution mass spectrometer (for secondary ion mass spectrometry and thermal ionization mass spectrometry) and a multi-technique instrument, respectively.

I suspect that readers looking for an introductory overview will be disappointed in the contents of this volume. It will be more useful to teachers of advanced courses in which surface techniques make an appearance along with other analytical chemical instrumentation, as there are useful examples and the applications chapters allow the importance of these surface techniques to be emphasized. The book could not be recommended for purchase by students, but would be a useful addition to the libraries of institutions where instrumental analytical chemistry is taught.

To address the need for an introductory overview text in this area properly, what is required is a publication in the RSC Paperback series. Such a text needs an author not editors, although Randell and Neagle's text could provide a considerable amount of useful material.

Julian Tyson

Photochemical Vapour Deposition
Edited by J. G. Eden. *Volume 122 in Chemical Analysis: A Series of Monographs on Analytical Chemistry and Its Applications.* Pp. xii + 194. Wiley. 1992. Price £43.95. ISBN 0-471-55083-3.

The average reader of *The Analyst* may not be familiar with the concept of chemical vapour deposition (CVD), so before commenting on this book let me give a thumbnail sketch of what it is about.

CVD is a process whereby a thin solid film is synthesized from the gaseous phase by a chemical reaction. It is this reactive process which distinguishes CVD from physical deposition processes. A wide range of layers can be produced by CVD and these include conductors, semiconductors, insulators and dielectrics, optoelectronic and optical layers, and coatings. The production of these layers forms the basis of a number of multi-million dollar industries, such as microelectronics fabrication and coating technologies. Most chemical reactions in CVD are thermodynamically endothermic and/or have a kinetic energy of activation associated with them. Generally this is an advantage since the reactions can be controlled by regulation of energy input. However, it does mean that energy has to be supplied to the reacting system and traditionally CVD processes have been initiated and controlled by the input of thermal energy to the substrate. For many applications, though, the high temperature required for deposition may cause thermal damage to the substrate; for example, crystalline stress may be introduced and interdiffusion between doped regions may occur. A solution to these problems is to use other forms of energy input that allow deposition at lower temperatures. One such energy input is to use photons and this has given rise to the technique of photochemical CVD, or photo CVD, which is the subject of this monograph.

'For any one working in the area of photochemical vapour deposition, or thinking of becoming involved with the technique, this small volume would serve as a good starting point and provide a useful introduction to the technique and to the literature available'.

The material in the book is presented in a logical manner starting with fundamental aspects of photochemical processes followed by practical issues of reactors, optical sources and associated equipment. Then there are three chapters on specific types of material, namely, metals, semiconductors, and dielectrics, followed by a chapter on miscellaneous materials. Finally, there are chapters on surface processes and future prospects. For any one working in the area of photochemical vapour deposition, or thinking of becoming involved with the technique, this small volume would serve as a good starting point and provide a useful introduction to the technique and to the literature available.

This volume is well written and is certainly authoritative, well referenced, up-to-date and it will, as already indicated, serve as a very valuable review for some time. Indeed, as someone who has a significant interest in thin-film preparation and properties, in general, and in CVD, in particular, I found this text interesting to read and I am sure I shall refer to it regularly in the future. However, as someone who has also contributed to this series some years ago and still with an interest in analytical chemistry, I think it is strange to find this volume in this series for, by the widest stretch of the imagination, it has little to do with analytical chemistry, at least in the generally accepted meaning of the term. The readers of *The Analyst* may think otherwise and be willing to spend over £40 on this volume. If they do they will get a valuable reference text, but what they should not expect is much enlightenment on such things as principles of analysis, analytical techniques, analysis of particular types of materials and substances, or an overview of analytical processes, all of which the volumes in the series normally deal with. Therefore, it is doubtful whether any analytical chemist would want to spend the money on this volume, in spite of its obvious merits.

Michael L. Hitchman

Laboratory Accreditation and Data Certification. A System for Success
By Carla H. Dempsey and J. D. Petty. Pp. xiv + 240. Lewis Publishers. 1991. £68.00. ISBN 0-87371-291-9.

The authors are chemists with considerable experience of quality assurance (QA) and both have worked in the US Environmental Protection Agency (EPA). Dr. Petty has wide analytical experience and has been responsible for working to the US Food and Drugs Administration 'good manufacturing practice' and 'good laboratory practice' requirements.

As expected, this book is extremely well written and produced. In the first four chapters, the authors critically discuss the need for laboratory accreditation and data certification, and current practices and principles. Most of the remainder of the book focuses on the EPAs Contract Laboratory Program (CLP) and the need to base CLP on broader quality management principles, in particular on Deming's approach to 'total quality management'.

The logic of their argument results in the conclusion that independent third-party accreditation and certification of analytical laboratories and data are required. Accreditation is needed to establish 'baseline credibility', and should be made by assessment of the laboratory quality system by a suitable independent body against an appropriate standard. The authors recommend that data certification should be based on the establishment of the laboratory's actual performance using evaluation samples. They further conclude that accreditation

'this book provides a logical and readable justification of accreditation and performance evaluation (usually known in this country as proficiency testing)'.

and performance evaluation must be carefully integrated into a single programme to provide purchasers of data with the necessary indicators of a credible system. They also provide the elements that must be included in the standard for accreditation.

The remainder of the book deals with the practicalities of implementing the accreditation and performance evaluation systems and their application to environmental and other types of laboratories.

For a QA professional, this book provides a logical and readable justification of accreditation and performance evaluation (usually known in this country as proficiency testing) and the discussion of Deming's 14 principles in a laboratory context leading to a standard for accreditation is most interesting. It also sheds considerable light on the problems caused in the USA by the common practice of second-party accreditation.

We are very fortunate in the UK to have a long and well-established tradition of third-party assessments and certification, of which accreditation by NAMAS to their standard is appropriate for most laboratories. Although it will be a valuable addition to analytical chemistry literature in the USA, this book will not be of much assistance to the majority of analytical chemists in the UK except for those actively employed in the management of QA systems.

E. J. Newman

Topics in Fluorescence Spectroscopy
Edited by Joseph R. Lakowicz. Volume 1. Techniques. Pp. xiii + 453. Plenum. 1991. Price US$79.50. ISBN 0-306-43874-7; Volume 2, Principles. Pp. xv + 432. Plenum. 1991. Price US$79.50. ISBN 0-306-43875-5; Volume 3. Biochemical Applications. Pp. xiv + 390. Plenum. 1992. Price US$79.50 (USA and Canada), US$95.40 (Export). ISBN 0-306-43954-9.

Few instrumental analysis methods can match the explosion of interest enjoyed in recent years by fluorescence spectroscopy. Rapid advances in optoelectronics, data handling and reagent synthesis have combined to increase the range of instrumentation and applications tremendously, and practitioners in biochemical and environmental sciences in particular have been quick to exploit these opportunities. It is significant that these three volumes, each containing eight mostly lengthy chapters written by experts from several countries, are by no means comprehensive in their coverage. However, more volumes are promised in due course, and if they match the standards of the first three, they will be mandatory reading for fluorescence enthusiasts.

The first volume ('Techniques') concentrates heavily (five chapters) on the many recent developments in time- and phase-resolved techniques: all this material is presented with authority and clarity and offers an excellent overall view of a most important area. The three remaining chapters cover correlation spectroscopy (an underrated approach with many applications), and the perhaps more familiar fluorescence microscopy and flow cytometry methods. The second volume ('Principles', should not this have been volume 1?) covers a much wider range of topics, including energy transfer,

'mandatory reading for fluorescence enthusiasts'.

anisotropy, quenching and polarization methods, and includes two welcome and fascinating chapters on aspects of data handling using least squares and global analysis approaches. Such topics do not always make for easy reading, but these contributions are very clear, again with some emphasis on the analysis of time-domain data. The oddity in this volume is the chapter on fibre-optic fluorescence sensors: though short it is well written, but surely in the wrong volume! (However, most libraries and researchers will doubtless want to buy all the volumes anyway.)

The third and most recent volume covers an interesting range of very specific application areas in the biomedical sciences. Most of these are not explicitly analytical in character, though the techniques described will often have general application. For example, some of the methods used to detect tyrosine fluorescence in proteins, in the presence of much more intense tryptophan emissions, might be applied in many situations where closely overlapping fluorescence spectra arise, and the careful experimental techniques required for the observation of room temperature phosphorescence in proteins will similarly have much broader relevance. Other chapters, such as the one on total internal reflectance fluorescence, remind us of the great versatility in sample handling of fluorescence analysis methods. There is a disappointingly short account of fluorescence in immunodiagnosis, and other major application areas which might have been expected (*e.g.*, the very widespread use of fluorescence in the determination of intracellular calcium and other ions; the growing interest in long-wavelength and near-IR fluorescence; matrix isolation methods; fluorescence enzyme assays *etc.*, are not covered in any depth, so we must look forward to further volumes.

These books are moderately priced by modern standards, and are well produced with very few errors. (Only the indexing, always difficult in multi-author works of this kind, is sometimes inadequate.) The overall impression is that the distinguished editor has brought together a scholarly and invaluable collection of essays in a fascinating area of chemistry. I strongly recommend these books to fluorescence researchers.

James N. Miller

Diode Array Detection in HPLC
Edited by Ludwig Huber and Stephan A. George. *Chromatographic Science Series. Volume 62.* Pp. viii + 400. Marcel Dekker. 1993. Price US$150.00. ISBN 0-8247-8947-4.

Of the many books that have been published over recent years on aspects of HPLC, this one is different in that it is solely

devoted to one very specialized topic, *i.e.*, UV detection using the diode array detector (DAD). This is an edited volume with the 14 chapters prepared by a team of 8 different authors. Since apart from one exception, both of the editors and all of the authors are employed by Hewlett-Packard, a first impression of this volume may lead to the conclusion that this is likely to be a sophisticated and, at a price of US$150.00, a somewhat expensive advertisement for the products of this company. However, although this is the case up to a point, in that just about all chromatographic and spectrochromatographic examples shown in the figures were acquired on HP equipment, this reviewer was impressed by the scope covered and that several competitor products were also featured especially in the earlier chapters.

The first five chapters are concerned with the development of and various features available with DADs, and probably contain the most useful contributions to this volume. The remaining chapters describe various applications.

The first two chapters are an excellent introduction providing a review of historical and modern developments. This treatment of describing the various approaches that have been investigated provides a very good insight into the details of the workings of DADs, which is very important to enable the reader to understand the features that these instruments can provide using a combination of the mass of data collected and the computing power available with modern PCs, which are described in Chapters 4 and 5. Chapter 4 is concerned with the methods available for spectral matching and peak purity and compares various algorithms that have been developed for these functions. Chapter 5 is concerned with chemometrics and examines in some detail, mathematical approaches to peak deconvolution and multicomponent analysis.

The following chapters include various applications of DADs commencing with the pharmaceutical industry where the author identifies the place of DADs in basic research and product development, clinical assays and drug metabolism, and finally in quality control and stability studies. The following chapter adds details on applications for clinical applications by giving a number of examples of analyses with different classes of drug products. The chapter on toxicological applications considers clinical toxicology, forensic drug analysis, doping control in sports (both human and equine) and even forensic fibre examination where the importance of the analysis of dyestuffs is demonstrated. Additional applications include amino acids, peptides and proteins; food and beverages; environmental; and chemical, petroleum and polymers.

The next chapter is concerned with the optimization of diode array detection particularly addressing the questions of sensitivity and selectivity and there is a final short chapter on the automation of DAD functions when applied to routine applications.

Overall, the book has been well prepared with few typographical errors, it is readable and most chapters are well referenced. It is probably most suitable as an introduction to this specialized detection technique for experienced chromatographers and for this purpose provides a very comprehensive treatment. However, considering the advertising value to a single supplier of this equipment, the price is rather high.

G. P. R. Carr

Introduction to Micellar Electrokinetic Chromatography
By Johan Vindevogel and Pat Sandra. *Chromatographic Methods Series.* Pp. x + 238. Hüthig. 1992. Price US$62.00; DM 88.00. ISBN 3-7785-2105-5.

This book addresses a rapidly emerging area of capillary electrophoresis (CE). Although the title modestly claims only an introduction to the subject, this book provides an excellent, in depth treatment of nearly all aspects of this subject.

This work is organized into four sections—fundamentals, instrumental aspects, resolution, and applications—which are further broken down into 13 chapters containing 108 figures, 24 tables and 574 references. Besides the 4 page table of contents, this concise monograph also includes a preface, introduction, postscript, 2 appendices (the second of which is a 3 page glossary of symbols and abbreviations), and a 4 page subject index.

Chapter 1 provides a good historical overview and distinguishes among the concepts of zone electrophoresis, isotachophoresis and isoelectric focusing. Chapter 2 describes the phenomena and underlying factors that affect electrophoretic mobility and electroosmosis. Separation theory for CE is described in Chapter 3, followed by a summary of non-ideal effects and the importance of ionic strength when pH effects are being considered. Electrochromatography is the subject of Chapter 4, where the significance of both column diameter and flow profile is clearly illustrated. In Chapter 5, the separation theory and modes of micellar electrophoretic chromatography (MEKC) are introduced, along with a summary of common anionic and cationic surfactants. Thermal effects, columns, injection and detection are the subject of Chapters 6–9, and the kinetic (efficiency) and thermodynamic (retention, elution range, *etc.*) aspects of resolution are described in Chapters 10 and 11, respectively. Finally, general and chiral applications of MEKC are reviewed in Chapters 12 and 13.

Although this book is a first edition, I have only a few minor criticisms, mostly directed at errors of omission. First, only a very brief discussion of selectivity in general terms was provided, in a section devoted primarily to the effect of organic modifier and surfactants on the elution range; a discussion of the hydrophobic selectivity of MEKC, essentially its potential to separate homologues, was omitted entirely. Second, although efficiency was discussed thoroughly in terms of plate height, its measurement and the deconvolution of extracapillary and intracapillary sources of band broadening were virtually ignored. Third, the measurement and properties of mixed surfactants and/or micelles was omitted, an area obviously relevant to future investigation in MEKC. Fourth, although an expression was provided for the retention factor (k') of a charged solute in terms of migration times or velocities, the converse expression for the solute migration time in terms of t_0, k', t_{mc} *etc.*, was omitted. Finally, the terse style and knowledge of chromatography that the authors assume are probably appropriate for most readers, but with only a few additional explanatory sentences here and there, and perhaps a few pages of general chromatography background, the authors could make their work considerably more accessible to the EKC novice who also lacks experience in gas chromatography or high-performance liquid chromatography.

These minor criticisms notwithstanding, I found this to be an excellent book. The scope of the book is appropriate and its objectives are fulfilled admirably. It is clear, concise, and, on the whole, well-organized and cross-referenced; the inclusion of titles in the references at the end of each chapter is something that more publishers should consider. Ideas were generally explained well, and it is also free of the usual number of typographical and proofreading errors that plague most first editions. An especially noteworthy feature of this monograph are the superb figures and tables, some taken from the literature, that illustrate subtle points that might escape the reader if presented in a textual format. Personal favourites include Table 5.1, an explanation of the iterative method for measuring t_{mc} using the migration data of a set of homologues; Table 8.1, the effect of capillary diameter on the amount of analyte injected hydrodynamically; and Figs. 11.3, 11.6 and

11.9, the influence of the phase ratio, electroosmotic flow, and the electrophoretic mobility of the micelles on the resolution.

In summary, this book belongs in the personal library of every MEKC practitioner as well as in every institutional library. Although some portions of this book may understandably become dated as research in this area continues, this book or any future editions will likely be the 'bible' of MEKC for several years.

Joe P. Foley

An Introduction to the Management of Laboratory Data: A Tutorial Approach Using Borland's Paradox Relational Database

By C. N. Hegarty. Pp. xii + 588. Royal Society of Chemistry. 1992. Price £85.00. ISBN 0-85186-219-5.

Analytical laboratories are drowning in the data produced from a variety of instrumental and classical analytical techniques. To help overcome the problem, databases and the associated software, called laboratory information management systems (LIMS) are used. This book joins three available titles on the subject.

Hegarty's book consists of 30 chapters (588 pages) and comes with an IBM compatible 3.5 inch disc containing a single user run time version of a LIMS system developed using Paradox 3. This book is aimed at laboratory supervisors and managers, who have a limited knowledge of computer programming, as an introduction to the use of a relational database for the management of laboratory data. The author does not assume any previous programming knowledge by the reader as the book contains step-by-step instructions to design a simple LIMS system.

Each chapter has an overview of the contents, which is very useful either for scanning the whole book or putting the reader into a receptive frame of mind for a specific topic. The book starts from a discussion on the organization of laboratory documentation. I found this an original point to start from that targets the function of a LIMS system immediately: administration not analysis. It was in this chapter that I felt that references to further reading would have been useful rather than on a single page at the back of the book. The book then moves into a presentation of electronic recording and gives a very concise and clear presentation of using Paradox for a LIMS system; covering areas such as graphical presentation of data, query by example, record locking and finishes with the pros and cons of the approach.

'all the information required for a functional LIMS system'.

From here the reader is taken into the application, starting with the concept of data tables and the information associated with a sample such as submitter, source, test procedures, staff and the hierarchy for approval of the results and report.

After this, the reader is taken through chapters covering the creation of menus to operate the system, log-in screens, work sheets, manual results entry (on-line entry has been excluded from consideration in Chapter 2), verify and approve results, and tables for monitoring laboratory performance and security. One of the final chapters lists all the scripts used to prepare the LIMS system for further customization and development by the reader. In short, all the information required for a functional LIMS system.

The concept and detail of the LIMS system presented here is excellent for an analytical laboratory. However, a LIMS system also serves the organization and there should be a reference to this. The book is not an academic treatise but focuses primarily on the practical aspects of LIMS system. I would encourage analysts to read the book and use the software, as it provides a non-commercial insight into LIMS systems. It would also help laboratory managers, if they have the time available, to gain an insight into the subject and help discuss the matter on a level playing field with the computer department. One area that is not exploited by the book is education: if a paperback version were available for students it would make an excellent introduction to the subject and make new graduates more attractive to industry rather than a new employer having to educate them from scratch.

R. D. McDowall

Spectroscopic Methods and Analyses. NMR, Mass Spectrometry and Metalloprotein Techniques
Edited by Christopher Jones, Barbara Mulloy and Adrian H. Thomas. *Methods in Molecular Biology. Volume 17.* Pp. x + 296. Humana Press. 1933. Price US$ 59.50. ISBN 0-89603-215-9.

This volume is the first part of a predicted trilogy on *physical methods of analysis* in this series. The overall undertaking is therefore a mammoth on with additional promised volumes on Optical Spectroscopy and Macroscopic Techniques (Volume 2) and Crystallographic Methods and Techniques (Volume 3). Unlike previous books in the series the present one does not, in general, adhere to the recipe and notes type format, maybe because of the coverage of the large instrument methods. The style is more a readable textbook for a relatively non-specialist scientific audience, but the bias is towards those working with proteins, oligosaccharides or DNA. Three of the chapters dedicated to proteins, Chapter 3 on peptide structure (M. P. Williamson), Chapter 15 on resonance Raman spectroscopy (R. S. Czernuszewicz) and Chapter 16 on X-ray absorption spectroscopy (C. D. Garner) do have useful notes sections and very informative methodological summaries as does Chapter 6 on the NMR of polysaccharides (C. Jones and B. Mulloy). Other chapters give a more introductory description of techniques being applied to all three classes of molecule, *i.e.*, Chapter 1, An Introduction to NMR (C. Jones and B. Mulloy), Chapter 7, Dynamic and Exchange Processes (L.-Y. Lian), Chapter 8, An Introduction to Mass Spectrometry (R. Wait), Chapter 9, Laser Desorption Ionization Mass Spectrometry (M. Karas and U. Bahr) and Chapter 12, Tandem Mass Spectrometry (C. E. Costello). There are additional specialist NMR chapters on Proteins in Solution (D. Neuhaus and P. A. Evans; Chapter 2), Drug DNA

'The content of the book, with respect to the molecules and techniques discussed, comprehensively covers the new physico-chemistry of macromolecules'.

Interactions (J. Barber, H. F. Cross and J. A. Parkinson; Chapter 4) and Carbohydrate Moieties of Glycoproteins (H. van Halbeek; Chapter 5). Proteins are then further covered with chapters on their analysis by Plasma Desorption Mass Spectrometry (P. Roepstorff; Chapter 10), Fast Atom Bombardment Mass Spectrometry (R. Wait; Chapter 11), Mössbauer Spectroscopy (D. P. E. Dickinson; Chapter 13) and Electron Paramagnetic Resonance Spectroscopy (R. Cammack; Chapter 14).

The content of the book, with respect to the molecules and techniques discussed, comprehensively covers the new physico-chemistry of macromolecules. All the major new methodologies in NMR spectroscopy (COSY, HMBC, HMQC, TOCSY, NOESY, ROESY) and mass spectrometry (FAB, LD, PD, ES) are introduced. The NMR studies are also

discussed with respect to the data on macromolecular interactions that can be obtained by X-ray crystallography, a current debate in the field on the relative merits of each technique. As stated on p. 88 'NMR spectroscopy can, if necessary, be used as an alterantive to X-ray crystallography. On rare and much publicized occasions it has even been used to correct information obtained by X-ray diffraction'. The authors go on to describe the diversity of NMR experimentation in terms of temperature, ionic strength, pH, dielectric constant *etc.* As we know both methods have their different advantages and drawbacks. Mass spectrometry is also necessary in the analysis armamentarium for high sensitivity detection. For those in the structural or conformational analysis field, this book and the two subsequent volumes provide a comprehensive guide to the choice of appropriate technique for a particular macromolecular problem.

Elizabeth F. Hounsell

Mass Spectral and GC Data of Drugs, Poisons, Pesticides, Pollutants and Their Metabolites. Second, revised and enlarged edition. Parts 1, 2 and 3

By K. Pfleger, H. H. Maurer, A. Weber. Pp. Part 1, xvi + 1266; Part 2, viii + 1004; Part 3, viii + 1954. VCH. 1992. Price DM 1290.00. ISBN 3-527-26989-4 (VCH Weinheim); 0-89573-855-4 (VCH New York).

The first edition of this book appeared in 1985. The second contains 4370 EI spectra ('1500 drugs and medicaments, 800 pesticides and pollutants and 2000 metabolites'). The spectra will soon be available in several (condensed) formats for computer scanning, but there is far more in this printed version than summaries of the spectra.

'The work seems destined to become a standard in its field'.

The first 61 pages of Part 2 (repeated in Part 3) contain explanatory notes, abbreviations and an alphabetical compound index. The spectra, 5 per page (*m/z* 4–221 and 222–777 u in Parts 2 and 3, respectively), are paginated consecutively (pages 1–1954). The spectra are arranged by ascending mass (nearest integer); from each nominal mass the spectra are ordered by retention index (alkane) on OV-101 and then, if necessary, alphabetically. Compounds with retention index <1000 are so designated. Replicate spectra are ordered by molecular ion (M^+) or the highest mass visible and also by major fragment ions (>80% of the base peak). This duplication is balanced by the enhanced practical value of the work.

The layout and general quality of the production are good. The spectra are represented graphically and structures are assigned in each case. Many previously unpublished metabolite spectra are said to be included. However, in this edition minor but nevertheless important peaks in the spectra are no longer enhanced by truncating common base peaks—this seems a retrograde step. The origin of the samples providing the spectra are included, but another simple key indicating any additional chemical evidence supporting the spectral interpretation would have been useful.

But what of Part 1? This consists of: introduction (2 pages); experimental (16 pages); introduction to EI mass spectrometry (2 pages); artifacts (4 pages); atomic masses (1 page); abbreviations (3 pages, duplicated in Parts 2 and 3); user's guide (2 pages); and references (2 pages). Useful background, but real life is not quite so straightforward, the use of perfluoroacylation to derivatize 6-acetylmorphine (Section 2.2.2.5), for example, may be unsound.[1] There are then 379 pages of tables of compounds for which spectra are available classified by name, category and retention index, and a further 420 pages of tables of 'Potential Poisons' (over 7500 entries) classified by molecular mass to 5 decimal places, name and category. Finally there are 417 pages of CAS cross-indexes of potential poisons by common name, registry number and index name.

The 'Potential Poisons' table is massive, but seems rather quaint in places; it includes water (!) and some anti-inflammatory agents are denoted as 'antiphlogistic'. Any analytical toxicologist worth his or her salt could find omissions (astaxanthin, a naturally-occurring analogue of canthaxanthin; atracurium, which gives rise to laudanosine *in vivo* and is widely used in clinical practice; cyclosporin; methyl *tert*-butyl ether; and so on). There are many inconsistencies: 2,4-D is classified as a herbicide but its isobutyl and isopropyl esters are listed as pesticides; cyanide hydrogen is a poisonous gas whilst prussic acid is an insecticide. . . . On the positive side, parent compounds, for which spectra are available in Parts 2 and 3, are included, but the exclusion of metabolites limits the usefulness of the formula mass listing. Reference to works, for example Ardrey *et al.*[2] (drugs) and Middleditch[3] (artifacts), which cover some of the compounds cited here, but for which spectra are not presented in Parts 2 and 3, would have further enhanced the practical value of this table.

When reviewing the first edition of this *magnum opus* Prof. R. A. de Zeeuw emphasized its value to experienced analysts. Whilst in full agreement with regard to Parts 2 and 3 of this edition, the value of some sections of Part 1 is less clear. It would be naive to think that mass spectroscopy has anything more than a supportive role in emergency toxicology. This being said, one cannot but admire the authors' devotion to the task in hand, their collection of CAS Registry Numbers alone is formidable! The work seems destined to become a standard in its field.

References

1 Ceder, G., and Eklund, A., in *Forensic Toxicology*, ed. Kaempe, B., TIAFT, Copenhagen, 1991, pp. 193–197.
2 Ardrey, R. E., Allan, A. R., Bal, T. S., Joyce, J. R., and Moffat, A. C., *Pharmaceutical Mass Spectra*, Pharmaceutical Press, London, 1985.
3 Middleditch, B. S., *Analytical Artifacts, GC, MS, HPLC, TLC and PC, J. Chromatogr. Lib., vol. 44*, Elsevier, Amsterdam, 1989.

R. J. Flanagan and T. E. Levitt

Conference Diary

Date	Conference	Location	Contact
1994			
April			
6–8	**Electroanalysis: A Tribute to Professor J. D. R. Thomas**	Cardiff, UK	**Dr. J. M. Slater,** Department of Chemistry, Birkbeck College, University of London, 29 Gordon Square, London, UK WC1H 0PP **Tel:** +44 71 380 7474. **Fax:** +44 71 380 7464
10–13	**ANATECH 94: 4th International Symposium on Analytical Techniques for Industrial Process Control**	Mandelieu La Napoule, France	**ANATECH 94 Secretariat,** Elsevier Advanced Technology, Mayfield House, 256 Banbury Road, Oxford, UK OX2 7DH **Tel:** +44 (0)865 512242. **Fax:** +44 (0)865 310981
10–15	**207th ACS National Meeting and 5th Chemical Congress of North America (with Sessions of Analytical Chemistry, Environmental Chemistry, Chemical Health and Safety, *etc.*)**	Mexico City, Mexico	**Mr. B. R. Hodson,** American Chemical Society, 1155–16th Street N.W., Washington, DC 20036, USA **Tel:** +1 202 872 4396.
10–16	**3rd International Conference on Methods and Applications of Radioanalytical Chemistry**	Kailua-Kona, Hawaii, USA	**Ned A Wogman,** Battelle, Pacific Northwest Laboratories, P.O. Box 999, P7-35, Richland, WA 99352, USA **Tel:** +1 509 376 2452. **Fax:** +1 509 376 2373
11–12	**Biosensors for Food Analysis**	Leeds, UK	**Mr. S. S. Langer,** The Royal Society of Chemistry, Burlington House, Piccadilly, London, UK W1V 0BN **Tel:** +44 71 437 8656. **Fax:** +44 71 734 1227
12–14	**13th Pharmaceutical Technology Conference**	Strasbourg, France	**Professor Mike Rubinstein,** 13th Pharmaceutical Technology Conference, 24 Menlove Gardens North, Liverpool, UK L18 2EJ **Tel:** +44 51 737 1993. **Fax:** +44 51 737 1070
12–15	**The Royal Society of Chemistry Annual Chemical Congress**	Liverpool, UK	**Dr. J. F. Gibson, Scientific Secretary,** The Royal Society of Chemistry, Burlington House, London, UK W1V 0BN **Tel:** +44 71 437 8656. **Fax:** +44 71 437 8883
17–19	**International Symposium on Volatile Organic Compounds (VOCs) in the Environment**	Montreal, Quebec, Canada	**Symposium Chairman, Dr. Wuncheng Wang,** US Geological Survey, WRD, P.O. Box 1230, Iowa City, IA 52244, USA. **Tel:** +1 319 337 4191, **Fax:** +1 319 354 0510; or **Co-Chairmen, Dr. Jerald Schnoor,** University of Iowa, Department of Civil and Environmental Engineering, Iowa City, IA 52242, USA. **Tel:** +1 319 335 5649, **Fax:** +1 319 335 5777; and **Dr. Jon Doi,** Roy F. Weston, Inc., 1 Weston Way, West Chester, PA 19380, USA **Tel:** +1 215 524 6167. **Fax:** +1 215 524 6175
18–22	**6th International Conference on Near Infrared Spectroscopy**	Lorne, Australia	**NIR-94, Peter Flinn,** Pastoral and Veterinary Institute, Mt. Napier Road, Private Bag 105, Hamilton, Victoria 3300, Australia **Tel:** +61 55 730915. **Fax:** +61 55 711523
19–22	**ANALYTICA'94: 14th International Conference on Biochemical and Instrumental Analysis**	Munich, Germany	Münchener Messe- und Ausstellungsgesellschaft mbH, Analytica '94/Werbung Postfach 12 10 09, D-8000 München 12, Germany **Tel:** +49 89 51 07 143. **Fax:** +49 89 51 07 177
May			
7–12	**Food Structure Annual Meeting**	Toronto, Ontario, Canada	**Dr. Om Johari,,** SMI, Chicago (AMF O'Hare), IL 60666-0507, USA **Tel:** +1 708 529 6677. **Fax:** +1 708 980 6698
8–12	**85th AOCS Annual Meeting & Expo**	Atlanta, GA, USA	**AOCS Education/Meetings Department,** P.O. Box 3489, Champaign, IL 61826-3489, USA **Tel:** +1 217 359 2344. **Fax:** +1 217 351 8091
8–13	**HPLC '94, Eighteenth International Symposium on Column Liquid Chromatography**	Minneapolis, MN, USA	**Ms. J. E. Cunningham,** Barr Enterprises, P.O. Box 279, Walkersville, MD 21793, USA **Tel:** +1 301 898 3772. **Fax:** +1 301 898 5596

Date	Conference	Location	Contact
8–13	**CLEO '94: Conference on Lasers and Electro-Optics**	Anaheim, CA, USA	**Meetings Department,** Optical Society of America, 2010 Massachusetts Avenue, NW, Washington, DC 20036-1023, USA **Tel:** +1 202 223 9034. **Fax:** +1 202 416 6100
9–13	**Focus 94–The Annual National Meeting and Exhibition of the Association of Clinical Biochemists**	Brighton, UK	**Focus 94,** P.O. Box 227, Buckingham, Buckinghamshire, UK MK18 5PN **Tel:** +44 2806 613. **Fax:** +44 2806 487
16–19	**24th Annual Symposium on Environmental Analytical Chemistry**	Ottawa, Canada	**Dr. M. Malaiyandi,** CAEC, Chemistry Department, Carleton University, 1255 Colonel By Drive, Ottawa, Canada K1S 5B6 **Tel:** +1 613 788 3841. **Fax:** +1 613 788 3749
16–20	**Deauville Conference: 13th International Symposium on Microchemical Techniques; 2nd Symposium on Analytical Sciences**	Montreux, Switzerland	**D'Conference 94,** 7 rue d'Argout, 75002 Paris, France **Tel:** +33 1 42 33 47 66. **Fax:** +33 1 40 41 92 41
16–20	**24th International IAEAC Symposium on Environmental Analytical Chemistry**	Ottawa, Ontario, Canada	**Dr. James F. Lawrence,** Food Additives and Contaminants, Health and Welfare, Tunney's Pasture, Ottawa, Ontario, Canada K1A 0L2
23–25	**ISPAC 7: International Symposium on Polymer Analysis and Characterization**	Les Diablerets, Switzerland	**Secrétariat,** ISPAC 7, CERMAV-CNRS, BP 53 X, 38041 Grenoble Cedex, France
24–27	**3rd Symposium on Molecular Chirality**	Kyoto, Japan	**Professor Terumichi Nakagawa,** Symposium on Molecular Chirality (SMC), Faculty of Pharmaceutical Sciences, Kyoto University, Yoshida-Shimoadachi-cho, Sakyo-ku, 606 Japan **Fax:** +81 48 471 0310 (Professor Hara)
24–27	**International Symposium on Metals and Genetics: Toxic Metal Compounds in Environment and Life 5; Interrelation between Chemistry and Biology**	Toronto, Ontario, Canada	**Professor B. Sarkar,** Department of Biochemistry, The Hospital for Sick Children, 555 University Avenue, Toronto, Ontario, Canada M5G 1X8
29–1/6	**42nd ASMS Conference on Mass Spectroscopy**	Chicago, IL, USA	**ASMS,** 815 Don Gaspar, Santa Fe, NM 87501, USA **Tel:** +1 505 989 4517.
30–2/6	**14th Nordic Atomic Spectroscopy and Trace Analysis Conference**	Naantali, Finland	**Ari Ivaska,** Abo Akademi University, Laboratory of Analytical Chemistry, Biskopsgatan 8, SF-20500 Abo Turku, Finland
30–1/6	**Scandinavian Symposium on Infrared and Raman Spectroscopy**	Bergen, Norway	**Dr. Alfred Christy,** Department of Chemistry, University of Bergen, N-5007 Bergen, Norway
June			
1–3	**Second International Symposium on Hormone and Veterinary Drug Residue Analysis**	Bruges, Belgium	**Professor C. Van Peteghem,** Symposium Chairman, Faculty of Pharmaceutical Sciences, University of Ghent, Harelbekestraat 72, B-9000 Ghent, Belgium **Tel:** +32 9 221 89 51 (ext. 235). **Fax:** +32 9 220 52 43
1–3	**Biosensors 94—The Third World Congress on Biosensors**	New Orleans, USA	**Kay Russell,** Conference Department, Elsevier Advanced Technology, Mayfield House, 256 Banbury Road, Oxford, UK OX2 7DH **Tel:** +44 (0) 865 512242. **Fax:** +44 (0) 865 310981
5–7	**VIth International Symposium on Luminescence Spectrometry in Biomedical Analysis—Detection Techniques and Applications in Chromatography and Capillary Electrophoresis**	Bruges, Belgium	**Professor Dr. Willy R. G. Baeyens,** Symposium Chairman, University of Ghent, Pharmaceutical Institute, Dept. of Pharmaceutical Analysis, Lab. of Drug Quality Control, Harelbekestraat 72, B-9000 Ghent, Belgium **Tel:** +32 (0) 9 221 89 51. **Fax:** +32 (0) 9 221 41 75
5–11	**24th ACHEMA**	Frankfurt, Germany	**Dechema,** Theodor Heuss-Allee 25, P.O. Box 970146, D-W-6000 Frankfurt am Main 97, Germany
6–8	**Conference on Plasma Science**	Santa Fe, NM, USA	**A. Perratt,** Los Alamos National Laboratory, Group X-10, MS D-406, P.O. Box 1663, Los Alamos, NM 87545, USA

Date	Conference	Location	Contact
8–11	**6th International Conference on Flow Analysis**	Toledo, Spain	**Professor M. Valcárcel/Dr. M. D. Luque de Castro,** (Flow Analysis VI), Departamento de Química Analítica, Facultad de Ciencias, E-14004 Córdoba, Spain **Tel:** +34 57 218616. **Fax:** +34 57 218606
12–15	**1994 PREP Symposium and Exhibit**	Washington, DC, USA	**Ms. Janet Cunningham,** Symposium/Exhibit Manager, Barr Enterprises, P.O. Box 279, Walkersville, MD 21793, USA **Tel:** +1 301 898 3772. **Fax:** +1 301 898 5596
13–15	**4th International Symposium on Field-Flow Fractionation**	Lund, Sweden	**Dr. Agneta Sjögren,** The Swedish Chemical Society, Wallingatan 24, tr. S-111 24 Stockholm, Sweden **Fax:** +46 8 106 678
15–17	**16th Symposium on Applied Surface Analysis (ASSD)**	Burlington, MA, USA	**Joseph Geller,** Geller Microanalytical, 1 Intercontiental Way, Peabody, MA 01960, USA **Tel:** +1 508 535 5595.
15–18	**The Second International Symposium on Speciation of Elements in Toxicology and Environmental and Biological Sciences**	Loen, Norway	**The Second International Symposium on Speciation of Elements in Toxicology and in Environmental and Biological Sciences,** Yngvar Thomassen, National Institute of Occupational Health, P.O. Box 8149 DEP, N-0033 Oslo 1, Norway
16–17	**14th International Symposium on Environmental Pollution**	Toronto, Canada	**Dr. V. M. Bhatnagar,** Alena Chemicals of Canada, P.O. Box 1779, Cornwall, Ontario, Canada K6H 5V7 **Tel:** +1 613 932 7702.
16–17	**18th International Conference on Analytical Chemistry and Applied Chromatography/Spectroscopy**	Toronto, Canada	**Dr. V. M. Bhatnagar,** Alena Chemicals of Canada, P.O. Box 1779, Cornwall, Ontario, Canada K6H 5V7 **Tel:** +1 613 932 7702.
19–21	**The 5th Nordic Symposium on Trace Elements in Human Health and Disease**	Loen, Norway	**Yngvar Thomassen,** Trace Elements in Human Health and Disease, National Institute of Occupational Health, P.O. Box 8149 DEP, N-0033 Oslo, Norway **Tel:** 47 22466850. **Fax:** 47 22603276
19–24	**20th International Symposium on Chromatography**	Bournemouth, UK	**Mrs J. A. Challis,** Chromatographic Society, Suite 4, Clarendon Chambers, 32 Clarendon Street, Nottingham, UK NG1 5JD **Tel:** +44 602 500596. **Fax:** +44 602 500614
20–23	**2nd Oxford Conference on Spectroscopy**	Ringe, NH, USA	**Dr. Art Springsteen,** Labsphere Inc., P.O. Box 70, North Sutton, NH 03260, USA **Tel:** +1 603 927 4266.
27–1/7	**Special FEBS Meeting on Biological Membranes**	Espoo, Suomi-Finland	**Professor Timo Korhonen,** Biochemical Society, European Federation of Biochemical Societies (FEBS), Department of General Microbiology, University of Helsinki, Mannerheimintie 172, SF-00300 Helsinki, Finland
July			
3–7	**International Chemometrics Research Meeting**	Veldhoven (Eindhoven), The Netherlands	**Mrs. Gerrie Westerlaken,** Conference Organizing Bureau VNW, Postbus 1558, 6501 BN Nijmegen, The Netherlands **Tel:** +31 80 234471. **Fax:** +31 80 601159
18–22	**XIII International Congress on Electron Microscopy**	Paris, France	**B. Jouffrey,** SFME 67, rue Maurice Gunsbourg, 94205, Ivry sur Seine cedex, France **Tel:** +33 1 46702844. **Fax:** +33 1 46708846
20–22	**Seventh Biennial National Atomic Spectroscopy Symposium**	Hull, UK	**Dr. Steve Hill,** Department of Environmental Sciences, University of Plymouth, Drake Circus, Plymouth, Devon, UK PL4 8AA
August			
2–6	**The Second Changchun International Symposium on Analytical Chemistry(CISAC)**	Changchun, China	**Professor Quinhan Jin,** Department of Chemistry, Jilin University, Changchun 130023, China **Tel:** +86 431 82233 (ext. 2433). **Fax:** +86 431 823907

Date	Conference	Location	Contact
8–10	**40th Canadian Spectroscopy Conference**	Halifax, Canada	**Dr. W. D. Jamieson,** Fenwick Laboratories Ltd., 5595 Fenwick Street, Suite 200, Halifax, NS B3H 4M2, Canada **Tel:** +(902) 420 0203. **Fax:** +(902) 420 8612
8–12	**IGARSS '94: 1994 International Geoscience and Remote Sensing Symposium**	Pasadena, CA, USA	**Meetings Department,** Optical Society of America, 2010 Massachusetts Avenue, NW, Washington, DC 20036-1023, USA **Tel:** +1 202 223 9034. **Fax:** +1 202 416 6100
14–18	**International Symposium on Bacterial Polyhydroxyalkanotes (ISBP '94)**	Montreal, Quebec, Canada	**ISBP Secretariat,** Conference Office, McGill University, 550 Sherbrooke St. West, West Tower, Suite 490, Montreal, Quebec, Canada H3A 1R9 **Tel:** +1 514 398 3770. **Fax:** +1 514 398 4854
21–26	**208th ACS National Meeting (with Sessions of Analytical Chemistry, Environmental Chemistry, Chemical Health and Safety, *etc*)**	Washington, DC, USA	**Mr. B. R. Hodson,** American Chemical Society, 1155–16th Street N.W., Washington, DC 20036, USA
24–26	**International Symposium on Capillary Electrophoresis**	Heslington, York, UK	**Dr. T. L. Threlfall,** Industrial Liaison Executive, University of York, Department of Chemistry, Heslington, York, UK YO1 5DD **Tel:** Direct line: 0904 432576 General Office: 0904 432511. **Fax:** +0904 432516
29–2/9	**13th International Mass Spectrometry Conference**	Budapest, Hungary	**Hungarian Chemical Society,** H-1027 Budapest, Hungary **Tel:** +36 1 201 6883. **Fax:** +36 1 15 61215
September			
4–7	**East European Furnace Symposium**	Warsaw, Poland	**Dr. Ewa Bulska,** University of Warsaw, Department of Chemistry, Ul. Pasteura 1, 02 093 Warsaw, Poland **Fax:** +48 (22) 22 59 96
5–6	**First International Symposium on Neuroelectrochemistry**	Coimbra, Portugal	**Profa. Dra. Ana Maria Oliveira Brett,** Departamento de Química, Universidade de Coimbra, 3049 Coimbra, Portugal **Tel:** +351 39 22826. **Fax:** +351 39 27703
5–9	**7th International Symposium on Synthetic Membranes in Science and Industry**	Tübingen, Germany	**Dechema,** P.O. Box 970146, D-W-6000 Frankfurt am Main 97, Germany
6–8	**RSC Autumn Meeting (with Analytical Session on Analytical Challenges in Toxicology and Pollution)**	Glasgow, UK	**Dr. J. F. Gibson,** The Royal Society of Chemistry, Burlington House, Piccadilly, London, UK W1V 0BN **Tel:** +44 71 437 8656. **Fax:** +44 71 734 1227
11–16	**EUCMOS XXII: XXIInd European Congress on Molecular Spectroscopy**	Essen, Germany	**GDCh-Geschäftsstelle, Abt. Tagungen,** Varrentrappestr. 40–42, Postfach 90 04 40, D-6000 Frankfurt am Main 90, Germany **Tel:** +49 69 79 17 358. **Fax:** +49 69 79 17 475
12–15	**Separations for Biotechnology**	Reading, UK	**SCI Conference Office,** 14/15 Belgrave Square, London, UK SW1X 8PS **Tel:** +44 71 235 3681. **Fax:** +44 71 823 1698
12–15	**3rd International Symposium on Environmental Geochemistry**	Krakow, Poland	**Helios Rybicka,** Faculty of Geology, Geophysics and Environmental Protection, University of Mining and Metallurgy, Al. Mickiewicza 30, PL-30-059 Krakow, Poland **Tel:** +48 12 333290. **Fax:** +48 12 332936
13–18	**3rd International Symposium on Mass Spectrometry in the Health and Life Sciences**	San Francisco, CA, USA	**Marilyn Schwartz,** Department of Pharmaceutical Chemistry, University of California, San Francisco, CA 9413-0446, USA
18–22	**Geoanalysis 94: An International Symposium on the Analysis of Geological and Environmental Materials**	Ambleside, UK	**D. L. Miles,** Analytical Geochemistry Group, British Geological Survey, Kingsley Dunham Centre, Keyworth, Nottingham, UK NG12 5GG **Tel:** +44 602 363100. **Fax:** +44 602 363200
19–21	**The Second International Conference on Applications of Magnetic Resonance in Food Science**	Aveiro, Portugal	**Dr. A. M. Gil,** Department of Chemistry, University of Aveiro, 3800 Aveiro, Portugal

Date	Conference	Location	Contact
19–21	**The Fourth Annual CIM Field Conference**	Sudbury, Ontario, Canada	**1994 CIM Field Conference,** c/o Sudbury Geological Discussion Group, P.O. Box 1233, Station B, Sudbury, Ontario, Canada P3E 4S7
19–23	**XIIIth International Symposium on Medicinal Chemistry**	Paris, France	**CONVERGENCES/ISMC '94,** 120 avenue Gambetta, 75020 Paris, France **Fax:** +33 1 40 31 0165
21–23	**7th International Symposium on Environmental Radiochemical Analysis**	Bournemouth, UK	**Dr. P. Warwick,** Department of Chemistry, Loughborough University of Technology, Loughborough, Leicestershire, UK LE11 3TU **Tel:** +44 509 222585 or +44 509 222545. **Fax:** +44 509 233163
21–23	**5th International Symposium on Pharmaceutical and Biomedical Analysis**	Stockholm, Sweden	**Swedish Academy of Pharmaceutical Sciences,** P.O. Box 1136, S-111 81 Stockholm, Sweden **Tel:** +46 8 245085. **Fax:** +46 8 205511
22–24	**12th National Conference on Analytical Chemistry**	Constanta, Romania	**Dr. G.-L. Radu,** Romanian Society of Analytical Chemistry 13 Bul. Carol I, Sector 3, 70346 Bucharest, Romania
25–28	**5th International Symposium on Chiral Discrimination**	Stockholm, Sweden	**Swedish Academy of Pharmaceutical Sciences,** P.O. Box 1136, S-111 81 Stockholm, Sweden **Tel:** +46 8 245085. **Fax:** +46 8 205511
25–30	**1994 European Workshop in Chemometrics**	Bristol, UK	**Janice Green,** School of Chemistry, University of Bristol, Cantock's Close, Bristol, UK BS8 1TS **Tel:** +44 (0)272 303030 (ext. 4421) or +44 (0)272 303672. **Fax:** +44 (0)272 251295
26–28	**Protozoan Parasites and Water**	York, UK	**IFAB Communications,** Institute for Applied Biology, University of York, York, UK YO1 5DD **Tel:** +44 (0)904 432940. **Fax:** +44 (0)904 432917
26–30	**16th International Symposium on Capillary Chromatography**	Riva del Garda, Italy	**Professor Dr. P. Sandra,** I.O.P.M.S., Kennedypark 20, B-8500 Kortrijk, Belgium **Tel:** +32 56 204960. **Fax:** +32 56 204859
October			
2–7	**29th Annual Meeting of the Federation of Analytical Chemistry and Spectroscopy Societies**	St. Louis, MO, USA	**FACSS,** P.O. Box 278, Manhattan, KS 66502-0003, USA **Tel:** +1 301 846 4797.
3–6	**PREP '94: 11th International Symposium on Preparative and Industrial Chromatography**	Baden-Baden, Germany	**GDCh-Geschäftsstelle, Abt. Tagungen,** Varrentrappestr. 40–42, Postfach 90 04 40, D-6000 Frankfurt am Main 90, Germany **Tel:** +49 69 79 17 358. **Fax:** +49 69 79 17 475
17–19	**3rd International Symposium on Supercritical Fluids**	Strasbourg, France	Congres 'Fluides Supercritiques' Mle Brionne, ENSIC B.P. 451-1, rue Grandville, F-54001 Nancy Cedex, France **Tel:** +33 83 17 50 03. **Fax:** +33 83 35 08 11
30–4/11	**OPTCON '94**	Boston, MA, USA	**Meetings Department,** Optical Society of America, 2010 Massachusetts Avenue, NW, Washington, DC 20036-1023, USA **Tel:** +1 202 223 9034. **Fax:** +1 202 416 6100
31–2/11	**ANABIOTEC '94: 5th International Symposium on Analytical Methods, Systems and Strategies in Biotechnology**	Minneapolis, MN, USA	**Anabiotec Conference Secretariat,** Elsevier Advanced Technology, Mayfield House, 256 Banbury Road, Oxford, UK OX2 7DH **Tel:** +44 (0)865 512242. **Fax:** +44 (0)865 310981
November			
6–12	**Third Rio Symposium on Atomic Spectrometry**	Caracas, Venezuela	**Professor José Alvarado,** Universidad Simón Bolívar, Departamento de Química, Laboratorio de Absorción Atómica, Apartado postal No. 89000, Caracas, 1080-A, Venezuela **Fax:** +58 2 938322/5719134/5763355/9621695
9–11	**11th Montreux Symposium on Liquid Chromatography–Mass Spectrometry (LC/MS; SFC/MS; CE/MS; MS/MS)**	Montreux, Switzerland	**M. Frei-Häusler,** Postfach 46, CH-4123 Allschwil 2, Switzerland **Tel:** +41 61 4812789. **Fax:** +41 61 4820805

Courses

Date	Conference	Location	Contact
1994			
April			
18–22	**Gas Liquid Chromatography Short Course**	Loughborough, Leicestershire, UK	**Mrs. S. J. Maddison,** Department of Chemistry, Loughborough University of Technology, Loughborough, Leicestershire, UK LE11 3TU **Tel:** +(5090) 222575.
May			
16–19	**Modern Practice of Gas Chromatography Short Course**	West Chester, PA, USA	**Sally Stafford,** Hewlett Packard, Little Falls Site, 2850 Centerville Road, Wilmington, DE 19808-1610, USA **Tel:** +302 633 8444.
23–25	**Fifteenth Annual Introductory HPLC Short Course**	West Chester, PA, USA	**Jim Alexander,** Rohm and Haas Laboratories, 727 Norristown Road, Spring House, PA 19477, USA **Tel:** 2135 619 5226.
24–26	**Fourth Annual Flow Injection Atomic Spectrometry Short Course**	Amherst, MA, USA	**Dr. Julian Tyson,** Department of Chemistry, University of Massachusetts, Amherst, MA 01003, USA **Tel:** +(413) 545 0195. **Fax:** +(413) 545 4856/4490
July			
4–6	**Problem Solving for Analytical Leaders**	Heslington, York, UK	**Dr. T. L. Threlfall,** Industrial Liaison Executive, University of York, Department of Chemistry, Heslington, York, UK YO1 5DD **Tel:** Direct line: 0904 432576 General Office: 0904 432511. **Fax:** +0904 432516
4–8	**High Performance Liquid Chromatography Short Course**	Loughborough, Leicestershire, UK	**Mrs. S. J. Maddison,** Department of Chemistry, Loughborough University of Technology, Loughborough, Leicestershire, UK LE11 3TU **Tel:** +(0509) 222575.
August			
21–24	**Capillary Electrophoresis Course**	Heslington, York, UK	**Dr. T. L. Threlfall,** Industrial Liaison Executive, University of York, Department of Chemistry, Heslington, York, UK YO1 5DD **Tel:** Direct line: 0904 432576 General Office: 0904 432511. **Fax:** +0904 432516
September			
4–8	**Molecular Graphics and Modelling Short Course**	Heslington, York, UK	**Dr. T. L. Threlfall,** Industrial Liaison Executive, University of York, Department of Chemistry, Heslington, York, UK YO1 5DD **Tel:** Direct line: 0904 432576 General Office: 0904 432511. **Fax:** +0904 432516
5–9	**AA/ICP-AES-ICP-MS Short Course**	Loughborough, Leicestershire, UK	**Mrs. S. J. Maddison,** Department of Chemistry, Loughborough University of Technology, Loughborough, Leicestershire, UK LE11 3TU **Tel:** +(0509) 222575.
6–9	**The Leeds Course in Clinical Nutrition**	Leeds, UK	**Mrs. Hilary L. Thackray,** Department of Continuing Professional Education, Continuing Education Building, Sprinfield Mount, Leeds, UK LS2 9NG **Tel:** +(0532) 333233.

Entries in the above listing are included at the discretion of the Editor and are free of charge. If you wish to publicize a forthcoming meeting please send full details to: *The Analyst* Editorial Office, Thomas Graham House, Science Park, Milton Road, Cambridge, UK CB4 4WF. Tel: +44 (0)223 420066. Fax: +44 (0)223 420247.

Analytical News and Information

Centres of Excellence in Analytical Chemistry Launch Unique Modular Multi-university MSc in Analytical Science

The Universities of Bradford, East Anglia, Loughborough, Surrey and York are collaborating to offer a Modular Multi-university MSc in Analytical Science commencing in October, 1994. The course is offered on a part-time basis to provide a programme specifically tailored for industrial analytical scientists.

Demand for well-trained analysts greatly exceeds supply, and this was the primary reason to offer the course through a consortium of universities. Each institution has its own fields of excellence in analytical chemistry, and combining their strengths means that not only will the students benefit from their expertise, but so will their employers.

The Editor of *The Analyst*, Harpal Minhas (HM), attended the launch of the Multi-university MSc in Analytical Science, at the King's Manor, York, on October 29, 1993 and later interviewed Dr. David M. Goodall (DMG), about the benefits of the new course.

HM: *How and why did the establishment of this degree arise?*

DMG: The impetus for this course was the increasing recognition of the need for trained analysts in industry and of the inadequacy of university resources available to satisfy that need, at least within the traditional perception of courses. Through our work in the Centre for Analytical Science and

'the equivalent of an MBA in Analytical Science'.

Instrumentation at the University of York, we have been engaged in discussion with senior managers from industry. We asked them what kind of a higher degree would meet the career development needs of high-flying staff within their companies. What they came up with was a course which provided analytical scientists with a thorough technical knowledge, interdisciplinary vision and skills in management and team leadership. Put another way, we should be heading towards the equivalent of an MBA in Analytical Science. Companies were enthusiastic about the idea of universities pooling their expertise, and about our goal to enhance the status of Analytical Science in the UK.

HM: *Is there a real need for this degree? How do you know?*

DMG: As was indicated earlier, we have talked widely over a period of three years to technical and analytical managers and directors in industry, both to establish their perception of where the current needs for training are and whether they would support such a project. We have had an overwhelming response both in terms of the need for relevant analytical education and training and of their wish to support such an initiative, in so far as the constraints of the recession allowed.

HM: *Who do you expect to enrol as students on this degree?* (i.e., *private individuals, industry wanting staff to have training in particular subjects?*)

DMG: The course is aimed primarily at analytical scientists in industry who wish to improve both their knowledge in depth

'we hope to attract participants who are seen by their managers as having a career in analytical management'.

and breadth of analytical matters. In particular, we hope to attract participants who are seen by their managers as having a career in analytical management. For this reason management and problem-solving skills as well as technical topics are stressed in the syllabus.

HM: *What are the requirements for students to be allowed on this course? Are the criteria the same as for the usual MSc students or will entry be based on ability to pay?*

DMG: The requirements will generally be those for usual MSc entry, *i.e.*, a BSc (normally a 2:2 or above) in an appropriate scientific discipline. However, some of the applicants may have achieved positions of responsibility within the analytical community *via* alternative routes. Substantial weight will be put on referees' reports, and additional evidence of suitability from written work and interview, in deciding whether to accept students with non-standard backgrounds.

HM: *Why five universities instead of one with open learning and a variable time limit? How long are students allowed to finish the course?*

DMG: The Modular Multi-university MSc was developed from continuing education short courses. All five of our collaborating partners have strengths in providing short courses for industrial analytical scientists. We wanted to bring this very successful style of teaching into the mainstream of university teaching, and what was needed was a way of developing and combining courses to give a recognised qualification. This was made possible by the award of £44,000 over two years from 1991–1993 by the University of York through UFC (Universities Funding Council) Continuing Education funding. Dr Terry Threlfall, who formerly worked in Rhône Poulenc and is now the Industrial Liaison Executive in the Department of Chemistry at York, was funded to work on a project to develop award-bearing courses and bring together a consortium of universities.

'The five universities have strengths in complementary areas, and the very broad base of expertise is a particular advantage of the MSc course'.

The five universities have strengths in complementary areas, and the very broad base of expertise is a particular advantage of the MSc course. This means that a very versatile higher degree can be offered, suitable for participants from a wide range of backgrounds including bioanalysis and materials analysis. Our industrial colleagues were very keen that each research project should be supervised by someone with an active research programme in that area. One university alone could not field the numbers of staff that would be necessary to provide research capabilities in all the required areas of analytical science.

As to the time available to complete the degree, there is a limit of 2–5 years, to take into account the individual circumstances of the participants.

HM: *How does this course differ from MSc courses already in existence at the five relevant universities?*

DMG: It differs from existing MSc courses in that the taught element is centred around intensive short courses. The time commitment away from the company will only be 6–7 weeks in total. Pre-reading and assessment will be conducted in the student's own time at home and the project work (equivalent

to 20 weeks full time) will be carried out in company time. The content of some of the individual modules will be similar to those available on full-time courses at participating universities, but parts of the core modules have been devised specifically to meet the needs perceived by industrial managers: Laboratory Management; Problem Solving; and Strategic Planning. The equivalence of these modules with full-time MSc course work has been exhaustively discussed between the university partners. It is not, and will not be, intended to be seen as, an easy option, involving less work than alternative MSc courses.

We are aiming for the highest quality: academic and industrial chief examiners will be appointed from the start of the course and have a remit to include validation of proposals for all modules and their assessment. Inter-institutional quality control will be an integral part of setting and maintaining standards.

HM: *Will students be free to take only the modules/subjects they want (particularly those in industry) and not bother taking the whole course?*

DMG: As we have pursued and discussed the degree, we have come to realise hidden advantages. Availability of expertise has already been mentioned. Versatility is yet another advantage. There are three options for participants: they can come on a short course as they always have done; they can elect to take the module associated with the course with its requirements for pre-reading, presentation and assessment of work, leading to credit points and a certificate for that module; or they can register for the MSc and build those credit points towards the degree.

HM: *With only those modules being chosen that are relevant to a particular student, is there not a danger that the course material chosen becomes less analytical chemistry and more of another related subject?*

DMG: There are no subjects in the syllabus other than analytical science and analytical/technical management topics. No one can hope to understand the entire subject area, particularly one as wide as analysis, and the MSc will be equivalent to a year's full-time study. The homogeneity of the training and its relevance is ensured firstly by the core modules, which have been drawn up on a consensus of what

'if analytical chemists are to be more than just "testers" they need to know about the physics and mathematics which underpin modern analytical methods'.

industry thought 'every analytical scientist ought to know', and by the appointment of an industrial and an academic supervisor for each participant to advise on the most suitable combination of the optional modules. At the launch meeting for the MSc Bill Sharples, formerly Chairman of the Analytical Chemists' Committee of ICI, eloquently traced the recent evolution of analytical chemistry. As he put it, if analytical chemists are to be more than just 'testers' they need to know about the physics and mathematics which underpin modern analytical methods. To train problem-solving scientists we must ensure that they understand the breadth of the subject. If these related disciplines are not also covered how can analytical team leaders harness the talents of the people who are working under them?

HM: *How will it work? Will each university have these extra students sitting in on their normal lectures for particular modules or will extra teaching facilities be required?*

DMG: Those registered for the MSc will come along to the short-course modules but, unlike normal short-course delegates, they will undertake the associated pre-course reading and post-course assessment. These modules differ from normal graduate courses and, typically, compress 40 hours of learning into 4 days. External academic and industrial tutors join the course team with staff from the university organising the module, and in many cases instrument companies providing state-of-the-art apparatus for the practical sessions. Each university organizes modules in areas of its strengths, thus, extra teaching facilities are not required and the modules are intended to be self-financing.

HM: *Will there be examinations as for usual MSc courses or is this degree based entirely on coursework?*

DMG: There will be a written examination following the final core module. Other modules will be assessed using a balance of practical work, problem-solving and paper exercises and critical reviews of the literature. The main aim will be to test understanding and the ability to use that understanding in a variety of contexts. The research project will be assessed on the basis of the dissertation submitted.

HM: *Do you have plans to allow other universities in the UK and Europe to take part in this course? If so, when?*

DMG: We are currently exploring the possibility of extending the consortium to include the Universities of Hull, Strathclyde, Swansea and UMIST. We have canvassed industry and are just starting negotiations in European universities, with the Netherlands being the obvious first target because of their strengths in analytical science and their experience in universities working together. However, initially we have launched with a small number of partners in order to make it manageable. The recent White Paper on Higher Education which has given increased credibility to Master's degrees has certainly helped acceptance of the concept of this initiative.

HM: *Will this MSc course produce an EC approved/recognized MSc equivalent? Will this course assist students with obtaining professional qualifications,* e.g., *MRSC or European Chemist?*

DMG: We are in negotiations with the Royal Society of Chemistry regarding the suitability of the course as a basis for acceptance on to the Register of Analytical Chemists. European equivalents will have to be negotiated when we begin talks with continental universities.

HM: *Will there ever be a modular Ph.D. course?*

DMG: A Diploma in Analytical Science, encompassing the taught modules but lacking the research project of the MSc, is our next target. Many people have welcomed our proposals in this area for staff who already have a higher degree and need to broaden their training. As to the question of the modular PhD, as the normal route through higher degree studies for *all* graduates will be MSc, followed by PhD, we see no problem with this. Candidates who successfully complete the MSc and wish to continue their advanced study will be qualified to register with any of the universities in the consortium. They will work under the joint direction of academic and industrial supervisors, as in the MSc project. The PhD would work very much like a current Co-operative Award in Science and Engineering (CASE) doctorate but with the research carried out in their workplace, complemented, where appropriate, by short periods at the university.

HM: *Thank you for your time and for agreeing to speak to* The Analyst *about the new course. I am sure that the given insight will be of value to prospective students.*

At the end of the interview, Dr. David M. Goodall added, 'Although the content of the course and of the modules has been discussed with industry, further comments and suggestions would be welcomed. The consortium is also considering other higher degree initiatives including an advanced Diploma course for those already possessing an MSc or PhD, and comments on these ideas would be invaluable.'

Future Issues will Include—

Amperometric Arrays in Flowing Solution Analysis—**Peter R. Fielden, Thomas McCreedy, Nigel Ruck and Danut-Ionel Vaireanu**

Recovery of Saxitoxin from Solution by Coprecipitation With Hydrated Iron(III) Oxide—**R. Guevremont, M. N. Quigley and A. S. Reto**

Application of Infrared Spectrometry to the Study of Tautomeric Equilibria and Hydrogen Bonding Basicity of Medical and Biochemical Agents: *N,N'*-Disubstituted Amidines—**Ewa D. Raczyńska, Christian Laurence and Michel Berthelot**

Study by Ultraviolet-Visible Derivative Spectrophotometry of Some Antibiotics. Part I. Molecular Interactions of Benzylpenicilline in Aqueous Solution—**Nicoleta Carp, Mihai Carp and Veronica Tufoi**

Studies on the Breakdown of Organoselenium Compounds in a Hydrobromic Acid–Bromine Digestion System—**Alessandro D'Ulivo, Leonardo Lampugnani, Ilias Sfetsios, Roberto Zamboni and Claudia Forte**

Surface-enhanced Raman Spectroscopy of 9-Phenylacridine on Silver Sol—**T. Iliescu, I. Marian, R. Misca and V. Smarandache**

Infrared and Nuclear Magnetic Resonance Studies of Some Surface Properties of Asbestos–Albumin Interactions—**Rodica Dumitru-Stănescu, Cristina Mandravel and Cristina Bercu**

Second-derivative Spectrophotometric Determination of Naproxen in the Presence of its Metabolite in Human Plasma—**M. Parissi-Poulou and I. Panderi**

Application of ^{57}Fe Emission Mössbauer Spectroscopy to the Investigation of the Physico-chemical Consequences of the Double Radioactive Decay ^{57}Ni → ^{57}Co → ^{57}Fe in the Solid State—**Michel Devillers and Jean Ladriere**

Enhanced Waveguide Raman Spectroscopy With Thin Films—**R. E. Hester and S. Ellahi**

Determination of Proanthocyanidins and Catechins in Beer and Barley by High-performance Liquid Chromatography With Dual-electrode Electrochemical Detection—**David Madigan, Ian McMurrough and Malcolm R. Smyth**

Spectrophotometric Determination of Phenols by Coupling With Diazotized 2,4,6-Trimethylaniline in a Micellar Medium—**J. S. Esteve Romero, L. Alvarez Rodríquez, M. C. García Alvarez-Coque and G. Ramis-Ramos**

Chemical Effects on the Intensity of Ti Kη (Radiative Auger Satellite) X-ray Fluorescence Spectra—**Jun Kawai, Takayuki Nakajima, Takehiro Inoue, Masaharu Yamaguchi, Hirohiko Adachi, Kuniko Maeda and Sadayo Yabuki**

Determination of Precious Metals in Rocks by Inductively Coupled Plasma Mass Spectrometry Using Nickel Sulfide Concentration. Comparison With Other Pre-treatment Methods—**Riitta Juvonen, Eeva Kallio and Tuula Lakomaa**

Kinetic Thermometric Determination of Vanadium by its Catalytic Action on the Oxidation of Chromotropic Acid by Bromate. Application to the Analysis of Atmospheric Aerosols—**J. Mateu, R. Forteza, V. Cerda and M. Colom-Altés**

Application of Isotope Ratio Monitoring Gas Chromatography–Mass Spectrometry to the Analysis of Organic Residues of Archaeological Origin—**R. P. Evershed, S. Charters, K. I. Arnot, J. Collister and G. Eglinton**

Determination of Metals in Sediments of Sinamaica Lagoon, Venezuela, by Atomic Absorption Spectrometry—**Marinela Colina de Vargas, Hilda Ledo de Medina and Katiuska Araujo**

Direct Determination of Polycyclic Aromatic Hydrocarbons in Environmental Matrices Using Laser Desorption Laser Photoionization Time-of-flight Mass Spectrometry—**Patrick R. R. Langridge-Smith, Anita C. Jones, Michael J. Dale and Simon J. T. Pollard**

Tandem Mass Spectrometric Investigation of the Phytosiderophores Mugineic Acid, Deoxymugineic Acid and Nicotianamine—**Peter T. M. Kenny and Kyosuke Nomoto**

Tandem Mass Spectrometry for the Determination of Deoxyribonucleic Acid Damage by Polycyclic Aromatic Hydrocarbons—**Joëlle Wellemans, Ronald L. Cerny and Michael L. Gross**

Multiple Stage Mass Spectrometry: The Next Generation Tandem Mass Spectrometry Experiment—**Gary L. Glish**

Laser Photoacoustic Spectrometry for Trace Gas Monitoring—**Markus W. Sigrist**

Unifying Theory of Errors for the Analytical Methods of Concentration-dependent Distribution, Immunoassay and Substoichiometric and Sub-superequivalence Isotopic Dilution—**J. Klas, Fedor Macesek**

Efficient Procedures for the Voltammetric Determination of Total Arsenic in Zinc and Cadmium Plant Electrolyte Process Streams and in Industrial Effluents—**Alan M. Bond, Robert I. Mrzljak, Terence J. Cardwell, R. W. Catrall, O. M. G. Newman, Bruce R. Champion and J. Hey**

Simultaneous Flow Analysis–Fourier Transform Infrared Determination of Benzene, Toluene and Methyl *t*-Butyl Ether in Petrol—**Miguel De La Guardia, S. Garrigues and Maximo Gallignani**

On-line Preconcentration and Flow Analysis–Fourier Transform Infrared Determination of Carbaryl—**Miguel De La Guardia, S. Garrigues, Ma Teresa Vidal and Maximo Gallignani**

Laser Mass Spectrometry of a Frozen Water Matrix in Environmental Analysis—**S. Alimpiev, V. Mlinsky, S. Nikiforov and M. Belov**

Application of Drift Spectroscopy and Chemometrics to the Discrimination of Dye Mixtures Extracted from Fibres from Worn Clothing—**Serge Kokot and C. Gilbert**

Stabilization of the Peptide Conformation on the Micellar Surface—**Yuri E. Shapiro, Viktor Ya Gorbatyuk, Anatoyli A. Mazurov and Sergei A. Andronati**

Quantitative Analysis of Small Volumes of Gas Mixtures by Fourier Transform Infrared Spectroscopy—**H. Pitsch, M. T. Gaudez, J. Florestan and J. C. Boulou**

Small Volume Batch-injection Analyser—**Joseph Wang and Liang Chen**

Developments in Spectroscopic Data Handling—**Anthony N. Davies**

Luminescence Lifetimes in Biological Systems—**D. Phillips**

Determination of Selenium in Biological Matrices Using a Kinetic Catalytic Method—**I. G. Gokmen and E. Abdelqader**

Simultaneous Determination of Cr(III) Complexes and Cr(VI) Fast Protein Anion-Exchange Liquid Chromatography by Atomic Absorption Spectrometry—**Radmila Milacic and Janez Stupar**

Novel View of the Electrochemistry of Gold—**L. D. Burke, D. T. Buckley and J. A. Morrissey**

The Second International Symposium on

Speciation of Elements in Toxicology and in Environmental and Biological Sciences

June 15-18, 1994, Loen, Norway.

AIMS

The Symposium will focus on recent speciation research related to the chemical, physical and morphological states of elements as they appear in various compartments in environmental and biological systems. The aims of the symposium are: to provide a forum at which recent progress in analytical methodology of element speciation can be discussed and to provide an opportunity for an interchange of ideas between analytical and other scientists investigating fundamental aspects of environmental and human toxicology, nutrition, or metal containing drugs.

THEMES

The main themes for the Symposium are:

A. Sampling, Characterization, Detection and Determination of Chemical or Particle Species

* In Air
* In Water
* In Soil
* In Biological Systems

B.Thermodynamic and Kinetic Aspects

C.Importance of Speciation in Environmental and Human Toxicology, Nutrition and Medicine.

* Speciation of the elements will be considered in the context of pathways to humans, exposure routes, uptake, distribution, metabolism, toxicological mechanisms and excretion.

SUBMISSION OF ABSTRACTS

All contributions (oral or poster) presented will be eligible for publication in a Special Symposium Issue of the journal *The Analyst*. Prospective authors should submit an abstract (A4 format) of one-page length, including tables and figures, by February 15, 1994(deadline).

ORGANIZING COMMITTEE

Yngvar Thomassen (*Symposium Chairman*) **Evert Nieboer** (*Programme Chairman*)

Rita Cornelis (*Gent, Belgium*) **Jytte Molin Christensen** (*Copenhagen, Denmark*)

Brit Salbu (*Aas, Norway*) **Wolfgang Frech** (*Umea, Sweden*)

Jan Aaseth (*Elverum, Norway*)

FOR FURTHER INFORMATION CONTACT: The Second International Symposium on Speciation of Elements in Toxicology and in Environmental and Biological Sciences, **Yngvar Thomassen**, National Institute of Occupational Health, P.O. Box 8149 DEP, N-0033 Oslo 1, Norway.

The 5th Nordic Symposium on

Trace Elements in Human Health and Disease

June 19-21, 1994, Loen, Norway

AIMS

The Symposium will focus on recent research related to trace elements and their relevance in human physiology and toxicology. The programme will emphasize cross-disciplinary issues and promote participant interaction. The conference is intended both for scientists in academia with expertise in toxicology, clinical and analytical chemistry, pathology, metabolic disorders, occupational and environmental health and nutrition, as well as environmental and health professionals.

THEMES

The main themes for the Symposium are:

* Environmental and Occupational Exposure
* Analytical and Clinical Chemistry
* Trace Element Imbalances Related to Human Diseases (*e.g.*, Cancer; Cardiovascular, Liver and Neurological Diseases)
* Dietary Levels and Critical Requirements (Essentiality *versus* Toxicity; Geomedicine)
* Reference Concentrations as Drugs, Chemotherapeutics, Diagnostic Agents, and Chelation Therapy
* Reproductive and Development Effects

SUBMISSION OF ABSTRACTS

The Organizing Committee cordially invites you to submit an abstract of original research related to the themes of the Symposium. Prospective authors should submit an abstract (A4 format) of one-page length including tables and figures by February 15, 1994(deadline). All contributions (oral or poster) presented will be eligible for publication in a Special Symposium issue of *The Analyst*

ORGANIZING COMMITTEE

Jan Aaseth, (*Symposium Chairman*) Hedmark Central Hospital, Norway

Jan Alexander, Institute of Public Health, Oslo, Norway

Evert Nieboer, McMaster University, Hamilton, Canada

Jetmund Ringstad, Ulleval Hospital, Oslo, Norway

Brit Salbu, Agricultural University, As, Norway

Yngvar Thomassen, (*Symposium Secretary*) Oslo, Norway

FOR FURTHER INFORMATION CONTACT: Trace Elements in Human Health and Disease, **Yngvar Thomassen,** National Institute of Occupational Health, P.O. Box 8149 DEP, N-0033 Oslo, Norway. TEL: 47 22466850; FAX: 47 22603276

Analytical Abstracts Now on CD-ROM!

Available in Macintosh™ and IBM Compatible Formats

The premier source of current awareness information in analytical chemistry is now available on a single SilverPlatter CD-ROM.

Analytical Abstracts on CD-ROM features:

- Approximately 170,000 items from 1980 onwards
- Easy to use SilverPlatter software
- Quarterly updates with more than 3,000 items
- Unlimited searching - no additional costs

Special Discount for Hardcopy Subscribers

Contact us today for further information and a FREE demo disk.

Judith Barnsby, Royal Society of Chemistry,
Thomas Graham House, Science Park, Milton Road,
Cambridge CB4 4WF, United Kingdom
Tel: +44 (0) 223 420066 Fax: +44 (0) 223 423623
Telex: 818293 ROYAL

AA

ROYAL SOCIETY OF CHEMISTRY
Information Services

Multi-Journal Searching Now Possible!

ONLINE ACCESS TO THE RSC PRIMARY JOURNALS

Keeping up-to-date with the chemical literature becomes increasingly difficult as the volume of text grows year by year. Manipulating data can be labour-intensive and time-consuming, while searching may not be as accurate nor as comprehensive as desired. Online search, on the other hand, is both quick AND thorough.

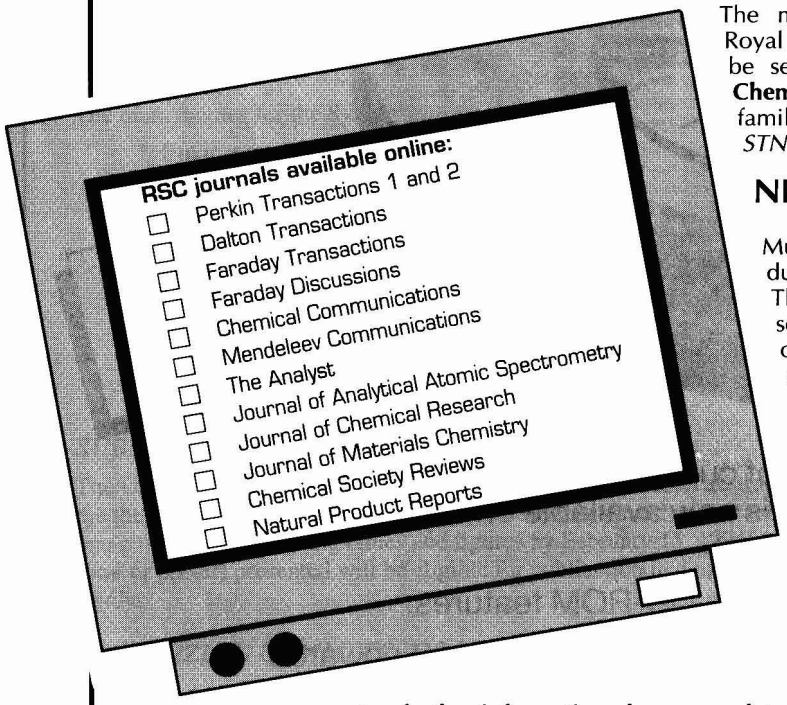

The main primary journals of the Royal Society of Chemistry can now be searched online as part of the **Chemical Journals Online** (**CJO**) family of full-text titles available via *STN International*.

NEW FEATURE!

Multifile searching has been introduced to the **CJO** database range. This enables you the user to search different files simultaneously, which makes searching simpler and faster than before.

The advent of RSC journals online is a boon to chemists, researchers and information specialists everywhere. If you want to cast your search net even wider, it will benefit you too!

For further information please complete and return the reply slip below:

☐ ***Please send me further details of*** **Chemical Journals Online.**

Name: .....

Position: .....

Organisation: .....

Address: .....

.....

.....

Please return to:
Sales and Promotion Department, Royal Society of Chemistry, Thomas Graham House, Science Park, Milton Road, Cambridge CB4 4WF, UK.
Tel: +44 (0) 223 420066. Fax: +44 (0) 223 423623.

ROYAL SOCIETY OF CHEMISTRY

Information Services

ROYAL SOCIETY OF CHEMISTRY

NEW AND RECENT ANALYTICAL BOOKS

Spectrochemical Analysis by Atomic Absorption and Emission

By Lauri H.J. Lajunen
University of Oulu, FInland

This **new** book describes both the theory of atomic spectroscopy and all the major atomic spectrometric techniques (AAS, Flame-AES, Plasma AES, AFS and ICP-MS), including basic concepts, instrumentation and applications.

Spectrochemical Analysis by Atomic Absorption and Emission is very wide in scope and will be extremely useful to both undergraduates and lecturers undertaking modern analytical chemistry courses. It contains many figures and tables which illuminate the text, covers various sample preparation methods and gives suggestions for further reading.

Contents:
Introduction; Theory of Atomic Spectroscopy; Atomic Absorption Spectrometry; Flame Atomic Emission Spectrometry; Plasma Atomic Emission Spectrometry; Inductively Coupled Plasma Mass Spectrometry; Atomic Fluorescence Spectrometry; Sample Preparation; Advantages and Mutual Comparison of Atomic Spectrometric Methods; Further Reading; Subject Index.

Softcover **xii + 242 pages**
ISBN 0 85186 873 8 **Price £18.50**
June 1992

Analytical Ultracentrifugation in Biochemistry and Polymer Science

Edited by S.E. Harding
University of Nottingham
J.C. Horton
University of Nottingham
A.J. Rowe
University of Leicester

Analytical Ultracentrifugation in Biochemistry and Polymer Science is the first book of its kind to appear for nearly two decades and gives as comprehensive a coverage as is possible of the present state-of-the-art, from the leading experts in the field. It describes the advances currently being made and assesses to what extent 'classical' methods are still applicable, providing an up-to-date guide for potential users and experienced researcher alike.

The book divides naturally into four parts. Part I describes the state-of-the-art in instrumentation including a detailed consideration of optical systems and data capture and analysis procedures. Part II focuses on sedimentation equilibrium methods for obtaining molecular weight, polydispersity and interaction information. Part III considers transport methods (both sedimentation and diffusive) and includes a detailed consideration of rigid and flexible particle conformation analysis, polydisperse and interacting systems and concentration dependence phenomena. Part IV looks at a wide range of applications to macromolecular systems in biochemistry and polymer science, including seed and membrane proteins, polysaccharides and glycoconjugates and synthetic macromolecular systems.

This important **new** book is the consequence of an exciting resurgence of interest in the technique, will assist researchers in biochemistry and polymer science to make the most of the exciting opportunity that now exists.

Hardcover **xiv + 630 pages**
ISBN 085186 345 0 **Price £85.00**
November 1992

Particle Size Analysis

Edited by N.G. Stanley-Wood
University of Bradford
R.W. Lines
Coulter Electronics Limited, Luton

Particle Size Analysis reviews the development of particle characterization over the past 25 years and also speculates on its future. Interest in the subject has increased enormously over the years and this book highlights the changes and advances made within the field.

This book is comprehensive in its coverage of particle size analysis and includes contributions on such characterization techniques as microscopy using fractal analysis, light diffraction, light scattering with the phase doppler technique, light observation, and photon correlation spectroscopy. A number of chapters address the interest in on-line in-stream particle size analysis and illustrate the progress being made in achieving this long sought after ideal of *in-situ* in-process particle characterization. Applications to other technological fields are detailed by chapters covering biological systems and the pharmaceutical industry. The subject of surface area determination is considered with particular emphasis on the measurements on porosity of powders, the characterization and comparability of reference materials, and the need for standards.

Particle Size Analysis should provide stimulating reading for technologists, scientists, and engineers involved in particle characterization and powder technology worldwide.

Special Publication No. 102

Hardcover **xx + 538 pages**
ISBN 0 85186 487 2 **Price £57.50**
June 1992

Bioanalytical Approaches for Drugs

including Anti-asthmatics and Metabolites

Edited by Eric Reid
Guildford Academic Associates
I.D. Wilson
ICI Pharmaceutical Division, Macclesfield

Methodological Surveys in Biochemistry and Analysis

Volume 22

Series Editor Eric Reid
Guildford Academic Associates

Bioanalytical Approaches for Drugs, including Anti-asthmatics and Metabolites gives a state-of-the-art account of the subject and focuses on assaying blood and other biological samples, especially drugs which are given in low dosage or which yield metabolites that need subtle investigation. It covers advances in HPLC, SFC, CZE, MS and other detectors, NMR, and automated sample handling, as well as diverse drugs. The book also looks at problems such as analyte lability, stereoselectivity and interferants.

This book is the latest volume in the 'Analysis' sub-series of **Methodological Surveys in Biochemistry and Analysis**, which is acknowledged as an integrated reference source, and contains a cumulative analyte index. It will be essential reading for researchers involved in analytical, medicinal, pharmaceutical and bio-organic chemistry.

Special Publication No. 110

Hardcover **xiv + 356 pages**
ISBN 0 85186 236 5 **Price £75.00**
September 1992

ROYAL SOCIETY OF CHEMISTRY

Information Services

To Order, *Please write to:*
Royal Society of Chemistry, Turpin Distribution Services Limited, Blackhorse Road, Letchworth, Herts SG6 1HN, United Kingdom.
or telephone (0462) 672555 quoting your credit card details. We can now accept Access/Visa/MasterCard/Eurocard.

Turpin Distribution Services Limited is wholly owned by the Royal Society of Chemistry.

For information on other books and journals, *please write to:*
Royal Society of Chemistry, Sales and Promotion Department, Thomas Graham House, Science Park, Milton Road, Cambridge CB4 4WF. UK.

RSC Members *should obtain members prices and order from :*
The Membership Affairs Department at the Cambridge address above.

FIRST FOLD HERE

THE ANALYST READER ENQUIRY SERVICE

For further information about any of the products featured in the advertisements in this issue, write the appropriate number on the postcard, detach and post.

FOLD HERE

THE ANALYST READER ENQUIRY SERVICE

MARCH'94

For further information about any of the products featured in the advertisements in this issue, please write the appropriate number in one of the boxes below.
Postage paid if posted in the British Isles but overseas readers must affix a stamp.

PLEASE USE BLOCK CAPITALS LEAVING A SPACE BETWEEN WORDS *Valid 12 months*

1 NAME

2 COMPANY

PLEASE GIVE YOUR BUSINESS ADDRESS IF POSSIBLE. IF NOT, PLEASE TICK HERE ☐

3 STREET

4 TOWN

5 COUNTY
POST CODE

6 COUNTRY

7 DEPARTMENT/
DIVISION

8 YOUR JOB TITLE/
POSITION

9 TELEPHONE NO

OFFICE USE ONLY REC'D PROC'D

FOLD HERE

Postage will be paid by Licensee

Do not affix Postage Stamps if posted in Gt. Britain, Channel Islands, N. Ireland or the Isle of Man

BUSINESS REPLY SERVICE
Licence No. WD 106

Reader Enquiry Service
The Analyst
The Royal Society of Chemistry
Burlington House, Piccadilly
LONDON
W1E 6WF
England

Second International Symposium on Hormone and Veterinary Drug Residue Analysis

Congress Centre Oud St. Jan, Bruges, Belgium, May 31–June 3, 1994

The above symposium will cover the following topics: sample pre-treatment, extraction and clean-up procedures (SPE, SFE, IAC, gel permeation, *etc.*) in drug residue analysis; analysis of hormone and veterinary drug residues; chromatographic techniques (high-performance liquid chromatography, capillary gas chromatography, thin-layer chromatography, *etc.*) and their detection by spectroscopic (UV, IR, MS, luminescence, *etc.*), electrochemical and other methods (FID, ECD, *etc.*); immunoaffinity techniques and immunoassays (RIA, CLIA, ELISA, FIA, dipstick technology, *etc.*); other techniques applied to hormone and veterinary drug residue analysis in biological samples of human and animal origin; metabolism, pharmacokinetics and toxicology of these compounds; quality control and reference materials; stability of residues in food of animal origin; legal aspects and control mechanisms regarding residues of veterinary drugs in food; and problems concerning consumption of meat originating from hormone treated animals with regard to doping analysis.

All papers must be presented in English. No simultaneous translation will be provided.

The deadline for receipt of abstracts is March 1, 1994.

The symposium papers will be published in *The Analyst*, subject to the usual review process. The manuscripts should be written in accordance with the Instructions for Authors for *The Analyst*, and be handed to the Secretariat before the end of the symposium.

For further information contact: Prof. C. Van Peteghem, Symposium Chairman, Faculty of Pharmaceutical Sciences, University of Ghent, Harelbekestraat 72, B-9000 Ghent, Belgium.
Phone: (32) 9/221.89.51 ext. 235
Fax: (32) 9/220.52.43

ANALAO 119(3) 367–480, 25N–40N (1994) MARCH 1994

The Analyst

The analytical journal of The Royal Society of Chemistry

CONTENTS

Cover picture: Cerenkov radiation in Harwell's irradiation pond. Print kindly supplied by AEA Technology.

Continued on Inside Back Cover–

Typeset and printed by Black Bear Press Limited, Cambridge, England

0003-2654(1994)3:1-0